Preface

This Conference on Advanced Materials, organized jointly by the Materials Research Society of Singapore (MRS-S) and the Institute of Materials Research and Engineering (IMRE) follows a successful inaugural meeting held in August 2004.

Recognizing the seminal contributions of Prof Shih Choon Fong as the Founding Director of IMRE and the Founding President of MRS-S, the conference incorporates a symposium on "Physics and Mechanics of Advanced Materials" to mark his 60th birthday. The symposium is a significant gathering of former associates of Prof Shih, all of whom are renowned researchers who have made a special effort to be here to honour Prof Shih's research achievements. We are particularly grateful to Prof. John W. Hutchinson, Harvard University, for delivering the opening lecture.

The materials research community has responded enthusiastically to this conference. There will be more than 40 invited presentations and a large number of posters highlighting the range of Singapore research in materials science and engineering. We are very grateful for the great interest shown and have tried to provide as many opportunities as possible for researchers to make presentations in either oral or poster form. The presentations will feature research on Nanomaterials, Biomaterials, Functional materials, Optoelectronics and Photonics, Polymers, Microelectronics and Characterization by advanced techniques over the three days of this conference.

To recognize the efforts of all poster presenters, the Materials Research Society will award five prizes for poster presentations.

With this conference, the Materials Research Society and IMRE provide a forum for the materials research community in the even years, between the "International Conference on Materials for Advanced Technologies (ICMAT)" held every odd year.

To reach out to a broader audience, a Public Lecture by Prof. James R. Rice, Harvard University, is scheduled. The title of the lecture is "The dynamics of subduction earthquakes, including past and future Sumatran events". We are grateful to Prof. Rice for sharing his expertise with the materials community and also with the general public. Thanks are due to the Prof Chan Eng Soon, Head of the Department of Civil Engineering at the National University of Singapore and his colleagues for joining with MRS Singapore in organizing this event.

We take this opportunity to thank Toshio Nakamura (SUNY Stony Book), Peter Moran (Singular ID, Singapore), Ares Rosakis (Caltec) and G. Ravichandran (Caltec) for their contribution towards the organization of the special symposium. It is their hard work that has made the event possible. Thanks are also due to Dr. Wong Chia Woan (IMRE) for coordinating the conference logistics and other members of MRS Management Committee for their cooperation.

We trust you will have a stimulating and enjoyable conference.

B.V.R. Chowdari
President & Organizing Chair
MRS Singapore

K.W. Lim
Executive Director
IMRE

Program
2nd MRS-S Conference on Advanced Materials
(Incorporating the Symposium on Physics and Mechanics of Advanced materials)

Wednesday, January 18, 2006

0730 Registration

0900 Welcome & Felicitation to Shih Choon Fong, Founding President of Materials Research Society of Singapore and Founding Director of IMRE
B.V.R. Chowdari, President, Materials Research Society of Singapore
K.W. Lim, Executive Director, Institute of Materials Research and Engineering
John W. Hutchinson, Harvard University, USA
Brian Moran, Northwestern University, USA

0930 Address by Shih Choon Fong, Founding President of Materials Research Society of Singapore and Founding Director of IMRE

0940 Opening Lecture: Thin Film Mechanics and Its Applications, John W. Hutchinson, Harvard University

1030 Coffee Break & Poster Viewing

Session I Chair: Freddy Boey, Nanyang Technological University

1100 I1 Nanofibers in Healthcare, Defense & Security, Environment and Energy, S. Ramakrishna[1,2,3] and W.E. Teo[1], [1]Nanoscience and Nanotechnology Initiative, National University of Singapore, [2]Department of Mechanical Engineering, National University of Singapore, [3]Division of Bioengineering, National University of Singapore

1120 I2 Carbon Nanotubes: Nonlinear Optical Properties and Applications, Ji Wei, Department of Physics, National University of Singapore

1140 I3 Silicon Nanowires for Devices, Ajay Agarwal, N. Singh, N. Balasubramanian and D.L. Kwong, Institute of Microelectronics

1200 I4 Ballistic Transport and Quantum Electron Charging in Carbon Nanotubes, Zhang Qing, School of Electrical & Electronic Engineering, Nanyang Technological University

1220 I5 Large Area Magnetic Nanostructures for Spintronic Applications, Adeyeye Adekunle, Information Storage Materials Laboratory, Department of Electrical and Computer Engineering, National University of Singapore

1240 Lunch & Poster Viewing

Session II Chair: Andrew Wee, National University of Singapore

1400 I6 Dilute Nitride-Antimonide as a Potential Material System for Communication Wavelength Photonics on Low-Cost GaAs Platforms, S.F. Yoon, S. Wicaksono, W.K. Loke, W.K. Cheah and W.J. Fan, Compound Semiconductor & Quantum Information Group, School of Electrical & Electronic Engineering, Nanyang Technological University

1420 I7 OLED Degradation Characteristics: 1/f Noise and Dark Spot Growth Kinetics, Chua Soo-Jin[1,2], Zhao Xin Yue[2] and Ke Lin[1], [1]Institute of Materials Research and Engineering, [2]Centre for Optoelectronics, Department of Electrical and Computer Engineering, NUS

1440 I8 A Photonic Integration Platform Based on Indium Phosphide, Chin Mee Koy[1], Mei Ting[2] and Hou Lianping[2], [1]Photonics Research Centre, School of Electrical and Electronic Engineering, Nanyang Technological University, [2]National Research Centre for Optoelectronic Technology, Institute of Semiconductors, Chinese Academy of Sciences, P.R. China

1500 I9 Electrode Modification for Enhancing OLED Performance, Zhu Furong, Institute of Materials Research and Engineering

1520 Coffee Break & Poster Viewing

Session III Chair: He Chaobin, Institute of Materials Research and Engineering

1600 I10 Computational Materials Design for Alternative Energy Applications, Wu Ping, Jing Hong Mei, Ong Phuong Khuong, Bai Ke Wu and Yu Zhi Gen, Institute of High Performance Computing, A*Star

1620 I11 Development of Nano-Structured Electrodes for Fuel Cells, Jiang San Ping, School of Mechanical and Aerospace Engineering, Nanyang Technological University

1640 I12 Development of Metal-N-H Complexes for Onboard Hydrogen Storage, Chen Ping, Xiong Zhitao, Wu Guotao, Hu Jianjiang, Liu Yongfeng and Yang Lefu, Physics Department, National University of Singapore

1700 I13 Direct Synthesis of H_2O_2 from the Elements, Stephan Jaenicke, Wang Xu and Jasmine Lee Lye Cheng, Department of Chemistry, National University of Singapore

1720 I14 Evaluating Structural Integrity Using Optical Techniques, H.M. Shang and Y.Y. Hung, Temasek Laboratories at NTU, School of Mechanical and Aerospace Engineering, Nanyang Technological University, Singapore; Department of Manufacturing Engineering and Engineering Management, City University of Hong Kong, Kowloon, Hong Kong

1740 I15 Multiferroism in Barium Titanate by Cobalt Substitution, T. Sritharan, A. Srinivas and F.Y.C. Boey, School of Materials Science & Engineering, Nanyang Technological University, Nanyang Avenue, Singapore

1800 End of the Session

Thursday, 19 January 2006

Session IV Chair: Yoon Soon Fatt, Nanyang Technological University

0900 I16 Cluster and Molecular Self-Assembly on Surface Nanotemplates, A.T.S. Wee[1], M.A.K. Zilani[1], Y.Y. Sun[1], H. Xu1, Lei Liu[1], W. Chen[1], X.Y. Gao[1], D.C. Qi[1], G.W. Peng[1], S.C. Tan[1], Y.P. Feng[1], X.-S Wang[1] and K.P. Loh[2], [1]Department of Physics, [2]Department of Chemistry, National University of Singapore

0920 I17 Electrical Transport Study of Inhomogeneous Magnetic Materials and Nanostructures, Wu Yihong, Department of Electrical and Computer Engineering, National University of Singapore

0940 I18 Quantum Dots for Cell Imaging Applications, Jackie Y. Ying, Yuangang Zheng, Subramanian Tamil Selvan and Nikhil R. Jana, Institute of Bioengineering and Nanotechnology

1000 I19 Nanolubrication: Patterned Lubricating Films for Magnetic Hard Disks, Zhang Jun, Data Storage Institute

1020 I20 Deformation & Failure Modes of a Nanofiber, S.Y. Ng[1], E.P.S. Tan[1], C.H. Sow[2] and C.T. Lim[1], [1]Division of Bioengineering & Department of Mechanical Engineering, National University of Singapore, [2]Department of Physics, National University of Singapore

1040 Coffee Break & Poster Viewing

Session V Chair: Feng Xiqiao, China

1100 I21 Functional Nanohybrids and Mesoporous Thin Films, John Wang, A.H. Yuwono and Zhang Yu, Department of Materials Science and Engineering, National University of Singapore

1120 I22 Dynamics of Colloidal Assembly Driven by an Alternating Electric Field, Liu Xiang Yang, Department of Physics, National University of Singapore

1140 I23 Magnetic Thin Films as High Density Storage Media, Ding Jun, Department of Material Sciences and Engineering, National University of Singapore

1200 I24 Direct Evidence for Anisotropic Strain Induced Shape Transition During Epitaxial Growth of Hexagonal Lattice FeGe on Ge(001), Yong-Lim Foo, Zhi Peng Li, Eng Soon Tok, Joyce Pei Ying Tan and Ming Lin, Institute of Materials Research and Engineering

1220 Lunch & Poster Viewing

Session VI Chair: A. Ramam, Institute of Materials Research and Engineering

1400 I25 Deformation and Fracture Mechanism in Thermoset and Thermoplastic Nanoclay Composites, Chaobin He, Instittute of Materials Reserach and Engineering

1420 I26 Synthesis and Characterization of SnO_2 Nanorods Thin Films as Gas Sensing Materials, O.K. Tan, H. Huang, Y.C. Lee and M.S. Tse, Microelectronics Center, School of Electrical and Electronic Engineering, Nanyang Technological University

1440 I27 Synthesis of CdS Nanocrystals from [(2,2'-bipy)Cd(SC{O}R)$_2$] (R = Long Alkyl Group) by Self-Capping, Chang-Tong Yang, Zhihua Zhang, Wee Shong Chin and Jagadese J. Vittal, Department of Chemistry, National University of Singapore

1500 I28 Analysis of Nanoindentation of Thin Film Structures, Zeng Kaiyang[1], Shen Lu[2] and Jiang Haiyan[3], [1]Department of Mechanical Engineering, National University of Singapore, [2]Institute of Materials Research and Engineering, [3]Department of Materials Science and Engineering, NUS

1520 Coffee Break & Poster Viewing

Session VII

1600 Poster Viewing and Judging

1800 End of the Session

Friday, 20 January 2006

Session VIII Chair: Teoh Swee Hin, National University of Singapore

0900 I29 Nanostructured Polymer Carriers for Drug/Gene Delivery, Yi-Yan Yang, Yong Wang, Li-Shan Wang and Li-Hong Liu, Institute of Bioengineering and Nanotechnology

0920 I30 Controlled Growth and Applications of Nanoscale Metal Oxide Materials, Sow Chorng Haur[1], T. Yu[1], Y.W. Zhu[1], P. Chen[1], A.T.S. Wee[2], X.J. Xu[2], C.T. Lim[3], J.T.L. Thong[4] and Z.X. Shen[1], [1]Department of Physics, Blk S12, Faculty of Science, National University of Singapore, [2]Department of Mechanical Engineering, National University of Singapore, [3]Department of Electrical and Computer Engineering, National University of Singapore, [4]Division of Physics and Applied Physics, Nanyang Technological University

0940 I31 Advanced CMOS Front-End Technologies for Sub-Tenth Nanometer Technology Node, Sungjoo Lee, Silicon Nano Device Lab, National University of Singapore

1000 I32 Different Functional Nanostructures Formed Selectively on Inert Substrates Wang Xue-sen, Department of Physics and NUS Nanoscience & Nanotechnology Initiative, National University of Singapore

1020 Coffee Break & Poster Viewing

Session IX Chair: Lim Seh Chun, National University of Singapore

1100 I33 Materials Design from First Principles, Feng Yuan Ping, Department of Physics, National University of Singapore

1120 I34 Frontier Research Opportunities at the Singapore Synchrotron Light Source, H.O. Moser[1], M. Bahou[1], B.D.F. Casse[1], E.P. Chew[1], M. Cholewa[1], C.Z. Diao[1], S.X.D. Ding[1], P.D. Gu[1], S.P. Heussler[1], L.K. Jian[1], J.R. Kong[1], Z.J. Li[1], Z.W. Li[1], Miao Hua[1], B.T. Saw[1], Sharain bin Mahmood[1], Li Wen[1], J. Wong[1], Ping Yang[1], X.J. Yu[1], X.Y. Gao[2], Tao Liu[2], A.T.S. Wee[2] and W.S. Sim[3], [1]Singapore Synchrotron Light Source, National University of Singapore, [2]Physics Department, National University of Singapore, [3]Chemistry Department/NUS

1140 I35 Scanning Probe Microscopy for Materials Characterization, Sean O'Shea, Institute of Materials Research and Engineering

1200 I36 Opening New Frontiers in Materials Processing Using Microwaves, Manoj Gupta and Wong Wai Leong Eugene, Department of Mechanical Engineering, National University of Singapore

1220 I37 Transferring Know-How from Nature's Biomaterial Synthesis Machinery to Materials Research, Suresh Valiyaveettil, Department of Chemistry, NUS-Nanoscience and Nanotechnology Initiative, National University of Singapore

1240 Lunch & Poster Viewing

Session X Chair: Timothy J. White, Nanyang Technological University

1340 I38 Simulation of Adatom Clustering on a Stepped Suface and the Effect of Surface Elasticity on the Interaction Between Suface and Inclusion, Shou-Wen Yu, Ji-Qiao Zhang, Gan-Yun Huang and Xi-Qiao Feng, Department of Engineering Mechanics, FML, Ministry of Education, Tsinghua University, Beijing

1400 I39 InP Based MEMS for Tunable Photonic Devices, A. Ramam, Vicknesh Shanmugan and J. Arokiaraj, Institute of Materials Research

1420 I40 Combination of Self Assembly with Lithography for Fabrication of 3D Photonic Crystal Devices, George X.S. Zhao[1], Qingfeng Yan[1] and S.J. Chua[2,3], [1]Department of Chemical and Biomolecular Engineering, National University of Singapore, [2]Department of Electrical and Computer Engineering, National University of Singapore, [3]Institute of Materials Research and Engineering (IMRE), Singapore

1440 **I41 Mathematical Modeling of Temperature Sensitive Hydrogels,** Erik Birgersson, Hua Li and Chun Lu, Institute of High Performance Computing, 1 Science Park Road, #01-01 The Capricorn, Singapore Science Park II, Singapore 117528

1500 **I42 From Optical MEMS to Photonic NEMS Devices,** Ai-Qun Liu, School of Electrical & Electronic Engineering, Nanyang Technological University, 50 Nanyang Avenue, Singapore 639798

1520 **I43 On the Design and Material Challenges in the Development of Interconnections for Ultra-Fine-Pitch Wafer Level Packages,** Andrew A.O. Tay, Nano/Microsystems Integration Lab, Department of Mechanical Engineering, National University of Singapore, Singapore-117576

1540 **Poster Award Presentations and Closing Remarks**

1600 **Coffee Break**

1630 **End of the Session & Conference**

Affiliated Program Organized Jointly by the Civil Engineering Department, NUS and MRS Singapore

1730 **Public Lecture @ Engineering Auditorium, Block EA, NUS: The Dynamics of Subduction Earthquakes, Including Past and Future Sumatran Events,** James R. Rice, Harvard University, USA

1830 **Refreshments**

Program
Symposium on Physics and Mechanics of Advanced Materials

Organizers:

B.V.R. Chowdari (MRS Singapore)
Toshio Nakamura (SUNY Stony Brook)
Peter Moran (Singular ID, Singapore)
Ares J. Rosakis (Caltech)
G. Ravichandran (Caltech)

Wednesday, January 18, 2006

0830 Registration

0900 Welcome & Felicitation to Shih Choon Fong, Founding President of MRS-S and Founding Director of IMRE
B.V.R. Chowdari, President, Materials Research Society of Singapore
K.W. Lim, Executive Director, Institute of Materials Research and Engineering
John W. Hutchinson, Harvard University, USA
Brian Moran, Northwestern University, USA

0930 Address by Shih Choon Fong, Founding President of MRS-S and Founding Director of IMRE

0940 Opening Lecture: Thin Film Mechanics and Its Applications, John W. Hutchinson, Harvard University, USA

1030 Coffee Break & Poster Viewing

Session I Chair: Ares J. Rosakis
Thin Films and Nano-Structures I

1100 I1 Nano-Mechanics of Solid Surface Suspension and Imprinting with Solid Surface Nano-Structures, Kyung-Suk Kim, Brown University, USA

1130 I2 Stamp Collapse in Soft Lithography, Yonggang Huang, University of Illinois at Urbana-Champaign, USA

1200 Lunch & Poster Viewing

Session II Chair: C.L. Briant
Thin Films and Nano-Structures II

1400 I3 Nanomechanics of Macroelectronics, Zhigang Suo, Harvard University, USA

1430 I4 Mechanics and Reliability of Low-k Dielectrics and Copper Interconnects, X.H. Liu, T.M. Show, M.W. Lane and E.G. Linger, IBM Watson Research Centre, USA

1500 I5 Effect of Surface Anisotropy on the Formation and Evolution of Heteroepitaxial Islands, Yong-Wei Zhang, National University of Singapore, Singapore

1530 Coffee Break and Poster Viewing

Session III Chair: Peter Moran
Fracture and Failure of Materials I

1600 I6 Dissolution Driven Crack Growth, Per Ståhle[1,3], Andrey Jivkov[2] and Christina Bjerkén[3], [1]Lund University, [2]The University of Manchester and [3]Malmö University

1630 I7 A Mechanism-Based Approach to Predict Ductile Crack Growth in Metallic Alloys, Xiaosheng Gao and Jinkook Kim, The University of Akron, USA

1700 I8 Analytical and Computational Modeling of Crack Initiation and Growth in High Temperature Materials, Noel O'Dowd and Catrin Davies, Imperial College London, UK

Thursday, 19 January 2006

Session IV Chair: G. Ravichandran
Fracture and Failure of Materials II

0900 I9 Shear Band Propagation from a Crack Tip Subjected to Mode II Shear Wave Loading, Zhizhou Zhang and Rodney J. Clifton, Brown University, USA

0930 I0 A Micromechanical and Experimental Study of Rupture Mechanisms in Mixed Mode Fracture, Jonas Faleskog and Imad Barsoum, Royal Institute of Technology, Sweden

1000 I11 Analyses of Fatigue Crack Growth by Crack-Tip Blunting and Re-Sharpening, Viggo Tvergaard, Technical University of Denmark, Denmark

1030 Coffee Break & Poster Viewing

Session V Chair: William R. Schowalter
Geo-Mechanics

1100 I12 Heating and Weakening of Faults in Earthquake Slip, James R. Rice, Harvard University, USA

1130 I13 Laboratory Earthquakes, Ares J. Rosakis, California Institute of Technology, USA

1200 Lunch

Session VI Chair: Yongwei Zhang
Bio-Materials

1300 I14 Influence of Human Disease States on Single-Cell and Cell-Population Mechanics, Subra Suresh, Massachusetts Institute of Technology, USA

1330 I15 Patterning Microscale Attractive and Repulsive Gradients for Cell Cultures, Peter Moran, Institute of Materials Research & Singular ID, Singapore

1400 I16 Engineering Nanoprobes for Imaging Gene Expression Dynamics, Gang Bao, Georgia Institute of Technology and Emory University, USA

1430 I17 A Composites-Based Approach for Constitutive Modeling of Soft Tissue with Applications to the Human Annulus Fibrosus, Brian Moran, Zaoyang Guo and Xiong-Qi Peng, Northwestern University, USA

1500 Coffee Break

Session VII Chair: Per Stahle
Advanced Materials I

1530 I18 Size Effects and Scaling in Discrete Dislocation Plasticity, A. Needleman[1], E. Van der Giessen[2], V.S. Despande[3], [1]Brown University, USA, [2]The Netherlands, [3]UK

1600 I19 Inter- and Intragranular Stresses in Nonlinear Ferroelectrics, A. Haug, P.R. Onck and Erik van der Giessen, University of Groningen, The Netherlands

1630 I20 Inverse Analysis to Determine Properties of Anisotropic Thin Films and Coatings, Toshio Nakamura and Yu Gu, State University of New York at Stony Brook, USA

1700 I21 Numerical Analysis of Deformation and Fracture During Indentation of Thin Hard Films on Soft Substrates, R. Narasimhan, Indian Institute of Science, Bangalore, India

Friday, 20 January 2006

Session VIII Chair: Viggo Tvergaard
Advanced Materials II

0900 I22 Bending of a Microbeam due to Adherent Molecules, L.B. Freund, Brown University, USA

0930 I23 Internal Compressive Stresses that Enable Ceramics to Exhibit a Threshold Strength, F.F. Lange, University of California at Santa Barbara, USA

1000 I24 A Finite Deformation Shell Formulation for the Analysis of Composite and Functionally Graded Material Structures, J.N. Reddy and R.A. Arciniega, Texas A & M University, USA

1030 Coffee Break & Poster Viewing

Session IX Chair: Zhigang Suo
Advanced Materials III

1045 I25 Alternative Approaches to Lightweight Construction, Hans Obrecht, Patrick Fuchs and Marcel Walkowiak, Universitaet Dortmund, Germany

1115 I26 Microstructural Changes During Superplastic Forming at Higher Strain Rates in Al-Mg Alloys, C.L. Briant[1], S. Agarwal[1], P.E. Krajewski[2] and A.F. Bower[1], [1]Brown University and [2]General Motors R&D Center, USA

1145 I27 Large Electrostriction in Ferroelectrics, G. Ravichandran, California Institute of Technology, USA

1215 Closing Remarks

1230 Lunch

Poster Presentations

Opening Lecture

Date: Wednesday, January 18, 2006
Time: 0940

Thin Film Mechanics and Its Applications

John W. Hutchinson
Division of Engineering and Applied Sciences, Harvard University
E-mail: hutchinson@husm.harvard.edu

Thin films are ubiquitous in modern technology as adhesives, protective and wear coatings, and as fundamental structures in electronic and photonic devices and packages. Layered structures comprised of films of metals, ceramics and polymers are commonly manufactured with large mismatches in elastic moduli and coefficients of thermal expansion to achieve special functional purposes. A rich trove of interesting deformation and failure phenomena for thin films has been observed. Considerable progress in understanding the mechanics underlying these phenomena has occurred over the last decade. Mechanics principles and approaches have been developed that provide guidelines for circumventing thin film failure modes. A overview of this progress will given with particular emphasis on delamination phenomena. Examples will be drawn from many application areas, including thermal barrier coatings for turbine engines, diamond coatings for wear enhancement, metal films on flexible polymer substrates for electronic data storage devices.

Public Lecture

Lecture at the National University of Singapore

Date: Friday, January 20, 2006
Time: 1730

The Dynamics of Subduction Earthquakes, Including Past and Future Sumatran Events

James R. Rice
Division of Engineering and Applied Sciences and Department of Earth and Planetary Sciences, Harvard University, Cambridge, MA, USA

The world's largest earthquakes occur at subduction zones, where the floor of an ocean dips under a continent. As demonstrated tragically in the December 2004 Sumatran event, the hazard arises not just from the seismic shaking but also from the possibility of tsunami excitation. The talk will review in elementary form the basic mechanics and geology of the earthquake process, including some special features of subduction earthquakes. Results will be shown on rupture propagation, slip, uplift, seismic shaking and tsunami generation in large events, including Sumatran. Two current research topics may improve the intermediate term predictability of such earthquakes. One is the discovery in some subduction zones of slow deformation episodes; these occur in the region slightly downward, along the descending seafloor, from where earthquakes nucleate, and cause episodic steps of stress on that seismogenic region. The second is evidence of an accelerating rate of release of energy in smaller earthquakes over tens of years before some large events. Other efforts which can improve earthquake survivability include the establishment of early warning systems based on automated rapid analysis of signals near the source region and wireless communication to population centers, the use of detailed seismic imaging and large scale computation to characterize the distribution of expected ground motions for candidate earthquakes, and the formulation, and enforcement, of appropriate building codes.

2nd MRS-S Conference Abstracts

I1 Nanofibers in Healthcare, Defense & Security, Environment and Energy

S. Ramakrishna*[,1,2,3] and W.E. Teo[1]
[1]*Nanoscience and Nanotechnology Initiative, National University of Singapore, 9 Engineering Drive 1, Singapore 117576, Singapore*
[2]*Department of Mechanical Engineering, National University of Singapore, 9 Engineering Drive 1, Singapore 117576, Singapore*
[3]*Division of Bioengineering, National University of Singapore, 9 Engineering Drive 1, Singapore 117576, Singapore*
*E-mail: seeram@nus.edu.sg

For any technology, the material of its product is one of the limitations in its application. Conversely, a technology that can fabricate products made of different materials will have wide-ranging applications. Electrospinning is one such versatile process for fabricating nanofibers. Nanofiber with its very high surface area to volume ratio has the potential to significantly increase the performance of many current technologies as well as creating new products. Its ability to form different fibrous assemblies allows application specific modifications at the same time. This meant that electrospun nanofibers can be used in areas from healthcare, defense and security to environment and energy applications. Tests using contact angle analysis has shown that a hydrophobic material achieves super hydrophobicity after electrospinning to form a fiber mesh. The relatively high production rate of electrospinning has led to several companies producing electrospun fibers on a commercial level. Research on using electrospun nanofibers in areas of healthcare and defense and security has shown promising results. More recently, researchers are beginning to explore the use of electrospun nanofibers in the field of environment and energy applications. Electrospinning is one of the few nanotechnologies with huge versatilities and which products are affordable to the general public.

I2 Carbon Nanotubes: Nonlinear Optical Properties and Applications

Ji Wei
Department of Physics, National University of Singapore, Singapore 117542
E-mail: phyjiwei@nus.edu.sg

Carbon nanotubes are nearly ideal, one-dimensional (1D) nanostructures with unique electronic and optical properties that recommend them highly for applications in photonics. The 1D character of carbon nanotubes also has important implications for the thermo-optical properties as well. In this presentation, I will start with a brief review on the electronic structures of carbon nanotubes. In particular, I will discuss their potential applications for optical limiting and ultra-fast all-optical switching. I will present our experimental investigations that demonstrate the potentials of carbon nanotubes. Our experimental results include three research projects that we have carried out. They are (i) optical limiting in solutions of multi-walled carbon nanotubes with nanosecond laser pulses, (ii) ultra-fast saturable absorption in multi-walled carbon nanotubes with femtosecond laser pulses; and (iii) alteration of the ultra-fast nonlinear response in composites which are made up of carbon nanotubes and semiconductor quantum dots.

I3 Silicon Nanowires for Devices

Ajay Agarwal*, N. Singh, N. Balasubramanian and D. L. Kwong
Institute of Microelectronics, Singapore
*E-mail: agarwal@ime.a-star.edu.sg

Uni-dimensional silicon nanowires (SiNW) have attracted attention as highly sensitive sensor element for label-free bio-molecular sensing as well as nanoscale transistors. Due to high surface-to-volume ratio, the electronic conductance of nanowires is sensitive enough for single molecule detection when such species gets attached to the suitably modified nanowire surface.

Fabrication of the SiNW is well exploited using vapor-liquid-solid (VLS) method, solution technique, direct lithography, etch and self-limiting oxidation process, etc. VLS method is the most used for the realization of nanowires using various metals and oxide as catalysts. For the easier adaptation of sensor fabrication technologies by the silicon industry, it is important that the processes are CMOS compatible. In present work, we present the fabrication process and electrical properties of lateral silicon nanowires formed on different silicon wafers using stress-limited oxidation technique. Further the paper deals with the application of silicon nanowires for gate-all-around transistors and biosensor. The details of nanowire bio-chemical sensor experiments, analysis of the results and the sensor mechanism will be elaborated.

I4 Ballistic Transport and Quantum Electron Charging in Carbon Nanotubes

Zhang Qing
Associate Professor
School of EEE, NTU
E-mail: eqzhang@ntu.edu.sg

When the characteristic dimension l of electronic devices is reduced down to nanometer scales, a few fundamental changes in the electronic properties of the devices must occur. For example, if the electronic mean free path is comparable to l, the electron transport will change from diffusive to ballistic mode. If the capacitance C of the sample is so small that $e^2/C \geq k_B T$ with e, T and k_B the unit charge, temperature and the Boltzmann constant, respectively, single electron charging effect is detectable. In this talk, the unique behaviors of carbon nanotube based field effect transistors are observed recently and they can be attributed to ballistic transport and quantum electron charging effects.

I5 Large Area Magnetic Nanostructures for Spintronic Applications

Adekunle Adeyeye
Information Storage Materials Laboratory, Department of Electrical and Computer Engineering,
National University of Singapore, 4 Engineering drive 3, Singapore-117576
E-mail: eleaao@nus.edu.sg

An exciting development in magnetism has been the use of controlled nanofabrication techniques such as lithography and other self assembly methods to create nanomagnets. Magnetic nanostructures possess very different properties from their parent bulk material. Ferromagnetic nanostructures provide an opportunity for the exploration of new physical phenomena and the development of technologically important devices. One of the main applications of magnetic nanostructures is in ultra-high density data storage and non-volatile memory.

In this talk, I will present the magnetic and transport properties of large area nanomagnets fabricated using deep ultraviolet lithography. We have used electron beam deposition technique and lift-off method to convert the developed resist patterns into magnetic nanostructures of different shapes and sizes. The uniformity of the nanomagnets was characterized using SEM and AFM. We observed that the structures are uniform, have the desired shapes and are reproducible over a large area. The magnetic and transport properties of the fabricated nanostructures are very different from the reference film and strongly depend on the size and shape of the nanostructures. Some of our recent findings will be presented. Finally, a simple micromagnetic modeling will be used to aid our understanding of the magnetization reversal processes in magnetic nanostructures.

I6 Dilute Nitride-Antimonide as a Potential Material System for Communication Wavelength Photonics on Low-Cost GaAs Platforms

S.F. Yoon*, S. Wicaksono, W.K. Loke, W.K. Cheah and W.J. Fan
Compound Semiconductor & Quantum Information Group
School of Electrical & Electronic Engineering
Nanyang Technological University
*E-mail: esfyoon@ntu.edu.sg

Compound semiconductor material and device research goes back a long way in Nanyang Technological University Singapore, with the founding of the Compound Semiconductor & Quantum Information Group in the eighties. This talk highlights recent research activities of the Group in the area of dilute nitride-antimonide materials and devices. In particular, the development of dilute nitride-antimonide materials using the molecular beam epitaxy process is described, and the potential of this material system for integration with a low-cost GaAs optoelectronics platform is highlighted. The talk will trace the growth and material characteristics and describe the application of the dilute nitride-antimonide system in PIN photodiodes. Results from photoluminescence, x-ray diffraction, secondary ion mass spectroscopy (SIMS), current-voltage (I-V) and photoresponsivity measurements will be presented. Post growth thermal annealing experiments will be described, and future strategies will be presented as a way forward for the research.

I7 OLED Degradation Characteristics: 1/f Noise and Dark Spot Growth Kinetics

Chua Soo-Jin*[,1,2], Zhao Xin Yue[2] and Ke Lin[1]
[1] *Institute of Materials Research and Engineering (IMRE)*
[2] *Centre for Optoelectronics, Department of Electrical and Computer Engineering, NUS*
*E-mail: elecsj@nus.edu.sg

Organic light-emitting diodes (OLEDs) have received considerable worldwide attention over the last decade due to their great potentials for flat panel display applications. The physical processes underlying the operation of organic light emitting diodes are charge injection from the metallic electrodes into the organic layers, charge transport across these layers through carrier hopping, electron-hole recombination and exciton emission. However OLEDs are beset by generation of dark spots which grow either during operation or while on the shelf. Their origins are principally due to moisture or oxygen ingress through pinholes in the OLED layers, or through interaction between the layers due to their difference in chemical potentials causing reactions and delamination. The latter can be assisted by the presence of moisture and oxygen and other ambient gases or may be photo-assisted. The characteristics of each of the processes are different and manifest itself through the variation of dark spot growth rate or kinetics and the noise it generates. Degradation can take place in the material or at the interfaces between the layers generating traps. These result in carrier number fluctuations and hopping time during charge transfer. This presentation will highlight the characteristics observed in the 1/f noise and the dark spot growth kinetics.

I8 A Photonic Integration Platform Based on Indium Phosphide

Chin Mee Koy*[,1], Mei Ting[1] and Hou Lianping[2]
[1] *Photonics Research Centre,*
School of Electrical and Electronic Engineering
Nanyang Technological University, Singapore 639798
[2] *National Research Centre for Optoelectronic Technology, Institute of Semiconductors, Chinese Academy of Sciences Beijing 100083, P.R. China*
*E-mail: emkchin@ntu.edu.sg

Optical communication has enabled the transmission of information with almost unlimited bandwidth. Yet photonic devices used in optical communication systems are relatively large, discrete and costly components. The challenge is to develop new systems that can transport greater quantities of data at ever decreasing cost. Photonic integration is one promising way to achieve this goal, and provides many of the same advantages as electronic integration. However, unlike transistors which form the bedrock building block for all of electronics, *no photonic equivalent of transistors exists.*

An integration platform must be able to tackle the large diversity of devices that exist (both active and passive), be scalable as more devices are integrated, and yet be as robust and simple as possible. In our architecture, this is achieved by having two levels of integration to accommodate both active and passive devices. In the first level,

quantum well epilayers are grown on the InP substrate. Multiple active devices can be integrated *horizontally* using a unique *bandgap engineering* technique developed in NTU. In the second level, a vertical coupler or spot-size converter is used to maximize the coupling between the optical chip and single-mode optical fiber. More generally, it can be used to provide optical interconnection between vertically separated layers. The whole structure requires only one-step growth and is robust.

I9 Electrode Modification for Enhancing OLED Performance

Zhu Furong
Institute of Materials Research and Engineering, 3 Research Lint Singapore 117602
E-mail: fr-zhu@imre.a-star.edu.sg

The electrode-organic interfacial properties play a critical role in determining the performance of OLEDs. A number of anode modification rcchniques and device architectures are developed for enhancing OLED performance. Accomplishments in developing tecbniques for engineering interfacial properties to ensure electron-hole current balance in OLEDs will be discussed. In practical applications, the visual contrast is more important than the brightress of image. As such, improving the visual contrast in OLED displays is another important issue to address with a significant technological implication. This talk will also discuss the progress in developing color tuning udttl graded anode thickness and gradient refractive index anode for enhancing the visual contrast of OLED displays.

I10 Computational Materials Design for Alternative Energy Applications

Wu Ping*, Jing Hong Mei, Ong Phuong Khuong, Bai Ke Wu and Yu Zhi Gen
*Institute of High Performance Computing, A*Star, Singpaore*
*E-mail: wuping@ihpc.a-star.edu.sg

Materials design requires scientific and engineering skills of diverse disciplines, therefore, computational science, which is widely regarded as the "third pillar" of 21st century scientific and engineering enterprise alongside theory and physical experiment, is naturally becoming very popular in the discovery of materials. This is especially true for the search of new materials for alternative energy applications that may reduce our dependence on fossil fuel. Computational models may provide a unique window through which unexpected materials behaviors can be revealed virtually that are otherwise impractical or impossible to figure out.

IHPC has developed a research roadmap for future energy applications. A number of materials design projects are undergoing in collaboration with other A*star research institutes and the two local Universities, which have already demonstrated how computational modeling plays a leading role in scientific discovery and technology advancement. At the presentation, I shall show a few case studies of materials design research for hydrogen storage, solid oxide fuel cells and energy saving devices.

I11 Development of Nano-Structured Electrodes for Fuel Cells

Jiang San Ping
School of Mechanical and Aerospace Engineering, Nanyang Technological University
E-mail: mspjiang@ntu.edu.sg

The performance of fuel cells, be it high temperature solid oxide fuel cell (SOFC) or low temperature polymer electrolyte and direct methanol fuel cells (PEFC & DMFC) are critically dependent on the microstructure of the electrode and electrode/electrolyte interface. For solid oxide fuel cells operating at intermediate temperatures of 600-800°C, the cell performance is primarily limited by the electrode polarization. In this talk, the development of nano-structure electrodes via an effective and simple ion impregnation approach for SOFC is introduced. In this method, nano-sized catalytic active phase such as Gd-doped ceria was introduced into the pre-sintered porous electrode. The results show that the ion impregnation is particularly effective to enhance the electrocatalytic activity of the conventional electrodes such as $(La,Sr)MnO_3$, Ni and $(La,Sr)(Cr,Fe)O_3$ electrodes for intermediate temperature SOFC applications. The relationship between the microstructure and electrochemical behavior of the impregnated electrodes is discussed. Finally, recent development in the layer-by-layer (LbL) self-assembly of polymer stabilized nanoparticles for polymer electrolyte and direct methanol fuel cells is briefly introduced.

I12 Development of Metal-N-H Complexes for Onboard Hydrogen Storage

Chen Ping*, Xiong Zhitao, Wu Guotao, Hu Jianjiang, Liu Yongfeng and Yang Lefu
Physics Department, NUS
*E-mail: phychenp@nus.edu.sg

Metal nitrides and imides exhibit strong affinity towards hydrogen molecules. Such strong interactions enable these substances to be used as potential materials for hydrogen storage. In the previous investigations, maximum of 11.5wt% and 7.0 wt% of hydrogen storage capacities have been determined in lithium nitride and lithium imide, respectively. However, relatively high operating temperatures place a serious restriction onto the application of those substances. It is clear that to lower down the operation temperatures the composition and structure of the subject material have to be altered in order to sit within a suitable thermodynamic range. Successful attempt has been made in Li-based ternary systems, such as Li-Mg-N-H and Li-Ca-N-H, in which considerable reduction in hydrogen absorption and desorption temperatures and uprising H_2 desorption plateau pressures have been achieved. Ternary imide $Li_2MgN_2H_2$, as an example, could reversibly store 5.8wt% of hydrogen at 180°C with desorption plateau pressure higher than 20 bars.

I13 Direct Synthesis of H_2O_2 from the Elements

Stephan Jaenicke*, Wang Xu and Jasmine Lee Lye Cheng
Department of Chemistry
National University of Singapore
*E-mail: chmsj@nus.edu.sg

Hydrogen peroxide is an ideal oxidant. In contrast to other oxidizing agent such as Cl_2, transition metal oxides, or nitric acid/nitrous oxides, the only byproduct of the oxidation is water. However, the current method of H_2O_2 synthesis by the autooxidation process is economical only at a large scale of 60,000 tons per year. Many applications of H_2O_2 for water treatment or bleaching require relatively small amounts of dilute H_2O_2. A method for the point of use generation of H_2O_2 is therefore highly desirable.

The formation of H_2O_2 is very exothermic, and is therefore entirely irreversible. However, the elements H_2 and O_2 can also combine to form water, and this reaction is even more highly exothermic. In order to produce H_2O_2 in good yield, a highly selective catalyst is required, and the parallel reaction to water as well as the unproductive further reduction of hydrogen peroxide according to the equation $H_2O_2 + H_2 \rightarrow 2H_2O$ have to be suppressed. We have investigated the formation of H_2O_2 from the elements over Pd and Pd/Pt catalysts supported on a number of different supports (activated carbon, various zeolites, silica). The experiments were done in three different reactors: an atmospheric tube reactor with continuous gas feed, a batchwise reaction in an autoclave at elevated pressure, and continuous continuous production in an inherently safe micro-reactor format with co-current flow of the reactant gases and the liquid phase through a stationary packed catalyst bed. Different solvents were examined, e.g. water and various alcohols, as well as water-alcohol mixtures. It was found that at room temperature, the addition of Br^- is required to enhance the selectivity to H_2O_2. The best results were obtained with Pd/Pt alloy catalysts supported on sulfonated carbon. A selectivity of 73% at a hydrogen conversion of 12% could be achieved in the autoclave. In the microreactor, the best results were 69% selectivity at 39% conversion in a single pass.

I14 Evaluating Structural Integrity Using Optical Techniques

H.M. Shang* and Y.Y. Hung
Temasek Laboratories at NTU,
School of Mechanical and Aerospace Engineering, Nanyang Technological University, Singapore
Department of Manufacturing Engineering and Engineering Management,
City University of Hong Kong, Kowloon, Hong Kong
*E-mail: mhmshang@ntu.edu.sg

A general theory that summarizes the working principles of various optical nondestructive techniques such as fringe- and grating- projection, moiré, holography and shearography will be presented. The general theory also illustrates that holography and shearography can be perceived as similar techniques except in the amount of image-shearing used during testing. The optical nondestructive testing process involves comparing the phase distributions of two slightly mis-matched optical gratings (known as the reference and the object gratings) and then extracting the phase-difference. Depending on the optical arrangement, the phase-difference depicts either the spatial coordinates or the first-order derivatives of the object surface relative to the reference surface. Various examples will be presented.

I15 Multiferroism in Barium Titanate by Cobalt Substitution

T. Sritharan*, A. Srinivas and F.Y.C. Boey
School of Materials Science & Engineering, Nanyang Technological University,
Nanyang Avenue, Singapore
*E-mail: assritharan@nut.edu.sg

Barium titanate, a good ferroelectric, could be induced with magnetic ordering by substituting the Ba or Ti ions by a magnetic ion. In this paper we disclose results of Co substituent. Compounds of general formulae $Ba_{1-x}Co_xTiO_3$ and $BaCo_xTi_{1-x}O_3$ were synthesized and characterized. It is shown that the crystal structure of $BaTiO_3$ is preserved and the ferroelectric polaization appears to decrease with increase of Co content. Ferromagnetic saturation is observed in magnetization versus magnetic field plots. When Co substitutes Ba, the saturation level increases with increase in Co content. However, when Co substifutes Ti, saturation level decreases after an initial increase for dilute concentrations. There appears to be a limit to Co dissolution at Ti sites but not at Ba sites within the concentrations investigated here. Some reasons are discussed.

I16 Cluster and Molecular Self-Assembly on Surface Nanotemplates

A.T.S. Wee*[,1], M.A.K. Zilani[1], Y.Y. Sun[1], H. Xu[1], Lei Liu[1], W. Chen[1], X.Y. Gao[1], D.C. Qi[1], G.W. Peng[1], S.C. Tan[1], Y.P. Feng[1], X.-S. Wang[1] and K.P. Loh[2]
[1] *Department of Physics, NUS*
[2] *Department of Chemistry, NUS*
*E-mail: phyweets@nus.edu.sg

The fabrication of molecular nanodevices necessitates the creation of structures at the molecular scale, i.e. <5 nm in size. The formation of self-assembled nanostructures by "bottom-up" methods is a field that has attracted great interest recently due to the potential applications of nanoscale devices. In this talk, I will present our latest results in cluster and molecular assembly with the aim of fabricating of nanostructures and molecular nanodevices. We propose "bottom-up" self-assembly methods in vacuo for the fabrication of such structures, using nanoscale templates that form spontaneously on surfaces under carefully chosen conditions. The combined use of STM, LEED and synchrotron experiments, as well as computational studies using tensor LEED analysis and DFT calculations on metal [1–3] and semiconductor single crystal surfaces is presented. The formation of oxygen-induced reconstructions on Cu(210) that can serve as 1D surface nanotemplates has been observed using STM [4] and LEED, and its detailed structure calculated by tensor LEED [5,6].

For the 6H-SiC(0001) wide bandgap semiconductor surface, a range of interesting surface reconstructions is observed [7]. Monodispersed 3-5 nm Co nanoclusters have been deposited on the C-terminated 6H-SiC(0001) 6?3 × 6?3*R*30? nanomesh template [8,9]. We have also observed the formation of Co-induced magic clusters on Si(111)-7×7 surface [10]. Finally, I will discuss recent synchrotron resonant photoemission and x-ray absorption results on some self-assembled monolayer molecules.

References

[1] Y.Y. Sun, H. Xu, Y.P. Feng, A.C.H. Huan, A.T.S. Wee, *Surf. Sci.* **548**, 309 (2004).
[2] Y.Y. Sun, H. Xu, Y.P. Feng, A.C.H. Huan, A.T.S. Wee, *Phys. Rev. Lett*., **93** (2004) 136102.
[3] Y.Y. Sun, H. Xu, J.C. Zheng, J.Y. Zhou, Y.P. Feng, A.C.H. Huan, A.T.S. Wee, *Phys. Rev. B* **68**, 115420 (2003).
[4] A.T.S. Wee, J.S. Foord, R.G. Egdell, J.B. Pethica, *Phys. Rev. B* **58**, R7548 (1998).
[5] Tan K.C., Guo Y.P., Wee A.T.S. and Huan C.H.A., *Surf. Rev. Lett*. **6,** 859 (1999).
[6] Y.P. Guo, K.C. Tan, H.Q. Wang, C.H.A. Huan, A.T.S. Wee, *Phys. Rev. B* **66**, 165410 (2002).
[7] X.N. Nie, H.Q. Wang, A.T.S. Wee, K.P. Loh, *Surf. Sci.* **478**, 57 (2001).
[8] W. Chen, K.P. Loh, H. Xu, A.T.S. Wee, *Appl. Phys. Lett.* **84**, 281 (2004).
[9] W. Chen, H. Xu, L. Liu, X.Y. Gao, D.C. Qi, G.W. Peng, S.C. Tan, Y.P. Feng, K.P. Loh, A.T.S. Wee, *Surf. Sci*., to appear.
[10] A.K. Zilani, Y.Y. Sun, H. Xu, Lei Liu, Y.P. Feng, X.-S. Wang, A.T.S. Wee, *Phys. Rev. B*, to appear.

I17 Electrical Transport Study of Inhomogeneous Magnetic Materials and Nanostructures

Wu Yihong
Department of Electrical and Computer Engineering, National University of Singapore
E-mail: elewuyh@nus.edu.sg

Inhomogeneity exists in virtually all material systems. Although its influence to material or device properties may be easily ignored in bulk materials, it is no longer the case for nanoscale systems. This has, in particular, become an important issue for new types of spintronic materials such as half metals and diluted magnetic semiconductors. In addition to chemical and structural inhomogeneity, magnetic inhomogeneity also affects the properties of these materials. In this talk, we will show how a differential conductance technique can be used to characterize inhomogeneity in Fe_3O_4 and ZnO:Co. The former is a half metallic material with anti-phase boundaries and the latter is a potential room-temperature magnetic semiconductor. In order to confine the inhomogeneity in a small region, we have fabricated Fe_3O_4 nanowires using the hard mask and ion milling technique. Detailed bias-dependence study of both the conductance and magnetoresistance curves for both the thin films and nanowires suggests that the electrical conduction in magnetite near and above the Verwey transition temperature is dominated by a tunneling mechanism across antiphase boundaries. The thickness of the effective potential barrier is found to decrease with the magnetic field which accounts for the negative magnetoresistance at high field. A simple model is invoked to explain the experimental results. As for the case of ZnO:Co, we report a systematic study of structural, optical, electrical and magnetic properties of $Zn_{1-x}Co_xO$ ($x = 0.08 - 0.41$) thin films co-doped with Al. Both co-doped (in which Co is co-sputtered with other elements) and δ-doped (in which Co is doped digitally in the host matrix) samples have been prepared and studied. Again, we will show that, in complementary with other techniques, the differential conductance technique is a powerful tool to reveal the inhomogeneity of diluted magnetic semiconductors.

I18 Quantum Dots for Cell Imaging Applications

Jackie Y. Ying*, Yuangang Zheng, Subramanian Tamil Selvan and Jana Nikhil R.
Institute of Bioengineering and Nanotechnology
*E-mail: jyying@ibn.a-star.edu.sg

Quantum dots are fluorescent semiconductor nanoparticles that offer narrow, tunable emission bands, and superior photostability compared to conventional organic dyes. They are of great interest as fluorescent labels for cellular imaging, biosensors, immunoassays and other biomedical applications. For biological applications, quantum dots need to be soluble and stable in water. They should demonstrate high quantum efficiency and show low non-specific binding under biological conditions.

In our group, several novel methods have been developed to generate water-soluble quantum dots. Quantum dots capped by either natural materials or synthetic materials have been synthesized or solubilized in aqueous solution and the fluorescence emission is tunable between 350 nm and 700 nm. The as-prepared QDs have a quantum yield (QY) up to 45% in aqueous phase, and the bandwidths of the fluorescence peaks is as narrow as 20 nm, comparable with most organo-metallically synthesized QDs. These QDs were highly soluble and stable in a wide pH range and in biological systems, and they show lower cytotoxicity compared with QDs prepared in other methods. These novel quantum dots are also surface-functionalized and conjugated with bioprobes for bio-labeling and cell imaging applications.

I19 Nanolubrication: Patterned Lubricating Films for Magnetic Hard Disks

Zhang Jun
Data Storage Institute
E-mail: Zhang_jun@dsi.a-star.edu.sg

Nanolubrication is emerging to be the key technical barrier in many devices. One of the key attributes for successful device lubrication is self-sustainability using only several molecular layers. For single molecular species lubrication, one desires bonding strength and molecular mobility to repair the contact by diffusing back to the contact. One way to achieve this is the use of mask to shield the surface with a patterned surface texture, put a monolayer on the surface and induce bonding. Then re-deposit mobile molecules on the surface to bring the thickness back to the desired thickness.

This paper describes the use of long wavelength UV irradiation (320–390 nm) to induce bonding of a perfluoropolyether (PFPE) on CNx disks for magnetic hard disk application. This allows the use of irradiation to control the degree of bonding on CNx coatings. The effect of induced bonding based on this wavelength was studied by comparing 100% mobile PFPE, 100% bonded PFPE, and a mixture of mobile and bonded PFPE in a series of laboratory tests. Using a lateral force microscope, a diamond-tipped atomic force microscope, and a ball-on-inclined

plane apparatus, the friction and wear characteristics of these three cases were obtained. Results suggested that the mixed PFPE has the highest shear rupture strength.

I20 Deformation & Failure Modes of a Nanofiber

S.Y. Ng[1], E.P.S. Tan[1], C.H. Sow[2] and C.T. Lim*,[1]
[1]*Division of Bioengineering & Department of Mechanical Engineering, NUS*
[2]*Department of Physics, NUS*
*E-mail: ctlim@nus.edu.sg

Biodegradable polymeric nanofibrous scaffolds have been widely used for tissue engineering. The stiffness of individual polymer nanofibers that make up the entire 3D scaffold not only determines the growth, motility and differentiation of cells, but also the structural integrity of the scaffold. Therefore, there is a need to study the nanomechanical properties of individual nanofibers. However, mechanical testing of a single nanofiber has not been widely performed due to its small size. Yet, such tests are important as the mechanical properties are found to vary significantly for nanofibers with diameters ranging from tens to hundreds of nanometers. In this study, the deformation and failure behaviors of polymer nanofibers of varying diameters undergoing stretch are investigated. Single nanofibers are stretched to predetermined strain levels that correspond to critical stages - namely linear elastic deformation, plastic yielding, strain hardening and failure. Any nanostructural rearrangement or changes within the nanofiber is observed at these critical stages. Results obtained can help us better understand the nanostructure-property relationship of polymer nanofibers that were previously not possible.

I21 Functional Nanohybrids and Mesoporous Thin Films

John Wang*, A.H. Yuwono and Zhang Yu
Department of Materials Science and Engineering, Faculty of Engineering, National University of Singapore Singapore 117576
*E-mail: msewangj@nus.edu.sg

A number of novel functional (electrical, optical and magnetic) properties have been demonstrated by mesoporous oxides and nanohybrids consisting of one or more nanocrystalline inorganic phases dispersed in a suitable polymeric matrix. Although several new synthesis routes have been attempted for fabrication of these nanostructured materials, there is often a lack of proper control in nanocrystallinity of the resulting mesoporous and nanohybrid structures, where the kinetics involved are restricted by the relatively low synthesis temperatures involved. To realize the well controlled mesoporous structures and nanohybrids of enhanced nanocrystallinity, we have devised surfactant and di-block polymer templatings, where the hydrophilic and hydrophobic structures are effectively used as the assembling blocks. In combination with an appropriate hydrothermal treatment in water vapor, we have successfully synthesized TiO_2-based mesporous and nanohybrid thin films with remarkably enhanced nanocrystallinity, where the rearrangement of flexible Ti-O-Ti bonds are promoted. In this talk, the wet-chemistry and several parameters involved in surfactant and di-block polymer templatings will be discussed for their effects on the resulting TiO_2-based mesoporous and nanohybrid thin films, as well as on the functional properties of these nanostructured materials.

I22 Dynamics of Colloidal Assembly Driven by an Alternating Electric Field

Liu Xiang Yang
Department of Physics, Faculty of Science, NUS
E-mail: phyliuxy@nus.edu.sg

The large and high quality colloidal crystals are playing an increasingly important role in the templating of photonic crystals, optical switching, drug delivery and biosensors. Here we demonstrate a charged colloidal particle assembling driven by alternating electric field. This system allows us to have direct imaging and in-situ observation on nucleation, in particular, pre-nucleation process which are explored in real space by the light microscope. By following their evolution, a set of important parameters of nucleation can be measured under different driving forces. The advantages of our system are direct visualization of the nucleation process for colloidal particle assembly and better control of the perfection of crystals based on the well-defined driving force. As far as we know, no quantitative control of the two-dimensional or three-dimensional (2D or 3D) colloidal crystallization has been performed from the view of nucleation and growth. We expect studies of this colloidal model system to contribute to our understanding of nucleation mechanism and growth for the high–quality colloidal crystals, which has the essential role in the various applications.

I23 Magnetic Thin Films as High Density Storage Media

Ding Jun
Department of Material Sciences and Engineering, National University of Singapore Singapore 119620
E-mail: msedingj@nus.edu.sg

Magnetic thin films with high coercivity and perpendicular anisotropy are interesting for the application as high density magnetic media. Recently, FePt is intensively investigated as high-density perpendicular recording media of the next generation. In our research, we have successfully fabricated high coercivity FePt thin films with a large perpendicular anisotropy and a low formation temperature. The effects of substrate, underlayer and doping have been investigated in order to obtain the high coercivity phase (L1) formed at a relatively low temperature.

The search for new magnetic thin film materials, we have achieved a coercivity as high as 12 kOe with a relatively large perpendicular anisotropy in Co-ferrite thin films. Because of the low price, excellent chemical stability and high mechanical strength, Co-ferrite thin films are promising for the application as high density magnetic recording media. In this presentation, the structure and magnetic properties of Co-ferrite will be reported. We have also studied the possible coercivity mechanisms. The presentation may include the magnetic properties of magnetic nanowires on AAO template and other magnetic thin

films which possess the potential as high density magnetic recording media.

I24 Direct Evidence for Anisotropic Strain Induced Shape Transition During Epitaxial Growth of Hexagonal Lattice FeGe on Ge(001)

Yong-Lim Foo*, Zhi Peng Li, Eng Soon Tok, Joyce Pei Ying Tan and Ming Lin
Institute of Materials Research and Engineering
*E-mail: yl-foo@imre.a-star.edu.sg

We observed epitaxial FeGe (hexagonal lattice) islands growth and shape transition on Ge(001) substrate at real time using an in-situ ultra-high vacuum transmission electron microscope. Islands are elongated due to anisotropic strain of 8.25% and 1.25% along their two orthogonal azimuths. Unlike previous reports, there is no shrinkage of island width during shape transition. Epitaxial strain is minimized by preferential growth of materials along azimuth of least mismatch, and this kinetic effect dominates over the increase in surface energy during wire formation.

I25 Deformation and Fracture Mechanism in Thermoset and Thermoplastic Nanoclay Composites

Chaobin He
Instittute of Materials Reserach and Engineering
3 Research Link, Singapore, 117602

Polymer/clay nanocomposites have been studied extensively as a new generation of polymeric materials. The nanocomposites often exhibit significantly improved Young's modulus, thermal stability and barrier performance. However, the effect of nanoclay on the fracture toughness is dependent on the nature of the matrix polymers. In thermosetting polymers such as epoxy, nanoclay can improve both the stiffness and toughness, whereas in thermoplastic polymers such as nylon6, the nanoclay usefully causes dramatic decrease of fracture toughness.

In this work, the deformation and fracture mechanisms of epoxy/clay and nylon6/clay nanocomposites have been studied by means of microscopic analysis and small angle X-ray scattering. It was found that, in epoxy/nanoclay systems, the formation of massive amounts of microcracks and the increase of the process zone are the major toughening mechanisms. Most of the microcracks initiated between clay layers, which developed within the tactoids and extended into the matrix as the strain increases. In nylon6/clay systems, most of the crazes initiated between clay and polymer matrix, which developed into cracks as the strain increases. The brittleness of the nylon6 nanocomposites can be attributed to their inability to generate high concentration of craze and micro-cracks at high clay loading, possible due to confinement effect.

I26 Synthesis and Characterization of SnO_2 Nanorods Thin Films as Gas Sensing Materials

O.K. Tan*, H. Huang, Y.C. Lee and M.S. Tse
Microelectronics Center, School of Electrical and Electronic Engineering,
Nanyang Technological University, 50 Nanyang Avenue, 639798, Singapore
*E-mail: eoktan@ntu.edu.sg (A/P O.K. Tan)

SnO_2 thin films have been deposited by rf inductively coupled plasma enhanced chemical vapor deposition (PECVD) using dibutyltin diacetate as precursor. The as-deposited SnO_2 thin films were post-treated in the inductively coupled plasma (ICP). After plasma treatment, uniform SnO_2 nanorods were grown on the SnO_2 thin films. The nanorods were formed by sputtering-redeposition mechanism. The effects of plasma treatment conditions on the morphologies of SnO_2 thin films were studied. The rf power and gaseous composition of the ICP plasma had great effects on growth of the SnO_2 nanorods from the SnO_2 thin films. The type of plasma was also very critical, and there were no nanorods grown on the SnO_2 thin films treated in capacitively coupled plasma. The SnO_2 nanorods thin films have also been successfully deposited by one-step PECVD and liquid injection PECVD. Due to the large surface-to-volume ratio and tiny grain size, the SnO_2 nanorods thin films showed much higher sensitivity, faster response and shorter recovery time compared to the as-deposited SnO_2 thin films with nanograins. Pd surface doping was used to modify the surface chemical state of the SnO_2 thin films. The selectivity to H_2 gas of the SnO_2 thin films was greatly enhanced by Pd surface doping.

I27 Synthesis of CdS Nanocrystals from [(2,2'-bipy)Cd(SC{O}R)$_2$] (R = Long Alkyl Group) by Self-Capping

Chang-Tong Yang, Zhihua Zhang, Wee Shong Chin and Jagadese J. Vittal*
Department of Chemistry, National University of Singapore, Singapore 117543
*E-mail: chmjjv@nus.edu.sg

Semiconductor nanomaterials have been extensively studied due to their special size dependent optical and electronic properties. However, control of the size and shape of nanomaterials is still challenging. The tunable band gap of nanoparticles finds potential applications in many areas such as light emitting diodes and photocatalysis. The single-source molecular precursor route for the preparation of high quality, monodispersed II-VI chalcogenide nanoparticles has proven to be an efficient approach. In this method several surfactants have been employed to passivate the nanocrystals by capping. Here we describe the synthesis of highly monodispersed CdS nanocrystals just by refluxing air stable single-source precursors [(2,2'-bipy)Cd(SC{O}R)$_2$] (R = long chain n-alkyl group, 2,2'-bipy = 2,2'bipyridyl) in toluene solution. The decomposed side products of the precursors serve as capping groups to stabilize the nanocrystals in solution. The XRD pattern of CdS sample indicates the formation of the cubic phase. The IR, XPS and NMR spectroscopy show that the capping agents are 2,2'-bipy and (RC{O})$_2$S from the precursor. The nanocrystals have been characterized further by electronic spectroscopy, photoluminescence, and transmission electron microscopy. The details will be presented during the talk.

I28 Analysis of Nanoindentation of Thin Film Structures

Zeng Kaiyang*,[1], Shen Lu[2] and Jiang Haiyan[3]
[1]*Department of Mechanical Engineering, NUS*
[2]*Institute of Materials Research and Engineering*
[3]*Department of Materials Science and Engineering, NUS*
*E-mail: mpezk@nus.edu.sg

This talk presents a methodology that can be used to determine the elastic modulus, hardness, yield strength and strain hardening exponent for thin metallic films from analyzing nano-indentation load (P) – penetration (h) curves. The method combines several analyses originally developed for bulk materials, including dimensional analysis; $P - h^2$ (load – penetration^2) analysis; $S - h$ (stiffness - displacement) analysis; $S^2 - P$ (stiffness^2 – load) analysis; and slope analysis. The key factors for this method are to determine the loading curvature ($K = P/h^2$), elastic modulus and contact stiffness *(S=dP/db)* for thin films in which the effects of substrate to the indentation measurement are minimum. It is found that by combining plots of $P - h$ (indentation load – displacement) curve; $P - h^2$ curve; $P - S$ curve, and $S^2 - P$ curve, one can readily identify substrate effects to the thin film properties measured by nanoindentation. Hence, this information is used together with the dimensionless functions, which were developed previously for bulk metallic materials, to determine the yield strength and strain hardening exponent for metallic thin films. This method has been applied to the nanoindentation of several thin film structures and has shown consistent results.

I29 Nanostructured Polymer Carriers for Drug/Gene Delivery

Yi-Yan Yang*, Yong Wang, Li-Shan Wang and Li-Hong Liu
Institute of Bioengineering and Nanotechnology
*E-mail: yyyang@ibn.a-star.edu.sg

Materials have played a very important role in the biomedical field. In particular, a number of biomaterials have been proposed based on natural and synthetic materials for drug delivery. However, the method of delivering drugs to specific cells and cell compartments remains a challenge. The aim of our study is to develop biocompatible polymer nanocarriers for transporting drugs/genes to specific tissues, thereby alleviating or eliminating the side effects associated with the use of conventional delivery systems and improving the efficacy of drug or gene therapy.

Two kinds of nanostructured polymer carriers have recently been developed in our laboratory to achieve this objective. One of the carriers is cationic core-shell nanoparticles self-assembled from biodegradable cationic amphiphilicopolymer. These cationic nanoparticles bind DNA strongly, and yield high luciferase and GFP expression levels in various cell lines, which is comparable to or higher than that induced by PEI (25 kDa, branched). Greater *in vivo* luciferase transfection efficiency was also achieved in mice bearing subcutaneous 4T1 tumors using these nanoparticles. The second canier is based on pH-induced temperature-sensitive polymer core-shell nanoparticles, the shell of which is conjugated with folate. It has been proven that these nanoparticles are able to transport anticancer drugs specifically to cancer cells, which overexpress folate receptor on the surface, and release the drug molecules intracellularly.

I30 Controlled Growth and Applications of Nanoscale Metal Oxide Materials

Sow Chorng Haur*, T. Yu[1], Y.W. Zhu[1], P. Chen[1], A.T.S. Wee[1], X.J. Xu[2], C.T. Lim[2], J.T.L. Thong[3] and Z.X. Shen[4]
[1]*Department of Physics, Blk S12, Faculty of Science, National University of Singapore, 2 Science Drive 3, Singapore 117542;*
[2]*Department of Mechanical Engineering, National University of Singapore, Blk E3A, 9 Engineering Drive 1, Singapore 117576;*
[3]*Department of Electrical and Computer Engineering, National University of Singapore, Blk E4, 4 Engineering Drive 3, Singapore 117576;*
[4]*Division of Physics and Applied Physics, Nanyang Technological University, 1 Nanyang Walk, Block 5, Singapore 637616*
*E-mail: physowch@nus.edu.sg

Nanoscale materials have attracted great interests from researchers. Two-dimensional nanostructures such as nanowalls,[1] nanosheets,[2] and nanojunctions or networks [3] are an important category of nanostructured materials with great potential as important components for nanoscale devices with various interesting functions. Thus, in the past decade, many techniques have been developed for the synthesis of such nanostructured materials. Some examples of these techniques include (i) chemical vapor deposition, i.e. vapor-liquid-solid growth,[4] vapor-solid growth,[5] oxide-assisted growth,[6] (ii) carbothermal synthesis,[7] and (iii) ethylene glycol-mediated synthesis,[8] In addition to the above mentioned techniques, a wide variety of nanoscale metal oxide materials with fascinating morphologies can be synthesized by heating pure metallic foils or wires in appropriate controlled atmospheres.[9,10] Recently we have obtained very encouraging results in the development of a very simple technique. Simply heating metal foil or metal-coated substrates in ambient on a hotplate allows us to controllably fabricate a wide variety of nanoscale metal oxide (Copper Oxide CuO[11], Cobalt Oxide Co_3O_4[12] and Iron Oxide Fe_3O_4[13] with fascinating morphologies. Such morphologies include CuO nanowires, Co_3O_4 nanowalls, Fe_3O_4 nanoflakes. Similar heating of a wide variety of substrates that were coated with metal films resulted in nanomaterials synthesized directly on the heated substrates[13,14]. Many of these nanoscale metal oxides are efficient field emitters[10–14] rendering them potentially attractive materials for possible applications. In this report, we will introduce details of the hotplate technique and discuss the results of characterizations of these nanoscale materials and present some of the potential applications of these nanoscale meal oxide materials.

References

[1] Mandelis A. and Christofides C. 1993. Physics, Chemistry and Technology of Solid State Gas Sensors Devices. New York: Wiley-Interscience.
[2] Moseley P.T. 1992. Materials selection for semiconductor gas sensors. Sensors Actuators B 6:149–56.
[3] Henrich V.E. and Cox P.A. 1996. Surface Science of Metal Oxides. Cambridge/New York: Cambridge.

[4] Pan Z.W., Dai Z.R. and Wang Z.L., Appl. Phys. Lett. 2002, 80, 309.
[5] Pan Z.W., Dai Z.R. and Wang Z.L., Science 2001, 9, 1947.
[6] Hu J.Q., Ma X.L., Xie Z.Y., Wong N.B., Lee C.S. and Lee S.T., Chem. Phys. Lett. 2001, 344, 97.
[7] Gundiah G., Deepak F.L., Govindaraj A. and Rao C.N.R., Topics in Catalysis 2003, 24, 137.
[8] Jiang X.C., Wang Y.L., Herricks T. and Xia Y.N., J. Mater. Chem. 2004, 14, 695.
[9] Dang H.Y., Wang J. and Fan S.S., Nanotechnology 2003, 14, 738.
[10] Jiang X.C., Herricks T., Xia Y.N., Nano. Lett. 2002, 2, 1333.
[11] Zhu Y.W., Yu T., Cheong F.C., Xui X.J., Lim C.T., Tan V.B.C., Thong J.T.L. and Sow C.H. Nanotechnology JAN 2005 **16** 1 88–92.
[12] Yu T., Zhu Y.W., Xu X.J., Shen Z., Chen P., Lim C.T., Thong J.T.L., Sow C.H., Advanced Materials 2005 17, 1595.
[13] Ting Yu, Yanwu Zhu, Xiaojing Xu, Kuan-Song Yeong, Zexiang Shen, Ping Chen, Chwee-Teck Lim, John Thiam-Leong Thong, Chorng-Haur Sow, Small in press.
[14] Y.W. Zhu, T. Yu, X.J. Xu, Y.J. Liu, C.T. Lim, A.T.S. Wee, J.T. L. Thong, C.H. Sow, Applied Physics Letters 87, 023103 (2005).

I31 Advanced CMOS Front-End Technologies for Sub-Tenth Nanometer Technology Node

Sungjoo Lee
SNDL (Silicon Nano Device Lab), ECE Dept, NUS
E-mail: elelsj@nus.edu.sg

The recent fast pace of MOSFET scaling is accelerating the introduction of new technologies to extend CMOS beyond the sub tenth nanometer technology node. Technologies addressing CMOS scaling include both new materials and advanced MOSFET structures. In order to overcome the intrinsic problems of conventional Si-based CMOS devices, the non-classical CMOS devices using new transistor structural designs and new materials have intensively been studied by the industries and academic communities. New transistor structures seek to improve the electrostatics of the MOSFET, providing a platform for the introduction of new materials and accommodating the integration needs of new materials. New materials include the high-K dielectric and electrode materials used in the gate stack, the conducting channel that have improved carrier transport properties, as well as new materials used in the source/drain regions with reduced resistance and carrier injection properties. The combination of new device structure and new materials enables new operating principles that may provide new behavior and functionality beyond the constraints of conventional CMOS. The SNDL, since it was established in 2000, has been working on the development of scientific and technological bases for future CMOS Front-End technologies. In this talk, the recent technological achievements of SNDL will be presented.

I32 Different Functional Nanostructures Formed Selectively on Inert Substrates

Wang Xue-sen
Department of Physics and NUS Nanoscience & Nanotechnology Initiative
National University of Singapore, 2 Science Drive 3, Singapore 117542
E-mail: phywxs@nus.edu.sg

Low-dimensional semimetals (e.g. Bi, Sb) are excellent thermoelectric materials, whereas MnSb is ferromagnetic material with spintronic application potential. We investigated the self-assembly of Sb, Bi and MnSb nanostructures on highly-oriented pyrolytic graphite (HOPG) in simple physical vapor deposition using *in situ* scanning tunneling microscopy (STM). When antimony (mostly Sb_4) is deposited on HOPG, STM images reveal that three-dimension (3D) spheres, quasi-2D films and 1D nanowires are formed. The lattice parameters of the 2D and 3D structures are close to those of α-Sb bulk. The Sb NWs appear to start in a compressed state, and with strain relaxation occurring in later growth stages. The formation of compressed-state Sb NWs is attributed to an enormous Laplace pressure induced by surface tension in a nanostructure. This provides an example to show the general trend in which surface/interface and related nanomechanical properties play decisive roles in the synthesis and the characteristics of nanostructures. Certain control of the dimensionality of Sb nanostructures self-assembled on HOPG has been accomplished. At room temperature and a low Sb flux, 3D islands grow exclusively, whereas at 100°C and a high flux, 2D and 1D structures are dominant. This is explained in terms of different activation energies of Sb_4 diffusion and conversion to chemisorption or dissociation state on HOPG. For Bi on HOPG, since the deposition flux consists of mostly Bi_2 and Bi_1, only 1D and 2D Bi nanostructures are observed. MnSb nanostructures synthesized on HOPG exhibited ferromagnetism at RT. For real device applications, we have also been exploring controlled growth of these functional nanomaterials on Si-based oxide and nitride surfaces.

I33 Materials Design from First Principles

Feng Yuan Ping
Department of Physics,
National University of Singapore
E-mail: hyfyp@nus.edu.sg

First principles methods based on density functional theory are used to investigate fundamental physical properties of materials for advanced technology, and to design new materials. The first principles methods are powerful in predicting properties of new materials and in design of new materials because they do not require experimental input and all physical quantities are computed self-consistently by solving quantum mechanical equations. Some of our recent work in this area will be discussed.

First-principles total energy calculations were carried out on hypothetical C_3P_4 and other group IV-V compounds, to investigate their possible structures and properties. Strikingly different structures and properties were predicted for the group IV-phosphides and nitrides. Pseudocubic-C_3P_4, in particular, was found to exhibits exceptional mechanical stability and interesting properties.

Functionalization of carbon and other nanotubes were studied using *ab initio* methods. It was found that the properties of the nanotubes can be significantly modified by doping the nanotubes with different atoms. For example, carbon substitution for either boron or nitrogen atom in the BN nanotubes induces spontaneous magnetization.

Based on first principles studies, we proposed a method for chemical tuning of metal effective work function or Schottky barrier heights (SBHs) for the metal gate-high-k oxide interface. Based on our calculation for Ni-ZrO_2 interfaces, a tunability as wide as 2.8 eV can be achieved for the SBHs, by including a heterovalent metal interlayer between the metal gate and the high-k oxide, which far exceeds the required tuning range. In addition, there exists a simple linear relationship between the effective work function and electronegativity of interlayer metal. The work provides a practical way of tuning the metal work function to satisfy the engineering requirement for the metal gate technology.

I34 Frontier Research Opportunities at the Singapore Synchrotron Light Source

H.O. Moser*, M. Bahou, B.D.F. Casse, E.P. Chew, M. Cholewa, C.Z. Diao, S.X.D. Ding, P.D. Gu, S.P. Heussler, L.K. Jian, J.R. Kong, Z.J. Li, Z.W. Li, Miao Hua, B.T. Saw, Sharain bin Mahmood, Li Wen, J. Wong, Ping Yang, X.J. Yu, X.Y. Gao[1], Tao Liu[1], A.T.S. Wee[1] and W.S. Sim[2]
Singapore Synchrotron Light Source/NUS
[1] *Physics Department/NUS*
[2] *Chemistry Department/NUS*
*E-mail: moser@nus.edu.sg

SSLS is providing high flux synchrotron radiation covering a spectral range from hard X-rays ($\approx$ 15 keV) to the far infrared (10 cm^{-1}). Operated permanently since November 2003, SSLS has served more than 230 users.

Methods available include

- Micro/nanofabrication based on the LIGA process at the LiMiNT facility,
- White light phase contrast imaging and tomography at PCIT,
- Soft X-ray spectroscopy for studying the electronic and magnetic properties of surfaces, interfaces, and nanostructured samples at SINS,
- Infrared spectro/microscopy at ISMI, and
- X-ray diffraction, reflectometry, absorption and fluorescence spectroscopy at XDD.

R&D work at SSLS comprises micro/nanofabrication, the analytical characterization of materials and processes, and the development of new systems for 4th generation synchrotron light sources.

Research highlights include the fabrication and characterization of the first THz electromagnetic metamaterials at LiMiNT and ISMI, the non-invasive in situ characterization of membrane filtration processes, the elucidation of the structure of carbon nanomesh at the surface of SiC, as well as the thickness, roughness, and density of highly porous polyaniline nanofiber films, the structure of $La_7Na_3(SiO_4)_6$ powders using anomalous dispersion, and the determination of the local structure around the Cl atom in compounds by means of low energy XAFS at XDD.

I35 Scanning Probe Microscopy for Materials Characterisation

Sean O'Shea
Institute of Materials Research and Engineering (IMRE)
E-mail: s-oshea@imre.a-star.edu.sg

Scanning probe microscopy Scanning Probe Microscopy (SPM) is a class of instruments for the characterization of surfaces with nanometer scale resolution. These instruments, most notably Scanning Tunneling Microscopy (STM) and Atomic Force Microscopy (AFM) allow materials to be characterized down to the atomic level. I will outline some of our activity in this area at IMRE and in particular will highlight our results on organic molecular films adsorbed at interfaces. Two areas will be discussed, as described below.

(i) Studying the electrical properties of molecular films. I will show data of adsorbed molecules on surfaces and our attempts to characterize the local electrical properties of the adsorbed molecules using STM and the method of BEEM (Ballistic Electron Emission Microscopy). This problem is of interest for polymer and molecular electronics.
(ii) Studying the mechanical properties of confined liquids. I will discuss the use of AFM in liquid environments to image and measure the physical properties of simple organic molecules adsorbed on solid surfaces. The basic measurement is the interaction force as a function of tip-sample distance i.e. a "force curve". The force curve allows study of nanometer scale adhesion, elasticity, friction and stiffness. One finds that even for liquid molecules squeezed between two surfaces with nanoscale volume, the liquid may order near the surface into discrete "solid-like" layers.

I36 Opening New Frontiers in Materials Processing Using Microwaves

Manoj Gupta and Wong Wai Leong Eugene
Department of Mechanical Engineering, NUS, Singapore 117576

The interrelationship between processing, microstructure, properties and performance is well known in the field of materials science. For the same material different properties can be realized by changing the processing route/methodology.

Amongst various processing techniques, microwave based techniques are relatively new, cost-effective and environment friendly. The use of microwaves in synthesizing polymers and ceramics based materials has been established for a few decades now, however, there are extremely limited research activities related to the synthesis of metal based monolithic, reinforced and nanomaterials.

In view of the advantages associated with microwaves, research activities were initiated in the year 2004 in Materials Laboratory of Department of Mechanical Engineering in NUS to use microwaves to synthesize metal based materials. Studies were targeted on: a) melting of metals/alloys such as aluminum, magnesium and lead free solders and b) sintering of metals, alloys, composites and nanomaterials. Target metals/alloys were chosen for applications in weight critical and electronic applications. Results obtained convincingly showed that metals, alloys and electronic solders can be conveniently melted using a domestic microwave oven and similar or enhanced mechanical properties can be realized from the microwave

processed materials with an inherent energy savings of about 75–80%.

I37 Transferring Know-How from Nature's Biomaterial Synthesis Machinery to Materials Research

Suresh Valiyaveettil
Department of Chemistry, NUS-Nanoscience and Nanotechnology Initiative,
3 Science Drive 3, National University of Singapore, Singapore - 117543.
E-mail: chmsv@nus.edu.sg

Design and synthesis of novel supramolecular architectures is an interesting area of research in the last two decades. Intermolecular interactions assisted self-assembly of small building blocks play an important role in obtaining the desired shape and function of the supramolecular architectures. Such approaches have been used by Nature to build interesting functional materials. Learning the fundamentals of this fascinating bioprocesses and modifying it to fit the synthesis of complex synthetic materials would provide new avenues for developing multifunctional materials. A combination of covalent synthesis with the self-assembly assisted formation of well-defined architectures (noncovalent synthesis) is used in our laboratory towards the design and synthesis of material synthesis. This presentation will focus on our recent efforts on design and synthesis of simple molecular building blocks for investigation of the self-assembly and our initial findings on the mechanism of hard tissue formation in Nature through the self-assembly processes. The combination of synthetic and biomimetic approaches allow us to develop interesting bionanomaterials in laboratory environment.

I38 Simulation of Adatom Clustering on a Stepped Suface and the Effect of Surface Elasticity on the Interaction Between Suface and Inclusion

Shou-Wen Yu*, Ji-Qiao Zhang, Gan-Yun Huang and Xi-Qiao Feng
Department of Engineering Mechanics, FML, Ministry of Education, Tsinghua University, Beijing 100084, China
*E-mail: yusw@mail.tsinghua.edu.cn.

Surface processes on a surface have attracted an increasingly intensive attention due to their extensive applications in the development of nano-structured materials and devices. Many surface processes are associated with adatoms and their evolutionary relocation. Based on Kukta's adatom model, the evolution of adatoms adsorbed on a surface is studied in the present paper. Both the effects of elastic interaction and van der waals interaction have been considered. It is found that the van der Waals interaction plays a more significant role in the clustering process of adatoms on a stepped surface. The adatoms are much easier to cluster on a surface with defects (e.g., steps) than on a smooth surface. By modeling the adatoms as point force dipoles, the interaction between adatoms and a subsurface inclusion is considered. Results show that adatoms tend to stay at the surface above the inclusion and different shape, size and eigen fields of the inclusion would induce various evolution patterns of the adatoms due to the interaction between themselves and that arises from the inclusion.

I39 InP Based MEMS for Tunable Photonic Devices

A. Ramam*, Vicknesh Shanmugan and J. Arokiaraj
IMRE, 3 Research Link, Singapore 117602
*E-mail: ram-akki@imre.a-star.edu.sg

This research work combines novel movable structures based on MEMS understanding, with InP photonic components for tuning and coupling applications in the 1.3/1.5 um wavelength domain. The intention is to combine a movable membrane activated by electrostatic (E-S) force in a Fabry Perot (F-P) cavity configuration with a photodetector (PD) device. Our attempt has been to combine the tunable membrane and the PD device onto an InP substrate in a monolithic manner. A membrane structure made out of InP epilayer, and activated by E-S force basically serves as an optical filter. An improvised wet releasing technique has been established to release 1 um thick, InP membrane structures, with InGaAs as sacrificial layer. The fabricated electrostatic actuators were characterized under DC and quasi static conditions, with an observed deflection of > 300 nm and a pull in voltage of 7 volts. The technique of wafer bonding InP to InP and InP to Si samples is established by optimizing the surface condition of the samples and the wafer bonding parameters. Successful bonds were achieved at low temperatures ($\sim 250°C$) and TEM analysis showed narrow interface (< 10 nm) between the two materials. Using waveguide concepts and wafer bonding approach a novel cross coupler and OADM device has been conceived.

I40 Combination of Self Assembly with Lithography for Fabrication of 3D Photonic Crystal Devices

George X.S. Zhao*[,1] Qingfeng Yan[1] and S.J. Chua[2,3]
[1] *Department of Chemical and Biomolecular Engineering, National University of Singapore*
[2] *Department of Electrical and Computer Engineering, National University of Singapore*
[3] *Institute of Materials Research and Engineering (IMRE), Singapore*
*E-mail: chezxs@nus.edu.sg

Many photonic devices require the exact placement of well-defined defects in the interior of a photonic crystal. Thus, defect engineering has been a great research interest. While traditional "top-down" lithography techniques have been demonstrated to be workable for fabricating photonic crystals with defects, they are time-consuming, expensive processes, and limited to particular materials. The self-assembly method, which utilizes self-assembled colloidal microspheres as template, is simple and cost-effective. However, the self assembly method alone cannot allow one to fabricate defects. This presentation discusses how to combine lithography with self assembly to embed various defects (point, line and planar defects) in three-dimensional photonic crystals.

I41 Mathematical Modeling of Temperature Sensitive Hydrogels

Erik Birgersson*, Hua Li and Chun Lu
Institute of High Performance Computing
1 Science Park Road, #01-01 The Capricorn
Singapore Science Park II, Singapore 117528
*E-mail: erik@IHPC.a-star.edu.sg

Recent years has seen a wide variety of applications of hydrogels due to one or several unique properties: ability to sense and react to specific changes in its environment; reversible volume changes of up to a thousand-fold or more; high biostability and biocompatibility. Some of the pharmaceutical and biological applications include drug delivery devices, tissue engineering, and artificial muscles.

The properties of hydrogels originate from their structure, comprising three-dimensional networks of cross-linked polymers, penetrating solvents and ions if charged. In its dry state, the hydrogel behaves as a solid as opposed to its swollen state, where the absorbed solvent lends it more liquid-like properties. Stimuli-responsive hydrogels can sense and respond to specific perturbations in its environment, such as temperature and pH. In order to gain an insight into the response of temperature-sensitive hydrogels, a mathematical model has been derived, non-dimensionalized, validated experimentally and analyzed. It considers conservation of momentum, energy and mass for the solid and polymer phase in both Lagrangian and Eulerian coordinates, and allows for a study of the deformation behavior after step changes in temperature as well as for temperature gradients. Characteristics such as stresses, osmotic pressures, deformations are studied both numerically and predicted via a scale analysis.

I42 From Optical MEMS to Photonic NEMS Devices

Ai-Qun Liu
School of Electrical & Electronic Engineering
Nanyang Technological University, 50 Nanyang Avenue
Singapore 639798
E-mail: eaqliu@ntu.edu.sg

In the past twenty years, the application of Microelectromechanical Systems (MEMS) technology to the fabrication of mechanical devices greatly stimulated extensive research in semi-conductor microsensors and microactuators. MEMS technologies have the advantage of batch processing to address the manufacturing and performance requirements of the sensor industry. The versatility of semiconductor materials and the miniaturization of VLSI patterning techniques promise new sensors with better capabilities and improved performance-to-cost ratio over those of conventionally machined devices.

This talk will introduce design and manufacturing of MEMS technologies from the viewpoint of optics and photonics physics. MEMS research at Nanyang Technological University will be presented. Examples and applications in different subject areas related to fiber optics communication will be described. These include design, materials, and optical switch, variable optical attenuator (VOA) and tunable laser. Specific devices on photonics bandgap (PBG) coupling, integrated filter and biophotonics integrated chip for cells shorting applications will also be discussed.

Various design and manufacturing issues will be introduced to explain the make of these devices using surface-micromachining and bulk-micromachining. Current research programs on PBG and biophotonics medical device will be briefed via some preliminary results in the areas of MEMS. This talk will be concluded with the future trends and research directions in MEMS from the viewpoint of physicists and electronic engineers.

Dr Ai-Qun Liu (A.Q. Liu) received his PhD degree in Applied Mechanics from National University of Singapore (NUS) in 1994. His MSc degree was in Applied Physics, and BEng degree was in Mechanical Engineering from Xi'an Jiaotong University. Currently, he is an Associate Professor at the Division of Microelectronics, School of Electrical & Electronic Engineering, Nanyang Technological University (NTU). He is also appointed as an *Associate Editor* for the IEEE Sensor Journal. Dr Liu's major research interests are MEMS design, simulation, fabrication and experiment.

I43 On the Design and Material Challenges in the Development of Interconnections for Ultra-Fine-Pitch Wafer Level Packages

Andrew A.O. Tay
Nano/Microsystems Integration Lab, Department of Mechanical Engineering,
National University of Singapore, Singapore-117576.
E-mail: mpetayao@nus.edu.sg

The tremendous demand for electronic products with higher processing speed, smaller, thinner and portable features has led the industry to move towards high performance devices with increased functionality and high interconnect density at very fine pitches. At the integrated circuit level, feature size is already below 100 nm making it truly nano. However, the sizes of interconnections between the chip and the printed circuit board are still comparatively large with the latest pitches at 150mm. In order to fully capitalize on the nano features of the IC, the pitches of chip-to-board interconnections have to be correspondingly reduced. However, this has great design and material challenges.

This paper describes the challenges of designing chip-to-board interconnections for ultra-fine-pitch wafer level packages. Several interconnection designs for 100 mm pitch interconnections together with some reliability data will be presented. For the first time in the world, we have successfully developed wafer level packages at 100mm pitch which meets the standard reliability requirements of surviving 1000 temperature cycles. Several solutions for pitches down to 20mm pitches will also be presented including those involving use of nanostructured materials. Some studies on enhancing properties of solders employed in joining processes in electronics packaging using nanomaterials such as carbon nanotubes and nanoparticles of nickel and molybdenum will also be described and results presented.

Symposium Abstracts

I1 Nano-Mechanics of Solid Surface Suspension and Imprinting with Solid Surface Nano-Structures

Kyung-Suk Kim
Division of Engineering, Brown University
Providence, RI 02912
E-mail: kim@engin.brown.edu

S*ome* analytical results on nano-meter-scale solid interface deformation are presented, based on experimental observations associated with solid surface suspension and imprinting caused by high grafting density contacts and molecular interactions at the interface. Carbon nano-tube arrays of high grafting density, greater than hundred million arrays per square millimeters, are used to study nano-scale contact suspension of plastically deforming gold and aluminum surfaces, and imprintability of high density nano-scale contacts. The imprintablity and stress induced chemical reaction are found to cause high friction resistance at the nano-meter-scale contact friction. Lateral force microscopy using a metal-coated micro-ball tip and nano-indentation with carbon nano-tube arrays are employed for the experimental investigation, and various atomistic simulations are used to model the nano-scale deformation phenomena.

I2 Stamp Collapse in Soft Lithography

Y. Huang
Department of Mechanical and Industrial Engineering, University of Illinois at Urbana-Champaign, Urbana, IL 61801, USA
E-mail: Huang9@uiuc.edu

We have studied the so-called roof collapse in soft lithography. Roof collapse is due to the adhesion between the PDMS stamp and substrate, and it may affect the quality of soft lithography. Our analysis accounts for the interactions of multiple punches and the effect of elastic mismatch between the PDMS stamp and substrate. A scaling law among the stamp modulus, punch height and spacing, and work of adhesion between the stamp and substrate is established. Such a scaling law leads to a simple criterion against the unwanted roof collapse. The present study agrees well with the experimental data.

I3 Nanomechanics of Macroelectronics

Zhigang Suo
Division of Engineering and Applied Sciences, Harvard University
E-mail: suo@deas.harvard.edu

For half a century, the technology of integrated circuits has been advancing by miniaturization. While the trend to *miniaturize features* will continue in the field of microelectronics, a new trend to *enlarge systems* is gaining momentum in the nascent field known as macroelectronics. Macroelectronics will be a platform for many technologies, such as flexible displays, medical imaging systems, and thin-film solar cells. The widespread use of the macroelectronic products will depend on their low costs and ruggedness, attributes that will come from new material choices and new manufacturing processes. For example, thin-film devices on thin polymer substrates lend themselves to roll-to-roll fabrication, and impart flexibility to the products. These large structures will have diverse architectures, hybrid materials, and small features; their mechanical behavior during manufacturing and use poses significant challenges to their development. This talk describes our ongoing work in the mechanics of macroelectronics, with emphasis on hybrid organic/inorganic structures of nanoscale features. More information is available at www.deas.harvard.edu/suo.

I4 Mechanics and Reliability of Low-k Dielectric and Copper Interconnects

X.H. Liu*, T.M. Shaw, M.W. Lane and E.G. Liniger
IBM TJ Watson Research Center
*E-mail: xhliu@us.ibm.com

To enhance chip performance and reduce power the microelectronics industry has been decreasing the resistance and capacitance constant in wiring the microprocessors. The wiring resistance has been reduced by replacing subtractive aluminum by damascene copper with improved reliability. However, when moving from oxide to low-k material the low dielectric constant is achieved at the expense of weak thermal mechanical properties, resulting in reliability challenges in copper/low-k integration and chip packaging. The modulus, hardness and fracture toughness of low-k material are lower than oxide. Therefore a tensile stress in a chip with low-k/copper interconnects can cause cracking and delamination. In this talk we will present the modeling to understand the effects of copper pattern on low-k dielectric cracking and the experiment to verify the model. A predictive tool to evaluate mechanical stability during copper/low-k integration has been developed to guide low-k material optimization and chip design.

I5 Effect of Surface Anisotropy on the Formation and Evolution of Heteroepitaxial Islands

Yong-Wei Zhang
Department of Materials Science and Engineering, National University of Singapore, 119260
E-mail: msezyw@nus.edu.sg

The self-assembled formation of three-dimensional heteroepitaxial island growth has been investigated by using a three-dimensional kinetic model. In the formulation, the surface evolution is induced by surface diffusion, which is in turn driven by the gradient of surface chemical potential. Surface condensation is assumed to depend on the difference between the surface chemical potential and the chemical potential of the vapor phase. The surface chemical potential includes elastic energy and surface energy. The effects of elastic anisotropy and surface energy anisotropy on the formation and evolution of heteroepitaxial islands have been studied in details. The simulations reveal that the uniformity, regularity, shapes and sizes of the self-assembled quantum dots strongly depend on the growth rate, elastic anisotropy, and surface energy

anisotropy. It is shown that calculations considering surface energy anisotropy and elastic anisotropy reproduce many features of experimental results, and demonstrate the significance of their influence on island formation and self-assembly in epitaxial growth.

I6 Dissolution Driven Crack Growth

Per Ståhle*[1,3], Andrey Jivkov[2] and Christina Bjerkén[3]
[1]*Lund University,* [2]*The University of Manchester and* [3]*Malmö University*
*E-mail: per.stahle@ts.mah.se

During corrosive dissolution of metal ions from a body surface, an oxide compound is produced. This compound forms a protective film that reduces the dissolution rate. When a few nanometres of depth is dissolved the dissolution rate becomes insignificant. However, repeated loading will damage the protective film with continued dissolution as a result. Below a threshold strain the film is believed to remain intact.

Under such synergetic action of corrosive processes and mechanical load an initially flat surface form irregularities and pits. The ratio between the threshold strain and the remotely applied strain is shown to control the shape of the pits. For small applied loads blunt cracks are formed. The model simulates how dissolution forms a pit that grows to become a crack in a single continuous process. The crack growth rate and the crack path are determined by the dissolution of material from the blunt crack tip. A crack growth criterion is not needed. For small loads the crack growth rate becomes independent of the applied load. Increasing load leads repeatedly to crack branching. The simulated cracks are observed to follow a near tip mode I path. Excessive branching follows the penetration of a bimaterial interface.

I7 A Mechanism-Based Approach to Predict Ductile Crack Growth in Metallic Alloys

Xiaosheng Gao* and Jinkook Kim
Department of Mechanical Engineering, The University of Akron, Akron, OH 44325, U.S.A.
*E-mail: xgao@uakron.edu

Ductile fracture in metallic alloys is a process of void nucleation, growth and coalescence. But due to sizeable difference between the characteristic length scales involved in the material failure process and the dimensions of the actual structural component, it is impractical to model every void in detail in structure failure analysis, especially for situations involving extensive crack propagation. For this reason, various forms of porous material models have been developed to describe void growth and the associated macroscopic softening during the fracture process. To simulate crack formation and propagation, a criterion for void coalescence is also needed. In this study, void coalescence is regarded as the result of localization of plastic flow between enlarged voids and the criterion for onset of coalescence is obtained in terms of the macroscopic equivalent strain (E_c) as a function of the macroscopic stress triaxiality ratio and Lode angle of the representative material volume. As an application, a numerical procedure is proposed to predict ductile crack growth in thin panels of a 2024-T3 aluminum alloy. Here the Gologanu-Leblond-Devaux porous plasticity model is used to describe the void growth process and the expression for E_c is calibrated using experimental data. The calibrated computational model is then applied to predict crack extension in fracture specimens having various initial crack configurations. The numerical predictions show very good agreement with experimental measurements.

I8 Analytical and Computational Modeling of Crack Initiation and Growth in High Temperature Materials

Noel O'Dowd* and Catrin Davies
Imperial College London
*E-mail: n.odowd@imperial.ac.uk

Creep crack initiation (CCI) in isotropic materials at high temperature is studied. Previous models have assumed that CCI occurs under a predominately steady state stress distribution. In this work methods are developed to predict the time for creep crack initiation (CCI) from a stationary sharp crack tip under conditions of small scale yield or widespread plasticity conditions on initial loading. At high temperatures the material is assumed to follow power law creep behavior. A multiaxial creep ductility model is introduced and failure is considered to occur at a material point when the accumulated equivalent creep strain reaches the multiaxial creep ductility. In this work the effects of creep strain accumulation during stress redistribution is taken into account and the time to crack initiation prediction from the analytical crack tip fields. At short times the stress fields are assumed to be dominated by J or K and at long times by the creep parameter C^*. Studies have been carried out using material properties representative of Type 316H stainless steel at 550°C. The predictions are compared to the results from 2D plane strain finite element (FE) analysis of a compact tension specimen and from experimental data for 316H stainless steel.

I9 Shear Band Propagation from a Crack Tip Subjected to Mode II Shear Wave Loading

Zhizhou Zhang and Rodney J. Clifton*
Brown University
*E-mail: javascript:press_email('clifton@engin.brown.edu')

Results are reported for pressure-shear plate impact experiments on pre-cracked 4340 VAR steel plates, with tempered martensitic microstructures, subjected to Mode II loading. Experiments show the propagation of a shear band ahead of the main crack. Simulations show good agreement between computed and recorded normal and transverse velocity-time profiles at the rear surface of the target. Introduction of a thermal-visco-plastic power law model, including a strain-failure model, leads to shear-band like features. Simulations using ABAQUS/Explicit include heat generation due to plastic working, and heat conduction. The predicted speed of propagation of the tip of the band is found to be substantially less than that corresponding to the measured extension of the shear band. Adjustments of parameters of the power-law plasticity model have little effect on the overall length of the band. Possible reasons for differences between predicted

and measured shear band speeds are discussed. Reduced shearing resistance in the rear part of the shear band and the possibility of a more unstable shear band formation mechanism are viewed as the most likely explanations for the relatively long shear bands observed.

I10 A Micromechanical and Experimental Study of Rupture Mechanisms in Mixed Mode Fracture

Jonas Faleskog* and Imad Barsoum
Deptartment of Solid Mechanics,
Royal Institute of Technology, SE-100 44 Stockholm, Sweden
*E-mail: jonasf@hallf.kth.se

Under general loading conditions ductile tearing in porous solids may involve several co-operating or even competing fracture mechanisms leading to crack growth. In the opening loading mode (mode I) high stress triaxiality promotes void growth and rupture occurs by link-up of voids of various sizes through necking of inter-void ligaments until impingement. In the shear loading mode (mode II/III) voids experience limited growth due to low stress triaxiality and final link-up between voids occurs through shear localization of plastic strain in the ligaments between voids.

This study focuses on the conditions that govern the transition between the two different link-up mechanisms associated with high and low stress triaxiality, respectively. A micro mechanical model is used, where It is assumed that the ductile rupture process is localized into a well defined planar layer. The model consists of an array of equally sized cells, each containing a spherical void. The array of cells is subjected to a combination of a tensile stress and shear stress with a superimposed hydrostatic pressure. The localized deformation characterizing both failure modes fits well into the general framework introduced by Rudnicki and Rice (1975) for plastic localization into a planar band, acting as a precursor to rupture. The kinematical conditions for the deformation across the band are utilized to analyze the transition between the two failure modes. The deformation gradient is homogeneous outside the band, and varies in a continuous manner with the position across the band. This model facilitates localization into a symmetric mode, a shear mode or a combination of both modes.

The transition between the two modes of failure was also experimentally studied by use of a double notched tube specimen. The tube was subjected to a combination of tension and torsion applied at a fixed ratio. By changing the ratio the stress triaxiality in the notched region could be controlled. Tests were carried out for a range of ratios of interest for mixed mode fracture.

I11 Analyses of Fatigue Crack Growth by Crack-Tip Blunting and Re-Sharpening

Viggo Tvergaard
Department of Mechanical Engineering, Solid Mechanics Technical University of Denmark, DK-2800 Kgs. Lyngby, Denmark
E-mail: viggo@mek.dtu.dk

Crack-tip blunting under tensile loads and re-sharpening of the crack-tip during unloading is one of the basic mechanisms for fatigue crack growth in ductile metals. This model gives part of the explanation for crack growth under cyclic loading, but does not account for other important crack growth mechanisms, such as effects of corrosion, debris, damage evolution, etc.

Detailed numerical studies of crack-tip blunting under cyclic loading have been carried out in the last few years, using finite strain plasticity to model the large deformations around the crack-tip, and it has been found that the purely ductile growth mechanism can fit into the Paris power law. However, such analyses are limited to the first two or three full load cycles, as very strong mesh distortion occurs in front of the crack-tip. The numerical model has been extended by incorporating remeshing techniques, and thus crack growth by the blunting mechanism has been simulated through several hundred load cycles. The method has been used to study the effect of an overload or of compressive underloads, and some of these results will be briefly reviewed. A recent publication has shown folding of the crack surface in compression, leading to striations. The influence of mesh refinement is used to study the possibility of this type of behaviour within the present method.

I12 Heating and Weakening of Faults in Earthquake Slip

James R. Rice
Harvard University
E-mail: rice@esag.harvard.edu

What physical processes determine how a fault zone weakens during earthquake slip? Field observations of mature faults, the focus here, suggest that slip in individual events occurs primarily within a thin shear zone, < 1–5 mm, within a finely granulated, ultracataclastic fault core. Relevant weakening processes in large crustal events are therefore likely to be driven by shear heating. It is suggested here that they involve (1) Thermal pressurization of pore fluid, and (2) Flash heating at highly stressed frictional micro-contacts, although at large enough slip, macroscopic melting and, in silica-rich lithologies, gel formation may be important too. Theoretical modeling of these mechanisms is constrained with lab-determined hydrologic and poroelastic properties of fault core material and high-speed friction studies. A testable prediction is of the shear fracture energies that would be implied if actual earthquake ruptures were controlled by those mechanisms. Seismic data has been compiled on the fracture energy of crustal events, including its variation with slip in an event. That data is plausibly described by the theoretical predictions, thus supporting the plausibility of thermal weakening.

I13 Laboratory Earthquakes

Ares J. Rosakis
California Institute of Technology

Recently, seismologists have discovered that some earthquakes are very slow with almost no energy radiated, while others excite strong and damaging seismic waves with extremely high rupture speed, sometimes believed to be super-shear (faster than shear-wave speed of the surrounding rock body). This variation reflects the difference in rupture physics dominating different tectonic

environments. As a result it has become very important to understand what causes the dramatic variation of rupture speed, and rupture behavior. We have embarked on this problem by constructing laboratory models of earthquakes and by using high-speed imaging of photo-elastic rupture patterns. We have defined a series of experiments to determine the behavior of rupture under spontaneous loading similar to that of crustal earthquakes. With these experiments we have demonstrated that under reasonable loading conditions similar to those for natural earthquakes, super-shear rupture propagation can occur. In such cases we have studied the conditions leading to transition of a sub-Rayleigh rupture to supershear and have related the rupture growth length needed for transition to system parameters. The experiments and analysis has resulted in a better understanding of transition behavior encountered during natural earthquake events such as the 2001 Kunlun earthquake in Tibet. This is probably the first experimental demonstration of super-shear rupture propagation under spontaneous loading. (Xia, Rosakis and Kanamori, *Science*, 2003).

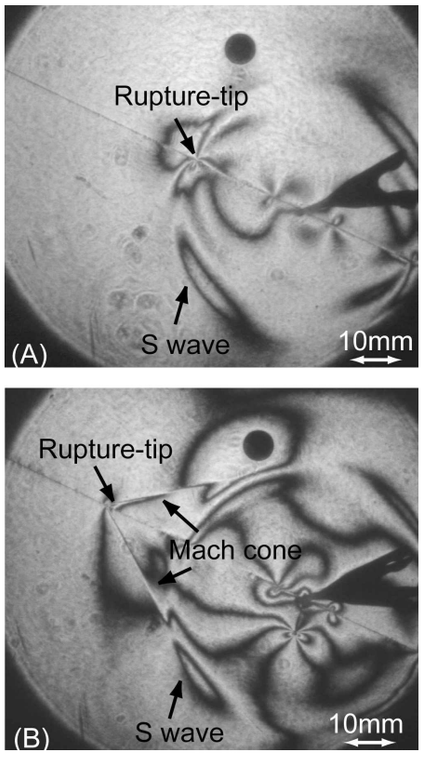

Motivated by such experiments we have also extended the work to observations of spontaneously nucleated events occurring, on frictionally held, bi-material interfaces. Previously, it was generally thought that if there is a velocity contrast the rupture preferentially grows toward the direction of sliding in the lower-speed side of the fault. In contrast to this, we have found that this is not necessarily the case; the rupture can propagate in both directions. In one direction, rupture always propagates at the Generalized Rayleigh wave speed (it is sub-shear) whereas in the opposite direction it may either be sub-shear or may transition to super-shear. This behavior could explain why the rupture in the recent Parkfield earthquake propagated to southeast whereas it propagated northwest in the previous two Parkfield earthquakes. It can also be used to explain field observations during the 1999 Izmit earthquake in Turkey. We hope that these results will help seismologists understand the basic physics of earthquakes and contribute to a better understanding of the vast diversity of earthquake characteristics. (Xia, Rosakis, Kanamori and Rice, *Science*, 2005).

I14 Influence of Human Disease States on Single-Cell and Cell-Population Mechanics

Subra Suresh
Massachusetts Institute of Technology
E-mail: ssuresh@MIT.EDU

Intracellular biochemical changes arising from the onset and progression of human diseases can cause substantial alterations in the molecular structure of cell membranes and the cytoskeleton. These structural changes, in turn, often lead to marked variations in the biomechanical and biorheological response of the affected cells, both in terms of single-cell mechanics and the motility and cytoadherence of a population of cells. In this presentation, controlled and systematic experimental results establishing direct connections between disease states and cell mechanics will be presented in the context of epithelial tumor cells and human red blood cells invaded by *P. falciparum* merozoites that induce malaria. The influence of specific subcellular molecular contributions to cell deformability will be demonstrated in both these examples through controlled biochemical assays or gene inactivation methods. The presentation will conclude with a survey of future opportunities to exploit these scientific findings for disease diagnostics and drug efficacy assays.

I15 Patterning Microscale Attractive & Repulsive Gradients for Cell Cultures

Peter Moran
Institute of Materials Research and Engineering & Singular ID, Pte Ltd
E-mail: peter.moran@singular-id.com

Extensive *in vivo* experiments and *in vitro* studies using liquid concentration gradients have shown that biomolecular gradients are vital for embryonic development. However, understanding how gradients of substrate-bound molecules or other attractive or repelling cues affect cell development has proven difficult due to the complexity of patterning such gradients on the microscale. Here we present two methods developed to pattern microscale gradients of substrate-bound proteins. Reaction of neuron stem cells to these patterns is also discussed. In addition substrates containing microheaters were developed allowing us to examine the effects and possible uses of microscale temperature gradients for cell patterning.

I16 Engineering Nanoprobes for Imaging Gene Expression Dynamics

Gang Bao
Department of Biomedical Engineering,
Georgia Institute of Technology and Emory university,
Atlanta, GA 30332

Living cells can sense mechanical forces and convert them into biological responses including ilterations in gene expression. Similarly, biological and biochemical signals are known to influence cellular abilities to sense, generate and bear mechanical forces. To gain a better understanding of the gene expression dynamics in response to external stimuli, we have developed nanostructured piobes to detect, localize, quantiff and monitor the expression of specific RNAs in living cells. In this talk I will demonstrate the living cell RNA detection capabilities using both Jual FRET (Fluorescence Resonance Energy Transfer) molecular beacons ani peptide-tinkid molecular beacons. We have sholm that, using a pair of molecular beacons that hibridize to adjacent regions on the same mRNA target, sensitive imagrng of specific mRNAs in live cells could be achieved. We have shown that peptide-linked molecular beacons could intemalize into living cells within 30 min with nearly 100% effrciency. We have further revealed intriguing details of RNA localization and co-localization in living cells, and studied the dynamics of RNA localization using molecular beacons in combination with FRAP (Fluorescence Recovery After Photobleaching). The application of these probes in cancer diagnosis, viral infectlon detection, and basic biomechanical and biological studies are illustrated.

I17 A Composites-Based Approach for Constitutive Modeling of Soft Tissue with Applications to the Human Annulus Fibrosus

Brian Moran*, Zaoyang Guo and Xiong-Qi Peng
Department of Mechanical Engineering,
Northwestern University
*E-mail: b-moran@northwestern.edu

A composites-based approach for modeling fiber-reinforced soft tissue is developed. The fiber is treated as a generalized neo-Hookean material and the matrix as neo-Hookean. A multiplicative decomposition of the deformation gradient into a fiber stretch part and a remaining shear deformation then permits the stored energy function to be developed in a straightforward manner which includes extending results for effective shear moduli in small deformation to the large deformation regime. The resulting model is in excellent agreement with a previous phenomenological model we have developed.

I18 Size Effects and Scaling in Discrete Dislocation Plasticity

A. Needleman*[,1], E. Van der Glessen[2] and V.S. Deshpande[3]
[1]*Brown University,* [2]*University of Groningen and*
[3]*Cambridge University*
*E-mail: needle@brown.edu

Plastic flow in crystalline materials is size dependent over length scales of the order of tens of microns and smaller. This size dependence arises in a variety of contexts; for example the grain size dependence of the flow strength, the indentation size effect and the size ependence of the thermomechanical response of thin films. One well-appreciated origin of size effects is associated with imposed plastic strain gradients and geometrically necessary dislocations. In addition, a sizedependent response can be obtained in circumstances where, at least in principle, a more or less homogeneous response is possible. Discrete dislocation plasticity analyses of various plastic flow and fracture processes will be used to illustrate a range of size effects. Particular attention will be given to the scaling, both with size and with material properties, that is redicted by the calculations.

I19 Inter- and Intragranular Stresses in Nonlinear Ferroelectrics

A. Haug, P.R. Onck and E. van der Giessen*
Materials Science Center, University of Groningen,
The Netherlands
*E-mail: E.van.der.Giessen@rug.nl

Ferroelectrics are crystalline inorganic materials consisting of domains with different polarization directions. The domains can be switched into different states by the application of an electric field or mechanical stress, and can thus become piezoelectric. In polycrystalline materials, as used in most applications, electric field and mechanical stress interact so as to maintain compatibility. We study the influence on switching caused by the interactions between neighbouring grains. The behaviour inside each grain is represented by the micromechanics model of Huber *et al.* (1999) which averages over multiple domains. The predictions of a self-consistent model of the polycrystal response are compared with those of a multi-grain model in which grains are represented individually. In one flavour of the multi-grain model, each grain is represented by a single finite element, while in the other the fields inside each grain are captured in more detail through a fine discretization. It is found that for different electrical and mechanical loading situations the overall response is only mildly dependent on the accuracy with which grain-to-grain interactions are captured. The resolution of the fields inside the grains however controls the accuracy with which intra- and intergranular stresses are predicted, which is key to predicting fracture processes in ferroelectrics.

I20 Inverse Analysis to Determine Properties of Anisotropic Thin Films and Coatings

Toshio Nakamura* and Yu Gu
State University of New York at Stony Brook
*E-mail: toshio.nakamura@sunysb.edu

Mechanical responses of thin films or coatings often display anisotropic behaviors. However, their small size scales often make determination of their properties difficult. This work introduces a simple yet versatile procedure with advanced data interpretation scheme to identify

key anisotropic parameters, namely, Young's moduli and yield stresses along longitudinal and transverse directions, respectively. Major advantages of this method are the minimal specimen preparations and the straightforward testing procedure. To enhance the accuracy of estimates, it utilizes two differently profiled nano-indenter heads, spherical and Berkovich. Prior to actual testing, detailed simulations were performed to verify the method's accuracy and robustness. In the experiment, a thermally sprayed NiAl coating which possesses process induced anisotropic features is considered. The load-displacement records from both spherical and Berkovich nano-indenters are post-processed with the proposed inverse analysis scheme. The estimated results predict different responses along the longitudinal and transverse directions. Separate tests are also conducted with micro-indenter heads with larger loads. They demonstrate lesser anisotropic effects but with more compliant responses. The latter observation is attributed to the unique morphology of thermally sprayed coatings, which inherently exhibit size effects.

I21 Numerical Analysis of Deformation and Fracture During Indentation of Thin Hard Films on Soft Substrates

R. Narasimhan*
Department of Mechanical Engineering,
Indian Institute of Science, Bangalore 560012, India
*E-mail: narasi@mecheng.iisc.ernet.in

Thin hard films deposited on soft substrates are employed in engineering applications where mechanical loads like those due to contact are experienced (for example, in cutting tools). It is important to understand the mechanics of deformation and fracture of these films in order to design better coating-substrate systems. Recent experimental work has shown that during spherical indentation, circumferential cracks may form outside the contact zone on the film surface or at the film-substrate interface directly underneath the indenter. The latter occur because the film experiences bending due to the contact load and behaves as a thin plate resting on a plastic foundation. In this paper, finite element simulations of spherical indentation of a thin hard film deposited on a soft substrate are first presented to understand the operative mode of deformation of the film corresponding to various stages of indentation. The transition from contact dominant behaviour to that governed by flexure of the film on the plastically yielding substrate is investigated from analysis of the load versus displacement curve as well as the stress distribution in the film. It is demonstrated that beyond a certain ratio of contact radius to film thickness, a/t, which depends on the substrate yield strength, the deflection profile and stress distribution in the film are accurately predicted by a plate bending model. In the second part of the paper, the behavior of flexure induced cracks emanating upwards from the interface is examined. The results show that when the crack length is small, predominantly mode I conditions prevail due to the bending stresses near the interface. As the crack length increases, the mode mixity gradually changes from mode I to mode II. It is observed that the crack growth process is stable up to a crack length of about a third of the film thickness and thereafter becomes unstable.

I22 Bending of a Microbeam due to Adherent Molecules

L.B. Freund
Division of Engineering, Brown University, Providence, RI USA
E-mail: freund@brown.edu

It has been demonstrated experimentally that a relatively high density of single-stranded DNA attached at one end to only one side of an elastic microbeam results in a measurable and reproducible curvature of the beam. The magnitude of the membrane force arising from the presence of the adherent molecules which induces the curvature can be estimated from the observations. However, the molecules are not bonded to each other in any way and the physical origin of the membrane force remains obscure. The purpose here is to undertake a systematic investigation of possible origins of this force on the basis of statistical mechanics of flexible molecules. Because single-stranded DNA is very flexible, the possibility that the force derives from the increased entropic free energy of the molecular chains as a result of mutual constraint exerted by the molecules on each other once they adhere to the surtace. It is found that membrane force of the magnitude of the served is readilv generated in this way, but the dependence of this force on length of the molecules is not entirely consistent with observations.

I23 Internal Compressive Stresses that Enable Ceramics to Exhibit a Threshold Strength

F.F. Lange
Materials Department,
University of California at Santa Barbara
E-mail: flange@engineering.ucsb.edu

It has been demonstrate, through theory and experiments, that compressive layers arrest large cracks (surface and internal) to produce a threshold strength, allowing an engineer to reliably design with brittle materials. The K function derived for a crack sandwiched between two compressive layers suggests that the threshold strength is proportional to the residual, compressive stress, the layer thickness, and inversely proportional to the distance between the compressive layers. All of these factors have been experimentally examined. Cracks that propagate straight though the layer obey the K function. Crack bifurcation, which occurs at higher compressive stresses, produces larger threshold strengths than predicted. Crack bifurcation is a new phenomenon that is still, little understood.

During the initial studies, differential thermal contraction during cooling from the densification temperature was used to develop the compressive stresses in laminar ceramics. More recently, we have used molar volume changes to induce the compressive stress. In one case, we have shown that the compressive stresses could arise when the compressive layer was formed with a mixture of un-stabilized zirconia and alumina, sandwiched between thicker layers of alumina. Ion exchanged glass plates that

are subsequently bonded together also produce a threshold strength. More recently, processing methods to surround prismatic and polyhedra macrostructures have also been developed.

I24 A Finite Deformation Shell Formulation for the Analysis of Composite and Functionally Graded Material Structures

J.N. Reddy* and R.A. Arciniega
Advanced Computational Mechanics Laboratory, Texas A & M University, College Station, TX 77843-3123
*E-mail: jnreddy@tamu.edu

Dedication: *This paper is dedicated to Professor Fong Shih on his 60th Birthday.*

In solid mechanics and structural mechanics the development of accurate shell theories has been one of the most important research activities. Finite element models of hear deformable plate and shell theories plagued with shear, membrane, and thickness locking phenomena.[1–3] Therefore, it is important to develop a consistent shell theory and associated finite element model that is both accurate and robust (i.e., does not suffer from any type of locking).

In the present study, a consistent shell theory for the analysis of multilayered composites and functionally graded shells is developed. A simple C^0 displacement finite element with higher-order interpolation polynomials is employed. This element is strictly free of membrane and shear locking. Comparisons of the present formulation with those found in the literature for typical linear benchmark problems involving isotropic and composite material cylindrical shells are found to be excellent.[3,4] Next, an extension of this element to geometrically nonlinear analysis of shells with applications to composite and functionally graded material shells are presented. The shell is assumed to undergo finite deflections and rotations but still experience small strains. The third-order shell theory is derived with exact nonlinear deformations and under the framework of the total Lagrangian description. The first-order shell theory is derived as a subset. Numerical examples for cylindrical shells are presented to illustrate the accuracy of the developed shell element.

Acknowledgment

The research results reported herein were obtained while the authors were supported by the Structural Dynamics Program of the Army Research Office (ARO).

References

1. Reddy, J.N., *Mechanics of Laminated Plates and Shells. Theory and Analysis*, 2nd ed., CRC Press, Boca Raton, FL, 2004.
2. Reddy, J.N., *An Introduction to Nonlinear Finite Element Analysis*, Oxford University Press, Oxford, UK, 2004.
3. J.N. Reddy and R.A. Arciniega, "Shear deformation plate and shell theories: from Stavsky to present," *Mechanics of Advanced Materials and Structures* **11**, pp. 535–582, 2004.
4. R.A. Arciniega and J.N. Reddy, "A consistent third-order shell theory with application to bending of laminated composite cylindrical shells," *AIAA Journal*, in print.

I25 Alternative Approaches to Lightweight Construction

Hans Obrecht*, Patrick Fuchs and Marcel Walkowiak
Universitaet Dortmund
*E-mail: hans.obrecht@udo.edu

From the point-of-view of economy and safety it is desirable to employ structures with a sufficiently high strength-to-weight ratio and a reasonably small imperfection-sensitivity. Unfortunately — due to the "unhappy coexistence of efficient shell design and the curse of imperfection-sensitivity" (B. Budiansky) - the goal of achieving both objectives simultaneously appears to be elusive. On the other hand, the results of extensive numerical studies recently performed at Dortmund suggest that the load-carrying capacities of certain structural configurations may indeed be improved significantly without a corresponding increase — or even with a notable decrease — in imperfection-sensitivity.

The presentation will focus on one such example — e.g. the axially compressed circular cylindrical shell partially filled with (and/or surrounded by) a compliant core material -, and results for the bifurcation behavior of grid structures with and without macroscopic auxetic properties will also be discussed. In both cases significant improvements in load-carrying behavior may be achieved with only a minor — or no — increase in weight.

I26 Microstructural Changes During Superplastic Forming at Higher Strain Rates in Al-Mg Alloys

C.L. Briant*[,1], S. Agarwal[1], P.E. Krajewski[2], and A.F. Bower[1]
**Division of Engineering, Brown University, Providence, RI 02912*
+General Motors R&D Center, 30500 Mound Road, Warren, MI 48090
*E-mail: Clyde_Briant@brown.edu

This paper reports an experimental and modeling study of deformation in 5083 Al-Mg alloys at elevated temperatures. Previous results have reported that some superplastic behavior can be observed in this material when it is tested in tension at strain rates as high as 0.3/s at 450°C. In this paper we first focus on the microstructural changes that are observed during the tests. The results show that at strain rates below 0.01/s little necking is observed in the samples at failure and the grains maintain a random orientation with respect to one another. At higher strain rates a strong texture develops and material in the neck of the sample becomes recryrstallized. The amount of recrystallization increases with increasing strain rate. Research has also been performed in which finite element calculations have been used to model superplastic deformation. This model takes into account both dislocation creep and grain boundary diffusion and gives good qualitative agreement with experiments.

I27 Large Electrostriction in Ferroelectrics

G. Ravichandran
California Institute of Technology, Pasadena, CA 91125, USA
E-mail: ravi@caltech.edu

Sensors and actuators based on ferroelectric materials are finding increasing use in applications related to mechanical, aerospace and biomedical fields. Most of the current devices rely on the linear piezoelectric behavior of formulations of PZT which provide strains of up to 0.2%. The nonlinear electromechanical behavior of ferroelectric materials is largely governed by the motion of domains and is affected by stress as well as electric field. A principle result of theoretical modeling is the mode of actuation in ferroelectric single crystals by 90° domain switching that could result in large strains. An experimental setup has been designed to investigate large strain actuation in single crystal ferroelectrics under combined electrical and mechanical loading. Experiments have been performed on single domain bulk crystals of barium titanate with (100) and (001) orientation. The electrostrictive response is shown to be dependent on the level of applied stress with a maximum strain of 0.9% measured at about 2 MPa. The *in situ* observations of the domain patterns using polarized light microscopy are presented. Continuum modeling and simulations are used to gain insights in to the mechanics and mechanisms of large strain actuation and dynamics of domain switching in ferroelectrics.

Poster Abstracts

P1 A Material that Combats Warfare Agents

Ramakrishnan Ramaseshan*,[1], Liu Yingjun[1], Barhate Rajendrakumar Suresh[1], Subramanian Sundarrajan[1], Neeta L Lala[1] and Seeram Ramakrishna[1,2]
[1]*NUS Nanoscience and Nanotechnology Initiative 2 Engineering Drive 3, Singapore 117576*
[2]*NUS Faculty of Engineering Dean's Office 9 Engineering Drive 1, Singapore 117576*
*E-mail: nnirr@nus.edu.sg

Military, firefighter, law enforcement, and medical personnel require high-level protection when dealing with chemical and biological threats (which include chemicals like Nerve gas, Mustard agent, Blood agents, biological toxins such as bacterial spores, viruses and rickettsiae) in many environments ranging from combat to urban, agricultural, and industrial. Current protective clothing is based on full barrier protection, such as hazardous materials (HAZMAT) suits, or permeable adsorptive protective over garments, such as those used by the U.S. military. The obvious limitations of these suits are overweight and moisture retention, both of which limit the user from donning them for longer periods.

Polymer nanofibers have been considered as excellent materials for this purpose owing to their light weight, high surface area and breathable (porous) nature of the membranes. The nanofibers were imparted with catalytic activity of β-Cyclodextrin and Iodosobenzoic acid, and the complex IBA-βCD which is known to have highly specific destructive effect on neurotoxic warfare agents. The compound IBA-βCD was synthesized in dimethyl formamide (DMF) reducing medium and mounted onto Polyvinylchloride (PVC) nanofibers which were electrospun from the same medium. The chemistry involved in the complexation has been explained. These catalytic fibers were tested with nerve gas simulants DMMP and Paraoxon. Decomposition studies were characterized using FT-IR spectra and UV spectrophotometry. The results show that all the three compounds β-Cyclodextrin, Iodosobenzoic acid and IBA-βCD are capable of hydrolyzing nerve agents to nontoxic products. The deactivation is higher when IBA-βCD is used, attributed to its high specificity. Presently kinetic measurements are being carried out to estimate the relative rates of decomposition. The catalytic nanofibers could be used as filters in face masks for defense or healthcare personnel or as a protective suit for the soldier in a battlefield as the case may be.

References

1. Ramakrishna, S., *et al*., An Introduction to Electrospinning and Nanofibers, World Scientific Publishing, Singapore (2005).
2. Gibson, P. W., *et al.*, AIChE J. (1999) 45, 190.

P2 Morpholoqy and Grain Size Study of Electrospun TiO_2 Nanofibers

A. Kumar[1], K. Fuiihara[2], Z.H. Zhou[3], J. Wang[3] and S. Ramakrishna*,[1,2,4]
[1]*Department of Mechanical Engineering,*
[2]*Division of Bioengineering,*
[3]*Department of Materials Science and Engineering,*
[4]*NUS Nanoscience and Nanotechnology Initiative, National University of Singapore, 9 Enqineerinq Drive 1, Singapore 117576*
*E-mail: seeram@nus.edu.sq

Electrospinning is a versatile technique to manufacture the desired organic and inorganic nano scale fibers. Potential applications of electrospun nanofibrous architecture include healthcare, biotechnology & environmental engineering, defense & security, and energy source such as photovoltaic devices. For photovoltaic devices, electrospunanofibrous architecture with high total surface-to-volume ratio would be a potential candidate since they may exhibit unique optical and electrical characteristics due to quantum size and confinement effect. lt is well known that optical and electrical properties of an inorganic semiconducting material are governed by its structure at varying length scales. For example, a refinement in grain and crystallite sizes in nanometer scale can result in an increase in bandgap, which is a parameter that can strongly affect a number of optical and electrical properties of an inorganic semiconducting nanofiber. Therefore, a systematic understanding on the relationships between the nanofiber structure and relevant physical properties is critically important for photovoltaic devices. In this report, TiO_2-based inorganic semiconducting nanofibers will be manufactured by the electrospinning method in combination with sol-gel. Several key nanostructural parameters will be controlled and optimized, including the crystallinity, grain size and fiber diameter in the nanometer scale, via proper processing control. Finally, optical property of the TiO_2 nanofibrous thin will be discussed.

P3 How to Control Molecular Structure of Electrospun Nanofibers?

R. Inai[1], M. Kotaki[2] and S. Ramakrishna[1,3,4]
[1]*Department of Mechanical Engineering,* [3]*Nanoscience and Nanotechnology Initiative,* [4]*Division of Bioengineering, National University of Singapore, 9 Engineering Drive 1, Singapore, 117576*
[2]*Molecular & Performance Materials Cluster, Institute of Materials Research & Engineering, 3, Research Link, Singapore, 117602*
E-mail: g0202463@nus.edu.sg

Electrospinning is a superior method for producing continuous nanofibers from most polymers. Due to the particular interests of electrospun nanofibers in tissue engineering fields, great efforts have been made to study the effects of processing parameters (solution properties, processing conditions, ambient conditions) on the morphology of electrospun biodegradable polymer fibers. However, due to limitations of characterization methods, structure-property relationship of electrospun polymer fibers has not been clarified yet.

In this study, semi-crystalline poly($_L$-lactide) (PLLA) were electrospun into nanofibers. Processing parameter (solution conductivity, polymer concentration, take-up velocity) effects on the internal molecular structure of electrospun PLLA nanofibers were investigated by

x-ray diffraction (XRD) and differential scanning calorimetry (DSC). Take-up velocity was found as a dominant parameter to induce a highly ordered molecular structure in the electrospun PLLA fibers compared to solution conductivity and polymer concentration, although these two parameters have been known to play an important role in controlling the fiber diameter. A collecting method of a single nanofiber by an electrospinning process was developed for the tensile tests to investigate structure-property relationships of the polymer nanofibers. The tensile results indicated that higher take-up velocity caused higher tensile modulus and strength due to the ordered structure developed through the process.

P4 Laser-Synthesized Carbon Nanoparticles and their Nonlinear Optical Limiting Performance

G.X. Chen[1,2], M.H. Hong[*,1,2,3,], L.S. Tan[1,2] and T.C. Chong[2,3]
[1]*NUS Nanoscience & Nanotechnology Initiative, 2 Engineering Drive 3, Singapore 117576*
[2]*Department of Electrical and Computer Engineering, National University of Singapore, 4 Engineering Drive 3, Singapore 117576*
[3]*Data Storage Institute, DSI Building, 5 Engineering Drive 1, Singapore 117608*
*E-mail: Hong_Minghui@dsi.a-star.edu.sg

Nonlinear optical limiting materials have attracted much research effort for their potential applications in nonlinear optical devices, optical communication and national defence, etc. Carbon nanoparticles are promising nonlinear optical limiting materials for wide-band optical responses towards nanosecond laser pulses. In this study, carbon nanoparticles were made by laser ablation of an immersed bulk carbon target in liquids. Transmission Electron Microscopy and UV-Vis spectroscopy were used to characterize the nanoparticles obtained. The nonlinear optical limiting effect was studied with a 7-ns Nd:YAG laser. The physical origin of nonlinear optical limiting in carbon nanoparticle system was investigated with time-resolved analysis of laser pulses and theoretical calculations.

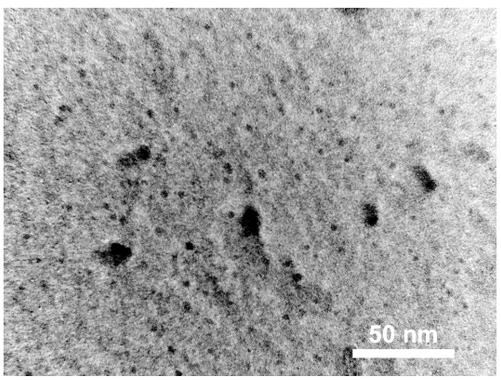

TEM image of carbon nanoparticles

P5 Implementation of Cracked AlGaN Template for V-Pits Reduction in InGaN/GaN Heterostructure

C.B. Soh[1], A.M. Yong[2], S.Y. Chow[3] and S.J. Chua[*,1,2]
Institute of Materials Research and Engineering, 3 Research Link, 117602, Singapore
*E-mail: elecsj@nus.edu.sg

In the growth of InGaN/GaN heterostructures and quantum well, inverted hexagonal V-defects are observed on the epilayer which is associated with mixed or pure screw-edge dislocations propagation and strain relaxation. The formation of V-defects is kinetically controlled by the reduction of Ga incorporation on the pyramidal wall of the $\{10\bar{1}1\}$ plane. In this work, InGaN/GaN is grown on conventional sapphire substrate and cracked AlGaN template. Cracked AlGaN would serve as a technique to reduce stress and hence dislocations propagation which subsequently reduced surface pits formation in the epilayer. The pits formation has been deterred with the implementation of the cracked AlGaN template and there is also a substantial PL emission enhancement. Although the V-pits density has been effectively reduced compared to the conventional sample without the implementation of the cracked AlGaN layer, the surface morphology is rougher and effort has to be taken to ensure that the u-GaN is adequately thick to effectively filled up the cracks and prevent its propagation to the epilayer.

P6 GaN-Based Semiconductor Saturable Absorber Mirror with SiO_2/Si_3N_4 DBR

Fen Lin[1], H.P. Li[2], H.F. Liu[1], W. Liu[3,4], W. Ji[2], S.J. Chua[1,3] and Ning Xiang[*,1]
[1]*Department of Electrical and Computer Engineering, National University of Singapore, Singapore 117576, Republic of Singapore*
[2]*Department of Physics, National University of Singapore, Singapore 117542, Republic of Singapore*
[3]*Institute of Materials Research and Engineering, Singapore 117602, Republic of Singapore*
[4]*Silan Azure Technologies, Hang Zhou 310018, P.R. China*
*E-mail: elexn@nus.edu.sg

A broadband GaN-based semiconductor saturable absorber mirror (SESAM) using SiO_2/Si_3N_4 distributed Bragg reflector (DBR) is reported. The SESAM works around 415 nm with InGaN multiple quantum wells (QWs) as absorbing material. The SiO_2/Si_3N_4 DBR provides a broad stopband of over 100 nm centered around 420 nm, which is much larger than that of the monolithically grown GaN/AlGaN DBR (around 15 nm at similar wavelength). The linear and non-liner transmission/absorption from the QWs and the reflectance from the DBR and the SESAM have been studied. Simulated data and experimental results are compared. Further optimized structure will be discussed. This SESAM can be applied in passively modelocking blue lasers to produce ultra-short optical pulses for data storage and spectroscopy applications.

P7 Ultrafast Nonlinear Optical Switching of ZnO Nanoparticles Beaded Multiwalled Carbon Nanotubes

Hendry Izaac Elim*, Yanwu Zhu, Jim-Yang Lee, Chorng-Haur Sow and Wei Ji†
Department of Chemistry & Biomolecular Engineering, NUS
4 Engineering Drive 4, 117576, Singapore
Department of Physics, National University of Singapore (NUS)
2 Science Drive 3, 117542, Singapore
E-mail: *cheehi@nus.edu.sg; †phyjiwei@nus.edu.sg

Ultrafast nonlinear optical switching of ZnO nanoparticles beaded multiwalled carbon nanotubes has been studied using femtosecond laser pulses at 780 nm. The nonlinear optical (NLO) measurements from as-grown MWNTs and ZnO-beaded MWNTs with 1 min and 5 min coating are put together to check the effects of ZnO nanoparticles. It has been observed that from ZnO/MWNTs with 1 min coating, the transmittance shows only slight reduction, compared with that from as-grown MWNTs. However, for the sample with 5 min coating, the normalized transmittance is significantly reduced. Such a reduction is believed to be induced by three-photon absorption in the presence of ZnO nanoparticles. With the total energy of three photons ($\sim$4.77 eV), a valence band electron can be excited to the conduction band in ZnO nanoparticle ($Eg = \sim 3.4$ eV). Such a nonlinear process gives rise to a positive contribution to the nonlinear absorption, as contrast to the saturable absorption. As a consequence, the resultant nonlinear absorption is the interplay between the three-photon absorption in ZnO nanoparticles and the saturable asorption in MWNTs. Such interplay provides effectively an effective way to control the nonlinear response by changing the concentration of the ZnO nanoparticles in our ZnO/MWNTs hybrid system. The observed optical nonlinearity has a recovery time of $\sim$1 ps. The large and ultrafast saturable absorption in ZnO-beaded MWNTs suggests that the samples can be used as saturable absorber devices.

P8 Optical Nonlinearities and Ultrafast Photo-Dynamics in Colloidal CdSe Quantum Dots

Yingli Qu and Wei Ji*
Department of Physics, National University of Singapore
*E-mail: phyjiwei@nus.edu.sg

Two-photon absorption (TPA), free-carrier absorption, refractive nonlinearities, and ultrafast dynamics of TPA-excited charge carriers in colloidal organic-coated CdSe quantum dots (QDs) are investigated with using both Z-scan and pump probe techniques. The wavelength scaling of the measured TPA coefficients from 720 nm to 950 nm shows the TPA in the CdSe QDs have an enhancement of at least an order of magnitude compared with its bulk counterpart. The negative sign of the third-order nonlinear index of refraction at 780 nm indicates the domination of optical stark effect; while the index change per excited carrier density is observed to be -10^{-21} cm^3 which is comparable with that of bulk CdSe. The degenerate pump-probe measurement at 780 nm reveals that the radiative recombination time for the TPA generated charge carriers is in nanoseconds when the number of excited electron-hole pair per dot is less than one. However, the Auger process will dominate the carrier relaxation and make the relaxation faster once the number of excited electron- hole pair per dot is greater than one and the Auger constant is determined to be 2.2×10^{-30} cm^{6}s^{-1}.

P9 CdS Nanocrystals Embedded Polymeric Film: For Ultrafast Nonlinear Optical Switching

Jun He* and Wei Ji
Department of Physics, National University of Singapore
*E-mail: phyhj@nus.edu.sg

We report the ultrafast nonlinear optical properties of cadmium sulfide nanocrystals (CdS NCs) embedded in a polymeric film. The CdS NCs of 2-nm radius are synthesized by an ion exchange method and highly concentrated in the two layers near the surfaces of the polymeric film. The two-photon absorption (2PA) coefficient and the optical Kerr coefficient are measured with femtosecond laser pulses at 800-nm wavelength. The one-photon and two-photon figures of merit are determined to be 3.1 and 1.3, respectively, at irradiance of $\sim$2 GW/cm^2. The observed nonlinearities have a recovery time of $\sim$1 ps and the two-photon-excited carrier dynamics have also been observed and discussed. Furthermore, we observe for the first time the interband 2PA saturation in CdS NCs under intense femtosecond laser excitation with 1.6-eV photon energy. The observation is compared to interband 2PA saturation in bulk CdS under the same experimental conditions. By using both Z-scan technique and transient absorption measurement, the saturation intensity are determined to be 190 GW/cm^2 for CdS NCs, which is 2 orders of magnitude greater than that for CdS bulk crystal. The 2PA saturation results are quantitatively in agreement with an inhomogeneously-broadened, saturated 2PA model. All these results demonstrate that CdS NCs embedded in polymeric film are a promising candidate for ultrafast nonlinear optical switching applications.

P10 Optical and Magnetic Properties of Metal Nanowires

Hui Pan, Chee KoK Poh, Yuan Ping Feng, Jianyi Lin and Wei Ji
Department of Physics, Faculty of Science, National University of Singapore, Science Drive 3, SG 117542
E-mail: G0202361@nus.edu.sg

Metal nanowires are of great interests in theoretical physics, solid state science and practical technological applications to future ultra-high-density magnetic recording media, magnetic devices and materials for optical, microwave applications. Template method is cheap and easy to operate, which can be used to produce nanowires with uniform diameters ranging from several nanometers to hundreds nanometer in large area. And highly ordered nanowires with uniform diameter, deposited in the anodic aluminum oxide (AAO) template, are essential to study their properties. Successful growth of single crystal nanowires of low melting point metals have been

reported, but growth of single crystal nanowires of high-melting-point metals was claimed to be very difficult if not impossible . Here, we presented that single crystalline Ni, Co, Zn, and Ag nanowires with preferred orientation can be successfully produced based on the AAO template. These nanowires show excellent optical limiting and magnetic properties.

P11 Surface Modification of Silicon Nanowires for Bio-Sensing

Y.L. Cai*, R.Z. Tan and A. Agarwal
*Institute of Microelectronics, A*Star*
*E-mail: caiyl@ime.edu.sg

This study reports the surface functionalization of silicon nanowire (SiNW) to capture and detect presence of biomolecules. Silicon oxide on the SiNW was treated with N-(2-aminoethyl)-3-aminopropyltrimethoxysilane and followed by Biotin N-hydroxy-succinimide ester (NHS-biotin) and streptavidin to create an oriented streptavidin monolayer that forms an affinity capture matrix for biotinylated biological molecules such as biotinylated DNA and biotinylated proteins. The streptavidin-biotin interaction is the strongest known non-covalent, biological interaction (association constant, $Ka = 10^{15}\ M^{-1}$) between protein and ligand [1]. The bond formation between biotin and streptavidin is very rapid and it is unaffected by wide extremes of pH, temperature, organic solvents and other denaturing agent. Biotin-streptavidin generates highly biocompatible surfaces and the existence of well documented protocols and techniques for the biotinylation of biomolecules helps to create suitable receptors for many different analytes. The use of biotin-oriented streptavidin helps to retain the activity of the streptavidin so that the binding between streptavidin and biotinylated biomolecules remains strong [2]. The specificity of biotin and streptavidin interaction ensures that biotinylated molecules bind only to the streptavidin affinity capture matrix and minimal attachment to other surfaces found on the device.

References

[1] Savage, D. *et al.* (1992) Avidin-Biotin Chemistry: A Handbook, Pierce Chemical Co., Rockford, IL.
[2] Robert S. Matson (2005) Applying Genomic and Proteomic Microarray Technology in Drug Discovery, CRC Press.

P12 Fabrication of Silicon Nanowires Using Stress-Retarded Oxidation

Trevor Lee Zong Ning*,[1] and Ajay Agarwal
Institute of Microelectronics, Singapore
[1] *also Material Science and Engineering Department, National University of Singapore, Singapore*
*E-mail: trevorleemiller@yahoo.com.sg

In the next few years, nanometer-wide silicon wires are expected to play a vital role in the development of microelectronics quantum devices. Different methods for the fabrication of the nanowires have been developed that are classified as bottom-up techniques such as the Vapor-Liquid-Solid (VLS) method and top-down techniques like stress-retarded oxidation.

In this work, we present the fabrication of silicon nanowires in CMOS compatible manner using stress-retarded oxidation The silicon nanowires were realized on SOI, bulk and poly-silicon wafers. The process includes definition of fin structures using lithography, etching of silicon and thermal oxidation. By controlling the fin dimensions and oxidation parameters, the final dimensions of the nanowires can be predicted. It is also observed that such a process is highly reproducible. The two ends of the nanowires were connected to the silicon, which were further connected to aluminum pads.

Using above mention process, nanowires with length ranging from 60 nm to 100 μm were fabricated. The fin CD was measured after different process steps to understand their significance. The cross-sectional dimensions of the wires were examined using TEM while device structures at various process steps were examined under SEM. The process details along with the results will be presented.

P13 Poly Silicon Nanowires for Sensors Applications

Liu Fangyue[1] and Ajay Agarwal
Institute of Microelectronics, Singapore
[1] *also at National University of Singapore, Singapore*
E-mail: U0205301@nus.edu.sg

Silicon nanowire field effect transistors were fabricated on polycrystalline silicon wafer using stress limited oxidation method, for the application of real-time sensors based on electrical measurements. This is a top-down approach, but additional size reduction could be done, that allow nanowire formation of 20 nm scale. Electrical measurements were done on nanowires while they were buried in oxide.

First electrical testing was done without any buffer solution on the wires. Since no significant conductance modulation of the structures was observed in the temperature range or 20 to 30°C, the strict control of temperature was not necessary during the sensing. Conductance measurements were done before and after delivering salt and acid solutions using different measurement schemes where short circuit was effectively prevented. The possible explanation for the change in conductance with ions in solution was formulated. The ability of nanowire field effect devices to detect chemical species in liquid solutions, the effect of hydrogen ion concentration or pH was studied before and after silanation. A much larger change with the pH was seen for silane-modified wires, in lower pH range.

Further, to understand the effect of dimensions on the wires' sensitivities, acid of same pH value was delivered to the sensors and their dependence was studied.

P14 Fabrication of Lithographically Defined Silicon Nanowires

W.W. Fang[1], N. Singh, A. Agarwal, G.Q. Lo and N. Balasubramanian
Institute of Microelectronics, Singapore-117685
[1] *Also with NUS*
E-mail: navab@ime.a-star.edu.sg; u0205187@nus.edu.sg

Silicon nanowires (SiNWs) have been hailed as the future nanoelectronics to fabricate multi-gate and gate-all-around

transistors. They also have potential uses in MEMS, NEMS as well as in the biological field such as bio-sensors. SiNWs can be fabricated using the bottom-up or top-down approach. The bottom-up approach uses some kind of self-assembly technique which has issue of growing the wires at desired locations and hence requiring methods like optical tweezers to re-position them. The top-down approach uses lithography to define the position and orientation of the wires and therefore the issue of placement does not arise. Also it is easier to dope lithographically defined nanowires to create good p-n junction based devices.

We demonstrate the fabrication of SiNWs with wire length ranging from 60 nm to 1850 nm using alternating phase shift mask lithography and self retarded oxidation process on bulk and SOI wafers. Our method fabricates wires down to 5 nm in diameter with good repeatability. We found that it is difficult to fabricate the wires of length shorter than the point spread function of the lithography tool due to exponential CD (critical dimension) increase with reduction in wire length. The pattern length/curvature dependency on the self retarded oxidation process is reported. We also demonstrate, for the first time, the curved SiNWs with different curvatures controlled by lithography.

P15 Influences of Triton X-100 on the Characteristics of Carbon Nanotube Based Field Effect Transistors

Jingqi Li and Qing Zhang*
Microelectronics Center, School of Electrical and Electronic Engineering, Nanyang Technological University, Singapore 639798
*E-mail: eqzhang@ntu.edu.sg

Triton X-100 is used as surfactant to disperse carbon nanotube (CNT) bundles. Its influences on the transfer characteristics of the carbon nanotube field-effect transistors (CNTFETs) fabricated with the dispersed CNTs by AC dieletrophoresis technique have been studied. We find that the surfactant at interface between the CNTs and Au electrodes can change the work function of the electrodes and therefore convert the CNTFETs from typical p-type to ambipolar characteristics. The adsorbed surfactants between the CNTs and SiO_2 result in a significant hysteresis in the transfer characteristics of the CNTFETs.

P16 Organophosphates Detection Using Carbon Nanotube Field Effect Transistor

Liu Ningyi, Cai Xianpeng, Lei Yu* and Zhang Qing†
School of Electrical and Electronics Engineering, NTU
School of Chemical and Biomolecular Engineering, NTU
E-mail: *YLei@ntu.edu.sg;†eqzhang@ntu.edu.sg

Organophosphates (OPs) are widely used toxic nerve agents found in agricultural pesticides, household products and chemical warfare agents. Due to its high production worldwide every year and extreme toxicity, innovative analytical tools/devices to monitor OPs are urgently demanded.

Single-walled carbon nanotubes (SWNTs) are of 1-D nanostructure, leading to a high sensitivity to variations of surrounding electrostatic environment. Meanwhile, SWNT based field effect transistors (SWNT-FET) can be integrated into IC chips with modern microelectronics technology. With these advantages, SWNT based detectors are going to have a high value of real-time detection of gas, small molecules and proteins.

Our SWNT based OPs detectors are built on SWNT-FETs coated with Organophosphorus hydrolase (OPH). The detection mechanism is attributed to the SWNT conductance change due to reaction of OPH catalyst and detecting OPs.

P17 Influences of Gate Electrode Structures on Memory Effects of Carbon-Nanotube Field-Effect Transistors

Hong Li, Qing Zhang* and Jingqi Li
Microelectronics Center, EEE, Nanyang Technological University, Singapore
*E-mail: EQZHANG@ntu.edu.sg

Back-gated and top-gated carbon nanotube field-effect transistors (CNTFETs) have been fabricated and characterized in ambient environment, respectively. AC dielectrophoresis technique is used to manipulate single-walled carbon nanotubes (SWNTs) to bridge the source and drain electrodes, which were pre-patterned on SiO_2/Si substrates. Electrical breakdown method is employed to eliminate the influence of metallic SWNTs on the performance of fabricated CNTFETs. The silicon substrates play a role of back gate. Such as-prepared backed-gated CNTFETs typically show p-type conduction channel behavior and hysteretic characteristics in the plot of the drain-source current versus gate voltage in ambient. After annealing the CNTFET at a temperature of 300°C and a pressure of 10 mbar for 20 minutes, we deposit a layer of Si_3N_4 on the top surface of the devices to serve as a top gate oxide. We find that the back-gated CNTFET shows p-type characteristics, while the same device with a top gate shows n-type behavior. Furthermore, the hysteresis loops for the top-gated CNTFET are significantly different from those of the back-gated structures. The effects of the top-gated structure on the behavior of the CNTFETs are discussed.

P18 Dispersion of Single-Walled Carbon Nanotubes with Different Surfactants

Hong Li, Qing Zhang*, Huilin Chai and Kianleng Lim
Microelectronics Center, EEE, Nanyang Technological University, Singapore
*E-mail: EQZHANG@ntu.edu.sg

Five different surfactants have been used to disperse highly purified single-walled carbon nanotubes (SWNTs) in their corresponding aqueous solutions. Efficiency of these surfactants on dispersing SWNTs has been studied systematically with various concentration, solvents, and ultrasonic agitation conditions, respectively. Uniformity and stability of the prepared SWNT suspensions are investigated in terms of comparing the as-prepared suspensions with corresponding ones stored for 10 days. Atomic force microscopy (AFM) and scanning electron microscopy (SEM) measurement are used to obtain the information about the SWNTs bundle thickness and length. We find that

Triton X100 ($C_{14}H_{22}O(C_2H_4O)_{100}$) and Sodium n-Dodecyl Sulfate could disperse the SWNTs, with an average SWNT bundle diameter below 20 nm, much more efficiently than 3-(triethoxysilyl)-propylamin, 3-mercaptopropionic acide and Garantieschein as surfactants. The mechanisms of the dispersion process for the surfactants are discussed.

P19 Influences of AC Electric Field on the Spatial Distribution of Carbon Nanotubes Formed between Electrodes

Ning Peng, Qing Zhang*, Jingqi Li and Ningyi Liu
School of Electrical and Electronic Engineering, Nanyang Technological University
*E-mail: EQZHANG@ntu.edu.sg

Influences of AC electric field on the spatial distribution of single wall carbon nanotubes (SWNTs) have been studied between two adjacent electrodes. The SWNTs are found to be well aligned with the electric field direction and the number density of the SWNTs attached to the electrodes is increased with the magnitude of the electric field. Induced AC dielectrophoresis force and torque on the SWNTs are analyzed to simulate the spatial distribution of the SWNTs. The influence of frequency and viscosity are taken into consideration. It is suggested that, the SWNTs rotate to align with the external field direction almost instantaneously once the electric field is applied. In contrast, the translation motion along the field gradient takes much longer time than the rotation. Both theoretical and experimental results show that perpendicular electrodes have better control over SWNT location than do parallel electrodes.

P20 Ferromagnetic Nanoscale Antidot Arrays

C.C. Wang[1], A.O. Adeyeye[1] and N. Singh[1,2]
[1]*Information Storage Materials Laboratory, Department of Electrical and Computer Engineering, National University of Singapore, 4 Engineering Drive 3, Singapore-117576*
[2]*Institute of Microelectronics, 11 Science Park Road, Singapore Science Park II, Singapore-117685*
E-mail: g0202259@nus.edu.sg

Advances in lithography and other controlled fabrication techniques have enabled researchers to design a wide variety of magnetic nanostructures to explore novel phenomena and applications. Magnetic antidot structures formed by extended regular arrays of holes have received a lot of attention due to the magnetic pinning properties introduced by the holes. Technologically, this peculiar structure has also been proposed for high density data storage. In this work, we have studied the magnetic properties of large area nanometric circular antidot arrays of square, honeycomb, and triangular symmetries using KrF lithography. $Ni_{80}Fe_{20}$ of thickness 30 nm was deposited using e-beam evaporation technique, followed by lift-off processes. The diameter of the holes is 250 nm and the pitch size is fixed at 400 nm.

We found that the lattice geometry induces a well-defined in-plane magnetic anisotropy, which conforms well to the symmetry of their respective unit lattice. The distribution of the easy axis (EA) and hard axis (HA) in the arrays is also strongly geometrically dependent, which is in good agreement with our micromagnetic simulations. We also observed that the magnetization reversal process of the antidot structure could also be tailored by the arrangement of the holes, which gives rise to distinct M-H hysteresis loops and magnetoresistance response.

P21 Magneto-Transport Properties of Pseudo Spin Valve Nanowires

S. Goolaup*[,1], A.O. Adeyeye[1] and N. Singh[1,2]
[1]*Information Storage Materials Laboratory, Department of Electrical and Computer Engineering, National University of Singapore, 4 Engineering drive 3, Singapore-117576*
[2]*Institute of Microelectronics, 11 Science Park Road, Singapore Science Park II, Singapore-117685*
*E-mail: goolaup@nus.edu.sg

Patterned pseudo-spin valve (PSV) nanostructures in which two ferromagnetic layers are separated by a non-magnetic spacer layer have attracted a lot of attention both from a fundamental viewpoint and because of their huge potential in applications such as miniaturized read head sensor. We have fabricated large area PSV nanowire arrays using deep ultra-violet lithography at 248 nm exposing wavelength, e-beam deposition and lift-off technique. The nanowires have width, 185 nm and edge-to-edge spacing of 185 nm. The Cu spacer thickness, t_{Cu}, was varied from 2 nm to 20 nm, while keeping the lateral dimensions and the $Ni_{80}Fe_{20}$ film thickness fixed. For whole range of t_{Cu} investigated, the magnetization loops for fields applied along the wire axis, display a distinct double step reversal due to the separate switching of the two $Ni_{80}Fe_{20}$ layers. For $t_{Cu} \leq 5$ nm, the exchange coupling mediates the reversal process, whereas, for $t_{Cu} \geq 10$ nm, the magnetostatic interaction between the layers dominates. For fields applied along the wire axis, we observed an evolution in the MR response, with the MR curve changing from a sharp peak to a well-defined plateau as t_{Cu} is increased from 2 nm to 20 nm. Our temperature dependent MR response reveals the presence of an exchange bias effect at 5 K, due to the formation of an anti-ferromagnetic phase.

P22 Microstructure and Magnetoelectronic Properties of Co Doped Half Metallic Fe_3O_4 Films and Devices

D. Tripathy[1], A.O. Adeyeye[1] and C.B. Boothroyd[2]
[1]*Information Storage Materials Laboratory, Department of Electrical and Computer Engineering, National University of Singapore, Singapore 117576*
[2]*Institute of Materials Research and Engineering, 3 Research Link, Singapore 117602*
E-mail: g0300880@nus.edu.sg

Half metals characterized by 100% spin polarization at the Fermi level, have attracted much scientific attention recently due to their potential for applications in spintronics based devices. Fe_3O_4 is one of the most promising half metallic materials due to its high Curie temperature (858 K). In the first part of this work, we have investigated the microstructural and magnetoelectronic properties of Co-doped Fe_3O_4 films which were fabricated at room temperature by co-sputtering Fe_3O_4 and Co targets. The presence of well defined grains separated by grain boundaries has been confirmed in the doped films using TEM. We observed that tunneling of spin polarized electrons across antiferromagnetic coupled grain boundaries dominates the transport properties of the films. Magnetic properties of

the doped films are highly dependent on the Co doping concentration and a drastic reduction in the coercivity H_C was observed at high Co concentration. In-plane MR curves show linear magnetic field dependence for the undoped films while a reduction in MR and departure from linear field-dependence is observed for the Co-doped films. In the second part of this work, we exploit the different coercivities exhibited by the Co-doped films with different doping concentrations to fabricate pseudo spin valve structures.

P23 Effect of Rapid Thermal Annealing to GaAsSbN Quantum Well and Bulk GaAsSbN Bulk Lattice-Matched to GaAs

S. Wicaksono, S.F. Yoon, W.J. Fan, W.K. Loke and Y.X. Dang
Compound Semiconductor and Quantum Information Group
School of Electrical and Electronic Engineering
Nanyang Technological University
E-mail: satrio@ntu.edu.sg

GaAsSbN is a promising material for GaAs-based optoelectronics. The diluted incorporation of nitrogen allows lattice-matching with GaAs substrate and greatly reduces the materials bandgap energy, simultaneously. GaAsSbN material has been proposed for GaAs-based optical communication and base material for heterojunction bipolar transistor applications. Rapid thermal annealing of dilute nitride has been reported to have improved the overall crystalline quality, although theoretically GaAsSbN should be less sensitive to thermal treatment as compared to InGaAsN, given the single group lll nature of GaAsSbN. Study on strained QW GaAsSbN/GaAs reveals optimum annealing temperature range of 650°C–750°C. Comparison with bulk GaAsSbN lattice-matched to GaAs (LM-GaAsSbN) with similar N concentration shows minimal energy bandgap blueshift and intensity improvement between the annealing temperatures range of 450°C–850°C. The intensity improvement and bandgap blueshift significantly increased for LM GaAsSbN with increased N concentration (∼2.7%) annealed at 700°C, which suggests group V sub-lattice rearrangement.

P24 Growth of GaAs on (100) Ge and Vicinal Ge Surface by Migration Enhanced Epitaxy

H. Tanoto*[,1], S.F. Yoon[1,2], W.K. Loke[1], E.A. Fitzgerald[3,2], C. Dohrman[3], B. Narayanan[4] and C.H. Tung[4]
[1]*Compound Semiconductor & Quantum Information Group*
School of Electrical and Electronic Engineering
Nanyang Technological University
[2]*Singapore-MIT Alliance*
E4-04-10, 4 Engineering Drive 3
Singapore
[3]*Massachusetts Institute of Technology*
Department of Materials Science & Engineering
Cambridge, MA 02139, USA
[4]*Institute of Microelectronics*
11 Science Park Road
Singapore Science Park II, Singapore
*E-mail: Hendrix@pmail.ntu.edu.sg

We present GaAs/Ge heteroepitaxy grown by solid-source Molecular Beam Epitaxy (SSMBE) with initial GaAs nucleation by migration-enhanced epitaxy (MEE) technique. Three samples were grown for this study; the first two samples, sample A and B, have surface orientation of (100) 6° offcut towards (111) plane. The third sample, sample C, has a nominal (100) surface orientation. These samples were subjected to different temperature during the MEE process, 450°C for sample A and C and 250°C for sample B. We examine the structures and the optical quality of the samples by cross-sectional Transmission Electron Microscope (XTEM) and 5 K photoluminescence (PL). Analyzing the XTEM images of sample A and B, we found that anti-phase domain (APD) still appear in sample A while it is suppressed in sample B. In sample A, two APDs propagating with 45° and 135° angle, as measured from the GaAs/Ge interface, met with each other at certain layer thickness leading to self-annihilation. Meanwhile, XTEM image of sample C show ApDs that propagated almost perpendicularly to the GaAs/Ge interface, making them less likely to self-annihilate. Finally, through the PL analysis, the best optical quality comes from sample B; which we believe mainly due to the total suppression of APD.

P25 Comparison of Lasing Characteristics of GaInNAs Quantum Dot Lasers and GaInNAs Quantum Well Lasers

C.Y. Liu*, S.F. Yoon and Z.Z. Sun
Compound Semiconductor & Quantum Information Group
School of Electrical & Electronic Engineering
Nanyang Technological University
*E-mail: liucy@ntu.edu.sq

Self-assembled GaInNAs/GaAsN single layer quantum dot (QD) lasers grown using solid source molecular beam epitaxy have been fabricated and characterized. The laser worked under continuous wave operation at room temperature with the emission wavelength ∼ 1.2 μm. The lowest obtained threshold current density in this work is ∼ 1.05 kA/cm^2 from a GaInNAs QD laser (50 × 700 μm^2) at 10°C. Temperature-dependent measurements have been carried out on the GaInNAs QD lasers. High-temperature operation up to 65°C was demonstrated from an unbonded GaInNAs QD laser (50 × 1060 μm^2), with high characteristic temperature (T_0) of 79.4 K in the temperature range of 10-60°C. For comparison, temperature-dependent operation has also been studied on the GaInNAs single quantum well (SQW) lasers. Unlike the relation between the cavity length and T_0 in GaInNAs SQW lasers, longer-cavity GaInNAs QD laser (50 × 1700 μm^2) showed lower T_0 of 65.1 K, which is presumably believed due to the nonuniformity of the GaInNAs QD layer.

P26 Nanoscale Selective Area Lateral Overgrowth of GaN

K.Y. Zang, Y.D. Wang, L.S. Wang, S.Y. Chow, S. Tripathy and S.J. Chua*
Institute of Materials Research and Engineering,
3 Research Link, 117602 Singapore,
and Singapore-MIT Alliance, E4-04-10, NUS,
4 Engineering Drive 3, 117576 Singapore
*E-mail: elecsj@nus.edu.sg

We have demonstrated nanoscale selective area lateral overgrowth of GaN on nanoscale patterned substrates, including nanoporous Si(111), nanoporous GaN and GaN

patterned with SiO_2 mask. Nanopore arrays were fabricated using anodized aluminum oxide templates as etch masks, resulting in an average pore diameter and pore spacing of about 60 and 110 nm, respectively. GaN were observed to be grown on top of the exposed nanostructured substrate by metal organic chemical vapor deposition. Nanoscale selective area lateral overgrowth of GaN was found to result in a significant reduction in the threading dislocation density, as characterized using cross-sectional transmission electron microscopy. All dislocations that were seen to bent to lie in the GaN (0001) basal plane during lateral overgrowth. Observation of E_2 phonon blue shifts in the Raman spectra indicate a significant relaxation of the tensile stress in the coalesced GaN films, due, at least in part, to the three-dimensional stress relaxation mechanism associated with growth on the relatively compliant porous silicon layer. Our results show that a single step lateral overgrowth of GaN is a simple and promising way to improve the crystalline quality of GaN layers for microelectronic applications.

P27 ZnO Thin Films Grown on p-GaN Using Hydrothermal Synthesis and Its Optoelectronic Devices Application

Le Hong Quang, Chua Soo Jin* and Eugene A. Fitgerald
*E-mail: elecsj@nus.edu.sg

ZnO thin films with the thickness 0.8–1 μm were deposited on p-GaN by hydrothermal synthesis at low temperature 100°C. The structural and optical properties of the as-grown ZnO films were investigated by X-Ray diffraction (XRD) and photoluminescence (PL) spectra. After annealing treatment the as-grown films in air at 600°C, 30 min, the ZnO films showed good crystallinity and optical properties with strong UV emission at 378 nm. In addition, a sharp UV emission peak at 369.45 nm with the FWHM 20 meV, which attributed to the bound exciton recombination, was also observed from the ZnO films at 80 K. Metal contact was formed on n-ZnO and p-GaN using Au and Ni/Au, respectively. The current-voltage characteristics of the fabricated n-ZnO/p-GaN heterojunction revealed rectifying behavior with a leakage current of 10^{-8} A at -10 V, a forward current 4×10^{-6}A at 10 V bias. The heterojunction also showed a good photoresponse, with the change of the current — voltage characteristics under ultraviolet illumination. Under UV illumination, the forward turn on voltage changed to 7.5 V. This result showed the ability to manipulate the electron transport in the ZnO based heterojunction devices.

P28 A Study of Charge Mobility Characteristics in a Novel PPV-PF Copolymer

Chellappan Vijila, Chen Zhikuan and Chua Soo Jin
Institute of Materials Research and Engineering
3 Research Link, Singapore 117 602
E-mail: c-vijila@imre.a-star.edu.sg

This paper reports a study of the absorption, photoluminescence and charge mobility characteristics of a novel electroluminescent polymer: poly{[2-(4',5'-bis(3"-methylbutoxy)-2'-phenyl)phenyl-1,4-phenylene vinylene]-co-(9,9-dioctyl-2,7-fluorenylene vinylene)} (PPV-PF). The π-π^* band gap of the polymer was estimated from the edge of the solid state absorption spectrum and found to be 2.48 eV. The photoluminescence spectrum exhibits clear vibrational features with a maximum at 2.44 eV. The charge mobility characteristics of the polymer were studied using the TOF photoconductivity measurement technique and an indium tin oxide (ITO)/polymer/Aluminium sandwich device structure. The TOF transients for positive charges are non-dispersive in nature, thus the transit time was obtained from the linear plot of photocurrent versus time. The hole mobility value was found to be in the range of 2.5×10^{-5} cm^2/V·s (1.6×10^5 V/cm) to 5.2×10^{-5} cm^2/V·s (3.7×10^5 V/cm) at 298 K which is one order of magnitude higher than that (1.7×10^{-6} cm^2/V·s) reported for MEH-PPV at an electric field of 2.5×10^5 V/cm. It was also observed that the hole mobility is almost independent of the applied electric field. This suggests that the introduction of fluorenylene unit to the PPV backbone results in a increase of hole mobility and degree of conformational order.

P29 Fabrication of Two-Dimensional Photonic Crystals in AlGaInP/GaInP Membranes by Inductively Coupled Plasma Etching

Ao Chen*[,1], Soo Jin Chua[1,2], Xin Hai Zhang[2] and Jian Rong Dong[2]
[1] *Singapore-MIT Alliance,*
National University of Singapore,
4 Engineering Drive 3, Singapore 117576
[2] *Institute for Materials Research and Engineering,*
3 Research Link, Singapore 117602
*E-mail: ao.chen@nus.edu.sg

The fabrication process of two-dimensional photonic crystals in an AlGaInP/GaInP multi-quantum-well membrane structure is developed. The process includes high resolution electron-beam lithography, pattern transfer into SiO_2 etch mask by reactive ion etching, pattern transfer through AlGaInP/GaInP layer by inductively coupled plasma (ICP) etching and a selective undercut wet etch to create the freestanding membrane. The chlorine-based ICP etching conditions are optimized to achieve a vertical sidewall. The 2-D photonic crystals of periodic air holes with the pitch $a = 200$ nm–480 nm and air filling ratio $f = 0.25$–0.35 are produced for both square and hexagonal lattices. The structure fabricated is characterized by photoluminescence measurements and surface-emitting lasing actions have been observed.

P30 GaN Faceted Epitaxy

Hailong Zhou, Soo Jin Chua and LianShan Wang
*E-mail: G0301203@nus.edu.sg

Epitaixal lateral overgrowth which occurs during GaN selective epitaxial has been studied using liner and designed shape mask features. The lateral growth varies between its maximum and minimum over a 30° angular span and exhibits hexagonal symmetry. Large variations in the lateral growth between the $\langle 1\underline{1}00 \rangle$ direction and $\langle 11\underline{2}0 \rangle$ direction are also obtained through variations in the growth temperature. Vertical growth follows an opposite trend to the lateral growth increase with the temperature

increase. Under proper growth conditions, lateral to vertical growth rate ratios maximum can be achieved, resulting in significant lateral mask overgrowth and coalescence of features without excessive growth times. And we also describe experiments to distinguish whether the lateral transport of material occurs via gas-phase diffusion or surface diffusion, either on the mask itself or on the epitaxial material. These results indicate that gas-phase diffusion dominates the transport of material during GaN ELO.

P31 Ostwald Ripening of Zinc Oxide by Post-Growth Annealing

S.T. Tan[1,2], X.W. Sun[1,*], X.H. Zhang[2], S.J. Chua[2], B.J. Chen[1] and C.C. Teo[3]
[1] *School of Electrical and Electronic Engineering, Nanyang Technological University, Nanyang Avenue, Singapore 639798, Singapore*
[2] *Institute of Materials Research and Engineering, 3 Research Link, Singapore 117602, Singapore*
[3] *School of Materials Science and Engineering, Nanyang Technological University, Nanyang Avenue, Singapore 639798, Singapore*
*E-mail: exwsun@ntu.edu.sg

Post-growth annealing was carried out on ZnO thin films grown by metal-organic chemical-vapor deposition. It was found from the scanning electron microscopy and atomic force microscopy measurements that the morphology of the thin films changed drastically after annealing. The as-grown thin films consist of fine nanoscale-sized sheets with random orientation. Upon annealing at 800°C, the ZnO nanosheets changed to three-dimensional nanoneedles. The different type of the mass transport mechanisms are discussed and correlated with the experimental results. A coarsening kinetics developed by the Lifshitz, and Slyozov [I.M. Lifshitz, and V.V. Slyozov, J. Chem. Solids Phys. **19**, 35 (1961)] and Wagner [C. Wagner, Z. Elektrochem. **65**, 581 (1961)] was used to estimate the activation energy of the coarsening process. The activation energy of the Ostwald ripening in ZnO films was estimated in the first attempt and the value is at around 1.33 eV. The sintering process was found to have a slightly higher activation energy than Ostwald ripening as observed in the experiments.

P32 Room Temperature Inductively Coupled Plasma Etching of InP Using CH_4/H_2, Cl_2/N_2 and $Cl_2/CH_4/H_2$

Chee-Wei Lee*, Mee-Koy Chin and Ting Mei
Photonics Research Centre, School of Electrical and Electronic Engineering, Nanyang Technological University, Singapore 639798
*E-mail: Cheewei_lee@pmail.ntu.edu.sg

We optimize room-temperature etching of Indium Phosphide (InP) using CH_4/H_2, $Cl_2/CH_4/H_2$ and Cl_2/N_2 Inductively Coupled Plasma (ICP) reactive-ion etch. A design of experiment (DOE) is used in the optimization. The results, in terms of etch rate, surface roughness and etched profile, are presented. The CH_4/H_2 recipe provides a relatively low etch rate ($\sim$ 100 nm/min) with possible polymer formation, but the gases are safer to use. The Cl_2-based recipes do not require substrate heating and thus can be more cost effective and widely applied. The $Cl_2/CH_4/H_2$ process is able to give a higher etch rate ($\sim$ 850 nm/min) and cleaner surface with less polymer formation compared to the conventional CH_4/H_2 process. The Cl_2/N_2 process produces even higher etch rate (as high as 2 μm/min), but rougher surface with slight sidewall undercut. The Cl_2/N_2 process also has no polymer formation due to the absence of methane gas. Both processes give very good selectivity against the silicon dioxide (SiO_2) etch mask. The selectivity of InP against oxide mask (up to 55:1) for the Cl_2/N_2 process is one of the highest reported so far. The etched structures possess reasonably good sidewall verticality and surface quality comparable to that obtained under elevated temperature condition (> 200°C).

P33 Inductively Coupled Argon Plasma-Enhanced Quantum well Intermixing and Multiple Bandgap Implementation for Photonic Integrated Circuit Application

D. Nie, T. Mei*, C.D. Xu and M.K. Chin
School of Electric and Electronic Engineering, Nanyang Technological University, Singapore 639798
*E-mail: etmei@ntu.edu.sg

Photonic integrated circuits (PICs) have advantages over discrete devices coupled through fibers. Fabrication of PICs requires in-plane lateral bandgap control across a single chip. Defects-enhanced quantum well intermixing (QWI) can perform the lateral bandgap control at a post-growth level. The bandgap control is based on the fact that the interdiffusion of the constituent atomic species in a metastable structure such as quantum wells (QWs) is enhanced by the existence of mobile point defects in the vicinity of a QW region in a rapid thermal annealing (RTA) process. The degree of bandgap modification is determined by the amount of mobile point defects, the RTA temperature and time. In the inductively coupled argon plasma-enhanced QWI, the bombardment from the high-density low-energy argon plasma generated in an inductively coupled plasma (ICP) chamber creates near-surface mobile point defects on a QW chip. During the subsequent RTA, these surface defects diffuse down to the QW region to enhance QWI. Multiple bandgap energies across a single chip have been achieved by selectively controlling the amount of near-surface mobile point defects without manipulating the RTA process using a multi-step plasma exposure process, or single plasma exposure process with gray mask technique or spatial defect modulation. To verify the integration capability, an extended cavity laser and an asymmetric multimode interference (MMI) wavelength monitor have been fabricated with their passive section intermixed using the inductively coupled argon plasma-enhanced QWI technique.

P34 Ring Resonator Based Filters

Yosef Mario Landobasa, Stevanus Darmawan and Chin Mee Koy*
Nanyang Technological University
*E-mail: emkchin@ntu.edu.sg

Ring resonators (RR) are waveguide realization of Fabry-Perot resonators which can be readily integrated in various array geometries to implement many useful functions.

Here we present various array configurations of RRs and derive their optical transmission properties (including the photonic bandgap feature) using the transfer matrix method. We discover that by using the complementary bandgap feature of the side-coupled RR and the coupled RR case, we can combine the two linear arrays to form a general 2-D lattice network of symmetric resonators which has a near-ideal bandpass filter characteristic, characterized by a flat top box-like amplitude response without out-of-band sidelobes, and a linear phase response.

On top of that, the nonlinear phase response of RR can be readily incorporated into a Mach-Zehnder Interferometer (MZI) to enhance the phase sensitivity and produce specific intensity output function. We present two generalized array configurations of ring-coupled MZI (side-coupled and coupled REMZI) and discuss their characteristics in terms of the amplitude and phase response of the ring arrays as well as the transmission output of the MZIs. The two types of array have distinct transfer functions and effective phase shifts, and can be tailored to phase-engineer a wide-range of MZI transmission functions.

P35 OLED Color Tuning with Graded ITO

Li-Wei Tan*, Furong Zhu, Kian Soo Ong and Xiaotao Hao
Institute of Materials Research and Engineering
*E-mail: lw-tan@imre.a-star.edu.sg

In contrast to the conventional multicolor OLEDs using different emission materials, a novel multicolor OLED using single electroluminescent emitting material was demonstrated. This device utilizes a graded transparent conductive oxide layer, which is also serves as the anode layer. The device has a simple architecture enabling fabrication of multicolor OLED displays at lower cost. The multicolor emission from single light-emitting material is achieved by varying the thickness of the graded transparent conductive oxide layer in the respective emitting zone. Since only single emissive material is used, there is no discrepancy in the durability of the different colors in the multicolor OLEDs. This is a major concern in multicolor OLEDs when emission materials with different lifetime are used.

P36 Transparent PM OLED Display

Chum Chan Choy, Li-Wei Tan and Furong Zhu*
Institute of Materials Research and Engineering
*E-mail: fr-zhu@imre.a-star.edu.sg

A laser ablation technology has been developed to create the pixel separation for matrix addressed OLED displays. This technology removes the need for lengthy photolithography processing, which is typically required for fabricating mushroom type insulators used in the conventional matrix addressed OLED displays. Our work demonstrates that it can be potentially very useful for mass production of high-resolution matrix addressed OLED displays. We have applied the laser ablation technique to form a see-through polymer light-emitting passive matrix display with a matrix of 96 × 64 with a display area of 28.77 mm by 19.17 mm.

P37 Contrast Enhancement of OLEDs

Liew Pooi Kwan, Candy Tan Mei Chern, Ong Kian Soo, Li Wei Tan and Furong Zhu
Institute of Materials Research and Engineering, 3 Research Link, Singapore 117602

In a conventional structure of the organic light emitting devices (OLEDs), OLEDs have a stack of organic layers sandwiched between an anode and a metallic cathode. The devices with this configuration are usually very reflective leading to a low contrast ratio. In many practical applications, the visual contrast is more important than the brightness of image. As such, improving the visual contrast in OLED displays is another important issue to address with a significant technological implication. In our work, we developed a new high contrast OLED architecture. The concept is based upon on using an optical destructive anode to reduce the ambient light reflection to enhance the visual contrast. Some experimental results of high-contrast OLED will be presented in the poster.

P38 Modeling of ZrO_2 Film Dynamic Growth on Silicon by ab initio Molecular Dynamics

Ling Dai[1], Shuo-wang Yang[2], V.B.C. Tan[1] and Ping Wu[2]
[1]*Mech. Eng., National University of Singapore*
[2]*Institution of High Performance Computing*
E-mail: G0306324@nus.edu.sg

Ab initio molecular dynamics simulations were carried out to model the deposition process of spuftering Zrconium atoms onto a natural oxidized Silica bulk in order to get a highdielectric-constant ZrO_2 thin film for the gate dielecfic strucnrre. During the dynamic simulations, the ZrO_2 thin film growing process was presented and investigated by atomic bonding analysis and inter-diffusion characterization. After the dynamic process, we found a thorough phase transformation of SiO_2/Si to a clear ZrO_2/Si interface. Studies on the interfacial sftucture and electron density-of-states proved that the ZrO_2/Si interface has good phase stabilities and adhesion properties. Many agreements were obtained between our simulation results and previous experimental and theoretical reports.

P39 Theoretical Study on Polyimide-Cu(100)/Ni(100) Adhesion

Jia Zhang[1,2], Michael B. Sullivian[1], Jianwei Zheng[1], Kian Ping Loh[2] and Ping Wu[1]
[1]*Institute of High Performance Computing, Singapore*
[2]*Department of Chemistry, National University of Singapore*
E-mail: g0301165@nus.edu.sg

The interfacial properties of polyimide (PI)/M (100) (M = Cu and Ni) were investigated using density functional theory (DFT). A PMDA-ODA monomer unit was used to represent the full PI and the surface was a represented by periodically repeated slabs. PI prefers the bridge and top sites on Cu(100) surface but only forms weak C = O-Cu interaction. PI favors the bridge site on Ni(100) surface and can form strong C-Ni, N-Ni and C = O-Ni bonds. The adsorption energies of PI on Cu(100) and Ni(100) surfaces are −0.58 eV and −4.7 eV, respectively. Compared to

the adsorption energies of O and O_2 on Cu(100) surface, the adsorption of PI on Cu(100) is not energy favorable, which leads to the easy oxidation of Cu particles in Cu/PI nanocomposite. The good adhesion at PI/Ni(100) suggests that Ni is a better candidate as a metal filler compared to Cu in the metal-polyimide composite.

P40 Characterization of the Cathode/ Electrolyte Interface in Solid Oxide Fuel Cells

Wei Wang, San Ping Jiang*, Hsien-Chi Yeh and Vincent Wei Wen Ho
School of Mechanical and Aerospace Engineering, Nanyang Technological University, Singapore 639798
*E-mail: mspjiang@ntu.edu.sg

The interface between the cathode and the electrolyte is critical for the O_2 reduction reactions in solid oxide fuel cells (SOFC). In this work, atomic force microscopy (AFM) and electrochemical impedance spectroscopy (EIS) were used to study the interfaces between two cathode materials (La, Sr)MnO_3, (La, Sr)(Co, Fe)O_3 (LSCF) and two electrolyte materials Y_2O_3-ZrO_2 (YSZ), Gd_2O_3-CeO_2 (GDC), under different polarization conditions. The effect of the sintering temperature of cathode coatings on the electrode behavior and interface topography/morphology was also investigated. The results present invaluable information of the active sites for the O_2 reduction on SOFC cathodes.

P41 First-Principles Study of the Influence of Doping Sr and Mn on the Electrical Conductivity of Perovskite $LaCrO_3$

Khuong P. Ong[1], Ping Wu*,[1] and S.P. Jiang[2]
[1]*Institute of High Performance Computing (IHPC), 01 Science Park Road, #01-01 The Capricorn, Singapore Science Park II, 117528*
[2]*School of Mechanical & Aerospace Engineering, Nanyang Technological University, 50 Nanyang Avenue, Singapore 639798*
*E-mail: Corresponding author

The electronic structure of $LaCrO_3$ has been studied by using the Full Potential Linearlized Augmented Plane Wave (FP-LAPW) method within the meta-generalized gradient approximation (meta-GGA) and meta GGA + U. Within the meta-GGA $LaCrO_3$ is an insulator with an energy band gap 1.1 eV which is much less than the experimental report 3.3 eV. In order to reproduce this energy band gap an effective U, $U_{eff} = 5.44$ eV has been used. The influence of Sr- and Mn-doping on the electrical property of $LaCrO_3$ has been studied within the meta-GGA calculations. It has revealed that doping of Sr/Mn on the La/Cr site, respectively, will produce metallic state for $La_{1-x}Sr_xCrO_3$ and $LaCr_{1-x}Mn_xO_3$.

P42 Synthesis and Characterization of Pt Catalysts on Multi-Walled Carbon Nanotubes by Intermittent Microwave Inadiation for Fuel Cells

Tian Zhi Qun and San Ping Jiang*
School of Mechanical and Aerospace Engineering, Nanyang Technological University, Singapore 639798
*E-mail: mspjiang@ntu.edu.sg

Polymer electrolyte and direct methanol fuel cells (PEFCs & DMFCs) are the most promising power sources. However, one of the most signifrcant barriers for the widegpread commercialization of PEFCs and DMFCs is the high cost of precious Pt and Pt alloy catalyst. One way to achieve this goal is by preparing the high activity catalyst tot reduce the amount of precious metal catalyst.

In this paper, Pt electocatalysts supported on multiwalled carbon nanotubes (Pt/MWCNTs) nanocomposites have been synthesized by a rapid intermittent microwave irradiation technique for PEFCs and DMFCs, using H_2PtCl_6 as Pt precursor. The Pt/MWCNT nanocomposites synthesized are characterized by XRD, XPS and TEM. The results indicate that Pt particle size and distribution on the MWCNTs support are affected significantly by the oxidation treatment of MWCNTs, the intermittent microwave irradiation procedure and the MWCNTs surface area. PtO_x ($x = 1$–2) species was firstly deposited on the surface of MWCNTs through the intermittent microwave inadiation and subsequently reduced to Pt(0) with the reflux in the presence of HCOOH. Pt/MWCNTs nanocomposites synthesized by this intermittent microwave irradiation method have achieved extremely uniform dispersed Pt nanoparticles with particle size of $\sim$3 nm. Electrochemical measurement indicates that Pt/MWCNTs nanocomposites synthesized by the intermittent microwave irradiation method display a significantly higher electrochemical active area and higher catalytic activity for methanol oxidation reactions in comparison to a commercial Pt/C catalyst.

P43 Hydrogen Desorption Properties of the Mg-Ca-N-H System

Y.F. Liu*, Z.T. Xiong, J.J. Hu, G.T. Wu and P. Chen
Physics Department, National University of Singapore
*E-mail: phylyf@nus.edu.sg

A new ternary Mg-Ca-N-H samples have been prepared by ball milling the mixture of $Mg(NH_2)_2$ and CaH_2 (1:1) with planetary ball mill machine, and the structure and hydrogen desorption performances were also studied. The results indicate that pure H_2 gas product can be formed during ball milling, and its amount was increased with prolonging ball milling time. After ball milling 72 hours, $\sim$3.5 H atoms ($\sim$3.57 wt%) were found to be detached from the starting material. Moreover, volumetric release and soak tests on the sample collected after 12 hours of ball milling show that hydrogen desorption starts at temperature right above 50°C. At temperature of 200°C, $\sim$2.0 wt% of hydrogen was desorbed. DSC measurement on the hydrogen desorption from the post-12h milled sample reveals that the overall heat effect is $\sim$28.2 kJ/mol-H_2, implying that Mg-Ca-N-H system could be a potential lower temperature hydrogen storage material. In addition, the high-pressure release testing reveals that hydrogen could not desorb from the post-12h milled sample at temperature below 200°C when 80 bars of hydrogen was applied. As temperature increased to 300°C more than 3.0 wt% of hydrogen was released, revealing that the equilibrium hydrogen desorption pressure is higher than 80 bars at temperature of 300°C. All these results indicate the Mg-Ca-N-H system may have good reversibility. However,

the difficulties in recharging the sample with hydrogen should be due to the high kinetic barrier.

P44 Ca-Na-N-H System for Reversible Hydrogen Storage

Zhitao Xiong, Guotao Wu, Jianjiang Hu, Lefu Yang and Ping Chen*
*E-mail: phychenp@nus.edu.sg

Ca-Na-N-H system was introduced and evaluated in this paper for reversible hydrogen storage. Similar to other amide-hydride systems already reported, interaction between $Ca(NH_2)_2$-NaH (1/1) was observed in the temperature range of 120–270°C with 1.1 wt% of hydrogen desorption, from which 0.96 wt% of hydrogen can be recharged. XRD and FTIR identified $NaNH_2$ and a solid solution of $Ca(NH_2)_2$ and CaNH as dehydrogenation products.

P45 Dependence of Dehydrogenation on Mechanical Ball Milling

Hu Jianjiang*, Xiong Zhitao, Liu Yongfeng, Wu Guotao and Chen Ping
Department of Physics, National University of Singapore
E-mail: phyhujj@nus.edu.sg

Mechanical ball-milling is a convenient way for conducting solid state reactions in addition to its usage in preparation of solid phase mixtures. In our study, chemical reactions were observed between $Mg(NH_2)_2$ and MgH_2 during ball milling, resulting in the release of hydrogen at room temperature. The as-milled samples with different milling time present various behaviors in the subsequent Temperature-Programmed-Desorption (TPD) tests. While NH_3 release started at 200°C for the sample with short milling time, it was effectively suppressed and postponed to above 300°C for samples with extended milling. The conversion of the amide and hydride to imide-like structure could be demonstrated by means of Fourier Transform Infrared Spectroscopy (FTIR) and x-ray Diffractometry (XRD). A total amount of 4.8 wt% of H_2 could be released from the investigated system.

P46 One-Pot Enzymatic Dynamic Kinetic Resolution of Secondary Alcohols by Zeolite Beta

S. Jaenicke*, Foo Kam Loon and Gaik Khuan Chuah
Department of Chemistry,
National Univesrity of Singapore
*E-mail: chmsj@nus.edu.sg

Enzymatic resolution is a useful method for obtaining enantiomerically pure compounds. Lipases have been widely used for the kinetic resolution of racemic secondary alcohols. In the presence of a suitable acyl donor, the enzyme selectively catalyzes the transesterification of one enantiomer in the racemate to the corresponding ester, while the other enantiomer remains unreacted. Subsequently, the mixture can be separated through normal separation techniques. However, the yield is limited to 50% if only one form of enantiomer is required. In principle, the yield could be increased to 100% if the enzymatic resolution is coupled with in-situ racemization of the secondary

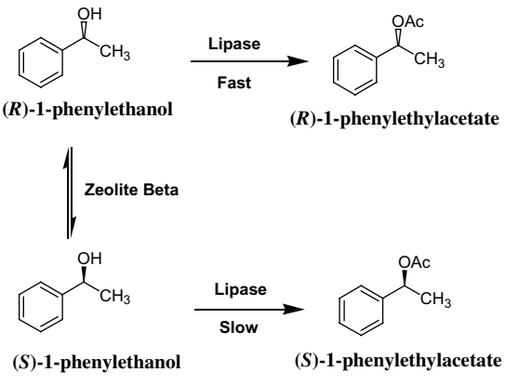

alcohol. This approach is called dynamic kinetic resolution (DKR).

Zeolite beta had been proposed as a racemization catalyst, and a very high ee was obtained when the DKR experiment was carried out in a liquid-liquid biphasic system. However, the presence of water leads to considerable unproductive hydrolysis of the acylation reagent.

A simple and convenient DKR reaction with a single liquid phase is preferably for industrial applications. The racemization potential of zeolite beta with different Si/Al and Si/Zr ratios had been tested. Zeolite Beta with a high Si/Al of 150 gives the best performance. The only side-product was styrene formed by dehydration of the 1-phenylethanol. Completely Al-free Zr-beta showed low reactivity, whereas materials with higher Al content had low selectivity and led to the formation of substantial amounts of styrene. It was found that the zeolite is also able to catalyze the transacylation reaction, thus leading to a loss in stereo-selectivity at long reaction times. This could be prevented by using a steric demanding transalkylation agent, vinyloctanoate, which is too big to fit in the pore system of the zeolite. In this way, 98%ee can be achieved at 83.6% conversion within 2 h.

P47 Potassium Phosphate as a Unique Solid Base in Phase Transfer Catalysis

G.K. Chuah, S. Jaenicke* and R. Vadivukarasi
National University of Singapore
Department of Chemistry
*E-mail: chmsj@nus.edu.sg

Phase-transfer catalysis (PCT) makes it possible to use simple bases such as aqueous OH^- to deprotonate weak organic acids in two-phasic systems. Thus, for the coupling reactions of C-H acidic compounds with suitable acceptors (ketones,alkylhalogenides, etc), cheap inorganic bases can be used, instead of expensive and difficult to handle reagents such as butyl lithium or sodium alkoxides. The marked enhancement of the basicity comes about because the acid-base equilibrium is coupled with the phase transfer equilibrium.

Potassium phosphate (K_3PO_4) has been proposed as a mild and selective solid base under solid-liquid phase transfer catalysis conditions. Whereas K_3PO_4 is only a weak base in an aqueous system, it is able to deprotonate C-H acidic compounds with a pK_A as high as 23 under phase-transfer conditions. The advantage of this reagent is that K_3PO_4 can be used in water-free systems, so that even hydrolysis-sensitive compounds can be prepared

which are not accessible under normal PCT conditions in aqueous/organic biphasic systems. It also does not evolve CO_2 on reaction with acids, which is a potential drawback when K_2CO_3 is used as solid base.

We describe the coupling reaction of methylmalonate with n-butylbromide under phase transfer conditions with K_3PO_4 as solid base. Various PTCs (18-crown-6, cetyl trimethyl ammonium bromide (CTMA), polyethylene glycols (PEG) of different molecular weight) were evaluated, with 18-crown-6 showing the best performance. In particular, we observed a strong dependence of the activity on the pre-drying conditions of the K_3PO_4. The activity could be correlated with water losses as determined by TGA and by high temperature XRD.

P48 Supported Ionic Liquid Phase Catalysts: Stereoselective Reduction of Ketones

Fow Kam Loon[1], Stephan Jaenicke*,[1] and Thomas Müller[2]
[1] *Department of Chemistry, National University of Singapore*
[2] *Institute of Technical Chemistry II, Technical University of Munich, Germany*
*E-mail: chmsj@nus.edu.sg

Heterogenizing of homogeneous catalysts is a strategy to improve process stability and economics. In most approaches, the homogeneous catalyst is immobilized by tethering the ligand to an insoluble support with a flexible linker. These approaches have generally not been adapted on an industrial scale. More successful is the liquid-liquid partition of the catalyst in one liquid phase in a liquid-liquid biphasic system, which is practiced in the SHOP (Shell Higher Olefine) process and the Ruhrchemie-Rhone-Poulenc process for the hydroformylation of propene.

We propose to make use of the special properties of ionic liquids as "designer liquids" where the properties can be modified widely. A thin film of an ionic liquid is coated on the surface of a stable carrier, and the homogeneous catalyst is dissolved in the ionic liquid phase.

The reduction of 1-phenylethanone to 1-phenylethanol was studied as a test reaction for the enantioselective reduction of pro-chiral ketones. Noble metal (Ru, Rh, and Pd) complexes with chiral phosphine ligands (BINAP) were dissolved in a thin film of supported phosphonium-salt based ionic liquid. All catalysts were tested in an autoclave at constant hydrogen pressure and their catalytic performances were compared to the corresponding homogeneous systems. The chemoselectivities of different noble metal complexes were investigated by measuring the kinetic constants of each step in the reduction of acetophenone.

The immobilised transition metal complexes generally showed a higher rate of reaction than the corresponding homogeneous catalysts. Although the chemoselectivity for reduction of the keto group was moderate, higher enantioselectivity (up to 74%) was observed for the immobilised catalysts as compared to the homogeneous catalyst. Except for the ruthenium complexes, the immobilised catalysts generally displayed a significantly higher stability compared to the corresponding homogeneous catalysts.

The immobilisation of organometallic complexes in a thin film of supported ionic liquid can afford enantioselective reduction of acetophenone at moderate reaction time. This multiphase catalytic system constitutes a straightforward method for developing heterogeneous catalysts from known homogeneous catalysts. The supported catalysts combine the advantages of homogeneous catalysts with those of heterogeneous catalysts. The immobilised catalysts can be handled like classic heterogeneous catalysts.

P49 Appraising Concrete Strength Using Shearography

H.M. Shang*,[1], Y.Y. Hung[2], C.Y. Yiu[3] and L. Liu[2]
[1] *Temasek Laboratories at NTU, School of Mechanical and Aerospace Engineering, Nanyang Technological University, Singapore*
[2] *Department of Manufacturing Engineering and Engineering Management, City University of Hong Kong, Kowloon, Hong Kong*
[3] *Department of Building and Real Estate, Hong Kong Polytechnic University, Hong Kong*
*E-mail: mhmshang@ntu.edu.sg

The importance of evaluating and monitoring the strength of concrete structures in existing buildings, especially in aging high rise buildings, can never be over emphasized. Core tests are commonly used to assess concrete strength. However, this process is lengthy involving drilling and gathering cored samples before test results are obtained. Various nondestructive testing techniques (e.g., surface hardness test, penetration resistance test and ultrasonic pulse velocity test) were developed to expedite the test process. Although they avoid damaging the test structure, practical limitations in using these techniques were reported. A new nondestructive testing method making use of shearography will be presented. The shearographic speckle pattern of the test surface is first recorded using a digital camera system. Another speckle pattern is recorded when the test surface is compressed by a punch traveling in a direction normal to the surface. Comparison of the two images results in a fringe pattern depicting the relative surface deflection in the vicinity of the indented region, hence enabling determination of the modulus of elasticity of concrete. Preliminary test results have demonstrated that this technique has great potential for developing into a practical tool for in-situ evaluation of concrete strength.

P50 Nondestructive Testing of Specularly Reflective Objects Using Fringe Reflection Technique

Y.Y. Hung[1] and H.M. Shang*,[2]
[1] *Department of Manufacturing Engineering and Engineering Management, City University of Hong Kong, Kowloon, Hong Kong*
[2] *Temasek Laboratories at NTU, School of Mechanical and Aerospace Engineering, Nanyang Technological University, Singapore*
*E-mail: mhmshang@ntu.edu.sg

For inspecting objects having mirror-like or specularly reflective surfaces, traditional optical techniques that are

normally developed for diffuse surfaces are no longer useful. A simple method will be presented for the detection of surface and sub-surface defects in such objects. In this method, a computer-generated fringe pattern is first programmed and then displayed on a TV monitor. When the TV monitor is placed in front of a specularly reflective object, the virtual image of the fringe pattern as seen by the observer (or as recorded by a camera) will be distorted in accordance with the slope of the object profile. Thus, if a planar surface is used as reference, the difference in distortion of the fringes observed from the object surface and the planar surface will describe the local slope of the object surface. If two virtual images of the fringe pattern on the test object are recorded, one before and another after the application of an incremental load, the corresponding change in the local slope of the object will be obtained from the recorded information. As slope-related information is retrieved, this technique is very sensitive to small deviations from the reference profile, hence enabling detection of sub-surface defects.

P51 Sonic-Shearography — An Optical Technique for Assessing Bonding Integrity in Structures

Y.Y. Hung[1] and H.M. Shang[*,2]
[1] *Department of Manufacturing Engineering and Engineering Management, City University of Hong Kong, Kowloon, Hong Kong*
[2] *Temasek Laboratories at NTU, School of Mechanical and Aerospace Engineering, Nanyang Technological University, Singapore*
*E-mail: mhmshang@ntu.edu.sg

Many useful optical nondestructive testing techniques were developed for surface profiling, displacement and strain measurements, and flaw-detection. These techniques have the advantage of being non-contacting and can provide full-field results very rapidly using high-speed portable computers. Shearography, a double-exposure interferometric technique giving direct measurement of surface slopes or surface displacement-gradients, has gained wide acceptance due primarily to its insensitivity to environmental instability during testing. When applied to detecting debonds in layered structures, vacuum stressing or thermal load-increments are frequently used between the two exposures. Steady-state periodic excitation is also used for detecting debonds in laminated panels: the structure is excited using a single frequency that is close to the resonance of the debonded region. However, the main drawback for using single excitation frequency is that the selected frequency may not be near the natural frequency, hence the inability to detect the debond. In this presentation, broadband-frequency excitation is used so that the surface of the test structure is excited continuously over a wide range of frequencies covering the natural frequencies of the debonded regions, thereby alleviating the drawback of the single-frequency excitation technique. This technique may also be applied to testing of improper mechanically fastened joints.

P52 Ruthenium as Barrier/Seed Layer for Cu/low-*k* Metallization: Crystallographic Texture, Roughness, Diffusion and Adhesion

M. Damayanti[*,1,2], T. Sritharan[1], Z.H. Gan[1], S.G. Mhaisalkar[1] and N. Jiang[3]
[1] *School of Materials Science and Engineering, Nanyang Technological University*
[2] *Chartered Semiconductor Manufacturing Ltd, Singapore*
[3] *Institute of Microelectronics, Singapore*
*E-mail: martina_dy@pmail.ntu.edu.sg

Ru is examined as barrier/seed layer in different layer stacks, with and without Ta, for a Cu/low-*k* system. Ru was found to promote a more pronounced Cu(111) texture than Ta, and the texturing appears to increase with increase of the Ru layer thickness. PVD Cu films on both Ru and Ru/Ta layers are adequately smooth with RMS roughness $\sim$0.8–1.4 nm. Ru crystals on a low-*k* layer have a columnar microstructure. Cu diffusion occurred into low-*k* through the 10 nm Ru barier after thermal anneal at 300°C for 1 h. The four point bend adhesion study demonstrates a sufficiently high Ru/low-*k* adhesion strength ($\sim$6 J/m^2) in comparison to Ta/low-*k* ($\sim$6.5 J/m^2).

P53 Monitoring Delocalization of Molecular Orbitals in 4-Fluoro-Benzenethoil Monolayer into Au(111)

Li Wang*, Wei Chen, Lei Liu and Andrew T.S. Wee[†]
Department of Physics, National University of Singapore
E-mail: *phywl@nus.edu.sg; [†]phyweets@nus.edu.sg

Molecules containing a high degree of -conjugation have been of great interest due to their novel and unique properties. Although it is accepted that the molecule/substrate junction plays a crucial role in these properties, the details on the coupling between molecule and supporting material still need to be understood.

Two types of 4-Fluoro-Benzenethoil monolayers on Au(111) were prepared by depositing molecules directly onto a clean Au(111) (sample A with a tilt angle of 62°) or forming a self-assembly monolayer in solution (sample B with 27°), the tilt angle being confirmed by x-ray absorption measurements. Resonant enhancements of the valence band electrons are observed in sample B when the photon energy sweeps across the C K-edge region, indicating the localized nature of the LUMO and LUMO+1 orbitals; in contrast, negligible resonant enhancement is detected in sample A, revealing that the excited electrons are considerably localized in the orbitals for sample A. Our results are in good agreement with DFT calculations (Transiesta program): strong hybridization between the molecular orbitals and Au occurs when the tilt angle increases from zero (molecule standing up on the surface) to 90 degrees (molecule lying on the surface), as a consequence, the molecular orbitals start to delocalize into Au substrate when lying down.

P54 Self-Organized Nanodot Formation on InP(100) by Argon Ion Sputtering

Tan Sian Khong[1] and Andrew Wee Thye Shen[2]
Department of Physics, National University of Singapore
E-mail: [1]scip1156@nus.edu.sg; [2]phyweets@nus.edu.sg

In recent years, the formation of nanostructures on semiconductor surfaces has attracted much interest due to their potential for applications in low-dimensional devices, particularly as ordered quantum nanodots for optoelectronics and quantum devices. Low energy ion sputtering using inert gases such as argon has been shown to be a promising non-lithographic, and hence simpler technique for the formation of surface nanostructures. In this work, we report the formation of self-organized ordered nanodots array on InP(100) by argon ion beam sputtering. We investigate the dependence of InP nanodot array formation on the ion beam incident angle, sample temperature, incident ion dose and ion current density. In our study, a hexagonal nanodot array with a coherence length of greater than 500 nm and mean dot diameter of 85 nm can be produced by 1 keV Ar^+ beam sputtering at normal incidence with the correct sputtering conditions. We have performed *in-situ* XPS analysis o the nanodot array and excess elemental In is found due to the preferential sputtering of P. Based on scaling theory, the temporal evolution of the sputtered surface can be divided into two different regimes: coarsening in the early-time regime and ordering in the late-time regime.

P55 Pentacene Thin Film Growth on Gold and Silver: Substrate Effect on Molecule Orientation and Film Structure

Yi Zheng[1], Dongchen Qi[1], N. Chandrasekhar[1,2], Xingyu Gao[1] and Andrew T.S. Wee[1,*]
[1]*Department of Physics, National University of Singapore, 10 Kent Ridge Crescent, Singapore, 119260*
[2]*Institute of Material Research and Engineering (IMRE),*
[3]*Research Link, Singapore, 117602*
E-mail: G0301319@nus.edu.sg

Pentacene thin film structure of more than one monolayer on gold substrates is currently controversial: some authors postulate a flat-lying layer by layer growth [1, 2], while the others declaring a dewetting and island growth with an upright orientation of molecules [3]. In this paper, pentacene thin films from 5 nm to 150 nm thickness on gold and silver have been studied using angle-dependent near-edge X-ray absorption fine structure (NEXAFS) spectroscopy. We observe that pentacene forms a well-defined thin-film structure on silver substrates with the long molecule axis perpendicular to the substrate plane. In contrast, for gold substrates, the strong dewetting effect leads to an island growth and a mixture of flat-lying and upright configurations.

References

[1] J.H. Kang and X.Y. Zhu, Appl. Phys. Lett. **82**, 3248 (2003).
[2] W.S. Hu, Y.T. Tao, Y.J. Hsu, D.H. Wei and Y.S. Wu, Langmuir **21**, 2260 (2005).
[3] G. Beernink, T. Strunskus, G. Witte and Ch. Woll, Appl. Phys. Lett. **85**, 398 (2004).

P56 Surface Science Studies at the SINS Beamline

Xingyu Gao*[,1], Dongchen Qi[1], Shi Chen[1], A.T.S. Wee[1], Ti Ouyang[2], Kian Ping Loh[2], Xiaojiang Yu[3] and Herbert O. Moser[3]
[1]*Physics Department, National University of Singapore*
[2]*Department of Chemistry, National University of Singapore*
[3]*Singapore Synchrotron Light Source, National University of Singapore*
*E-mail: phygaoxy@nus.edu.sg

Synchrotron radiation based techniques, such as X-ray photoemission spectroscopy (XPS) and X-ray absorption spectroscopy (XAS)/X-ray absorption near edge structure (XANES), are powerful tools for studying novel materials from thin films to nanostructures with surface sensitivity. These techniques can offer unique electronic, magnetic, chemical, and even some structural information. The SINS beamline at Singapore Synchrotron Light Source (SSLS) is ideal for the photoemsisison (XPS/UPS) and XAS to study the surface, interface, and nanostructure science. As an example, the study of negative electron affinity of diamond (100) surface induced by Diels-Alder reaction of 1,3 butadiene dosed on the diamond surface is presented. It gives apossible combination of NEA effect with organic functionalization of diamond surfaces. C K-edge XANES study of various samples are also presented, which include nanographite, polymer film and hydrogenated diamond.

P57 Growth and Characterization of Ferromagnetic MnSb Films on HOPG

Zhang Hongliang, Sunil S. Kushvaha, Andrew T.S. Wee and Wang Xuesen
Department of Physics and
NUS Nanoscience & Nanotechnology Initiative
National University of Singapore
E-mail: g0403679@nus.edu.sg

MnSb is a promising spintronic material due to its high spin polarization. Here, ferromagnetic MnSb crystallites and films (with thickness of 100 nm) were grown on highly orientated pyrolytical graphite HOPG by co-evaporation of Mn and Sb in ultrahigh vacuum. The surfaces of these structures were investigated by *in situ* scanning tunneling microscopy (STM). With large scale STM images, the films featured essentially hexagonal-shaped surface morphology. When down to atomic resolution, STM images shown that the MnSb surface exhibited 2×2 reconstruction regarding MnSb(0001) plane. Further *ex situ* X-ray photoelectron spectroscopy study on the core level revealed that the Mn 2*p* peaks shift 3 ev with respect to pure Mn, indicating the formation of MnSb compound. Magnetic properties of the polycrystalline films measured by vibrating sample magnetometer (VSM) will also be presented.

P58 Surface XAFS Using a Total Electron Yield Detector

T. Liu*, X.Y. Gao, Andrew Wee, P. Yang and H.O. Moser
Surface Science Laboratory, Physics Department, National University of Singapore, 2 Science Drive 3, Singapore 117542
*E-mail: phylt@nus.edu.sg

When a beam of X-rays of a few keV impinges upon matter, it produces secondary emissions including X-ray fluorescence, primary, Auger and secondary electrons. By changing the energy of the incident synchrotron X-ray beam and measuring the intensity of total electron yield (TEY) as a function of X-ray energy, the X-ray absorption fine structure spectra at the absorption edge of a specific element can be collected, due to the fact that the collected TEY is closely associated with the X-ray absorption coefficient of the element. A simple detector using this principle was developed at the XDD beamline with photon energy range of 2.5–10 keV at the Singapore Synchrotron Radiation Light Source (SSLS). Compared with conventional XAFS using transmission and fluorescence mode, the XAFS in TEY mode is thought to be a surface sensitive technique and works efficiently for thick and concentrated specimens which cannot be measured by other modes of XAFS, and it also suffers less from the self-absorption effect than in fluorescence mode.

The performance of this detector has been tested at XDD. It is shown that the measured spectra are closely related to the ambient between the samples and the collecting anode. In helium ambient, the most significant oscillations of XAFS can be achieved; however the oscillating amplitudes are still smaller than those measured in transmission mode. The mechanism of this reduction of amplitude is analyzed and discussed. The XAFS spectra measured from pure metal foils proves that this mode is very surface sensitive: any contaminations at the surface can induce a distortion of spectra, so a clean surface is a critical requirement for obtaining real structural information.

Despite its limitations, XAFS in TEY mode is promising for XAFS studies to obtain elemental information such as valence state, local symmetry, atomic arrangement of atoms specifically at the surface or near surface. Some examples will be presented to demonstrate the performance of this technique.

P59 Gold and Silver Coated Carbon Nanotubes: An Improved Broad-Band Optical Limiter

K.C. Chin*, A. Gohel, W.Z. Chen, H.I. Elim, G.L. Chong, C.H. Sow and A.T.S. Wee
NUS Nanoscience and Nanotechnology and Department of Physics, National University of Singapore, 2 Science Drive 3, Singapore 117542
*E-mail: nnickc@nus.edu.sg

5-nm-thick coatings of polycrystalline gold and polycrystalline silver were deposited on multiwalled carbon nanotubes. Their optical limiting (OL) properties were studied as a suspension in water at 532 nm and 1064 nm wavelengths by nanosecond laser pulses. Results show that they possess stronger OL performance compared to pure carbon nanotubes at 532 nm. We propose surface plasma absorption (SPA) of Au and Ag as the mechanism responsible for the enhancement of nonlinear scattering effects. These new composite nanomaterials are promising candidates as broad-band optical limiter for the protection of optical sensors in the visible and infrared wavelength ranges.

P60 Materials Patterning by Atomic Force Microscopy Nanolithography

Xian Ning Xie*, Hong Jing Chung, Chorng Haur Sow and Andrew Thye Shen Wee
NUS Nanoscience and Nanotechnology Initiative (NUSNNI)
*E-mail: nnixxn@nus.edu.sg

Atomic force microscopy (AFM) offers a versatile tool for nanoscale patterning and fabrication. In this work, we present our recent results[1–7] on AFM nanolithography and characterization for creating nanostructures and diagnosing local electrical features. We investigated the pattern formation by AFM nanolithography on various substrates including silicon, silicon carbide and polymers. The pattern formation mechanism and growth kinetics, etc. were explored. The impact of capillary-condensed water bridge, tip polarity and tip operating velocity on structure formation were discussed. The capability of conducting AFM for spatially resolved diagnosis of local electrical properties was also demonstrated.

References

1. X.N. Xie, H.J. Chung, C.H. Sow, K. Adamiak and A.T.S. Wee, *J. Am. Chem. Soc.*. 127 (2005) 15562.
2. X.N. Xie, H.J. Chung, C.H. Sow, A.A. Bettiol and A.T.S. Wee, *Advanced Materials* 17 (2005) 1386.
3. X.N. Xie, H.J. Chung, C.H. Sow, and A.T.S. Wee, *Appl. Phys. Lett*. 86 (2005) 192904.
4. X.N. Xie, H.J. Chong, C.H. Sow and A.T.S. Wee, *Appl. Phys. Lett*.. 86, 023112 (2005).
5. X.N. Xie, H.J. Chung, H. Xu, X. Xu, C.H. Sow and A.T.S. Wee, *J. Am. Chem. Soc*. 126, 7665 (2004).
6. X.N. Xie, H.J. Chung, C.H. Sow and A.T.S. Wee, *Appl. Phys. Lett*. 84, 4914, (2004).
7. X.N. Xie, H.J. Chung, C.H. Sow and A.T.S. Wee, *Chem. Phys. Lett*. 388, 446 (2004).

P61 A Multilayer Magnetic Force Microscopy Tip and Comparison of Its Imaging Performance with Conventional Tips

Han Gang*, Wu Yi Hong and Zheng Yuan Kai
Department of Electrical and Computer Engineering, National University of Singapore
*E-mail: Han_gang@dsi.a-star.edu.sg

Magnetic force microscopy (MFM) has become an effective tool for investigating magnetic nanostructures by detecting the magnetic stray field distribution of magnetic samples due to its high sensitivity and high spatial

resolution. The performance of MFM is largely determined by its scanning tip. Tips with a higher spatial resolution, higher sensitivity and better stability are always demanded for both fundamental and application researches. Much work has been done to improve spatial resolution by using either high aspect ratio or multilayer coated tips. In this work, we present the fabrication and testing of a multilayer tip in which a central FM layer is antiferromagnetically (AFM) coupled with two thinner FM layers at both sides via an ultrathin Ru layer. The bare tip was coated with a multilayer structure: Ta(5)/NiFe(2)/IrMn(10)/CoFe(4)/Ru(1.0)/CoFe(10)/Ru(1.0)/CoFe(4)/IrMn(10)/Ta(10), with the figures inside the brackets indicating the thickness of each layer in nm. The coating was performed on one side of the bare tip with the presence of an applied magnetic field along the tip axis direction. The performance of the tip has been tested by imaging the longitudinal media. The improvement of spatial resolution and sensitivity has been confirmed by comparing the imaging performance with that of conventional tips.

P62 Structural, Magnetic and Transport Properties of Ge:Mn Thin Films

Hongliang Li, Yihong Wu*, Tie Liu, Zeliang Zhao and Zaibing Guo
Department of Electrical and Computer Engineering, National University of Singapore, 4 Engineering Drive 3, Singapore 117576
Data Storage Institute, DSI Building, 5 Engineering Drive 1, Singapore 117608
*E-mail: elewuyh@nus.edu.sg

Recently Ge-based group IV diluted magnetic semiconductors (DMSs) have received much attention due to their potential applications in spintronic devices. Although intensive studies have been carried out, room temperature ferromagnetism has not been achieved yet. In this work, Ge:Mn polycrystalline thin films with high T_c phases (Mn_5Ge_2, Mn_5Ge_3 and $Mn_{11}Ge_8$) were fabricated on GaAs (001) substrates at a growth temperature of 300°C by varying Ge:Mn flux ratio using molecular beam epitaxy. Raman peak of Ge crystalline phase at a position of 297 cm^{-1} was observed in all samples and the peak intensity decreases with increasing Mn doping concentration. High-resolution TEM analysis was done to examine the microstructure, and the results indicated that high T_c phases were embedded in a diluted magnetic semiconductor matrix. Morphology investigation on the growth samples with AFM indicated a dominant three-dimension growth. The island sizes decreased with decreasing Mn doping concentration. Temperature-dependent and field-dependent magnetization showed T_c values of 335 K, 295 K and above 400 K for $Mn_{11}G_8$, Mn_5Ge_3 and Mn_5Ge_2, respectively. Semiconducting behaviors were observed in the samples and the ratio of ρ_{300}/ρ_{5K} varied with different Mn doping concentration. Differential conductance studies at different temperatures will be done to study the transport properties at the interface between the high T_c phases and diluted magnetic semiconductor matrix with possible applications to spintronics devices.

P63 Transport Properties of High T_c Ge:Mn Granular Wire

Tie Liu[1,2], Yihong Wu*,[1] and Hongliang Li[1,2]
[1]*Department of Electrical and Computer Engineering, National University of Singapore, 4 Engineering Drive 3, Singapore 117576, Singapore*
[2]*Data Storage Institute, DSI Building, 5 Engineering Drive 1, Singapore 117608, Singapore*
[3]*Institute of Materials Research and Engineering (IMRE), 3 Research Link, Singapore 117602, Singapore*
*E-mail: elewuyh@nus.edu.sg

Special attention has been given to group IV semiconductors due to their compatibility with existing silicon technologies. Ge host may also provide the simplest system for investigation of the fundamental origin of the DMS effect. In this work, Ge:Mn granular thin film were fabricated on GaAs (001) substrate at growth temperature of 300°C with molecular beam epitaxy. Raman, TEM and AFM measurements show the granular Mn_5Ge_2 structure embedded in Ge matrix. Temperature-dependent magnetization measured using SQUID shows the T_c above 350°C. To study the transport property of this sample, Ge:Mn thin film was fabricated into 5 μm width bar and connected with four-point electrodes. Differential conductance was measured at temperature from 5 K to 400 K using SQUID. The R-T curve can be explained using hopping conduction. Focused Ion Beam was used to further decrease the width of the Ge:Mn bar down to 1 μm and 100 nm. Differential conductance and R-T curves were compared before and after FIB.

P64 Disorder Induced Bands in First Order Raman Spectra of Carbon Nanowalls

Wang Haomin*, Wu Yihong, Choong Kaishin Catherine, Zhang Jun, Teo Kie Leong, Ni Zhenhua and Shen Zexiang
Department of Electrical and Computer Engineering, National University of Singapore
*E-mail: Wang_Haomin@dsi.a-star.edu.sg

Carbon can be grown into different forms of nanostructures such as fullerene, nanotubes and nanowalls or graphite sheets. Unlike fullerene and nanotubes which are stable thermodynamically, ultrathin graphite sheets tend to become stable only when they are supported by other materials or form self-supported and curved network structures such as the carbon nanowalls (CNWs). In contrast to fullerene and nanotubes which can be synthesized with very high crystalline quality, the open-boundary nature of CNWs inevitable makes the nanowalls highly defective, in particular at the edges. As a simple but powerful tool for investigating the phonon structures of various types of carbons, Raman spectroscopy is particularly suitable for studying the structural properties of carbon nanowalls. In this work, Raman spectra of carbon nanowalls grown using microwave plasma enhanced chemical vapor deposition were analyzed. A typical Raman spectrum of carbon nanowalls exhibits three main bands, i.e., the G, D and D' bands centered at about 1580, 1350 and 1620 cm^{-1}, respectively. The peak intensity ratio of D to G band (I_D/I_G) was found to be strongly influenced by the ratio of the total edge length of carbon nanowalls over the area of CNWs sample which is accessible by the laser beams, suggesting

that the strong D band is originated from the defects at the edges. The addition of water during the growth process resulted in the increase of relative intensity of the D band, which is attributed to the increase of defects formed by water assisted oxidization of the nanowalls.

P65 Water and Biological Compatibility of Poly(3,4-Ethylenedioxythiophene)

Emril Mohamed Ali*, Hsiao-hua Yu, Shujun Gao and Jackie Y. Ying
Institute of Bioengineering and Nanotechnology, Singapore
*E-mail: emril@ibn.a-star.edu.sg

Conducting polymer is a unique organic semiconducting material that can integrate organic chemistry with electronic and electrical system such as MEMS devices. The polymers can be directly coated onto exposed electrode surfaces by electropolymerization, which simplifies its integration process with MEMS devices. As a result, the polymer could be an ideal platform for biosensor application. However, one major issue with functional conducting polymer is its water and biological compatibility. Among all conducting polymers, poly(3,4-ethylenedioxythiophene) (PEDOT) is of particular interest due to its unique molecular structure and physical properties. Herein, we will demonstrate the compatibility of PEDOT in biological serum, electrolytes and buffers. In addition, PEDOT demonstrates low cytotoxicity on various cells. The combination of these properties makes it ideal as a robust biosensor.

P66 Silica-Incorporated Polyelectrolyte Fibrous Scaffolds for Tissue Engineering

Benjamin C.U. Tai*, Andrew C.A. Wan, Kwong-Joo Leck and Jackie J.Y. Ying
Institute of Bioengineering and Nanotechnology
*E-mail: btai@ibn.a-star.edu.sg

The synthesis of silica-incorporated polyelectrolyte fibres is described in this work. The incorporation of the inorganic silica component into the fibres was achieved by combining the polymerization of hydrolysed tetraethylorthosilicate (TEOS) with the process of interfacial polyelectrolyte complexation between chitosan and alginate. The presence of silica in the fibres was verified using photoacoustic Fourier-transform infrared spectroscopy as well as energy dispersive X-ray (EDX) analysis. Furthermore, the swelling behaviour of the polyelectrolyte fibres as a function of the amount of silica incorporated was investigated using light microscopy. The results indicate that the maximum swelling ratio of the fibres decreases with increasing silica incorporation, reaching a minimum of approximately 300% when 17% (v/v) of hydrolysed TEOS was used. With its reduced swelling properties, the silica-incorporated polyelectrolyte fibres could be processed by hydroentanglement to obtain non-woven porous, fibrous scaffolds. Through this aqueous, room-temperature fiber process, specific biomolecules and ligands could be presented to achieve "tailor-made" scaffolds for tissue engineering applications.

P67 Molecular Dynamics Simulation on the Stretching of a Nanofiber

M. Deng[1], S.Y. Ng[2], V.B.C. Tan*[,1,3] and C.T. Lim[1,2,3]
[1]*Department of Mechanical Engineering,*
[2]*Division of Bioengineering and*
[3]*Nanoscience and Nanotechnology Initiative*
*E-mail: mpetanbc@nus.edu.sg

Molecular dynamics simulation together with first principle DFT calculations were used to elucidate experimental observations of the response of PCL nanofibers subjected to tensile loads. Physical testing reveals that when PCL fibers of nominal diameters 50∼250 nm are stretched, multiple necked regions form at strains of up to 60%. On further loading, the fibers thin down uniformly with no discernable localised deformation. By restraining some parts of a PCL molecular chain model to represent the polycrystalline nature of PCL fibers, atomistic simulations of the chain under tensile strain replicated the transition from a multiple neck fiber to a uniform fiber as the strain increases from 60% to 200%. The simulations show that this phenomenon is result of stiff crystalline phases thinning out at a higher strain than the compliant amorphous phases of the fiber.

P68 Investigation of the Rheological Properties of Fibroblasts Using Micropipette Aspiration

E.H. Zhou[1,3], C.T. Lim*[,1,2] and S.T. Quek[2]
[1]*Division of Bioengineering,*
[2]*Department of Mechanical Engineering and*
[3]*Department of Civil Engineering,*
National University of Singapore
*E-mail: ctlim@nus.edu.sg

Single cell biomechanical experiments and computational modeling are increasingly being used to evaluate the mechanical properties of living cells. Here, we will model the micropipette aspiration experiment to obtain the viscoelastic properties of single cells. We will extend the commonly used standard linear solid model into the standard neo-Hookean solid model to model the large deformation of adherent-type cells in response to micropipette aspiration. The effects of pipette radius and fillet radius on the rheological behaviour of the cell will also be systematically studied. Based on the computational results, three relationships will be obtained to interpret the mechanical response arising from the micropipette aspiration of the cytoskeleton-rich cells.

P69 Nanomechanical Characterization of Hard-Tissues

Gayathri Subramanyam[1], Teo Kay Wah Alvin[1], Lim Chwee Teck[2] and Suresh Valiyaveettil*[,1]
[1]*Department of Chemistry, National University of Singapore, Singapore 117 543*
[2]*Department of Nano Biomechanics Laboratory, Division of Bioengineering, National University of Singapore, Singapore 117576*
*E-mail: chmsv@nus.edu.sg

Biominerals are usually composites containing a very low percentage of organic matrix amidst a dense mineral

phase. These biocomposites are renowned for their mechanical strength and toughness. The hierarchical structural arrangement of the mineral in combination with the astute placement of the organic matrix (containing biomacromolecules) imparts very special mechanical properties to the composites. In the present study, we investigate the nanomechanical properties of the shells of giant clams, *Tridacna squamosa* (Mollusca, Bivalva), at various stages of the biomineral formation. The shells were sampled at different stages of growth for our investigations. The morphological studies on the shells were carried out using scanning electron microscopy (SEM). The compositions of the shells were analyzed using FTIR, XRD, Raman spectroscopy. We identified the adult shell to be comprised of the mineral aragonite and about < 1% of proteoglycans as the organic matrix. The juvenile shells were composed of an addition metastable amorphous phase that eventually transforms to a more stable aragonitic phase. Understanding the mechanistic aspects involved here may shed light on hard-tissue fabrication in natural systems.

References

1. S. Kamat, X. Su, R. Ballarini and A.H. Heuer, *Nature* 2000, 405, 1036–1040.
2. I.M. Weiss, N. Tuross, L. Addadi and S. Weiner, *J Exp Zool*, 2002, 293, 478–491.

P70 Tissue Engineering of Skin Using Nanofibrous Scaffold

E.J. Chong[1,4], Y.Z. Zhang[1,2], C.T. Lim[*,1,2,4], T.T. Phan[1,3] and S. Ramakrishna[1,2,4]
[1]*Division of Bioengineering,*
[2]*Department of Mechanical Engineering,*
[3]*Department of Surgery, and*
[4]*Nanoscience and Nanotechnology Initiative*
*E-mail: ctlim@nus.edu.sg

The current design for a tissue engineering (TE) skin substitute is that of a biodegradable scaffold through which fibroblasts can be seeded, migrate and populate. This artificial 'dermal layer' needs to 'take' to the wound, which is not always successful for the current artificial dermal analogues available. The high cost of these artificial dermal analogues also makes its application prohibitive both to surgeons and patients, and in specific cases, ethical issues may be involved too. In this study, a nanofiber construct is produced by electrospinning nanofibers onto a Tegaderm™ wound dressing as a cost-effective scaffold for fibroblast integration and proliferation. It is hoped that this will result in a fibroblast populated three-dimensional dermal analogue which could be feasible for layered applications approach to build up thickness of dermis prior to re-epithelialisation. The results obtained in this study suggest that the fibroblasts populated TG-NF construct, achieved significant cell adhesion, growth and infiltration results. Thus, this is a successful first step for the TG-NF construct in establishing itself as a suitable three-dimensional scaffold for autogenous fibroblasts population, which is important in the treatment of dermal wounds. Further studies and analysis are ongoing to confirm the use of TG-NF construct as a suitable dermal analogue for layered application in wound healing.

P71 Nanohybrid Thin Films of Functional Titania (TiO_2) and Lead Zircomium Titanate (PZT) Nanoparticles by Block Copolymer Templating

Akhmad Herman Yuwono*, Zhou Zhaohui and John Wang
Dept. of Materials Science and Engineering,
Faculty of Engineering,
National University of Singapore,
Blk EA # 07-40, 9 Engineering Drive 1, Singapore 11576
E-mail: scip1063@nus.edu.sg

Nanohybrid thin films consisting one or more nanocrystalline ceramic phases in an appropriate polymer matrix represents a new class of potentially important functional materials for a number of applications. While most of the existing synthesis routes for such nanohybrids lead to a lack in uniformity of the inorganic-organic nanostructures, we have successfully devised a novel templating synthesis route, where poly(methylmethacrylate)-b-polyethylene oxide (PMMA-PEO) and polystyrene-b-polyethylene oxide (PS-b-PEO) block copolymers are employed as the building block for obtaining highly ordered arrays of titania (TiO_2) and lead zirconium titanate (PZT) nanoparticles. By controlling the processing parameters involved in the templating procedures, nanocrystalline oxide particles of 3 to 7 nm in sizes can be assembled in the hexagonal and cubical hierarchical structures. Such bottom-up fabrication techniques are attractive for generating patterns which are smaller in size than those produced by lithography techniques. Besides, the technique is also simple and cost-effective. The resulting highly ordered arrays of functional nanostructures are promising for a number of technologically demanding areas, as many optoelectronic, micromechanical and biomedical devices are continually miniaturized.

P72 Effects of $SrRuO_3$ Buffer Layer on Film Textures and Electrical Properties of $BiFeO_3$ Thin Films

Gao Xingsen, Zhen, Rongyan, Xue Junming and Wang John
Department of Materials Science and Engineering,
Faculty of Engineering
National University of Singapore
Singapore 117576
*E-mail: msewangj@nus.edu.sg

$BiFeO_3$ thin films have been extensively investigated recently, owing to its unique magnetic and electrical properties, which promise for a wide range of device applications. However, it is technologically challenging to realize well defined $BiFeO_3$ thin films on silicon wafers. This paper reports a RF sputtering process for depositing desired $BiFeO_3$ thin films on $Pt/SiO_2/Si$ substrates. Single phase $BiFeO_3$ was successfully deposited by RF magnetron sputtering on $Pt/SiO_2/Si$ substrates at an ambient temperature range of 500–650°C, when a thin $SrRuO_3$ buffer layer was employed as a buffer layer, while a large amount of impurity phase occurs without such buffer layer. The significant effects of the buffer layer were also observed on

the ferroelectric, dielectric, and leakage properties of the $BiFeO_3$ thin films. It not only acts as seedings for nucleation of $BiFeO_3$ phase, but also changes the interfacial behaviors, hence greatly improving the electrical properties. $BiFeO_3$ thin films exhibit well established hysteresis loop of square shape with an enlarged polarization, which is desirable for nonvolatile ferroelectric memories.

P73 Fe_3O_4 Nanoparticles in Polymer Matrix

Zhaohui Zhou and John Wang*
Department of Materials Science and Engineering, Faculty of Engineering, National University of Singapore
*E-mail: msewangj@nus.edu.sg

A wet chemistry approach has been devised successfully for *in-situ* formation of magnetic spinel nanoparticles in Nafion membrane. When trivalent Fe cations are used, amorphous precipitates with an interconnecting morphology were observed at the formation temperature of 60°C, which was attributed to the unique structure of the membrane. An increase in reaction temperature resulted in a slightly enhanced nanocrystallinity. Nanoparticles of $Fe(OH)_3$ formed at 120°C showed a very weak magnetization (0.11 emu/g at 5 T). When both Fe^{2+} and Fe^{3+} cations were present in the membrane, the magnetization of the resulting nanocomposites was enhanced dramatically (Ms of 1.7 emu/g) as a result of the formation of a spinel magnetic phase Fe_3O_4, which was derived from the intermediate phase $Fe(OH)_3$. In the presence of the polymer matrix, the crystallite size, phase formation process and morphology of the nonoparticles formed within the membrane can be controlled and adjusted by several experimental parameters and conditions involved, such as the ion-exchange time, reaction temperature and reaction time.

P74 Structures and Dielectric Anomalies of $Pb_{0.7(1-x)}Ca_{0.7x}La_xTiO_3$

H.P. Soon and J. Wang
Department of Materials Science and Engineering, Faculty of Engineering, National University of Singapore, Singapore 117576
*E-mail: msewangj@nus.edu.sg

By increasing x from 0.10 to 0.60 for $Pb_{0.7(1-x)}Ca_{0.7x}La_{0.2}TiO_3$, transitions from normal ferroelectric to dipolar glass and then to quantum paraelectric-like behaviour (QPB) are observed. Raman spectra of these compositions explicitly indicate the formation and growth of dipolar clusters upon cooling from 425 to 80 K, which has not been commonly observed in the typical relaxors. More interestingly, a non-vanishing E(1TO) mode that corresponds to the displacement of *A*-site cation with respect to Ti^{4+} and oxygen octahedral, has been obtained at $\sim 40\,cm^{-1}$ for $Pb_{0.7(1-x)}Ca_{0.7x}La_{0.2}TiO_3$ with $0.50 \leq x \leq 0.60$, where the predicted local phase transition temperatures for these compositions are −348 and −897 K respectively. Detailed analyses on the Raman spectra of $Pb_{0.7(1-x)}Ca_{0.7x}La_{0.2}TiO_3$ with $0.30 \leq x \leq 0.40$ suggested coexistence of a new QPB and tetragonal phases, where the amount of tetragonal phase increases with decreasing x. The *ab* intio indexing performed to the synchrotron XRD traces of $Pb_{0.7(1-x)}Ca_{0.7x}La_{0.2}TiO_3$ with $x = 0.55$ and 0.60 suggested an average cubic structure in contrast to the superlattice structure of $CaTiO_3$ that resulted in the positive soft E(1TO) mode down to 0 K. In this study, the crystal structure and occurrence of anomalous thermal hysteresis at $0.30 \leq x \leq 0.40$ and QPB at $0.55 \leq x \leq 0.60$ are plausibly correlated.

P75 Ferroelectric Properties of Heterolayered PZT Films with PT Buffer Layer

F.C. Kartawidjaja, Z.H. Zhou and J. Wang
Department of Materials Science and Engineering, Faculty of Engineering, National University of Singapore, Singapore 117576
E-mail: g0500513@nus.edu.sg

Heterolayered ferroelectric $Pb(Zr_{1-x}Ti_x)O_3$ (PZT) thin films, consisting of alternating $PbZr_{0.7}Ti_{0.3}O_3$ and $PbZr_{0.3}Ti_{0.7}O_3$ nanolayers, have been successfully fabricated via a sol gel route from metal-alkoxide solutions. The multilayer structures are successfully realized by alternating spin-coatings on $Pt/Ti/SiO_2/Si$ substrate. $PbTiO_3$ (PT) layer was chosen as a buffer layer to suppress PbO volatilization, thus avoiding the formation of rosette structure. A preferential (001)/(100) orientation is present in the heterolayered films thermally annealed at 500°C and then at 600°C for 1 hour, due to the coupling and interaction between the alternating layers assisted by annealing temperature. The heterolayered thin films showed superior ferroelectric and dielectric properties, as compared to $PbZr_{0.7}Ti_{0.3}O_3$ and $PbZr_{0.3}Ti_{0.7}O_3$ multilayered films. The remanent polarization and coercive field of six-heterolayered PZT film were measured to be $38.9\,\mu C/cm^2$ and 90.38 kV/cm, respectively. Their dielectric constant and dielectric loss at 100 Hz were 1270 and 0.0397, respectively. The much improved ferroelectric properties of the heterolayered films suggest that there is coupling mechanism between the alternating layers with different structure (rhombohedral and tetragonal). A further interesting phenomenon is that the reversible polarization gives a higher contribution to hysteresis loop of the heterolayered PZT films, as compared to the multilayered PZT thin films. This is attributed to the switching of 180° domains in the heterolayered films.

P76 Ordered Mesoporous 70 wt% SiO_2-30 wt% CaO Bioactive Glasses as Drug Carriers

D. Lukito, J.M. Xue* and J. Wang
Department of Materials Science and Engineering, Faculty of Engineering, National University of Singapore
*E-mail: msexuejm@nus.edu.sg

Bioactive glasses of high bioactivities are excellent candidates for bone filling applications. However, when they are used as bone filler, inflammation of bone caused by a pyogenic organism might occur. In this paper, antibiotic gentamicin used to treat the inflamation was incorporated into the ordered mesoporous bioactive glasses. The drug release profiles are monitored and the effects of drug loading on bioactivities have been studied. In order to optimize the drug release behaviors, PLGA biodegradable polymer

was employed to encapsulate the drug loaded bioactive glasses to form composite microspheres. Effects of the microsphere encapsulation on bioactivities of the composites have been investigated. The results showed that bioactivities of the drug loaded bioactive glasses were reduced as compared to those of the bioactive glasses without drug loadings while PLGA microsphere encapsulation on drug loaded bioactive glasses did not further inhibit the bioactivities.

P77 Functional Nanohybrids and Mesoporous Thin Films

John Wang*, A.H. Yuwono and Zhang Yu
Department of Materials Science and Engineering, Faculty of Engineering, National University of Singapore, Singapore 117576
*E-mail: msewangj@nus.edu.sg

A number of novel functional (electrical, optical and magnetic) properties have been demonstrated by mesoporous oxides and nanohybrids consisting of one or more nanocrystalline inorganic phases dispersed in a suitable polymeric matrix. Although several new synthesis routes have been attempted for fabrication of these nanostructured materials, there is often a lack of proper control in nanocrystallinity of the resulting mesoporous and nanohybrid structures, where the kinetics involved are restricted by the relatively low synthesis temperatures involved. To realize the well controlled mesoporous structures and nanohybrids of enhanced nanocrystallinity, we have devised surfactant and di-block polymer templatings, where the hydrophilic and hydrophobic structures are effectively used as the assembling blocks. In combination with an appropriate hydrothermal treatment in water vapor, we have successfully synthesized TiO_2-based mesporous and nanohybrid thin films with remarkably enhanced nanocrystallinity, where the rearrangement of flexible Ti-O-Ti bonds are promoted. In this talk, the wet-chemistry and several parameters involved in surfactant and di-block polymer templatings will be discussed for their effects on the resulting TiO_2-based mesoporous and nanohybrid thin films, as well as on the functional properties of these nanostructured materials.

P78 Kinetics of Incorporation in 2D Crystal Growth

Tian-Hui Zhang and Xiang-Yang Liu*
Physics Department, Blk S12, Faculty of Science, National University of Singapore, 2 Science Drive 3, Singapore 117542
*E-mail: phyliuxy@nus.edu.sg

Kinetics of the incorporation of individual particle in crystal growth is studied in colloidal system. The two-dimensional crystallization of negatively charged colloidal particles is induced by alternating electric field. Digital imaging records the dynamic process in a resolution which allows us to resolve the motion of individual particles. It is found that there are two kinds of distinct kinetics which dominate the small crystal nuclei and large crystal cluster respectively. This further understanding of the incorporation may help us apply effective control on the crystal growth, especially the growth of small crystal nuclei.

P79 Antifreeze Protein: From Interfacial Structure to Antifreeze Effect

Ning Du*, Xiang Y. Liu and Choy L. Hew
Biophysics & Micro/nanostructures Lab, Department of Physics, National University of Singapore, 10 Kent Ridge Crescent, Singapore 119260
*E-mail: phydn@nus.edu.sg

Antifreeze Proteins (AFPs), occurring in some polar animals and plants, are capable of inhibiting ice freezing at subzero temperatures. The antifreeze effect of Antifreeze Proteins on ice nucleation, which was neglected in most studies, was examined based on a "micro-sized ice nucleation" technique in this study. It follows from our experiments antifreeze proteins can inhibit the ice nucleation process by adsorbing onto both the surface of ice nuclei and dust particles, which leads to an increase of the ice nucleation barrier and the desolvation kink kinetics barrier, respectively. It was found that the antifreeze activity of AFPs can be enhanced either by their aggregation at higher concentration or by adding electrolyte into AFPs solutions. This promotion in antifreeze activity is attributed to the rise of surface activity for AFPs aggregates compared to AFPs monomers, and the screening effect of electrolyte to the surface charge of AFPs molecules, respectively. This study enables us to obtain a comprehensive understanding on the antifreeze mechanism of AFPs for the first time.

P80 Two Scenarios of the Colloidal Phase Transitions

Ke-Qin Zhang and Xiang Y. Liu*
Department of Physics, National University of Singapore, 2 Science Drive 3, Singapore 117542
*E-mail: phyliuxy@nus.edu.sg

Solid-liquid phase transitions form one of the fundamental topics in condensed matter physics. Their study has received a new impulse since phase transitions can be observed at the microscopic level by employing the development of direct imaging in model colloidal systems. Unlike the atoms in conventional materials, the individual colloidal spheres can be imaged with a conventional light microscope on time scales compatible with standard video equipment [1]. Therefore the microscopic structure and dynamics of colloidal suspensions can be studied with atomic-like resolution.

A two-dimensional assembly of charged colloidal particles induced by an alternating electric field was studied in real space by means of digital video microscopy. The phase transitions occur from a highly ordered colloidal monolayer to an isotropic suspension by changing the field strength and frequency (in the appropriate range). In particular, it is found that the strength-dependent phase transition is an infinite-order phase transition rather than a frequency-dependent phase transition, which is a second-order phase transition [2].

References

1. K.Q. Zhang and X.Y. Liu, *Nature* **429** (2004) 739–743.
2. K.Q. Zhang and X.Y. Liu, Unpublished.

P81 Phase Transition of Colloidal Particles under Alternating Electric Field

Yu Liu, Janaky Narayanan and Xiang-Yang Liu
E-mail: G0304884@nus.edu.sg

The two-dimensional (2-D) assemblies of colloidal particles above the electrode surface subjected to ac polarization are studied by varying the frequency and field strength in the absence and presence of added electrolyte. For a given field strength, a lower and an upper cut-off frequency can be identified between which the assembly has a crystalline structure, namely, a long range bond-orientational and translational order. Outside this frequency window, the structure undergoes a crystal-liquid transition. The variation of the translational and bond-orientational correlation functions with frequency suggest the existence of a hexatic phase in which the particles retain the remnants of the crystalline long-range orientational order, but has a liquid-like translational order. This suggests a frequency driven KTHNY transition in 2-D colloidal assembly. The electrohydrodynamic (EHD) flow[1–4] is used to calculate the equilibrium distribution of the particles as the resultant of the two opposing forces — the Stoke's force due to EHD velocity and the screened Coulomb interaction between the colloidal particles. The role played by the EHD flow in the particle aggregation, the existence of a frequency window for colloidal aggregation, the decrease in EHD velocity and hence the increase in inter-particle separation at high frequencies, and the dependence of the equilibrium inter-particle separation on ionic strength and ζ-potential are investigated.

References

1. F. Nadal, F. Argoul, P. Hanusse and B. Pouligny, Phys. Rev. E. **65**, 061409 (2002).
2. W.D. Ristenpart, I.A. Aksay and D.A. Saville, Phys. Rev. Lett. **90**, 128303 (2003).
3. P.J. Sides, Langmuir **19**, 2745 (2003).
4. Y. Liu, J. Narayanan and X.-Y. Liu (submitted to J. Chem. Phys).

P82 Preparation, Microstructure and Magnetic Properties of Co-Ferrite Thin Films with High Coercivity Using Pulsed Laser Deposition

Jianhua Yin[1,2], Jun Ding[*,1], Binghai Liu[1], Xiangshui Miao[2] and Jingsheng Chen[2]
[1]*Department of Material Sciences and Engineering, National University of Singapore, Singapore 119620*
[2]*Data Storage Institute, 5 Engineering Drive 1, Singapore 117608*
*E-mail: msedingj@nus.edu.sg

Co-ferrite films with high coercivity are interesting for various applications including high density magnetic recording and MEMS devices. In this work, Co-ferrite films on (100)-SiO_2 single crystal substrates have been systematically prepared at different substrate temperatures ($27 \sim 900$°C) and under different oxygen working pressure ($2 \times 10^{-2} \sim 2 \times 10^{-7}$ torr). The thickness of all these films was kept at approximate 100 nm. The structure and magnetic properties of the film were analyzed by XRD, AFM, TEM, and AGFM. Co-ferrite film with high room temperature coercivity approximate 10.5 kOe was successfully obtained with substrate temperature at 550°C and under 2 mtorr working pressure. The hysteresis loop of the film using AGFM shows a high perpendicular anisotropy. The XRD patterns and SAED results of the film indicate a large microstrain as well as a texture structure compared with that of the Co-ferrite target. HRTEM micrograph of the film shows that the grain size is approximate 15 nm. AFM image of the film indicates a smooth surface with the root mean square (rms) of surface roughness below 1 nm. The angular dependence of the coercivity of the Co-ferrite film reveals that the stoner-wohlfarth rotation is the predominant magnetization reversal mode. Furthermore, the negative δM deviation means that there is strong dipole interaction between the nanocrystalline grains, which may result in the high coercivity of Co-ferrite films. In summary, the High coercivity of Co-ferrite thin films may be related to the nanocystalline grain size, texture structure, large microstrain, and strong de-coupling interaction between grains.

P83 Fabrication of Alumina Nanowires Using AAO Templates

S. Thongmee[1], J.B. Yi[1], P. Hui[2], J.Y. Lin[2,3] and J. Ding[1]
[1]*Department of Materials Science and Engineering, National University of Singapore, Singapore 117576*
[2]*Department of Physics, National University of Singapore, Singapore 117542*
[3]*Institute of Chemical and Engineering Sciences, Singapore 627833*
E-mail: G0403276@nus.edu.sg

Alumina nanowires were synthesized on anodic aluminium oxide (AAO) templates using electrodeposition. The report presents a new method for AAO template in the fabrication of alumina nanowires. A high yield of alumina nanowires are obtained by etching AAO template in solution of chromic acid. We studied the effects of etching period and concentration of solution. The templates were exposed to air for different time periods varying from 15 hours to 2 months. After the exposure in air, the templates were etched by a solution of 2 wt% chromic acid for 15 min. We found that the alumina nanowires at 15 hours in air are clustered together without an ordered domain and there are pores under the wires. The templates that exposed to air for longer time (2 months) will lead to the formation of the very thin nanowires. The wires are uniform, longer and cover the entire of the template. The thinness of the wire is probably due to the fact that the samples were dried for a longer period. The AAO templates were immersed in solution of chromic acid for different periods of time. In addition, the effect of chromic concentration (1–4 wt%) on the formation of nanowires has been carried out. It is found that the formation of wire is very slow with low concentration. The concentration of 4 wt% chromic acid can form alumina nanowires.

P84 Studies of High-Frequency Magnetic Properties for Rodshaped Half-Metallic CrO_2 Ultrafine Particles

L.Z. Wu[1], J. Ding[1], L.F. Chen[2] and C.P. Neo[3]
[1]*Department of Materials Science, National University of Singapore, Singapore*
[2]*Tamasek Laboratories, National University of Singapore, Singapore*
[3]*DSO National Laboratories, 20 Science Park Drive, Singapore 118230, Sinsapore*
E-mail: Scip1361@.nus.edu.sg

The static and high-frequency magnetic properties (Complex intrinsic permeability μ_i and effective permeability μ_{eff}) have been studied for rod-shaped half-metallic CrO_2 ultrafine particles and composite with non-magnetic matrix. Effective permeability of composite consisting of CrO_2 inclusions embedded in a nonmagnetic matrix (epoxy resin) was calculated using effective medium theory. The theoretically calculated permeability spectra were then compared with experimentally measured permeability spectra of the composite. The results show that CrO_2 have national resonance frequency at around 8 GHz, which is attributed to the relatively large value of the shape anisotropy. The permeabilities μ_0' and μ_{max}'' of are 1.4–1.2 and ~ 0.4, respectively, for composites with 20% (by volume) CrO_2 rod-shaped powders with aspect ration 8:1. The parameters indicate that the rod-shaped CrO_2 may be a good candidate for electromagnetic compatibility and other practical applications at high frequency.

P85 Structural and Property Studies of Co-Doped-ZnO Thin Films Fabricated by Pulsed Laser Deposition Technique

L.H. Van[1,3], M.H. Hong[1,2] and J. Ding[1,3]
[1]*NUS Nanoscience and Nanotechnology Initiative, National university of Singapore, SG 117542*
[2]*Department of Electrical and Computer Engineering, National University of Singapore, SG 117576*
[3]*Department of Material Science and Engineering, Faculty of Engineering, National lJniversity of Singapore, SG 117678*
E-mail: G0306148@nus.edu.se

The structure and properties of Co-doped-ZnO thin films fabricated by Pulse Laser Deposition (PLD) are investigated in this work. Highly crystalline zincite structure was synthesized on (006) Al_2O_3 single crystal sapphire substrate. The growth temperature was ranged from 25°C to 800°C and the 0_2 partial pressure was set constant at 1×10^{-4} Torr. The zincite started to form at a relatively low temperature, 100°C. The XPS results shown that only 5% Cobalt were doped into the ZnO matrix while the XRD shown that only single zincite (002) phase is formed with no cobalt segregation is detected. The full width at half maximum of the zincite (002) peak rocking curve is 0.25°. The thin films are optically transparent from 400 nm to 800 nm and all films showed ferromagnetic property at room temperature. The magnitude of the ferromagnetism is strongly dependent on the substrate deposition temperature. Semiconductors properties of carrier concentration and resistivity were also studied by Hall Effect measurement. The thin films preserve its semiconductor electron carrier density at the range of 10^{21} cm^{-3}. The resistivity increased with the increasing deposition temperature.

P86 Dipolar Interaction of Co/CoO Bilayer by Sputtering

Jiabao Yi and Jun Ding
NUS
E-mail: Scip1124@nus.edu.sg

Co/CoO nanocomposite films were deposited by sputtering with an oxygen partial pressure of 0.0075, 0.015, 0.023, 0.03 mTorr. Co particles in the films were gradually isolated by CoO with the increasing of oxygen partial pressure according to the analysis by HRTEM. Co particles in the film deposited with 0.03 mTorr were found totally isolated by CoO. However, the film still shows ferromagnetism. It is due to the exchange coupling between Co and CoO, which was proved by depositing small amount of Co particles were deposited SiO_2 matrix showing a paramagnetism. Asymmetrical hysteresis loops with shoulder were observed in the film with 0.0023 mTorr O_2 at room temperature and in the film of 0.0075 mTorr at low temperature (4 k). The phenomenon may due to the competition of dipolar interaction of the Co particles and exchange coupling energy. ZFC and FC loop of the films showed that the blocking temperature decreased with the increasing of oxygen partial pressure. For Co particles in the SiO_2 matrix, if the Co amount increased to a certain amount (e.g. 10%), the composite film showed a ferromagnetism, suggesting the dipolar interaction (exchange coupling) is large enough to beat the thermal vibration energy.

P87 Direct Observation of Single-Walled Carbon Nanotube Growth at the Atomistic Scale

Ming Lin, Joyce Pei Ying Tan, Chris Boothroyd, Kian Ping Loh, Eng Soon Tok and Yong-Lim Foo*
Institute of Materials Research and Engineering
*E-mail: yl-foo@imre.a-star.edu.sg

The growth dynamics of single-walled carbon nanotube (SWNT) is observed in real-time using an in-situ ultra-high vacuum transmission electron microscope at 650°C. The SWNTs preferentially grow on smaller sized catalyst particles (diameter ≤ 6 nm) with three distinct growth regimes (incubation, growth and passivation). All the observed SWNTs grow via a base-growth mechanism with C diffusion on active Ni catalyst sites. Under the same experimental conditions, formation of carbon nanocages was observed on larger Ni catalyst particles. The evolution of SWNT or nanocages is dependent on catalyst size, and this can be rationalized from both energetics and kinetics considerations.

P88 NiGe on Ge(001) by Reactive Deposition Epitaxy: An in-situ UHV-TEM Study

Ramesh Nath, Chi Wen Soo, Chris Boothroyd, Mark Yeadon, Dong Zhi Chi, Hai Ping Sun, Yan Bing Chen, Xiao Qing Pan and Yong-Lim Foo*
Institute of Materials Research and Engineering
*E-mail: yl-foo@imre.a-star.edu.sg

We use a UHV-TEM, equipped with an electron-beam evaporator directed at a heating stage in the pole-piece, to follow the reaction pathway of Ni on Ge(001) substrate at 300°C. Using reactive deposition, we illustrate that epitaxial orthorhombic NiGe (a = 5.381 Å, b = 3.428 Å, c = 5.811 Å) phase can be grown directly without the initial formation of metal-rich Ni2Ge phase. The epitaxial orientation of the NiGe islands and the underlying Ge(001) substrate were found to be NiGe(01)//Ge(001) and NiGe[010]//Ge[110].

P89 Segregration of Mechanically Milled Agglomerated Silicon Nanocrystals

H.W. Lau and O.K. Tan*
Nanyang Technological University
*E-mail: eoktan@ntu.edu.sg

Silicon nanocrystals (Si nc) have stirred the research fields for its potential in light emission and charge trapping capability. Synthesis of Si nc is often expensive and tedious. These methods include ion implantation, chemical vapour deposition and electrochemical etching. In this conference, we report on the mechanical milling of Si powder to nanometric size with an average size of 10 nm. This method poses a bulk and inexpensive method of Si nc synthesis. However, agglomeration of Si nc is a serious problem with the usage of method of ball milling. Large particles can cause emission deficiency and lateral charge spreading. The need to segregate these agglomerates is critical. In our approach, an organic solvent (texanol-based) is used to embed the Si nc. Upon homogenizing, these agglomerates are being segregated. Transmission electron microscopic images featuring the segregation of these agglomerates are taken. Coupled with dynamic light scattering results, the particles sizes are further verified. This poses possible avenue of inexpensive and bulk production of Si nc-based optical and memory devices.

P90 The Characterization of Low Temperature Nano-Sized $SrTiO_{3-\delta}$-Based Oxygen Gas Sensor

Y. Hu* and O.K. Tan
Sensors & Actuators Lab, Microelectronics Centre, School of EEE,
Nanyang Technological University, 50 Nanyang Avenue, Singapore 639798
*E-mail: huying@ntu.edu.sg or yinghu67@yahoo.com.cn

Strontium Titanate ($SrTiO_3$) is a very important material for oxygen sensors. In this work, Pt-doped and un-doped nano-sized $SrTiO_{3-\delta}$ powders were synthesized at room temperature using high-energy ball milling technique. The thick film technology was adopted to fabricate the sensors. The powder particle sizes and micro-structural properties of the materials were characterized by XRD and TEM. The sensing properties to 20% O_2 in background N_2 were carried out by the gas sensor characterization system using National Instruments Labview 6.1 system. Experimental results show that the powder particle sizes are milled down to around 30 nm. The highest relative resistance ($R_{N2}/R_{20\%O2}$) of 6.35 is obtained for un-doped nano-sized $SrTiO_{3-\delta}$ sensors with annealing at 400°C and operating at 40°C. The 40°C operating temperature is much lower than that of the conventional low temperature semiconducting oxygen gas sensors (300–500°C) and $SrTiO_3$ oxygen sensors (> 700°C). This can extend the application of the semiconducting oxygen gas sensors from the conventional high and medium temperature to the lower operating temperature areas such as the medical, environmental and domestic fields etc. For 20% O_2 operating at 40°C, the Pt-dopant effectively decreases the response time from 1.6 minutes for un-doped material to 50 sec. for doped material. It is due to the grain size decreasing and dopant catalysis.

P91 Growth and Characterization of SnO_2 Nanorod Array by Plasma Enhanced Chemical Vapor Deposition

Y.C. Lee, O.K. Tan, H. Huang and M.S. Tse
Microelectronics Center, School of Electrical and Electronic Engineering,
Nanyang Technological University, Singapore 639798
E-mail: n030083@ntu.edu.sg

SnO_2 nanorod array have been successfully prepared on SiO_2/Si wafer by RF inductively coupled plasma enhanced chemical vapor deposition (PECVD) using dibutyltin diacetate as precursor. The as-deposited SnO_2 nanorods were well crystallized Cassiterite structure even without additional substrate heating during deposition. The effects of two main deposition parameters, i.e. substrate distance and RF power, on the growth of the SnO_2 nanorods have been studied. The diameter and the length of the nanorods decreased with the continuous increase of substrate distance and RF power. The tailoring of SnO_2 nanorods microstructure was hence achievable by independent control of the growth parameters. The gas sensing properties of the SnO_2 nanorod array were studied. Due to the high surface-to-volume ratio of the SnO_2 nanorods, the SnO_2 nanorod array showed good sensitivity to reducing gases CO and H_2. The SnO_2 nanorods were further doped by Pd and enhanced selectivity to H_2 gas was achieved in the Pd-doped SnO_2 nanorods.

P92 La_2S_3 Thin Films from Metal Organic Chemical Vapor Deposition of Single-Source Precursor

Lu Tian, Ti Ouyang, Kian Ping Loh and Jagadese J. Vittal*
Department of Chemistry,
National University of Singapore, Singapore 117543
*E-mail: chmlohkp@nus.edu.sg or chmjjv@nus.edu.sg

Rare earth chalcogenides have been extensively studied because of their potential applications in electronic, optical, superconducting devices, cold cathode configurations, current controlled devices, switching devices,

photoconducting cells and thermoelectric components. Also rare earth elements make them very attractive for the fabrication of new permanent magnets. Thin films of Lanthanum sulfide (La_2S_3) have been prepared from tris(N,N-diethyldithiocarbamato)(2,2'-bipyridyl) lanthanum (III) precursor ($[La(bipy)(S_2CNEt_2)_3]$) by using metal organic chemical vapor deposition (MOCVD) on different substrates for the first time. The preparative parameters, such as substrate temperature and the nature of substrate, are optimized to get well-defined cubic phase (γ) lanthanum sulfide thin films. The optimized films are characterized by means of X-ray powder diffraction (XRPD) techniques, scanning electron microscopy (SEM), High Resolution Transmission Electron Microscopy (HRTEM) and in-situ X-ray photoelectron spectroscopy (XPS). Electrochemical impedance study indicates that the as-deposited La_2S_3 thin film shows n-type characteristics. This new route may open the way to the creation of nanostructures.

P93 Inorganic Complexes Retain Diethylether Well above Its Boiling Point through $OH_2 \cdots OEt_2$ Hydrogen Bonding

Lu Tian and Jagadese J. Vittal*
Department of Chemistry,
National University of Singapore, Singapore 117543
*E-mail: chmjjv@nus.edu.sg

There has been a sustained interest in the solids that hold onto their gaseous and very volatile guests due to their potential applications as hydrogen, methane and other gas storage materials. Understanding the host-guest interactions is essential in controlling and retaining the guests in the crystal lattice.

The presence of low boiling liquids in the crystal lattice often poses problems in X-ray crystallography. Diethylether (Et_2O) with relatively low boiling point (34.6°C) is no exception as it is frequently used as a precipitant liquid to grow single crystals. The solid state structures of the complexes $[M(2,2'\text{-bpy})(SC\{O\}Ph)_3(H_2O)]\cdot Et_2O$ where M = La (**1**), Pr (**2**) and Sm (**3**) have been found to have an eight-membered ring formed by strong hydrogen bonds between two Et_2O solvates and two aqua ligands. All the three complexes are able to retain Et_2O above its boiling point through O-H $\cdots$ O hydrogen bonds. The inception temperatures for the weight loss of Et_2O are 82, 69 and 51°C for **1**, **2** and **3** respectively.

In summary, the crystal structures and thermal dehydration properties of three unusual lanthanide complexes that retain Et_2O well above its boiling point through O–H $\cdots$O hydrogen bonding has been studied. Further the onset temperature of Et_2O loss from the solid could be controlled by the size of the metal ions in these complexes. Et_2O-free solid **1** is able to take back Et_2O quantitatively.

P94 Synthesis of $CuInSe_2$ and $AgInSe_2$ Nanoparticles from Single Source Precursors

Meng Tack Ng and Jagadese J. Vittal*
Department of Chemistry, 3 Science Drive 3,
National University of Singapore, Singapore 117543
*E-mail: chmjjv@nus.edu.sg

The ternary compound $CuInSe_2$, which belong to the I-III-IV_2 family, has emerged as a leading material for high efficiency and radiation-hard solar cell applications.[1] This material also a candidate for the anode material of photochemical devices due to its high performance and high output stability.[2] $AgInSe_2$ also belong to I-III-IV_2 chalcopyrites family which is well known for its application in non-linear optical devices. It has been proposed as one of the most useful NIR material for the preparation of Schottky diodes and solar cells.[3] To date, many methods (e.g., solvothermal, microwave assisted polyol synthesis, chemical vapor deposition) have been reported to synthesize these metal chalcogenides either in the form of thin film or nanoparticles.[4] Among the reported methods, single precursor approach has drawn our attention due to its advantage in controlling the stoichiometry of the final metal selenide and a relatively mild condition required to synthesize $CuInSe_2$ and $AgInSe_2$. For this purpose, we have synthesized two phosphine capped bi-metallic selenocarboxylates, $[(PPh_3)_2AIn(SeC\{O\}Ph)_4]$ (A = Cu (**1**) & Ag (**2**)) and characterized by various analytical techniques. By heating both **1** and **2** in a suitable surfactants, $CuInSe_2$ nanoparticles with sizes less than 10 nm and $AgInSe_2$ nanostrip were obtained. The details of our investigations will be presented in the poster.

References

[1] A. Rockett and R.W. Birkmire, *J. Appl. Phys.* 1991, 70, 81. C. Guillen, J. Herrero, *Sol. Energy Mater.* 1992, 23, 31.
[2] D. Cahen, G. Dagan, Y. Mirovsky, G. Hodes, W. Giriat and M. Lubke, *J. Electrochem. Soc.* 1985, 132, 1062.
[3] P.P. Ramesh, O.M. Hussain, S. Uthanna, B.S. Naidu and P.J. Reddy, *Mater. Lett.* 34, 1998, 27.
[4] M.A. Malik, P. O'Brien, N. Revaprasadu, *Adv. Mater.* 1999, 11, 1441. B. Li, Y. Xie, J. Huang, Y. Qian, *Adv. Mater.* 1999, 11, 1456. B.M. Basol, *Thin Solid Films* 2000, 361, 514. K.K. Banger, M.H.-C. Jin, J.D. Harris, P.E. Fanwick, A.F. Hepp, *Inorg. Chem.* 2003, 42, 7713.

P95 Group 12 Metal Selenocarboxylates: Single Source Precursor for ZnSe and CdSe Nanoparticles

Meng Tack Ng and Jagadese. J. Vittal*
Department of Chemistry,
3 Science Drive 3,
National University of Singapore, Singapore 117543
*E-mail: chmjjv@nus.edu.sg

Group 12 chalcogenide quantum dots are of current interest as the bulk materials are one of the best known groups of semiconductors. Such materials that absorb or emit in the blue or near-UV regions of the electromagnetic spectrum are being extensively studied owning to their potential uses in optical sensors and lasers. Recently, we have successfully synthesized both zinc and cadmium selenocarboxylates, $[M(SeC\{O\}R)_2]_n$(M = Zn, R = CH_3-p-C_6H_4 (**1**); M = Cd, R = Ph (**2**)) in good yield. These compounds are found to be good single source precursors for preparing the corresponding ZnSe and CdSe nanoparticles by thermally decomposed them in hot mixture of long-chain alkylphosphines and alkylamines. The synthesized CdSe

nanoparticles are highly monodispersed and the size or band gap energy of this nanoparticle can be controlled by changing the reaction temperature and the concentration of tri-n-octylphosphine. The synthesized ZnSe nanoparticle is found to be less sensitive to the experimental conditions as compared with CdSe nanoparticle. In our case, only ∼5 nm highly monodispersed ZnSe nanoparticle was prepared that exhibits strong luminescence property with narrow emission peak. The details of our investigation will be presented in the poster.

P96 Effect of Environmental Calcium/Phosphate on Acid Resistance of Glass-Ionomers (Poster)

Wang Xiao Yan[1], Zeng Kaiyang*[,2] and Adrian Yap[1] and Shen Lu[3]
[1]*Department of Restorative Dentistry, NUS*
[2]*Department of Mechanical Engineering, NUS*
[3]*Institute of Materials Research and Engineering*
*E-mail: mpezk@nus.edu.sg

This study investigated the effect of environmental calcium (Ca) and phosphate (P) on acid resistance of glass ionomer cements (GICs). Two types of highly viscous GICs (HVGICs) (Fuji IX Fast [FN]; KetacMolar [KM]) were used in this study. Specimens were fabricated following manufacturers' instructions and subsequently exposed to water or acidic conditions (pH 3) with varying Ca/P levels. After 4 weeks, specimens were subjected to a nano-indentation test with continuous stiffness measurement (CSM) technique for depth hardness and modulus. The sectioned surface was observed using a scanning electron microscopy (SEM). It was found that a surface reaction layer formed for both FN and KM exposed to acidic conditions. The surface layer was not uniform and hardness/modulus of the layer increased with the indentation-penetration depth at varied magnitude. The thickness and depth hardness/modulus of the surface layer were dependent on environmental phosphate levels. Results suggest that the presence of high level of phosphate may improve the acid resistance of GICs.

P97 Interfacial Adhesion and Delamination Characterized by Wedge Indentations — A Finite Element Study

Jiang Haiyan[1], Zeng Kaiyang*[,2] and Yong-wei Zhang[1]
[1]*Department of Materials Science and Engineering, NUS*
[2]*Department of Mechanical Engineering, NUS*
*E-mail: mpezk@nus.edu.sg

This study presents a study of characterizing interfacial adhesion property of thin film system during wedge indentation experiments by using finite element method (FEM). A traction-separation law is used to describe the interface adhesion due to the presence of large-scale yielding condition during delaminations. The effects of dominant parameters of the traction-separation law, i.e., interface energy and interface strength, on the initiation of interface delamination during indentation was investigated by parametric studies. A critical indentation load was used to characterize the interface delamination. Increasing either the interface energy or the interface strength will cause an increase in the critical indentation load to initiate interface delamination. A methodology, which is capable of determining the interface adhesion property of thin film/substrate systems, has been proposed based on the results of parametric studies. The onset and propagation of interface delaminations during indentations were also investigated and found to initiate in pure shear (mode II), and subsequently transits in to a mixed mode with further propagation. The onset of interface delamination will cause a sudden decrease in the load-penetration curve and the stiffness of the whole system will decrease after the interface delamination.

P98 Analysis of Nanoindentation of Thin Film Structures

Zeng Kaiyang*[,1], Shen Lu[2] and Jiang Haiyan[3]
[1]*Department of Mechanical Engineering, NUS*
[2]*Institute of Materials Research and Engineering*
[3]*Department of Materials Science and Engineering, NUS*
*E-mail: mpezk@nus.edu.sg

This talk presents a methodology that can be used to determine the elastic modulus, hardness, yield strength and strain hardening exponent for thin metallic films from analyzing nano-indentation load (P) – penetration (h) curves. The method combines several analyses originally developed for bulk materials, including dimensional analysis; $P - h^2$ (load – penetration^2) analysis; $S - h$ (stiffness – displacement) analysis; $S^2 - P$ (stiffness^2 – load) analysis; and slope analysis. The key factors for this method are to determine the loading curvature ($K = P/h^2$), elastic modulus and contact stiffness ($S = dP/dh$) for thin films in which the effects of substrate to the indentation measurement are minimum. It is found that by combining plots of $P - h$ (indentation load – displacement) curve; $P - h^2$ curve; $P - S$ curve, and $S^2 - P$ curve, one can readily identify substrate effects to the thin film properties measured by nanoindentation. Hence, this information is used together with the dimensionless functions, which were developed previously for bulk metallic materials, to determine the yield strength and strain hardening exponent for metallic thin films. This method has been applied to the nano-indentation of several thin film structures and has shown consistent results.

P99 Nanoindentation of Polymeric Materials (Poster)

Zeng Kaiyang*[,1], Shen Lu[2], Yang Shuang[3] and Zhang Yong-wei[3]
[1]*Department of Mechanical Engineering, NUS*
[2]*Institute of Materials Research and Engineering*
[3]*Department of Materials Science and Engineering, NUS*
*E-mail: mpezk@nus.edu.sg

Nano-indentation of polymeric materials is great challenge due to the effects of polymer visco-elasticity or even visco-plasticity. This work presents a series recent study of nanoindentation of Polymethylmethacrylate (PMMA) with different molecular weight and epoxies with different cross-linking density. The effects of visco-elasticity of

the polymers to the indentation experiments have been studied using a generalized model and non-linear curve fitting of the indentation data at the constant load experiments. Elastic modulus, delayed elasticity, and viscocity were derived from the nano-indentation results. Based on this work, a methodology for performing nanoindentation on polymeric materials was proposed. Effects of polymer structures and composition to the nanoindentation experiments were also discussed.

P100 Influence of Pegylation on Gene Expression of Cationic Polymer Micelles

Yong Wang* and Yi-Yan Yang
Institute of Bioengineering and Nanotechnology
*E-mail: ywang@ibn.a-star.edu.sg

The stability of DNA/cationic polymer complexes is one of the major obstacles for gene transfection and poly(ethylene glycol) (PEG) has been used to elongate the lifespan of DNA complexes *in vivo*. We have recently synthesized cationic micelles based on biodegradable and cationic P(MDS-*co*-CES), which had positive charges on the surface. These micelles induced high gene transfection efficiency in various cell lines, comparable to or higher than PEI. In this study, PEG was conjugated onto P(MDS-*co*-CES) with various molecular weights. Pegylated polymer micelles had a reduced DNA binding ability. In addition, the pegylated micelles with higher grafting degree of cholesterol also reduced DNA binding ability when compared to that of pegylated micelles with lower cholesterol grafting degree. Thus, pegylated micelles yielded lower luciferase transfection efficiency in four different cell lines tested. However, the pegylated polymer with higher cholesterol grafting degree achieved greater luciferase expression level. In conclusion, the core-shell structure with positive charges on the surface is a crucial requirement to achieve high gene transfection efficiency. However, the transfection efficiency has to be compromised when pegylation is introduced to prolong lifespan of the complexes *in vivo*.

P101 Smart Core-Shell Nanoparticles for Targeted Anticancer Drug Delivery

Lihong Liu* and Yi-Yan yang
Institute of Bioengineering and Nanotechnology
*E-mail: lhliu@ibn.a-star.edu.sg

In this study, we reported pH-triggered thermally responsive core-shell nanoparticles self-assembled from the amphiphilic tercopolymer poly(*N*-isopropylacrylamide-*co*-*N,N*-dimethylacrylamide-*co*-10-undecenoic acid) [P(NIPAAm-*co*-DMAAm-*co*-UA) conjugated with cholesterol and folic acid. These nanoparticles exhibited a pH-dependent lower critical solution temperature (LCST). In a normal physiological environment, the LCST of the nanoparticles was well above the normal body temperature. In an acidic environment, however, the LCST was below 37°C, leading to the deformation of the core-shell nanoparticles and to the eventual release of drug molecules. Cholesterol was grafted to the hydrophobic segment of P(NIPAAm-*co*-DMAAm-*co*-UA) to improve the hydrophobicity of the core so that highly hydrophobic anticancer drugs such as paclitaxel can be easily encapsulated. In addition, folic acid was conjugated to the free amine group of P(NIPAAm-*co*-DMAAm-*co*-UA). Doxorubicin was used as a model anticancer drug. 4T1 mouse mammary carcinoma cells and human oral epidermal carcinoma KB cells were employed as folate receptor-expressing cells, and A549 human lung carcinoma cells were used as folate receptor-deficient cells. The doxorubicin-loaded core-shell nanoparticles with folate were much more cytotoxic to 4T1 and KB cells as compared to doxorubicin-loaded P(NIPAAm-*co*-DMAAm-*co*-UA) nanoparticles without folate. These multi-functional polymer core-shell nanoparticles may make a promising carrier for delivering anticancer drugs.

P102 Preparation and Properties of Porous Poly(N-Isopropylacrylamide)/Alginate IPN Hydrogels

Jian-Tao Zhang*[,1,2], Shi-Wen Huang[1], Ya-Nan Xue[1], Ren-Xi Zhuo[1] and Yi-Yan Yang[2]
[1]*Key Laboratory of Biomedical Polymers (Wuhan University), Ministry of Education; College of Chemistry & Molecular Sciences, Wuhan University, Wuhan 430072, P. R. China*
[2]*Institute of Bioengineering and Nanotechnology, 31 Biopolis Way, The Nanos, #04-01, Singapore 138669, Singapore*
*E-mail: jtzhang@ibn.a-star.edu.sg

A series of novel macroporous hydrogels based on the interpenetrating networks (IPN) of poly(*N*-isopropyl acrylamide) (PNIPAAm) and alginate were prepared by a sequential method. The PNIPAAm networks were firstly synthesized by radical polymerization in the presence of alginate using poly(ethylene glycol) 6000 (PEG6000) as a pore-forming agent to obtain the porous Semi-IPN hydrogels. The second alginate networks were then cross-linked by divalent cations (Ca^{2+}) to form Full-IPN hydrogels. The IPN hydrogels were characterized for their morphologies, thermal behaviors and mechanical strength using scanning electron microscope, differential scanning calorimeter and dynamic mechanical analyzer. The results show that the PEG-modified IPN gels were of obviously macroporous structures, and in comparison to normal PNIPAAm gel, porous Full-IPN hydrogels presented the same lower critical solution temperature (LCST), while their mechanical properties were greatly enhanced due to the incorporation of the second cross-linked alginate networks. Their swelling properties such as temperature dependence of equilibrium swelling ratio, shrinking and reswelling kinetics in water were also investigated. The shrinking rates of the porous Semi- and Full-IPN hydrogels were much higher than those of conventional PNIPAAm hydrogel when the temperature was raised above their LCST. These macroporous hydrogels may have great potential in biomedical applications.

P103 Development of Luminescent Hybrid Materials and Thin-films from Functional Polymers

S. Sindhu[1], S. Jegadesan[1,2], L. Hairong[2], C.H. Sow[1,3], and S. Valiyaveettil*[,1,2]
[1] *NUS Nanoscience & Nanotechnology Initiative, National University of Singapore, 2 Science Drive 3, Singapore 117542,*
[2] *Department of Chemistry, National University of Singapore, 3 Science Drive 3, Singapore 117543,*
[3] *Department of Physics, National University of Singapore, 2 Science Drive 3, Singapore 117542*
*E-mail: chmsv@nus.edu.sg

Nature uses various macromolecules to produce highly complex structures through self-assembly process. This knowledge of such controlled assembly can be used in the design and develop new synthetic structures with interesting properties. Herein, we report the role of modified conjugated polymers in the nucleation, growth and morphology of calcium carbonate ($CaCO_3$), an important natural material. In situ incorporation of sulfonated poly(*p*-phenylenes) (PPP) into highly porous calcium carbonate matrix was achieved and the detailed structure-property relationship of the morphological changes in $CaCO_3$ was investigated. Synthetic conditions are tuned properly to obtain hybrid thin films of the polymers and calcium carbonate. Such films can also be patterned using laser lithography. A simple, focused laser beam was used to fabricate structures with different shapes on the polymeric films by mass removal of the polymer by evaporation. These patterned films are important candidates for biological and micro-optics applications.

P104 Direct Focused laser Fabrication of SU-8

F.C. Cheong*, B. Varghese and C.H. Sow
National University of Singapore, Physics Department
*E-mail: phycfc@nus.edu.sg

SU-8 photoresist is an important material used in the development of micro-devices. Cross-linked SU-8 structures have been known for their thermal stability and their strong resistance to standard solvent, acid and base. Due to the inert properties of this polymer, it is difficult to further modify or remove SU-8 once it is completely cured.

We report an effective process to pattern cured and baked SU-8 photoresist on glass using focused laser beam. Laser fabrication has been an important tool in various fields of research. Making use of this laser cutting method, we are able to create interesting and useful two-dimensional SU-8 structures. The shapes and sizes of the structures created can be controlled by varying the power of the laser, angle of incident of the focused laser beam, the relative speed with which the laser beam traverse through the SU-8 film and the magnification of objective lens used. Besides two-dimensional structures, this method also allows us to generate three-dimensional structures.

P105 Germanium p-MOSFETs with Pt-Germanide Schottky Source/Drain, HfO_2 Gate Dielectric and TaN Gate Electrode

Rui Li[1], H.B. Yao[1,2], S.J. Lee*[,1], D.Z. Chi[2], M.B. Yu[3] and D.L. Kwong[3]
[1] *Silicon Nano Device Lab., Department of Electrical & Computer Engineering, National University of Singapore, Singapore, 119260,*
[2] *Institute of Materials Research and Engineering, Singapore*
[3] *Institute of Microelectronics, Singapore*
*E-mail: elelsj@nus.edu.sg

Schottky Source/Drain transistors using Pt-germanide and HfO_2/TaN gate stack are fabricated on Ge -substrate with conventional self-aligned top gate process. Pt-germanide was formed by RTA 30 nm Pt on n-type (Sb-doped) (100) Ge wafer at 400°C in N2 ambient, which is also the highest temperature throughout the fabrication process.

It was found that Pt-germanide provide promising properties for p-MOSFET; negative effective hole barrier height, low resistivity, atomically sharp junction with Ge with good morphology. The characterization of $PtGe_2$ Schottky Source/Drain Ge p-MOSFETs with HfO_2 gate dielectrics and TaN gate electrode demonstrated the significant I_{off} reduction compared to NiGe Schottky Source/Drain and conventional B-doped Ge p-MOSFETs, while maintaining the comparable I_{on} current.

P106 High Ge Concentration Strained SiGe on Insulator MOSFET with Schottky Barrier Source/Drain, High-k Gate Dielectric and Metal Gate

Fei Gao[1,2], Sungjoo Lee*[,1], Li Rui[1], S. Balakumar[2], Chi Dong-Zhi[3], Chin-Hang Tung[2] and Dim-Lee Kwong[2]
[1] *Silicon Nano Device Lab, Department of ECE, National University of Singapore, Singapore*
[2] *Institute of Microelectronics Engineering, Singapore*
[3] *Institute of Materials Research Engineering, Singapore*
*E-mail: elelsj@nus.edu.sg

Single crystalline strained SGOI (SiGe-on-insulator) is realized by oxidizing SiGe amorphous film deposited on silicon-on-insulator substrates by a co-sputtering technique. After a two-step oxidation process and a cyclic annealing step, SGOI with uniform Ge concentration has been achieved. Crystalline properties and strain analysis of the SGOI layers are investigated by TEM, FFT, micro-Raman, EDX and XRD. The overall strain in these SGOI films is beneficial for the improvement of the hole mobility of the MOSFET. Subsequently, We demonstrate high Ge SGOI MOSFET using Schottky S/D (source/drain) and HfO_2/TaN gate stack integrated with conventional self-aligned top gate process. Unlike high temperature S/D activation needed for conventional transistor, low Schottky barrier S/D formation temperature contributes to the excellent capacitance-voltage characteristic and low gate leakage current. SGOI structure suppresses the junction leakage problem, resulting in good agreement between the source current and drain current.

P107 STM Investigation of Ce and Zr Nanostructures on Si(111)

Ce Zhang, Sunil Singh Kushvaha, Wende Xiao, Bin Lu and Xue-Sen Wang
Department of Physics and NUSNNI, NUS, Singapore 117592
E-mail: G0403190@nus.edu.sg

In recent years, various types of silicides have received great attention for their unique electric properties, high-temperature stability, and compatibility with silicon technology. In addition, formation of silicide should be considered when growing high-k dielectric (e.g. CeO_2, ZrO_2) layers on Si. In this study, surface morphology and nanostructures of Zr and Ce on Si(111) under different experimental conditions were investigated though scanning tunneling microscopy (STM), Auger electron spectroscopy (AES) and low energy electron diffraction (LEED). Different coverage of Zr was deposited on Si(111) at room temperature, followed by annealing at temperatures ranging from 200° to 850°. Wire-like, triangular and rectangular-shaped islands with different atomic structures were observed on the surface. Ce was deposited on Si(111) at room temperature or at substrate temperature 500°. Various superstructures were observed after annealing at different temperatures (ranging from 500° to 1200°). Although most of the Ce/Si superstructures in this experiment were reported by others previously, phase transition related to the annealing temperature and coverage is still under investigation.

P108 Growth of Crystalline Sb and Bi Nanostructures on Highly Oriented Pyrolytic Graphite

Sunil Singh Kushvaha, Zhijun Yan, Hongliang Zhang, Wende Xiao and Xue-sen Wang
Department of Physics and NUSNNI, NUS, Singapore 117542
E-mail: G0301195@nus.edu.sg

Group V elements (e.g. As, Sb, Bi) are known to show rich allotropic transformation by applying high pressure due to shifting of semi-metallic bonding character to metallic or covalent side. In this framework, a question arises whether an allotropic modification of these elements (especially Sb and Bi) can be realized at nano-scale in self-assembly. We fabricated Sb and Bi nanostructures of different shape and size on highly oriented pyrolytic graphite (HOPG) by simple vapor deposition in ultra-high vacuum, studied these structures using in-situ scanning tunneling microscopy (STM). Three-dimensional (3D), 2D and 1D structures of Sb were observed whereas only 2D and 1D structures of Bi were obtained at room temperature (RT). Shapes of Sb structures were controlled in self-assembly by varying the flux and substrate temperature. At low flux and RT, mostly 3D islands of Sb were observed at steps and defect sites. Exclusively 2D and 1D structures of Sb were observed at high flux and 375 K. 2D structures of Sb and Bi show same bulk rhombohedral crystal structure whereas 1D structure of both elements show a significant deviation from bulk phase. Although the exact growth mechanism of these quasi-1D Sb and Bi structures and their crystalline structures are not very clear, it is considered an allotropic modification of Sb and Bi on graphite at the nano-scale.

P109 Abnormally Large Contraction at the Second Interlayer Spacing on the Fe(111) Surface

Y.Y. Sun* and Y.P. Feng
Department of Physics,
National University of Singapore
*E-mail: physyy@nus.edu.sg

Multilayer relaxations on clean metal surfaces are normally found to be damped into the bulk. However, by a re-analysis on an old LEED I-V data from the Fe(111) surface, we found an abnormally large contraction at the second interlayer spacing (about −15% of the bulk spacing), while the relaxations of the first and third spacings are −10% and +13%, respectively. We have conducted first-principles calculations on this surface and the LEED results have been confirmed, where the relaxations of the first three spacings from the first-principles calculations are −8%, −17% and +14%, respectively. The openness of the Fe(111) surafce, while still being a low-index surface of high-symmetry, may account for this anomalous behavior of the this surface.

P110 Crystallization of Al_2FeZr_6 Amorphous Alloys Prepared by Mechanical Alloying

Ouyang Yi Fang[1,2], Chen Hong Mei[2], Feng Yuan Ping[2] and Zhong Xi Ping[1]
[1]*Department of Physics, Guangxi University, Nanning 530004, P.R. China*
[2]*Department of Physics, National University of Singapore, Singapore 117542*
E-mail: Phyv3@nus.edu.sg

Amorphous Al_2FeZr_6 alloy was prepared from elemental powders by mechanical alloying. The microstructure evolution was identified by X-ray diffraction. The thermal stability of amorphous Al_2FeZr_6 was determined by DTA. There are two overlapped exothermic peaks observed in curves of DTA. This indicates that two exothermic reactions in the procedure of crystallization of amorphous Al_2FeZr_6 alloy. The effective activation energies of crystallization were evaluated using Kissinger's plot. The evaluated values of effective activation energy corresponding to the first and the second exothermic reactions are 266 and 299kJ/mole respectively. The products of crystallization of amorphous Al_2FeZr_6 alloy are binary intermetallic compounds $AlZr_2$ and $FeZr_2$ instead of intermetallic compounds Al_2FeZr_6. It was explained by comparing their relative stabilities based on enthalpies of formation of intermetallic compounds.

P111 Zinc-Blend NiO: A Possible Spin Electrode for Wide Gap Semiconductors from DFT Calculation

Wu Rongqin, Liu Lei, Peng Guowen, Yang Ming and Feng Yuan Ping
Department of Physics,
National University of Singapore
E-mail: g0203654@nus.edu.sg

Calculations based on spin density functional theory (DFT) with and without on-site Coulomb interaction and exchange U-J are performed to study the spin-polarized

electronic properties of zinc-blend NiO (zb-NiO) under equilibrium and strains. Pure DFT calculation predicts a hole-pocket at Γ point for the majority spin but with the inclusion of a small U-J the majority spin becomes semiconducting with the minority spin being metallic. Calculations with U-J = 2 eV shows that the half-metallicity is conserved with lattice constant a compressed to 4.38 angstrom and expanded to 4.62 angstrom, suggesting zb-NiO is a promising half-metallic electrode for those technologically important wide-gap semiconductors in the field of spintronics.

P112 Gold Nano Particles Deposited on CuO for CO Oxidation

Sun Han, Zhong Ziyi, Feng Yuanping and Lin Jianyi*
2 Science Drive 3, Blk S12 C/O Physics department, Department Office, NUS, 117542,Singapore
*E-mail: Lin_Jianyi@ices.a-star.edu.sg

Gold catalysts have recently been attracting rapidly growing interests due to their potential applicability to many reactions of both industrial and environmental importance. A series of gold/copper-oxide catalysts have been prepared by the deposition-precipitation method. Four kinds of CuO substrates were used as the substrates: self-made CuO micro cubic; self-made CuO nano flakes; commercial CuO; commercial CuO nano particles. Gas chromatography analysis was carried out to determine the CO oxidation conversion rate. The reaction gas used for CO oxidation was 5% CO 5% O2 in He. Both CuO supported Au catalysts and CuO substrates were active for CO oxidation. But the gold supported on CuO showed much better CO oxidation activities compared with bare CuO substrates. Au/CuO samples with different Au loadings and different calcination temperatures were synthesized to compare their CO oxidation activities. SEM, XRD, BET were also used to characterize these samples. It can be concluded that both substrates' structure and their particle size can affect the activity of the Au-CuO system.

P113 High-Resolution Reflectometry and Diffractometry at SSLS

P. Yang*, E.P. Chew and H.O. Moser
Singapore Synchrotron Light Source (SSLS), National University of Singapore
5 Research Link, Singapore 117603,
*E-mail: slsyangp@nus.edu.sg

High resolution experiments of X-ray specular reflectivity at grazing incidence angle and Bragg diffraction at higher angle can be conducted using a high-resolution Huber 4-circle diffractometer system 90000-0216/0. X-ray beam was conditioned to select desired wavelength by a focus mirror and a Si (111) channel-cut monochromator (CCM). The diffractometer features typical high-precision 0.0001° in step size for omega and two-theta circles (the best 0.00005° if needed). Slit system for incident and reflected (diffracted) beam can be adjusted in both vertical and horizontal directions. Such set-up yields X-ray beam with vertical divergence adjustable from 0.001° to 0.02°, ΔE/E from 1.4 to 14 g10^{-4} and 1000 times of flux in high-resolution setting at 8 keV, compared to a conventional lab source. Usable photon energy ranges from about 2.3 to 12 keV.

Structural characterization by reflectometry and diffractometry of low-*k* films, polymers, sol-gel Si, GeSi semiconductor layered system, Ni-alloy silicides, optic disc, ZnO_2 magnetic semiconductor layers, $GaAs/In_{0.25}Ga_{0.75}As$ multi-quantum wells, $[SiC/AlN]_{20}$ superlattices have been done. Anomalous scattering powder diffraction can also be performed using selected wavelengths near the absorption edges.

P114 X-Ray Absorption Fine Structure Spectroscopy at SSLS

P. Yang*, T. Liu†,1, Z.W. Li, Miao Hua and H.O. Moser
Singapore Synchrotron Light Source (SSLS), National University of Singapore
5 Research Link, Singapore, 117603,
[1] *SSLS collaborator: Surface Science Laboratory, Physics Department,*
National University of Singapore, 119260,
*E-mail: slsyangp@nus.edu.sg
†E-mail: phylt@nus.edu.sg

X-ray absorption fine structure (XAFS) spectroscopy has been set up in the X-ray demonstration and development (XDD) beamline at SSLS, with an energy range of 2.3 to 10 *keV*, which can be available to cover the K-edge of elements from S to Zn, and the L-edge of rare earth and some heavy metals from Zr to Ta. As a unique technique of probing the local structure of atoms, giving information on valence state, symmetry and local geometry, XAFS has been widely applied to a variety of fields. Samples that can be analyzed range from liquids, metals, catalysts, to biological systems, and minerals.

The basic set-up allows three modes of measurements to be performed: transmission for concentrated samples, fluorescence mode for diluted one and total electron yield mode for thin film and surface studies. Monitoring the intensity of synchrotron light source as intense as 10^9 photons/s, an accurate energy scan is performed by a channel-cut Si (111) monochromator, with a scan energy resolution of a few *eV* (this will be improved by using a pair of source slits in the front-end, to be 2 *eV* or so) and a scan repeatability of less than 0.15 *eV*.

Some examples of applications will be presented that have been successfully carried out using XAFS spectroscopy at SSLS.

P115 A Proposal for Singapore Magnetism Characterization Facility (SMCF) by Using Synchrotron Radiation

Yu Xiaojiang*, Vladimir Zabluda† and Herbert O. Moser†
Singapore Synchrotron Light Source, National University of Singapore
E-mail: *slsyxj@nus.edu.sg; †zvn@iph.krasn.ru; ‡slshom@nus.edu.sg

Singapore synchrotron light source (SSLS) is 700 MeV compact superconductor light source with bending magnetic field intensity 4.5 T and critical energy is 1.47 keV. We propose to build a new beamline for material science to cover energy range from 500–2000 eV by grating monochromator, around 1000 (E/Δ E) resolving power, and photon

polarization can be adjustable between linear and circular polarization. A multilayer mirror can be interchangeable with the gratings under UHV to give best reflection at 1900 eV of about 3% resolution, which lets GRAD analyzer working at high energy with reasonable flux. The main chamber of End-station will be equipped with a GRAD [1] analyzer operated as grazing-emission X-ray fluorescence mode, which comprises 40 multilayer mirrors, half of which multilayers are repeated with 100 Cu/C bilayers, detecting fluorescence energy range from 500–800 eV; and the left mirrors' multilayers are repeated with 100 Cr/C bilayeres for fluorescence energy range 750–2000 eV. The GRAD with 40 multilayer mirrors formed a ring shape detector as a 360 degree analyzer and total solid acceptance 0.3–1.0 sr, is a wavelength dispersion detector coped with the poor resolution for light elements and limited dynamic range of solid state detector. The GRAD can be used to detect the contamination on super flat surface and infer the composition, density and thickness of the multilayers. A XPEEM, 7 T superconductor magnet also installed in the main chamber. Experiments such XAS and XMCD can be done at this facility which is thought useful for magnetism and layer structure materials research.

References

[1] A.N. Buzykaeva, N.V. Kovalenko, S.V. Mytnichenko and V.A. Chernov, *Nuclear Instruments and Methods in Physics Research* **A 470**, 135 (2001)

P116 Development and Applications of the Phase Contrast Imaging and Tomography (PCIT) at SSLS for Advanced Materials Characterization

M. Cholewa*, Yang Ping, Ng May Ling, Li Zhi Juang, H.O. Moser and Yeukuang Hwu[1]
Singapore Synchrotron Light Source (SSLS), National University of Singapore (NUS), 5 Research Link, Singapore 117603
[1]*Institute of Physics, Academia Sinica, 128 Academia Road, Nankang, Taipei, Taiwan*
*E-mail: slsmc@nus.edu.sg

Recent results achieved at an existing phase contrast imaging and tomography (PCIT) beamline[1–3] at the Singapore Synchrotron Light Source (SSLS) have shown that high resolution (down to 0.7 μm) of 2-dimensional (2D) and 3-dimensional (3D) imaging could be extremely useful tool for advanced materials characterisation. A white (broadband) synchrotron radiation with limited coherence could produce refraction and diffraction based edge enhancement. With a white radiation it is possible to obtain a high photon flux that could be exploited for real time radiology (100 ms per frame), high lateral resolution and high speed in 2D imaging and 3D tomography.

X-rays are uniquely suited for microscopy as their short wavelength allows high spatial resolution. Their interaction with matter provides three contrast mechanisms that include absorption contrast, phase contrast, and diffraction contrast. The high penetrating power favors nondestructive imaging of large and opaque structures, as is well known in X-ray computed tomography (X-ray CT) for human medical applications[4]. In recent years a 2D and 3D imaging capabilities have been developed at the PCIT beamline at SSLS.

References

[1] W.L. Tsai, H.M. Chang, Y. Hwu, P.C. Hsu, H.L.Tsai, G.M. Chow, P.C. Ho, S.C. Li, H.O. Moser, Y. Ping, S.K. Seol, H. Je, A. Groso and G. Margaritondo, "Imaging cells with refractive index radiology", *Biophysical Journal*, **Vol. 87** (6) Dec. (2004) 4180–4187.
[2] A. Yeo, P. Yang, A.G. Fane, T. White and H.O. Moser, "Noninvasive Observation of External and Internal Deposition During Membrane Filtration by X-ray Microimaging (XMI)", *Journal of Membrane Science*, **250** (2005) 189–193.
[3] W.L. Tsai, P.C. Hsu, Y. Hwu, J.H. Je, P. Yang, H.O. Moser, A. Groso and G. Margaritondo, "Edge-enhanced Radiology with Broadband Synchrotron X-rays", in H.O. Moser, ed., Synchrotron Radiation in Materials Science (SRMS-3), *Nucl. Instr. and Meth.* **B199** (2003) 436–440
[4] E. Seeram, Computed Tomography", W.B. Saunders (2001).

P117 Micro/Nano Fabrication at the Singapore Synchrotron Light Source – Support to Advanced Material Research

L.K. Jian, H.O. Moser*, B.D.F. Casse, S.P. Heussler, J.R. Kong, B.T. Saw and Sharain bin Mahmood
Singapore Synchrotron Light Source/NUS
E-mail: moser@nus.edu.sg

SSLS is operating the compact 700 MeV electron storage ring Helios 2 that produces synchrotron radiation from two superconducting dipoles which run at a magnetic flux density of 4.5 T. The characteristic photon energy is about 1.5 keV. Micro/nanofabrication is covered with the LiMiNT facility (Lithography for micro/nano-technology). LiMiNT can do micromachining as a one-stop shop using the full LIGA process (LIthographie, Galvanoformung, and Abformung, first developed in Germany, is based on a combination of lithography, electroforming and replication processes). LiMiNT is run partly as a foundry, partly as a research lab. Under the foundry aspect, work is done for customers in various fields of applications. The own research aims at setting up nanolithography processes to batch process high aspect ratio devices. In this report, the technology capability of the LiMiNT in micro/nano fabrication and some application cases in support advanced material research are presented.

P118 Optimized Metallization for Molecular Devices

Jie Deng*,[1], Wulf Hofbauer[1], Saw Beng Tiam[2], Herbert O. Moser[2] and Sean O'Shea[1]
[1]*IMRE, 3 Research Link, Singapore 117602, Republic of Singapore*
[2]*SSLS - NUS, 5 Research Link, Singapore 117603, Republic of Singapore*
*E-mail: j-deng@imre.a-star.edu,.sg

Devices based on thin molecular films (i.e. self-assembled monolayers) require reliable contacts. For such vertically aligned architectures, the capping electrode can only be deposited after the molecular layer. Most deposition

methods for the top metallization layer are potentially damaging to organic molecules. Beyond the risk of chemical and thermal damage, diffusion of the electrode material through pinholes can also lead to shorts through the molecular layers.

We report on our work to optimize materials and our deposition process, and to increase the yield of electron beam lithographically defined cross-bar tunnel devices based on self-assembled monolayers. The devices are classified by their electrical (I-V) characteristics. Apart from stable working and shorted devices, we also find junctions that switch between high- and low-conductivity states, suggesting field induced formation and destruction of filaments traversing the molecular layer.

P119 Scanning Tunneling Microscopy at Liquid/Monolayer Interfaces.

Gosvami N.*[,1], Sinha S.K.[1], Sean O'Shea[2] and M. P. Srinivasan[3]
[1]*Department of Mechanical Engineering, National University of Singapore, 9 Engineering Drive 1, Singapore 117576, Singapore*
[2]*Institute of Material Research and Engineering, 3 Research Link, Singapore 117602, Singapore*
[3]*Department of Chemical Engineering, National University of Singapore, 4 Engineering Drive 4, Singapore 117576, Singapore*
*E-mail: ngosvami@nus.edu.sg

Studies on self-assembled monolayer (SAM) systems have been rigorously pursued in the last two decades as SAMs are promising candidate for variety of applications (molecular lubrication, molecular electronics, corrosion resistance, wetting control etc.) and can be used as a model system to understand structure-property relationship at molecular scale. To study the properties of these systems is a challenging task. Scanning probe microscopy techniques (scanning tunneling microscopy and atomic force microscopy) are extremely powerful tools to study such systems at molecular scale. SPM in liquids has an added advantage of reduced contamination and possibilities to understand liquid-SAM interface properties. Plethora of SPM studies in liquids has been performed to understand molecular structure and properties of SAMs and SAM-liquid interfaces. The most serious concern for the application of SAMs is their stability in variety of environment. We have employed low current scanning tunneling microscopy in liquid (hexadecane) environment to study the desorption mechanism of alkanethiol SAM molecules bonded to Au(111) surfaces. The observation reveals that alkanethiol SAM desorbs at a faster rate in hexadecane when deposited under ambient conditions, while SAMs deposited at elevated temperature ($\sim 50°C$) have much slower desorption rate due to the reduced defect density such as domain boundaries and etch pits.

P120 Improvement in Physical and Mechanical Properties of Magnesium Reinforced with Nano-Size MgO Particles

C.S. Goh, J. Wei* and M. Gupta
Department of Mechanical Engineering National University of Singapore, 10 Kent Ridge Crescent, Singapore 119260
[1]*Singapore Institute of Manufacturing Technology 71 Nanyang Drive, Singapore 638075*

Magnesium (Mg) composites are attracting increasing scientific and technological interests due to their weight critical applications. While fiber reinforced Mg composites have been popularly used in some high-end industries, such as the aerospace sector, particulate reinforced Mg composites are gaining attention due to their increased fabrication rate, reduced reinforcement and production cost. Conventional micron-size particulate reinforced Mg composites are constantly faced with the problems of particle cracking and particle matrix interfacial failures. These problems inevitably lead to low ultimate strength and ductility in the conventional Mg composites. In an attempt to overcome these entrenched issues and to look for further improvement in properties, the use of nano-size particles are investigated. Accordingly, Mg reinforced with up to 1 volume percent of nanosize MgO was synthesized using the disintegrated melt deposition technique followed by hot extrusion. The thermal stability of the Mg nanocomposites increases with higher additions of MgO. TEM analysis shows good interfacial adhesion between Mg and MgO. Mechanical property results reveal an improvement in macrohardness, yield and tensile strengths of the nanocomposites relative to pure Mg. The Mg nanocomposites synthesized exhibited excellent combination of properties that were distinctly superior when compared to the conventional Mg composites containing micron-size reinforcements.

P121 Effect of Presence of Different Reinforcements on the Properties of Sn-Ag-Cu Solder

S.M.L. Nai[1,2], J. Wei[2] and M. Gupta*[,1]
[1]*Department of Mechanical Engineering National University of Singapore, 9 Engineering Drive 1, Singapore 117576*
[2]*Singapore Institute of Manufacturing Technology 71 Nanyang Drive, Singapore 638075*
*E-mail: mpegm@nus.edu.sg

In this study Sn-Ag-Cu based nanocomposite systems with different reinforcements, namely: (1) multiwalled carbon nanotubes (MWCNTs), (2) titanium diboride (TiB_2) particulates and (3) yttria oxide (Y_2O_3) particulates were succesfully synthesized using the powder metallurgy technique. Micron size lead-free solder particles were blended together with varying amount of reinforcement. Blended powder mixtures were then compacted, sintered and finally extruded at room temperature. The extruded materials were characterized for their wettability, thermal and mechanical properties. Wettability property of the composite solders was found to improve with a threshold addition of reinforcements. Moreover, the results of thermal property characterization exhibited an overall decrease in CTE values for the composite solders, which might lead to better thermal mismatch between the interconnect material and substrate. Lastly, the mechanical results showed an increase in overall strength of the composite solders. An attempt is made in the present study to correlate the variation in amount of reinforcement with the properties of the resultant nanocomposite materials. These advanced interconnect materials will benefit industries like the

microelectronics flip chip assembly and pacaging, MEMS systems and NEMS systems.

P122 Molecular Engineering of Fluorescence Conjugated Polymers for Chemical- and Biosensors Applications

Muthalagu Vetrichelvan[1] and Suresh Valiyaveettil[2]
[1]*Singapore-MIT Alliance, E4-04-10, 4 Engineering Drive 3, Singapore – 117546.*
[2]*Department of Chemistry, 3 Science Drive 3, National University of Singapore, Singapore – 117 543.*
E-mail: chmsv@nus.edu.sg

The design and synthesis of fluorescence sensor with high selectivity and sensitivity for transition metal ions, toxic chemicals and biomolecules is interesting owing to its application potentials. Conjugated polymers for chemical and biological sensors are good candidates for developing such sensors because of the possibility of investigating analyte induced changes in optical and conducting properties. A series of copolymers comprising of alternating substituted phenylene and aromatic units with hetero donor systems were designed and synthesized using Suzuki-poly condensation reaction. Depending on the complexation abilities of the polymer backbone with the transition metals, phenols, carboxylic acids and other anions, fluorescence emission from the polymer was quenched. Another series of water soluble poly(para phenylene)s with the sulfonate side chain groups was also synthesized and investigated as fluorescence biosensors for the cationic biomolecules such as cytochrome-C and viologen derivatives *etc.* The presentation will address on the synthesis, characterization and fluorescence sensing applications of these conjugated polymers by the addition of external stimuli will be presented in detail.

P123 Nanopatterning of Conjugated Polymer Using Electrochemical Nanolithography

Subbiah Jegadesan[1,2], Sindhu Swaminathan[2], Rigoberto C. Advincula[3] and Suresh Valiyaveettil
[1]*Department of Chemistry,*
[2]*NUS- Nanoscience and Nanotechnology Initiative, 3 Science Drive 3, National University of Singapore, Singapore - 117543.*
[3]*Department of Chemistry, University of Houstan, Houstan, TX 77204-5003*
E-mail: chmsv@nus.edu.sg

Electrochemical lithography techniques have allowed the formation of nanostructures through selective deposition of metallic nanoparticles such as silver, copper and platinum on conducting substrates and also through surface modifications via oxidation of inorganic semiconductor/conducting substrates. In recent years, scanning probe microscope (SPM) based electrochemical nanolithography have attracted attention for the fabrication of nanostructures with a size range from sub-100 nm to micron size features using suitable films on conducting or semiconducting substrates. Here, we use this technique, to form the precisely controlled corona type pattern on electroactive precursor copolymer with controlled applied voltage and tip speed. The multielectroactive group on the copolymer facilitates a conductive patterning based on relief height formation as well as corona size distribution. Also, the formation of a conductive nanopattern on the copolymer film was investigated using a conducting atomic force microscopy (C-AFM).

P124 Preparation of Hybrid Thin-Films via Self-Organization of Conjugated Polymers and Nanomaterials

M.H. Nurmawati[1], R. Renu[1], C. Rein Hansen[1], P.K. Ajikumar[2], S. Valiyaveettil*[,1,2]
[1]*Department of Chemistry,*[2]*Singapore-MIT Alliance.*
[1]*3 Science Drive 3, National University of Singapore, Singapore 117543.*
[2]*4 Engineering Drive 3, Singapore 117546*
*E-mail: chmsv@nus.edu.sg

Emerging demands for miniaturized devices are causing the widely used top-down lithographic methods to reach a practical bottleneck. Manufacturing complex structures with long range lateral order and orientation have been investigated by many research groups. On the other hand, the bottom-up approach, less prevalent approach so far, makes use of self- organizing intriguing components in which the shape control only involves selection of choice of material and self-organization conditions. The latter method is currently being actively investigated to achieve desirable thin film configuration and properties. Subtle adjustments in casting environment conditions allow remarkable control in the consequent thin film morphologies. Herein the present study delineates the fabrication of micro-structured blue light-emitting thin films of novel, functionalized amphiphilic poly(*p*-phenylene)s (PPPs) which are being investigated as potential candidates for advanced polymer electronic and optical applications. In addition to this we demonstrate how controls of interplaying interaction forces afford large area of periodic and intricately patterned conjugated thin polymer-nanoparticle hybrid films. The thin film morphology and the consequent photo-physical properties of these organic and organic-inorganic hybrid structures are also investigated. The present talk will focus on the design of a conjugated polymer for simple and efficient preparation of self-organized functional microstructured thin films.

P125 Development of Luminescent Hybrid Materials and Thin-Films from Functional Polymers

S. Sindhu[1], S. Jegadesan[1,2], L. Hairong[2], C.H. Sow[1,3] and S. Valiyaveettil*[,1,2]
[1]*NUS Nanoscience & Nanotechnology Initiative, National University of Singapore, 2 Science Drive 3, Singapore 117542,*
[2]*Department of Chemistry, National University of Singapore, 3 Science Drive 3, Singapore 117543,*
[3]*Department of Physics, National University of Singapore, 2 Science Drive 3, Singapore 117542.*
*E-mail: chmsv@nus.edu.sg

Nature uses various macromolecules to produce highly complex structures through self-assembly process. This knowledge of such controlled assembly can be used in

the design and develop new synthetic structures with interesting properties. Herein, we report the role of modified conjugated polymers in the nucleation, growth and morphology of calcium carbonate ($CaCO_3$), an important natural material. In situ incorporation of sulfonated poly(*p*-phenylenes) (PPP) into highly porous calcium carbonate matrix was achieved and the detailed structure-property relationship of the morphological changes in $CaCO_3$ was investigated. Synthetic conditions are tuned properly to obtain hybrid thin films of the polymers and calcium carbonate. Such films can also be patterned using laser lithography. A simple, focused laser beam was used to fabricate structures with different shapes on the polymeric films by mass removal of the polymer by evaporation. These patterned films are important candidates for biological and micro-optics applications.

P126 Free Standing InP Thin Film Membranes on Si Substrates by Direct Wafer Fusion

Jesudoss Arokiaraj

In the optical telecommunication arena, applications such as real-time video-conferencing, internet has seen tremendous increase in handling high data rate transmission through the optical networks. Increasing this data rate and configuration capability will push the electronic components to their limits. This is a major issue of future photonic networks. Many promising technology-drivers have enabled to realize huge-capacity and high-complexity systems. Each technology possesses its own advantages and drawbacks. In order to integrate several functions on a same substrate, hybridization of different technologies has become a very interesting option.

The study here is focused on the hybridization of a thin InP semiconductor membrane onto an oxidized Si substrate using direct wafer bonding. The formation of native oxide on Si by a chemical process and InP by oxygen plasma exposure, aids in the contact bonding at room temperature spontaneously. Thermal annealing at 220°C for 45 minutes ensures atomic level bonding. InP substrate removal, defines a two micron InP thin film membrane bonded to Si. The thin film revealed excellent crystalline and structural quality by photoluminescence and double crystal x-ray diffraction. The free standing membrane was released by a combination of wet etching (BHF and KOH) and stress mapping was done by micro-Raman.

P127 Development of Surface Micromachined InP Based Photonic MEMS

Vicknesh Shanmugan

Compound semiconductor micromechanical structures offer enormous potential for convergence of photonics and microelectromechanical systems (MEMS). The use of these micromechanical structures with integrated photodetectors, to achieve tunable Fabry-Perot interferometers have been proposed earlier for fiber optic communications employing Wavelength Division Multiplexing (WDM) around 1.55 mm. The variation of the Fabry-Perot cavity length in these devices is achieved by electrostatic actuation induced movements of a Distributed Bragg Reflector (DBR) mirror suspended by beams. We have successfully developed a repeatable process to fabricate InP-based membranes using standard semiconductor fabrication techniques and a low-cost release & drying process. The fabrication techniques involve, optimized dielectric DBR stack deposition, membrane pattern definition, plasma etching to expose the sacrificial layer and metallisation to actuate the devices upon sacrificial release. The samples are subjected to sacrificial release by wet etching in H_2SO_4:H_2O_2: H_2O (1:1:8) followed by rinsing in DI water. Keeping the samples in DI water, they are frozen to 20°C below the freezing point and sublimed to vapor using a sublimation drying system. InP-based free standing structures with air gaps below the membranes and beams are observed under SEM. White Light Interferometer is also used to map the heights of various features on a released structure.

P128 Optical Add/Drop Multiplexing (OADM) Using InP Based Waveguides

Jesudoss Arokiaraj and Vicknesh Shanmugan

An optical add and drop multiplexer with the simultaneous functions of wavelength selection and routing of the selected signal, plays an important role in wavelength division multiplexing (WDM) networks. InGaAsP/InP vertical cross-coupler filters as OADMs are of particular interest because of their inherent monolithic integration with other optoelectronic devices, simple architectures and wavelength tunability.

Here we demonstrate a monolithic vertical cross-coupler based on a new architecture and adhesive wafer bonding approach. The cross-coupling occurs in a vertical direction with two sets of waveguides monolithically integrated on a semiconductor substrate. Since the waveguides are fabricated on a thin semiconductor film, bonded on a BCB coated Si substrate, the quality of the film was characterized at each process step, by photoluminescence, double-crystal x-ray diffraction and micro-Raman. The fabricated vertical coupler was characterized for the filtering effect using a waveguide set-up, where light from a tunable laser-fiber (1500 nm) was passed through an upper waveguide, coupled to the lower waveguide and correspondingly detected with an IR camera. The detailed analysis of the investigation will be presented.

P129 3D Scaffolds for Cell Culture Replicated from Self-Assembled Colloidal Crystals

Wang Likui, Siow Pi Choo, Yan Qingfeng, Sim King Huei, (George) X.S. Zhao*
Department of Chemical and Biomolecular Engineering, National University of Singapore
*E-mail: chezxs@nus.edu.sg

A three-dimensional (3D) macraporous hydroxyapatite (HA) scaffold with interconnected pores, ideal for cell culture, was synthesized by using colloidal crystal as template. PMMA beads of diameters in the range of 106–125 μm were synthesized and assembled into colloidal crystals. During the self assembly process, N,N-dimethylformamide was used as a solvent to aid the packing of the beads

and to create interconnected areas between the beads. HA was synthesized and infiltrated into the colloidal crystal through filtration under stirring. After several times of infiltration and removal of polymer beads through calcination, a macroporous 3D HA structure was obtained. The macroporous structure was characterized by SEM, TGA, XRD, and Hg porosimety. It was found that the structure have pores of around 100 μm interconnected by small necks. The size of the pores is suitable for bone cell growth and the interconnected necks facilitate the transfer of nutrient in the process of cell growth. The pore size can be easily controlled by the polymer bead size, and the neck diameter can be adjusted by N,N-dimethylformamide concentration. The porosity of the structure can be as large as more than 90%, which is ideal for cell culture.

P130 Photocatalytic Decomposition of Formic Acid Under Visible Light Irradiation Over V-Ion-Implanted TiO_2 Thin Film Photocatalysts Prepared on Quartz Substrate Using the Ionized Cluster Beam (ICB) Deposition Method

Jinkai Zhou[1], Masato Takeuchi[2], Ajay K. Ray[1], Masakazu Anpo[2] and (George) X.S. Zhao[1,*]
[1]*Department of Chemical and Biomolecular Engineering, National University of Singapore*
[2]*Department of Applied Chemistry, Osaka Prefecture University, Osaka, Japan*
*E-mail: chezxs@nus.edu.sg

Unique visible-light-responsive TiO_2 photocatalysts ($\lambda >$ 450 nm) were successfully developed by implantation of V ions into the TiO_2 thin films prepared on a quartz substrate by an ionized cluster beam (ICB) deposition method. The TiO_2 thin film photocatalysts were characterized by XRD, UV-vis, XPS, FE-SEM and AFM. After V ions implantation into TiO_2 thin film, the photocatalytic activity of the thin films for the decomposition of formic acid into CO_2 and H_2O was found to proceed efficiently under visible light irradiation longer than 450 nm. The origin of an enhancement of photocatalytic reactivity of the V ion implanted TiO_2 thin film was attributed to the modification of the electronic properties of TiO_2 thin film photocatalyst by the efficient substitution of the lattice Ti ions with V ions by ion-implantation, a physical doping method, which allows the doping of V ions with a high dispersion state.

P131 Template Synthesis of Graphitic Hollow Carbon Spheres

Fabing Su[1], Yong Wang,[1,2] Jim Yang Lee[1,2,3] and (George) X.S. Zhao*,[1]
[1]*Department of Chemical and Biomolecular Engineering, National University of Singapore*
[2]*Singapore-MIT Alliance, National University of Singapore*
[3]*Institute of Materials Research and Engineering (IMRE), Singapore*
E-mail: chezxs@nus.edu.sg

Recently, many novel porous carbons prepared by using templating strategies, ranging from microporous carbons, mesoporous carbons, to macroporous carbons, have been reported. These template-synthesized carbons possess many prominent characteristics, such as high surface area, relatively uniform pore size, ordered structure, and interconnected pore network, enabling them to find applications as catalyst supports, electrode materials, adsorbents, and optical materials, etc.

In this work, we prepared hollow carbon spheres with a graphitic carbon shell using the chemical vapor deposition (CVD) method in the presence of colloidal silica spheres as sacrificial template. The present preparation route involves carbon deposition by CVD of benzene vapor on the external surface of the silica spheres, followed by removal of the silica template using HF solution. The CVD mechanism was proposed. Nitrogen adsorption, thermogravimetric analysis (TGA) and X-ray diffraction (XRD) techniques were used to characterize the samples. The microscopic features of samples were imaged using field emission scanning electron microscope (FESEM) and field-emission transmission electron microscope (FETEM). The electrochemical properties of the carbon materials as anode electrodes in rechargeable lithium-ion batteries were evaluated.

P132 Thickness Dependence of Mechanical Properties of BD™ (Low-k) Thin Films

V.N. Sekhar*,[1], S. Balakumar[2], S.K. Sinha[1], Lu Shen[3] and A.A.O. Tay[1]
[1]*Nano/Microsystems Integration Lab, Department of Mechanical Engineering, National University of Singapore, Singapore-117576.*
[2]*Institute of Microelectronics, 11 Science park Road, Science Park II, Singapore-117685.*
[3]*Institute of Materials Research and Engineering, 3 Research Link, Singapore-117602.*
*E-mail: vnsekhar@nus.edu.sg

In Cu/low-k interconnect technology Black Diamond™ (low-k) has been identified as potential material for interlayer dielectric applications due to its better electrical and dielectric properties. But in dielectric material processing the key issue is the trade-off between dielectric and mechanical properties, results poor mechanical reliability. Hence it is very important to study the mechanical properties of the BD films. In present study we focus on thickness dependence of mechanical properties of the BD films. BD thin films of six different thicknesses 100, 300, 500, 700, 1000 and 1200 nm were deposited on 8" Si wafer by using PECVD technique for the present study. Nanoindentation and nanoscratch tests of the BD films were performed on Nano Indenter® XP (MTS Corp.) system using respective attachment. Hardness and elastic modulus of the BD films were characterized by using nanoindentation CSM technique. Significant difference in measured elastic modulus of the BD films observed. AFM scans of the residual indentation marks reveal that pile-up is prominent in thin film (100–500 nm) and sink-in is prominent in thick films (700–1200 nm). Adhesion strength of the BD films was characterized by using the nanoscratch ramp loading technique. Measured critical load (Lc) of the films and scratch width are increasing as the thickness of the film increases. Scratch failure mode is not same for all films and changes as the thickness varies. The nanoindentation and nanoscratch response of the BD thin films of six different thicknesses is not same and it is expected mainly

due to molecular reorganization in thin/ultra thin films. The present studies are very useful to estimate mechanical reliability of the patterned BEOL interconnects because the feature size of the BD thin films varies from few tens of nano meters to few microns.

P133 Surface NH_3 Anneal on Strained-$Si_{0.5}Ge_{0.5}$ for Metal-Oxide-Semiconductor Applications with HfO_2 as Gate Dielectric

Jidong Huang[1,2], Nan Wu[1], Qingchun Zhang[1], Chunxiang Zhu[1], M.F. Li, Andrew A. O. Tay[2], Zhi-Yuan Cheng[3], Chris W. Leitz[3] and Anthony Lochtefeld[3]
[1]*Silicon Nano Device Lab, Department of Electrical and Computer Engineering, National University of Singapore, 10 Kent Ridge Crescent, Singapore, 119260*
[2]*Nano/micro Systems Integration Lab, Department of Mechanical Engineering, National University of Singapore, 10 Kent Ridge Crescent, Singapore, 119260*
[3]*AmberWave Systems Corporation, 13 Garabedian Drive, Salem, NH 03079, USA*

In this study, metal-oxide-semiconductor capacitors were fabricated and characterized on compressively strained-$Si_{50}Ge_{50}$/ on $Si_{0.8}Ge_{0.2}$ virtual substrates by using metal-organic chemical vapor deposition HfO_2 as gate dielectric and TaN as metal gate electrode. It is demonstrated that surface nitridation treatment using NH_3 annealing prior to HfO_2 deposition effectively prevent the growth of GeO_x at the interfacial layer which exists on SiGe surface with direct deposition of HfO_2. X-ray photoelectron spectroscopic analysis suggests that the nitridation process tends to occur to Si atoms rather than to Ge atoms and results in the formation of an interfacial layer of SiN_xO_y on the SiGe surface. Capacitors with the surface nitridation treatment show good capacitance-voltage characteristics with negligible hysteresis and much smaller interface trap charge density in comparison with those of capacitors made without nitridation treatment. The surface nitridation seems to be a promising method for the formation of high quality high-k gate stack on strained-SiGe substrate.

P134 Germanium n^+/p Junction Formation by Excimer Laser Thermal Process

Jidong Huang[1,2], Nan Wu[1], Qingchun Zhang[1], Chunxiang Zhu[1], Andrew A.O. Tay[2], Guoxin Chen[3], and Minghui Hong[3]
[1]*Silicon Nano Device Lab, Department of Electrical and Computer Engineering*
[2]*Nano/micro Systems Integration Lab, Department of Mechanical Engineering*
[3]*Laser microprocessing Lab, Department of Electrical and Computer Engineering*
National University of Singapore, 10 Kent Ridge Crescent, Singapore, 119260

We demonstrated the first germanium n^+/p junction activated by laser thermal process. The substrates used for this study were phosphorous ion implantation gallium-doped p-type (100) germanium wafers. The annealing process was carried out by a KrF excimer laser with a wavelength of 248 nm.

The effect of laser energy fluence and irradiation pulse number on the redistribution of dopant atoms and the electrical properties of junction have been investigated. The secondary-ion-mass-spectrometry results indicate that step-like dopant profiles are formed with dopant atoms extending deeper upon increased laser fluence and successive pulse number. After being irradiated at laser energy fluence of 0.16 J/cm^2 with two successive pulses, the junction exhibits a sheet resistance of $\sim$50 Ohm/sq for n^+ region, a comparable I-V characteristic and much less phosphorus dopant diffusion in comparison with those formed by rapid thermal process annealing.

P135 Properties of Sn-3.8Ag-0.7Cu Solders Functionalized With Nanoparticles

K. Mohan Kumar[1,2], V. Kripesh[2] and Andrew A.O. Tay[1,*]
[1]*Nano/Microsystems Integration Lab, Department of Mechanical Engineering, National University of Singapore, Singapore-117576.*
[2]*Institute of Microelectronics, 11 Science park Road, Science Park II, Singapore-117685.*
*E-mail: g0203709@nus.edu.sg

The objective of the present work is to improve the mechanical, microstructural and melting properties of Sn-3.8Ag-0.7Cu solder by functionalizing them with minute amounts of nano-nickel and nano-molybdenum nanoparticles. Bulk Composite solders of up to 4wt% of nanoparticles were synthesized. The composite specimens were characterized by X-ray diffraction (XRD) and Field-Emission Scanning Electron Microscopy (FE-SEM). Melting characteristics of the nano particle-reinforced solders were determined using Differential Scanning Calorimetry (DSC). Microstructures of the composite solders were observed by FE-SEM at higher magnification for the observation of nano particle distribution in the solder matrix.

Mechanical properties of the composite specimens were compared with those of the pure solder specimens. It was found that the ultimate tensile strength (UTS) of Sn-3.8Ag-0.7Cu solder increased by 71% with the addition of 2.8 wt% of nano-molybdenum, while that of Sn-3.8Ag-0.7Cu solder specimens increased by 38% with the addition of nano-nickel. Hardness values of the nanoparticle reinforced composites have shown higher Vickers hardness values compared to their unreinforced counterparts. The enhanced mechanical properties of nano-particle functionalized solders which will be discussed in detail. The fractrographic examination conducted by FE-SEM indicated the existence of ductile features in the form of dimples in all the composite solders with different weight proportions of reinforcement. It is evident from the micrographs that much reduced ductility is observed in the specimens reinforced with the higher wt% of nano-ni and nano-mo addition. The optimum wt% reinforcement of nanoparticles for the best mechanical properties was determined. It was observed that the corresponding hardness values of the varying wt% of nano-ni composite solders varied from 158.9 MPa to 189.3 MPa, depending on the wt% of the reinforcement. Solders with 4 wt% nano-nickel addition had exhibited higher hardness values owing to the presence of the homogeneous distribution of nano-ni in

the solder matrix. In the case of Sn-3.8Ag-0.7Cu composite solders, functionalized with nano-mo hardness values were increased from 158.9 MPa to 234.4 MPa.

P136 Processing of the Nanotube Doped Solders and Their Mechanical and Properties for Fine Pitch Interconnection Applications

K. Mohan Kumar[1,2], V. Kripesh[2] and Andrew A.O. Tay[1,*]
[1] *Nano/Microsystems Integration Lab, Department of Mechanical Engineering, National University of Singapore, Singapore-117576.*
[2] *Institute of Microelectronics, 11 Science park Road, Science Park II, Singapore-117685.*
*E-mail: g0203709@nus.edu.sg

In the current study, the effect of nano-tube addition on the microstructural, mechanical and thermal behaviors of the Eutectic 63Sn-37Pb, Sn-3.8Ag-0.7Cu lead-free solders were investigated. The nano-tube functionalized composite solders were examined using X-ray diffraction (XRD) and Field-Emission Scanning Electron Microscopy (FE-SEM). Thermal behaviors of the SWCNT-reinforced solders were determined using Differential Scanning Calorimetry (DSC).

According to the XRD measurements, 63Sn-37Pb composite solders show the diffraction peaks for Tin (Sn), Lead (Pb), Carbon (SWCNT), while Sn-3.8Ag-0.7Cu composite solders exhibit the diffraction peaks for Sn, Ag_3Sn, Cu_6Sn_5 and Carbon (SWCNT). The intensity of carbon peaks increased with the increase in wt% of SWCNT addition to the solder matrix. The higher the carbon content the greater the intensity for the SWCNTs observed in the XRD spectra. Microstructures of the composite solders were observed by FE-SEM at higher magnification for the observation of the CNT distribution. It was observed that the corresponding hardness values of the varying wt% of SWCNT composite solders varied from 119.65 MPa to 167.7 MPa, depending on the wt% of the reinforcement. Solders with 1 wt% SWCNT addition had exhibited higher hardness values owing to the presence of the homogeneous distribution of SWCNT in the solder matrix. In the case of Sn-3.8Ag-0.7Cu composite solders, hardness values were increased from 158.9 MPa to 187.3 MPa.

Mechanical testing was carried out on both Sn-Pb and Sn-Ag-Cu based composite solder specimens. The Ultimate tensile strength (UTS) of the both composite solders with different wt% of nano-tube additions was compared with that of the virgin 63Sn-37Pb and Sn-3.8Ag-0.7Cu solder specimens. The UTS of the composite solders is shown to increase with the increasing wt% of nano-tubes until certain wt% of the SWCNT reinforcement. It was found that the ultimate tensile strength (UTS) of 63Sn-37Pb solder increased by 28% with the addition of 0.3 wt% of CNTs, while that of Sn-3.8Ag-0.7 Cu solder specimens increased by 49% with the addition of SWCNTs upto 1wt%. The enhanced mechanical properties of CNT-reinforced solders could be due to the possible load-transfer mechanisms of the CNTs. The fractrographic examination conducted by FE-SEM indicated the existence of ductile features in the form of dimples in all the composite solders with different weight proportions of reinforcement. It is evident from the micrographs that much reduced ductility is observed in the specimens reinforced with the higher wt% of CNTs.

P137 Infrared Spectro/Microscopy at SSLS — Applications to Material Science and Characterization of Organic Compounds

Mohammed Bahou*[,1], Li Wen[1], Xiande Ding[1], B. Didier F. Casse[1], Sascha P. Heussler[1], Herbert O. Moser[1], Wee-Sun Sim[2], Jin Gu[2] and Yves-Laurent Mathis[3]
[1] *Singapore Synchrotron Light Source, National University of Singapore, 5 Research Link, Singapore 117603*
[2] *Department of Chemistry, National University of Singapore, 3 Science Drive 3, Singapore 117543*
[3] *Institute for Synchrotron Radiation/ANKA, Forschungszentrum Karlsruhe, Postfach 3640, D-76131 Karlsruhe, Germany*
E-mail: slsmb@nus.edu.sg

Singapore Synchrotron Light Source (SSLS) is commissioning its new beamline for Infrared Spectro/MIcroscopy (ISMI). The infrared light is extracted from the edge region of dipole D1 of the compact superconducting electron storage ring Helios 2 as manufactured by Oxford Instruments. The nominal source point is located at half the maximum field, i.e., at 2.25 T. The light is collected with a water cooled plane mirror and relayed into a Bruker IFS 66 v/S vacuum Fourier transform interferometer by two toroidal mirrors, a second plane mirror, a rotational ellipsoidal mirror, and, finally, a plane mirror. Near the beam waist, a wedged diamond window is placed to separate ultra high vacuum on the upstream side from fore vacuum on the downstream side. The IFS 66 v/S is coupled with a Hyperion 2000 microscope and a UHV chamber for in situ reflection-absorption infrared spectroscopy (RAIRS).

With this optical configuration a bright infrared source with a spectral range extending from 15000 cm-1 to 10 cm-1 is achieved. The Optical design and the performance of the ISMI beamline will be presented. Experimental results of electromagnetic metamaterials, lamellar grating mirror will be presented. Application of Attenuated Total Reflection (ATR) measurements on Ganoderma spores will be presented.

P138 Cathodic Properties of $Li(Co_{1-x}Al_x)O_2$ (x=0.05-0.25) Prepared by Molten Salt Method for Li-Ion Batteries

M.V. Reddy, G.V. Subba Rao and B.V.R. Chowdari*
Department of Physics, National University of Singapore Singapore 117542
*E-mail: phychowd@nus.edu.sg

Lithium cobalt oxide, $LiCoO_2$ is presently used as the cathode material in commercial lithium ion batteries. However, due to the reversible crystal structure transitions that occur during charge-discharge operations for $x \geq 0.5$ in $Li_{1-x}CoO_2$, the utilizable capacity is restricted to $x < 0.5$. Studies have shown that dopants like Al or Mg can suppress the phase transitions thereby offering scope for increasing the capacity. Presently we prepared

$Li(Co_{1-x}Al_x)O_2$, x = 0.05–0.25 phases by using a one-pot molten salt method at 850°C in air and characterized by X-ray diffraction, Rietveld refinement, SEM and other methods. Cathodic properties were studied at ambient temperature in cells with Li-metal as the counter electrode by cyclic voltammetry (CV), galvanostatic charge-discharge cycling and Impedance spectroscopy. Single-phase compounds with hexagonal layer structure formed for all x. The CV showed that the redox couple, $Co^{3+/4+}$ is at ∼ 4.1–4.2 V for x ≥ 0.05, a value slightly higher than that shown by pure $LiCoO_2$ and the structural transitions that occur at 4.1–4.2 V are suppressed. As a consequence, the cyclability of $Li(Co_{1-x}Al_x)O_2$ is improved. Thus, for x = 0.15 and 0.20 stable capacities of 125 and 105 (± 3) mAh/g respectively, were obtained up to 60 cycles in the range, 2.5-4.3 V at the current rate of 30 mA/g. Higher initial capacities were noted for x ≤ 0.10 in the above voltage range and for all x with an upper cut-off voltage of 4.4 or 4.5 V. However, long-term cycling (up to 125 cycles) showed small capacity-fading.

P139 Incorporation of Noble Metal Nanoparticles in to Three-Dimensionally Ordered Macroporous TiO_2

Madhavi Srinivasan*, Guo Jun and Tim White
School of Materials Science and Engineering, Nanyang Technological University
*E-mail: madhavi@ntu.edu.sg

Titania (TiO_2) is a well known photocatalyst used in the decomposition of organic/ inorganic pollutants under ultra-violet (UV) light. Porous TiO_2 exhibits improved photocatalytic activity owing to its low density, high surface area, high porosity and increased adsorption/ diffusion properties of the target organic molecules. The deposition of noble metals on to these TiO_2 particles enhances the efficiency of photocatalytic reactions by promoting interfacial charge-transfer processes. In view of this, we have incorporated Au and Pt nanoparticles in to three-dimensionally ordered macroporous (3DOM) TiO_2. The 3DOM TiO_2 was synthesized by colloidal crystal templating using an alkoxide precursor and polystyrene spheres. Metal nanoparticles were deposited onto these porous structures by sodium borohydride reduction of the respective metal chlorides. Detailed synthesis and characterization of these metal/semiconductor nanocomposites will be presented.

P140 Sol-Gel Synthesis of Rare Earth Apatite, $Ca_2Nd_8(SiO_4)_6O_2$

S.C. Lim, T. White, Z. Dong and M. Srinivasan
E-mail: sclim@ntu.edu.sg

Silicate apatites of the type $Ca_2(REE, ACT)_8(SiO_4)_6O_2$ are potential host matrices for immobilization of rare earth element (REE) fission products and actinides (ACT) due to their radiation resistance. The neodymium-bearing apatite $Ca_2Nd_8(SiO_4)_6O_2$ is a suitable crystallochemical surrogate for waste forms containing light REEs and trivalent actinides. Conventionally, these apatites are synthesized by solid state methods at temperatures as high as 1700°C. In an effort to reduce the synthesis temperature and to increase the surface area of these materials, we have adopted soft chemistry processing routes to obtain single phase apatite. Using alkoxide precursors, these apatites can be synthesized at temperature as low as 600°C – 700°C. Detailed characterization of the synthesized materials was undertaken using X-ray diffraction and scanning/transmission electron microscopy.

P141 Molecular Dynamics Simulation Study of Transport of Liquid Water Through Carbon Nanotubes

Z.S. Liu[1], H.J. Gao[2], Y. Kong[2] and C. Lu[1]
[1]*Institute of High Performance Computing, 1 Science Park Road, #01-01 The Capricorn, 117528 Singapore*
[2]*Max Planck Institute for Metals Research, Heisenbergstrasse 3, 70569 Stuttgart, Germany*

Transport of molecules through molecular pores is essential for many biological processes. In recent years, the pursuit of new types of molecular transporters is an active area of research, due to the high impermeability of cell membranes to foreign substances and the need for intercellular delivery of molecules. The carbon nanotubes (CNTs) have been shown that it can be as building blocks in nanotechnology. The special geometry and interesting properties of CNTs offer various potential applications, such as nanoscale electronic devices, nanoscale sensors, selective molecular filters, support materials for catalysis, and removal of noxious organic chemicals. In order to determine the biocompatibility, potential utilities, and applications of novel nanomaterials in biological processing, the interaction between nanotubes and the materials of living systems should be investigated. As there exist an analogous water channels in living cells and CNTs can serve as prototypes for biological channels, it is more imperative to first study the behavior of water confined in CNTs.

In this presentation, the molecular dynamics simulation results for transport of water molecules through carbon nanotubes will be reported. In the simulation, short uncapped single-walled carbon nanotubes with different length and diameter as well as different helicity are modeled and simulated by MD software MPDyn. From simulation results, we will show that in specified cases, such as certain nanotube diameter and helicity, the initially empty nanotube channel can be filled by water from the surrounding reservoir, and remain occupied by certain number of water molecules during the entire process. A one-dimensionally ordered chain of water molecules is formed. The study demonstrated that the carbon nanotubes, with their rigid nonpolar structures, may be further exploited as unique molecular channels for water and others, with the channel occupancy and conductivity tunable by changes in the local channel polarity and solvent conditions.

P142 Room-Temperature Ferromagnetic $Zn_{0.95}Co_{0.05}O$ Diluted Magnetic Semiconducting Thin Films by Pulsed Laser Deposition

Zhang, Yuebin[1]; Liu, Qing[1]; Sritharan, Thirumany[1]; Li, Sean[2]
[1]*School of Materials Science and Engineering, Nanyang Technological University, Singapore 639798*
[2]*School of Materials Science and Engineering, The University of New South Wales, Sydney, NSW 2052, Australia*
E-mail: eybzhang@ntu.edu.sg

Co-doped ZnO thin films with room-temperature ferromagnetism have been successfully synthesized on (001) Si substrates by pulsed-laser deposition using a $Zn_{0.95}Co_{0.05}O$ ceramic target. Their microstructural properties are carefully studied using atomic force microscopy, x-ray diffraction and high-resolution transmission electron microscopy. The oxidation state of Co and the ratio of Co/Zn are examined by x-ray photoelectron spectroscopy, and magnetic measurements are performed using SQUID. Results show that a single-phase crystalline Co-doped ZnO film was grown with (002) preferential orientation and some edge dislocations formed during the film growth. The origin of room-temperature ferromagnetism is explored. The presence of nanoclusters of any magnetic phase can be ruled out. The dislocations, coupled with oxygen vacancy, may contribute to the ferromagnetic properties in the diluted magnetic semiconductor.

P143 Lubricant Film Uniformity Control for Magnetic Hard Disks

Y.R. Koh[1,2], J. Zhang[2], Y.H. Wu[1] and L. Boris[2]
[1] *ECE Department, National University of Singapore, Singapore 117576*
[2] *Data Storage Institute, 5 Engineering Drive 1, Singapore 117608*
E-mail: Zhang_jun@dsi.a-star.edu.sg

Lubricant film on hard disks is required to be uniform in order to minimize contact with slider which can affect the recording quality. Uniformity as deposited is important due to the limited effect of buffing. A typical dip-coated disk will show streaks and bands with different lubricant uniform thickness. Vibrations together with a band of thicker region across the middle of the disk resulted from constant withdrawal speed has been identified as the major cause of such non-uniformity. The results show that lubricant film thickness increases as withdrawal speed increases and vice versa. To achieve better uniformity, techniques including anti-vibration method are developed to remove the centre band and streaks of lubricant on the magnetic hard disk.

P144 Textured Growth of FeCo for Soft Underlayers in CoCrPt:SiO_2 Perpendicular Recording Media

C.S. Mah*, M.J. Liau[1], S.N. Piramanayagam and J.Z. Shi
Data Storage Institute, 5 Engineering Drive 1, Singapore 117608.
[1]*ECE Department, National University of Singapore, Singapore.*
E-mail: MAH_Chee_Shong@dsi.a-star.edu.sg

Soft magnetic underlayer of a double-layered perpendicular recording medium plays a crucial role in perpendicular recording technology, as the layer helping the writing process. At present, the most common soft magnetic underlayer is an amorphous material based on CoZr alloy. This underlayer exhibits a lower noise compared to many other materials. However, with an amorphous soft underlayer, a thick intermediate layer is needed to generate a good c-axis orientation of cobalt grains. On the other hand, if a crystalline soft underlayer with a fcc(111) phase is used, with suitable fcc(111) texture, Co-based recording media can grow with a hcp(002) texture. In such a case, very thin intermediate layer is sufficient to provide hcp(002) texture. In this study, we have investigated the effect of composition of CoFe alloy and suitable underlayers on the fcc(111) orientation and the subsequent Co(002) texture.

FeCo films were prepared by co-sputtering of Fe and Co targets. The films were prepared on Ta, Ta/Pd seedlayers and without seedlayers on glass substrates. It can be seen that the XRD pattern is different in the case of Ta/Pd underlayers, as compared to those on Ta underlayers. The Pd(111) induces a clear FeCo – fcc(111) phase. The films deposited on Ta/Pd underlayers also showed a reduced $\Delta\theta_{50}$ compared to films with Ta seedlayers only. The squareness and coercivity was greatly reduced when Ta/Pd underlayers were used. These results indicate that the texture of FeCo can be improved by suitable underlayers.

P145 Magnetic Intermediate Layer for Perpendicular Recording Media

C.S. Mah*, S.N. Piramanayagam, J.Z. Shi, J.M. Zhao, J. Zhang and Y.S. Kay
Data Storage Institute, 5 Engineering Drive 1, Singapore 117608
*E-mail: MAH_Chee_Shong@dsi.a-star.edu.sg

Recently, CoCrPt:oxide based alloys have been considered as perpendicular recording medium. In these media, the grains are separated by oxygen based grain boundary. Low noise, large SNR and smaller grains have been observed in the recording media based on these materials. Areal densities higher than that achieved by longitudinal recording have also been demonstrated. It is expected that these materials can be used in the hard disk drives for areal densities, as high as 600 Gb/in2. Some of the challenges for these materials towards very high areal densities are reduction of grain size & grain size distribution, reduction of c-axis dispersion (50, as observed by XRD), and reduction of intermediate layer thickness.

CoCrPt:oxide media has a few layers of materials as the intermediate layer. An increase in the $\Delta\theta$50 is observed when the Ru intermediate layer thickness is reduced. However, the reduction in the intermediate layer would help in the writing process. A novel concept that we propose is the use of magnetic intermediate layers. Under suitable deposition conditions, the magnetic material will help to improve the hcp(002) growth and during the writing process, it will pass the flux from head to SUL effectively. AGM, XRD and spin-stand measurements show acceptable SUL performance. This method has potential to solve the problem of intermediate layer thickness reduction.

P146 Effect of PEG on Rapamycin Release from Biodegradable Polymer Matrices

Xintong Wang, Subbu S. Venkatraman, and Yin Chiang Freddy Boey*
School of Materials Science and Engineering, Nanyang Technological University
*E-mail: MYCBOEY@ntu.edu.sg

Rapamycin-loaded polymer films of poly (lactic-co-glycolic acid) (PLGA) were produced. PEG was incorporated into polymer film as a plasticizer. Rapamycin release properties were studied in both polyethylene glycol (PEG) plasticized and unplasticized polymer matrices. Rapamycin release from PLGA 53/47 was mainly controlled by polymer degradation. The addition of PEG significantly changed the properties of PLGA and rapamycin release profile as well. PEG plasticized PLGA gave a zero-order release and expedited the degradation of polymer. However, a higher loading as l0% of pEG showed no further acceleration effect than 5% PEG on rapamycin release.

P147 Effect of Low Voltage Electron Beam on Biodegradable Polycaprolactone

N.K. Chia, Subbu Venkatraman and F.Y.C. Boey*
School of Materials Science and Engineering, Nanyang Technological University
*E-mail: MYCBOEY@ntu.edu.sq

The purpose of this study is to examine the effect of low energy electron beam on biodegradable polymers (PCL), and to understand their radiation-induced degradation mechanisms.

The degradation of these films was studied by measuring the changes in their molecular weights and morphological properties. The PCL film was irradiated and observed to undergo radiation-induced degradation through chain scission, as observed from a drop in its average molecular weight Mw with increasing radiation dose.

In-vitro study show that the average molecular weight for the PCL films is not affected by hydrolysis during immersion in pH 7.4 buffer solution after irradiation. The irradiation has ciused the molecular weight to drop initially with increased dosage. However it is stable during the period of immersion. Thus the effect of chain scission resulting in the drop of average molecular weight for PCL film is more significant during irradiation than hydrolysis.

After irradiation, result shows that the enthalpy of fusion for PCL films increases with dosage. The increase in enthalpy of fusion could due to the breakdown of amorphous region by chain scission thus resulting in the increase in the degree of crystallinity.

P148 Study of Micellar Aggregates of Star-Shaped PLA/PEO Copolymers

Pan Jie, Boey Yin Chiang, Fredd* and Subbu S. Venkatraman
NTU/MSE
*E-mail: MYCBOEY@main.ntu.edu.sg

Amphiphilic star-shaped block copolymers with varying compositions of hydrophilic poly (ethylene oxide) (PEO) and hydrophobic poly poly (L-lactic acid) (PLA) were synthesized by ring opening polymerization. In aqueous medium, the amphiphilic copolymer can self-assemble to form micellar aggregates below 200 nm. With the study of Static light scattering (SLS) and TEM, we assumed a vesicle-like structure for these novel micellar aggregates. With the x-ray photon electron spectrum (XPS) study, surface segregation of micellar aggregates on surface was noticed. These micellar aggregates show promising application in the controlled drug delivery field.

P149 Floating Alginate Beads For Gastric Retentive Drug Delivery

Tang Yong Dan, Boey Yin Chiang, Freddy* and Subbu S. Venkatraman
School of Material Science and Engineering, NTU
*E-mail: MYCBoey@ntu.edu.sg

Floating dosage forms allow prolonged gastric retention of drugs of interests hence provide a plausible way of local sustained release. In this paper, a type of multi-unit floating alginate gel beads was synthesized with calcium alginate, sunflower oil, a drug of interest through an emulsification gelation process. The alginate beads with oil were able to keep buoyant on the simulated gastric fluid for 24 hrs while the non-oily beads could not. Two kinds of drug with different hydrophilicities, ibuprofen and niacinamide, were tested respectively in the study. The more hydrophobic ibuprofen was released in a sustained manner for 24 hrs, while the hydrophilic niacinamide release was released in a burst manner. The oil partition was believed to be the major cause that ibuprofen release was extended.

P150 Excitonic Gain in Wurtzite $Mg_xZn_{1-x}O$-ZnO Strained Quantum Wells

A.P. Abiyasa, S.F. Yu, S.P. Lau and W.J. Fan
School of Electrical & Electronic Engineering, Nanyang Technological University, Block S2, Nanyang Avenue, Singapore 639798
E-mail: agus0004@ntu.edu.sg

Excitonic gain of wurtzite $Mg_xZn_{1-x}O$-ZnO quantum wells (QWs) is studied theoretically. The valence electronic band structure of $Mg_xZn_{1-x}O$-ZnO QWs, with the influence of biaxial strain and exciton-phonon interaction are taken into consideration, is calculated based on a 6×6 Hamiltonian. The conduction-valence band-offset ratio and conduction band deformation potential constant of $Mg_xZn_{1-x}O$-ZnO QWs are found to be 60/40 and −6.8 eV, respectively, from the available experimental data. The influence of biaxial strain on the peak excitonic gain of ZnO/$Mg_xZn_{1-x}O$ QWs for various well-width and Mg mole fraction is also investigated.

P151 Pressure-Sensitivity and Plastic Dilatancy Effects on Crazing in Polymers

Huck Beng, Chew; Tian Fu, Guo and Li, Cheng*
National University of Singapore
Department of mechanical engineering
*E-mail: mpecl@nus.edu.sg

Unlike metals, the yielding of polymeric materials exhibit pressure-sensitivity and the plastic flow is non-volume preserving. Fracture of these materials is often preceded by the formation of small crack-like defects known as crazes. In this study, the effects of pressure-sensitivity α and plastic dilatancy β on craze nucleation and growth are examined. A computational study is first performed to gain insights into the effects of α and β on the extent of plastic dissipation in a center-cracked tension specimen. The contribution of these parameters to craze growth is further examined by placing a single row of discrete voids ahead of a crack within a small-scale yielding boundary layer model. Results show that high pressure-sensitivity can induce large-scale damage, significantly increasing the plastic zone size and the extent of craze growth. In contrast, plastic dilatancy suppresses the craze growth and raises the stress carrying capacity of the material. This study offers some evidence of pressure-sensitivity as a major contributor to the formation of microporous crazing zones in polymers.

P152 Hydrothermal Epitaxy of Perovskite Films at 170°C

Gregory K.L. Goh* and Kelvin. Y.S. Chan
Institute of Materials Research and Engineering
*E-mail: g-goh@imre.a-star.edu.sg

Due its close lattice match with $KNbO_3$, $KTaO_3$ is ideal as a substrate or buffer layer for the growth of epitaxial $KNbO_3$ films which have the largest reported electromechanical coupling constants. Doped with niobium, the cubic phase of $KTa_{1-x}Nb_xO_3$ (KTN) is a good candidate material for electro-optic applications like band filters, light modulators and IR detectors. As bulk single crystals of $KTaO_3$ and KTN are difficult and expensive to grow, attention has been focused on the growth of epitaxial films. Hydrothermal epitaxy is a low temperature and potentially cost effective method of film growth that requires greater understanding.

In this study, epitaxial $KTaO_3$ films were grown hydrothermally on single crystal $SrTiO_3$ substrates by reacting Ta_2O_5 powder in a 7M KOH solution at 170°C. It was observed that the $KTaO_3$ film formed by the island growth mode and that buckling cracks were present after a critical film thickness. Determination of the residual strain due to grain coalescence, lattice mismatch and thermal expansion mismatch indicated that differential contraction between the substrate and film during cooling generated sufficient compressive stress to cause film buckling at regions where a separation between the film and substrate was present.

P153 Crystallinity and Cracking of Solution Deposited TiO_2 Films

Gregory K.L. Goh* and M.A. Bing
Institute of Materials Research and Engineering
*E-mail: g-goh@imre.a-star.edu.sg

Anatase TiO_2 is an important technological material that can be used for photocatalytic applications like antifogging, self cleaning, and solvent purification. An increasingly common method for oxide film growth is the use of low-temperature aqueous solutions to deposit crystalline films because temperature sensitive substrates polymers and organics can be used. As solution methods are cost effective, they may have a potentially significant impact on commercialization and not just for research.

In this study, the crystallinity of the anatase film was raised by increasing the growth temperature from 50 to 200°C. The higher growth temperature improved the crystallinity of the film from 70 to 90% because hydrolysis and dehydration was more complete. Despite this, the photocatalytic properties of the film appeared to improve with increasing growth temperature not because of greater crystallinity, but because the 200°C film had the larger internal surface area due to a different film formation mechanism. Also, for the first time, the cause of film cracking when a critical thickness is reach is investigated for photocatalytically active anatase TiO_2 films. It is important to understand such mechanical stability issues if solution deposited TiO_2 films are to be commercialized successfully.

P154 GaN Faceted Epitaxy

Hailong Zhou, Soo Jin Chua and LianShan Wang
E-mail: G0301203@nus.edu.sg

Epitaixal lateral overgrowth which occurs during GaN selective epitaxial has been studied using liner and designed shape mask features. The lateral growth varies between its maximum and minimum over a 30o angular span and exhibits hexagonal symmetry. Large variations in the lateral growth between the <11$\underline{0}$0> direction and <11$\underline{2}$0> direction are also obtained through variations in the growth temperature. Vertical growth follows an opposite trend to the lateral growth increase with the temperature increase. Under proper growth conditions, lateral to vertical growth rate ratios maximum can be achieved, resulting in significant lateral mask overgrowth and coalescence of features without excessive growth times. And we also describe experiments to distinguish whether the lateral transport of material occurs via gas-phase diffusion or surface diffusion, either on the mask itself or on the epitaxial material. These results indicate that gas-phase diffusion dominates the transport of material during GaN ELO.

P155 MicroFE Analyses of Human Femur Post-Arthroplasty

Jeremy Teo Choon Meng*,[1], Zhenlan Wang[1], Chee Kong Chui[1], Kuanming Si-hoe[1], Chye Hwang Yan[2], Sim Heng Ong[2], Shih-Chang Wang[3] and Swee Hin Teoh[1]
[1]*Department of Mechanical Engineering, National University of Singapore*
[2]*Department of Electrical Engineering, National University of Singapore*
[3]*Department of Diagnostic Radiology, National University Hospital*
*E-mail: mpetcmj@nus.edu.sg

The modeling of the microstructure of biological materials such as bone is an important step towards understanding their long-term stability. In this study we focus on the femur. Hip prostheses are required to be affixed into the femur as well as to withstand physiological loading over millions of cycles. Stresses are distributed over the entire cross-section of the femur in the normal hip. After hip arthroplasty, loading differs due to different prosthesis design and affixationmethod. Current methods to evaluate

the effectiveness of prosthesis or affixation includes, cadaveric testing and finite element analyses (FEA). FEA is attractive as numerous test can be carried out on a single specimen, experimental unknowns are eliminated and reproducibility in results are certain. However, the microporous cancellous bone in FEA is assumed as a continuum solid, which may not reflect the actual transfer of load from prosthesis to femur. In this study, we attempt to employ microFEA to visualize the load transfer before/after hip arthroplasty, cement andcement-less affixation method as well as a prosthesis with surface modification to aid in load transfer. We automatically generated microFE models of the femur and prosthesis directly from microCT imagesand digitally registered the image datasets to mimic hip arthroplasty. As an initial study, a 2D simulation was performed mid-frontal section of the femur and prosthesis.

P156 Permeability Testing of Irregular Cellular Solids Using Computational Fluid Dynamics and MicroCT Imaging

Jeremy Teo Choon Meng*,[1], Shih-Chang Wang[2] and Swee Hin Teoh[1]
[1]*Department of Mechanical Engineering, National University of Singapore*
[2]*Department of Diagnostic Radiology, National University Hospital*
*E-mail: mpetcmj@nus.edu.sg

Knowledge on the ease of fluid transport, or permeability, across cellular solids is important for complete characterization of materials. Aluminum foams used as lightweight heat exchangers, biopolymeric scaffold constructs for tissue engineering and knowledge of PMMA flow into cancellous bone are some important applications requiring permeability data. Permeability testing of materials is technically challenging requiring constant pressure head or fluid flow, uniformly tight seal between material and flow chamber interface and degassed fluid to name a few. Computational fluid dynamicas (CFD) can overcome these stringent requirements. However, it is not possible to model such irregular cellular solids for analyses using conventional CAD software. Here we employ microCT imaging technology to automatically extract intricate irregular geometry for CFD simulation of permeability test. As an initial study, we perform permeability testing analyses on simple, but highly variable, cellular solids such as polymeric scaffolds to intricate cellular solids with complex geometries such as cancellous bone. We performed linear correlation studies, single and multivariable, to determine microarhictectural properties that influence permeability directly. Connectivity (Tb.Pf) of the cellular solid can yield a R^2 value of 0.64 ($p = 8.01E\text{-}06$) and together with architecture pattern (SMI), spacing (Tb.Sp) and material thickness (Tb.th) a R^2 value of 0.93 is obtained.

P157 Micro-CT Imaging of Bone Microstructure Under Compression Loading Using Radiotranslucent Mechanical Testing Rig

Si-hoe K.M., Jeremy Teo and Teoh S.H.
National University of Singapore
Department of Mechanical and Production Engineering
E-mail: mpetcmj@nus.edu.sg

The relationship between microstructure and mechanical properties of bone is an important field of study. How the spongy bone, trabecular structure, deform with applied load has recently been highlighted to be critical in understanding many osteoporotic anomalies which can lead to fatal fracture. To date, there has been no micro-CT study of the bone microstructure of whole vertebrae under mechanical loading. This is now possible with the development of the Radio-translucent mechanical testing rig (RTR) used in conjunction with a Shimadzu micro-CT scanner.

Preliminary tests were conducted to verify the feasibility of the rig design in exerting a compression force large enough to cause initial failure in a vertebral body. Stepwise compression loading was conducted on a single porcine vertebra and the loading data was compared to results obtained from an industrial grade MTS compression testing machine. Finally, the ability of the RTR to yield high quality micro-CT scans of a porcine vertebra prior to, and at a compression failure strain of 12.1% was to be verified.

The stepwise compression loading conducted in the rig was found to effectively approximate a continuous loading of the same specimen in a MTS compression testing machine, as the deviation of the compressive forces exerted (at various strain levels) by both machines did not exceed $\pm$ 60.0 N. Finally, resultant micro-CT images (isotropic resolution 32.80 μm) of porcine vertebra trabecular microstructure loaded in the rig were obtained using the Shimadzu scanner. For the first time, trabecular microarchitecture detail of a whole vertebra buckling under 12.1 % failure compression strain loading was studied using a voxel-data visualization software.

P158 Characterization of Bone Material Property using Transfer Functions

Zhenlan Wang*,[1], Shu-Rong Weng[1], Chee-Kong Chui[1], Jeremy Teo Choon Meng[1], Chye-Hwang Yan[2], Sim-Heng Ong[2,3] and Swee-Hin Teoh[1]
[1]*Department of Mechanical Engineering, National University of Singapore*
[2]*Department of Electrical Engineering, National University of Singapore*
[3]*Division of Bioengineering, National University of Singapore*
*E-mail: mpewzl@nus.edu.sg

Modeling the heterogeneity in biological materials such as bone is important in computer assisted planning of surgery to reduce invasiveness. To be specific, parts of bone could be weakened via disease such as cancer. In this study we focus on the development of a spine invasive map to provide surgeons with an intuitive representation of the underlying bone material properties. This characterization is achieved via visualization using material sensitive transfer functions. The transfer functions assume a linear correlation between the strength of bone and its various characteristics such as bone density in the form of porosity of cancellous/cortical bone from medical images, and stiffness and elastic/plastic property measured via experiments. The selection of a transfer function for a specific material is automatic, and will result in the assignment of a unique shade of colors to the material. We attempt

to standardize the coloring scheme used to represent different material properties, so as to have a single unique representation. This will remove the needed for repetitive legend tables looking up. There is a need to study an extensive database of bone images and the underlying material properties. Clinical evaluations are also required to determine the usefulness of these visual characterization methods.

P159 Behavior of Piezoelectric Tubular Transducers in Relation to Tube Geometry

Ng Kuang Chern Nathaniel*, Li Tao, Ma Jan and Boey Yin Chiang, Freddy
Nanyang Technological University
*E-mail: ngkc@ntu.edu.sg

Piezoelectric tubular transducers are used in a wide range of applications, and as ultrasonic motors, they have been shown to outperform their electromagnetic counterparts of mm-order diameters and below. Two key material properties, the mechanical quality factor, Qm and the piezoelectric constant, d31 have been shown to govern the performance of such motors. Characterization of tubes of various materials and geometries are characterized in terms of resonance frequency, the dynamic bending displacement, and the vibration velocity, and constitutive relationships are derived. A comparison is made showing that the factor, Qm ' d31, indeed governs the performance of such motors. For both hard and soft PZT, linear relationships are observed between the vibration velocity and a geometric term. These results indicate a possible dependence of the material constants, Qm and d31 on the geometry of the tube, due to the frequency dependence of the constants. In the case of hard PZT, the vibration velocity shows an apparent independence of the geometric term, which opens to the question: how small can the geometry of the transducer be reduced without a reduction in the vibration velocity?

P160 Measuring Material Properties of Bone Using CT Imaging

Lei Yang*[,1,4], Chee Kong Chui[1], Sim Heng Ong[2,4], Shih-Chang Wang[3], Swee Hin Teoh[1] and Chye Hwang Yan[2]
[1]*Department of Mechanical Engineering, National University of Singapore*
[2]*Department of Electrical Engineering, National University of Singapore*
[3]*Department of Diagnostic Radiology, National University Hospital*
[4]*Division of Bioengineering, National University of Singapore*
*E-mail: leiyang@nus.edu.sg or g0402682@nus.edu.sg

Porosity of bone directly affects the mechanical characteristics of the tissue. With higher mineral content, the cortical bone is stiffer than trabecular bone, can withstand greater stress but less strain. Dual-energy x-ray absorptiometry (DXA) provides an effective measure of bone mineral density (BMD), reflecting the bone mineral content averaged across a specific region of interest. However, this technique only produce a two dimensional projected measurement of the bone mineral density. In this study, we will attempt to use 3D CT imaging to provide a measurement of the 3D bone mineral density. The process requires the precise measurement of the beam spectral intensity for the 80 kVp and 120 kVp setting. Phantoms from different 'pure' materials will first be constructed. We will scan these phantoms using the clinical CT machine from NUH. With the scan images and the material attenuation characteristics, we then proceed to estimate the beam spectral intensity. Estimation will be performed for both 80 kVp and 120 kVp. After which, we will scan a subject using the two kVp settings and perform a dual energy processing to obtain the 3D mapping of the bone mineral density. This work has potential applications for bone research and osteoporosis related research.

P161 Frequency Selective Composites with Randomly Distributed Conductive Fibers

L. Liu, S. Matitsine and Y.B. Gan
Temasek Laboratories, NUS
5 Sports Drive 2
Singapore 117508
E-mail: tslll@nus.edu.sg

Frequency selective composites (FSC) with band-stop properties can be obtained using half-wavelength conductive fibers embedded in a dielectric or magnetic host matrix via the spray method. The fibers can be periodically or randomly distributed in composites, both of which have interesting electromagnetic properties for practical applications, such as EMC/EMI shielding and antenna with low EM signature. The case of randomly distributed fibers is, however, more attractive due to its simpler and more convenient fabrication.

The transmission coefficient of FSC with randomly distributed conductive fibers of high volume concentrations was investigated with free space measurement and FEM (finite element method) calculation. Dependence of the effective permittivity of composites on the volume concentration and length of inclusive conductive fibers was obtained from the fitting of Lorentzian model. Cluster effects of overlapping fibers can explain why relaxation frequency is a function of concentration but resonance frequency even at high concentration is still close to that of single fiber. It was demonstrated that the current model can accurately predict the microwave properties of fiber composites.

P162 Application of Poly (ε-caprolactone) Films in Vascular Tissue Engineering Applications

Mark Chong Seow Khoon*[,1], Lee Chuen Neng[2] and Teoh Swee Hin[3]
[1]*Graduate Program in Bioengineering, National University of Singapore*
[2]*Department of Cardiac, Thoracic and Vascular Surgery, National University Hospital*
[3]*Department of Mechanical Engineering, National University of Singapore*
*E-mail: mpetsh@nus.edu.sg

Synthetic small diameter vascular grafts face severe limitations. In particular, permanent synthetic grafts fabricated from material such as Dacron are prone to occlusion due to neo-intimal hyperplasia. This pathological condition arises due to mechanical mismatch, as well as an inability of the host tissue to remodel the synthetic material. Tissue engineering represents a possible solution these issues. Guided regeneration techniques, in which a bioresorbable graft is implanted and eventually replaced by living tissue in vivo, demonstrate potential for such applications. The neotissue will then be capable of remodelling and adapting to biomechanical requirements. In this study, we investigate the possible use of poly (-caprolactone) (PCL) films for the development of vascular grafts. We demonstrate a method of functionalizing the films surface with a high density of carboxylic groups, while retaining the mechanical properties. We further show that biomolecules, such as heparin, can be incorporated onto the surface to improve biocompatibility. From these results, we propose that PCL films can be used in the design of resorbable vascular grafts.

P163 Controlled Patterning of Polystyrene Nanodots in Large Area by Near-Field Optical Enhancement

M.H. Hong[1,2,3,*], G.X. Chen[1,2], Y. Lin[1,2], Y. Zhou[3], Z.B. Wang[3], Q. Xie[3], L.S. Tan[1,2] and T.C. Chong[2,3]
[1]*Department of Electrical and Computer Engineering, National University of Singapore, 4 Engineering Drive 3, Singapore 117576*
[2]*NUS Nanoscience & Nanotechnology Initiative, 2 Engineering Drive 3, Singapore 117576*
[3]*Data Storage Institute, DSI Building, 5 Engineering Drive 1, Singapore 117608*
*E-mail: Hong_Minghui@dsi.a-star.edu.sg

Nanofabrication has attracted much research interest in recent decades. However, conventional nanofabrication techniques always involve complex experimental systems and complicated processing recipes. Thus, cost effective and high-efficiency substitute methods are greatly demanded. In this report, we propose a simple approach to create polystyrene nanodots over a large sample area with a fast processing speed. A monolayer of polystyrene microspheres was self-assembled on silicon wafer. Laser irradiation of the monolayer led to melting of the microspheres. The nanodots were produced in the following resolidification process. The morphology of polystyrene nanodots can be tuned by varying the input laser energy. Theoretical analysis revealed that the intense near-field optical enhancement under polystyrene microspheres plays a key role in this nanofabrication process.

P164 Elastic Properties of Ni_3Sn_4 from Density Functional Theory Calculations

N.T.S. Lee, V.B.C. Tan and K.M. Lim
Department of Mechanical Engineering, National University of Singapore
E-mail: g0202429@nus.edu.sg

The elastic properties of the intermetallic compound Ni_3Sn_4, found in modern solder interconnects, have been obtained with calculations based on Density Functional Theory (DFT) and the method of Hashin-Shtrikman and Hill. The presence of intermetallic compounds in excessive amounts affects the mechanical behaviour of the entire solder joint and is detrimental to its reliability. Hence, in evaluating the reliability of the joint, accurate knowledge of the properties of the intermetallic compounds is critical. Existing data is sparse and experimental testing is often difficult, thus calculations of mechanical properties with DFT can play a role. The value of the polycrystalline Young's Modulus obtained in our calculations (160 GPa) is in favourable agreement with the sparse experimental data currently available (118–142 GPa). This study thus adds to the body of evidence that validates DFT as a reliable method in predicting the elastic properties of materials.

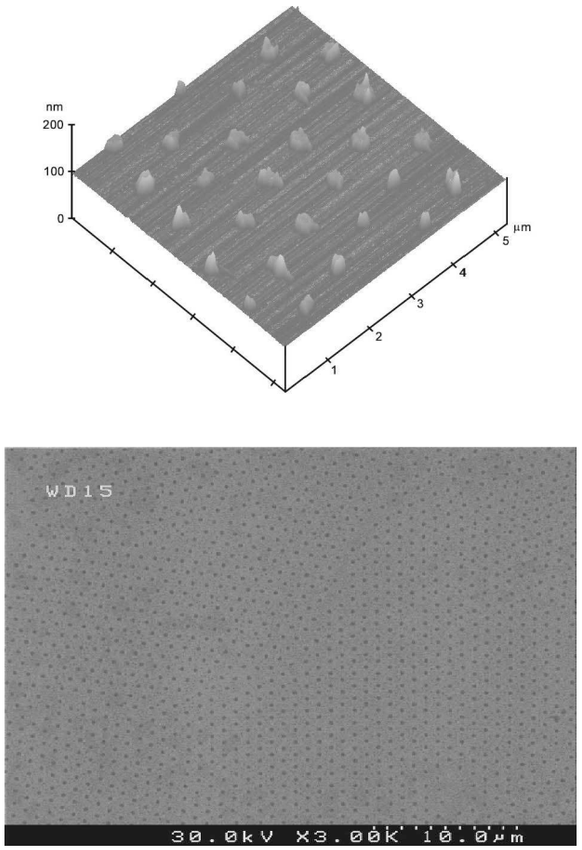

Fig. 1. AFM and SEM images of patterned polystyrene nanodots

P165 Hollow Fiber Membranes for Water, Chemical, Pharmaceutical and Environmental Industries: Historical Development and Technology Challenges Ahead

(Neal) Tai-Shung Chung
Department of Chemical & Biomolecular Engineering National University of Singapore
E-mail: chencts@nus.edu.sg

Polymeric hollow fiber membranes are market driving high-performance products. In many cases, polymeric hollow fiber membranes were produced prior to the fundamental understanding of detailed fabrication mechanisms.

Even today, most membrane scientists admit that they understand hollow fiber forming mechanism qualitatively, but not quantitatively. New hollow fiber membranes were prepared or invented mainly based on our experience, empirical data, limited qualitative and scientific understanding, and luck. Therefore, polymeric membranes have emerged as one of the fastest growing research areas in these days.

In this presentation, we will review technology breakthroughs for water, chemical and gas separation and biomedical applications in the last 5 decades and the challenges awaiting us. A critical examination on the fundamentals of asymmetric and composite hollow fiber spinning and membrane formation will be carried out. We will start the basic principle of dope preparation and principle of phase inversion process for desalination. Various technologies to develop high performance hollow fiber membranes will be reviewed and compared in terms of their uniqueness, impact, and the remaining uncertainties in these technologies. Following which, we may discuss the applications of membranes for various industries and challenging ahead.

P166 Self Assembly of Nanoparticles on Substrate Surface in Application to PECVD

P. Rutkevych, K. Ostrikov and S. Xu
Plasma sources and Applications Center (PSAC)
National Institute of Education (NIE)
Nanyang Technological University (NTU)
1 Nanyang Walk, Singapore 637616
E-mail: ng0205128t@mail.nie.edu.sg

Most reactive plasmas are optimal environment for intensive growth of clusters, nano- and even micro-particles (also known as dust particle). Recently it has been shown that such particles under certain conditions can be deposited on the substrate surface [1]. Levitating in the gas phase these particles are known to self-assemble into voids, crystals and other formations, however this self-assembly happens not only in the gas phase. In this paper we describe mechanisms governing the particle movement onto the substrate in case of irregular surface shape, which is often observed in deposition experiments.

In particular, we present two-dimensional simulation of nanoparticle kinetics, assuming the threshold condition for particle deposition are fulfilled and the particle movement is determined mainly by the electric field and ion-drag force. We have found that the particles tend to land the substrate in the vicinity of previously formed peaks, rather than smooth surface. Equilibrium shape of the formed nanostructures obtained for a range of particle sizes and biases applied to the substrate. The results are compared with experiments on carbon nanoparticle deposition and can be used for controlled growth of nanostructures in PECVD reactors.

References

1. P.P. Rutkevych, K. Ostrikov, and S. Xu. *Phys. Plasmas*, **12**:103507, (2005).

P167 Structure, Hardness and Adhesion Studies of Multilayer Ti/TiB_2 Coatings on High Speed Steel

N. Panich[1,2,*], S. Hannongbua[2] and Y. Sun[3]
[1] *School of Materials Science and Engineering, Nanyang Technological University, Singapore 639798*
[2] *Metallurgy and Materials Science Research Institute, Chulalongkorn University, Thailand 10330*
[3] *School of Engineering & Technology, De Montfort University, Leicester LE1 9BH, UK*
*E-mail: panich@pmail.ntu.edu.sg

Coatings are usually used to improve the functional properties of many engineering components. Indeed, a recent exciting development has been studied by designing the structure of these engineering coatings through the use of multiple layers of different materials. This study addresses at the development of multilayer Ti/TiB_2 coatings with increased adhesion to the substrate and retained high hardness. Multilayer Ti/TiB_2 coatings were deposited on stationary high speed steel substrates by magnetron sputtering. Multilayer Ti/TiB_2 coatings were evaluated with respect to fundamental properties such as structure, fractured cross-section, surface roughness, hardness, modulus and coating adhesion. It was found that the adhesion of resultant coatings was increased with increased alternate Ti/TiB_2 layers, whilst the hardness was slightly increased. However, in order to achieve good adhesion and hardness, the deposition time of TiB_2 should be longer than 30 min for developing the preferred (001) peak. It is also noted that with increasing the coating layer, the surface roughness increases significantly.

P168 Rewritable, DRAM and WORM-Type Molecular/Polymer Memories

Q.D. Ling[1], Yan Song[2], E.Y.H. Teo[2], S.L. Lim[1], Chunxiang Zhu[2], D.S.H. Chan[2], D.-L. Kwong[3], K.G. Neoh[1] and E.T. Kang*,[1]
[1] *Department of Chemical and Biomolecular Engineering, National University of Singapore, 10 Kent Ridge, 119260, Singapore*
[2] *SNDL, Department of Electrical and Computer Engineering, National University of Singapore, 119260, Singapore*
[3] *Institute of Microelectronics, 11 Science Park Road, Singapore Science Park II, 117685, Singapore*
*E-mail: cheket@nus.edu.sg

Non-volatile molecular memory devices, based on non-conjugated and conjugated polymers containing electron donor-acceptor structures and europium complex moieties, were demonstrated in Al/polymer/ITO sandwich structures. The devices exhibited distinctive high-conductivity (ON-state) and low-conductivity (OFF-state) states that could be accessed by applying voltage pulses of different polarities. It was found that the device based on the non-conjugated copolymer of *N*-vinylcarbazole and Eu-complexed vinylbenzoate (PKEu) was rewritable, and thus can be used as a flash memory. It exhibited an ON/OFF current ratio up to 10^4, switching response time of $\sim 20\,\mu s$, read cycles of more than 10^6, and write/erase voltages around $4\,V/-2\,V$. The device based on the conjugated copolymer of 9,9-dihexylfluorene and

Eu-complexed benzoate (PF6Eu) was a write-once read-many-times (WORM) electronic memory, with a high ON/OFF current ratio up to 10^7, stable ON- and OFF-states up to 10^8 read cycles at a read voltage of 1 V, and projected stability up to 10 years at a constant voltage stress of 1 V. Differing from the flash and WORM memory devices based on the polymers containing metal complexes, the device based on a conjugated copolymer (PFOxPy) containing both electron-donor and -acceptor groups, but without a metal complex moiety behaved as a dynamic random access memory (DRAM).

P169 Intermediate Range Ordering of Transport Pathways in Ion Conducting Glasses

Stefan Adams,[1] Andreas Hall[2] and Jan Swenson[2]
[1] *NUS, Department of Materials Science and Engineering 1 Engineering Drive 2, Singapore 117576*
[2] *Chalmers University of Technology, Göteborg (SWEDEN)*
E-mail: mseasn@nus.edu.sg

A fundamental understanding of the microscopic ion conduction mechanism in glasses is a longstanding problem, mostly because the inherent disorder of the glassy state renders an exact description of ion sites impossible. Here, ion transport mechanism and conduction pathways are examined by bond valence analysis of local structural models of in metal halide doped Ag, Li and Na diborate or metaphosphate glasses produced by reverse Monte Carlo fitting to experimental diffraction data or by molecular dynamics simulations. The number of available sites for the mobile ions and the resulting intermediate-range structure strongly depend on the type of mobile ion and on the dopant. Differences are particularly pronounced for the highly doped glasses, where e.g. AgI is introduced more homogenously in the B-O network with the formation of pronounced conduction pathways between neighbouring borate segments, while LiCl and NaCl are distributed more inhomogeneously. The local dimensionaliy of the ion transport pathway network reflects these features. The characterisation of the pathways is discussed in relation to the experimentally observed ionic conductivity. A comparison of results for static Reverse Monte Carlo models and molecular dynamics trajectories as the basis of the bond valence analysis reveals specific advantages of each type of structure models.

P170 An Evaluation of the Effects of Stiffness of Polycaprolactone (PCL) Membrane on Cell Proliferation

Puay-Siang Tan and Swee-Hin Teoh
National University of Singapore
*E-mail: mpetps@nus.edu.sg

Polymers made of polycaprolactone (PCL) have emerged as promising biomaterials in the recent years. The fabrication of PCL into ultra thin and flat membranes has been well documented. The process consists of roll milling, followed by heat pressing and finally biaxially stretching that allows the production of solvent-free PCL membranes. The biocompatibility of PCL films has also been proven in vitro. In the native environment, cells proliferate on matrices of different stiffness depending on the cell type. For example, bone cells proliferate in hard environments while skin cells prefer softer environments. It is predicted that cells will grow better on a substrate that mimics more closely its physiological milieu. The current experiment investigates two cell types, namely, chondrocytes and fibroblasts. The stiffness of the biaxially-stretched PCL membranes was controlled by manipulating its thickness. The thickness was maintained in the range of 5–30 μm. Cell proliferation and viability studies were conducted using confocal microscopy, MTT and AlamarBlue assays. The assays results indicated that fibroblast cells showed enhanced proliferation in less stiff membranes while chondrocytes proliferated better on stiffer membranes. Similar results were observed in the cytoskeleton staining of both cell types. In conclusion, stiffness of the PCL membrane can affect cell proliferation.

P171 Tunable Light Emission from Porous Silicon Using Focused Helium Irradiation

E.J. Teo, M.B.H. Breese, A.A. Bettiol, D. Mangaiyarkarasi, F. Champeaux, F. Watt and D.J. Blackwood
Department of Materials Science and Engineering
*E-mail: msetej@nus.edu.sg

In this work, high energy focused helium beam irradiation has been used prior to electrochemical etching of silicon for the production of controlled light emission from patterned porous silicon. The ion beam increases the local resistivity of the silicon, which changes the emission properties of the porous silicon formed. It is found that the emission wavelength is red-shifted with increasing dose of the beam. An increase of up to 150 nm in wavelength has been observed on a medium resistivity silicon wafer. This technique enables us to tune the colour emission of porous silicon from green to red on the very same wafer. This phenomenon can be explained by the quantum confinement model, which correlates the longer wavelength to an increase in the silicon nanocrystal size formed in the irradiated regions. We demonstrate the versatility of this technique to fabricate various multi-colour patterns by varying the dose of the beam.

P172 Effect of Surface Coating on the Biodistribution of Superparamagnetic Iron Oxide (SPIO) Nanoparticles in Tumor-Bearing Nude Mice

Joachim S.C. Loo[1,2], J. Ma[1], Freddy Y.C. Boey[1], Prasanna K. Mishra[2], Mary E. Harvey[3], Stephen J. Russell[3] and Kah-Whye Peng[3]
[1] *School of Materials Science and Engineering, Nanyang Technological University, Singapore*
[2] *Biochemistry and Molecular Biology, Mayo Clinic College of Medicine, Rochester, MN, USA*
[3] *Molecular Medicine Program, Mayo Clinic College of Medicine, Rochester, MN, USA*
*E-mail: joachimloo@ntu.edu.sg

Particulate systems or nanoparticles for drug or gene delivery have attracted considerable interest for cancer therapy.

However, one major limitation is that they are prone to phagocytosis. Surface modification, through surface coating, is one approach that has been reported to minimize phagocytosis. Dextran has been frequently used as a surface coating, whereas starch, known to have better haemorheological effects than dextran, has been less studied. From magnetic resonance (MR) imaging of live mice, it was found that regardless of surface coating, SPIO was still dominantly taken up by the MPS macrophages and accumulated in the liver and spleen. However, dextran-coated SPIO were also found to accumulate in tumour xenografts due to the leaky vasculature of the tumour, as observed from histology and ICP-MS results. Starch-coated SPIO, though larger in size than the dextran-coated SPIO, were also deposited in the tumour because of its better haemorheological effects, thus increasing vasculature leakiness of the tumour. Uncoated SPIO, on the other hand, was found to be massively taken up by the macrophages due to the lack of a hydrophilic stabilizing polymeric coating. It is conclusive that coated particles have better tumour targeting properties as compared to uncoated particles.

P173 Constitutive Modeling of Blood Vessels Using Combined Energy Function for Surgical Simulation

Chee-Kong Chui*,[1], Poh-Sun Goh[2], Zhenlan Wang[1], Chong-Jin Ong[1], Swee-Hin Teoh[1] and Ichiro Sakuma[3]
[1] *Department of Mechanical Engineering, National University of Singapore, Singapore*
[2] *Faculty of Medicine, National University of Singapore, Singapore*
[3] *Graduate School of Frontier Sciences, University of Tokyo, Tokyo, Japan*
*E-mail: mpecck@nus.edu.sg

A number of constitutive models are available for modeling the passive material properties of blood vessels. Nevertheless, to develop a constitutive formulation that is computational efficient for surgical simulation and sophisticated enough to predict in a clinically relevant manner the mechanical behavior of the vessel up to failure remains a challenging problem. We are proposing to use a combined logarithmic and polynomial based strain energy function to model the deformation of vessels. Based on the tensile properties (longitudinal direction) of various blood vessels reported in literature, the combined energy function is used to model the nonlinear stress-strain relationship. It can be observed that at low strain, the logarithmic component in the model was small, and the polynomial component was the dominant one. The roles of these components were reversed in high strain. There was no change in polarity of the material parameters in the curve fitting process. This is desired for implementing the material model in finite element methods. We are repeating the analysis considering the tensile properties (transverse direction) of the blood vessels. Human vascular models will be re-constructed from dynamic MR images. The material and geometrical representation could be used to simulate vessels deformation during catheterization.

P174 Methods and Experiments of Ultrasonic Monitoring for Bone Remodeling

Erin Teo Yiling*, Chui Chee Kong, V. Shim and Teoh Swee Hin
Department of Mechanical Engineering, National University of Singapore
*E-mail: erinteo@nus.edu.sg

Non-invasive monitoring of the remodeling process in bone is particularly important in the research for better treatment and prevention of osteoporosis. In this study, we focus on *in vivo* monitoring of bone remodeling processes using ultrasonic equipment. Ultrasonic evaluation was chosen due to its non-destructive and non-invasive nature. The aim is to enable the rate of bone fusion to be monitored on a regular basis. This could improve the post-implantation surgical treatment process by avoiding or reducing the number of review progresses for bone regeneration. The capabilities of ultrasonic instruments for mechanical properties evaluation could help bone material characterization in monitoring bone remodeling at different stages. Currently, we use a single transducer as an emitter and receiver for experimentation. The data are analyzed in the form of velocity and wavelength of ultrasonics through the media, elastic modulus, and images of the *in vitro* biological specimen. A microCT scan of the same biological specimen has been planned. A comparison could help correlate the ultrasound findings with that from microCT scan in the microstructure level. We will be using the developed ultrasonic scanning techniques to monitor bone development in a rat femoral model that has a three dimensional polycaprolactone scaffolds implanted.

P175 Non-Volatile Memory Structure Using Au Nano Crystals as Charge Storage Material

Faizhal B.B., F.J. Ma and Won Jong Yoo
Silicon Nano Device Lab
E-mail: g0500358@nus.edu.sg

The memory properties of flash devices with uniformly sized and distributed nano crystals as the charge storage material using pre-made Au nano particles are investigated. These pre-made 20 nm, 10 nm and 5 nm Au particles of small size deviation were deposited discretely from each other on 5 nm SiO_2 tunnel oxide from Au colloidal solution. These nano particles are deposited by electrostatic attraction and adhesion to an aminosilane adhesion agent, *N*-(2-Aminoethyl)-3-(trimethoxysilyl)propylamine (APTS), on the tunnel oxide by immersion in 0.5% (v/v) of diluted APTS. Atomic force microscope (AFM) images of the deposited 20 nm Au nano particles show a density of $\sim 3.2\times10^{10}\,\mathrm{cm}^{-2}$ with a uniform and well isolated distribution. Metal-oxide-semiconductor capacitor structures were then fabricated after capping with 300 Å of SiO_2. A counter-clockwise hysteresis of the capacitance-voltage (C-V) plot of ~2.3 V for a sweep voltage of +/−9 V is observed. From the C-V hysteresis, an asymmetrical positive and negative voltage shift has been observed with respect to the fresh device.

P176 Nanoparticles of Biodegradable Polymers for New-Concept Chemotherapy

Feng Si-Shen
Department of Chemical & Biomolecular Engineering and Division of Bioengineering,
National University of Singapore
E-mail: chefss@nus.edu.sg

This presentation will demonstrate through a full spectrum of research how nanoparticles of biodegradable polymers could radically change the current practice of chemotherapy with paclitaxel used as a prototype drug due to its excellent effects against a wide spectrum of cancers. Paclitaxel-loaded poly(lactic-co-glycolic acid) (PLGA) nanoparticles were prepared by a modified solvent extraction/evaporation technique with d-α-tocopheryl polyethylene glycol 1000 succinate (TPGS) as emulsifier. The nanoparticles were characterized by various state-of-the-art techniques, including laser light scattering for size and size distribution, FESEM and AFM for surface morphology, XPS for surface chemistry, zeta-potential for surface charge, DSC for physical status of the drug in nanoparticles, HPLC for drug encapsulation efficiency and *in vitro* drug release. Cellular uptake of fluorescent nanoparticles was visualized by CLSM and measured by microplate reader with Caco-2 cells employed as i*n vitro* model of the gastrointestinal barrier for oral chemotherapy. *In vitro* intracellular trafficking of nanoparticles was visualized by Cryo-SEM and TEM. *In vitro* HT-29 cell viability was accessed by MTT. *In vivo* pharmacokinetics measurement showed that the therapeutic effects and the sustainable therapeutic time of the nanoparticle formulation could be 4.9 times higher and 2.48 times longer for the NP formulation than those for the Taxol® formulation.

P177 Surface Functionalized Magnetic Nanoparticles for Biomedical Applications

Feixiong Hu, Shy Chyi Wuang, Koon Gee Neoh* and En-Tang Kang
Department of Chemical and Biomolecular Engineering
National University of Singapore
10 Kent Ridge, Singapore 119260
*E-mail: chenkg@nus.edu.sg

Surface functionalization of superparamagnetic magnetite nanoparticles with average diameters $\sim$ 6 nm was carried out to increase their potential for biomedical applications. These particles were either surfacefunctionalized with poly(poly(ethylene glycol) monomethacrylate) (P(PEGMA)) via surface-initiated atom-transfer radical polymerization (ATRP) or with poly(N-isopropylacrylamide) (P(NIPAAM)) also via ATRP followed by immobilization of heparin, an anti-coagulant. The modified nanoparticles were characterized using Fourier Transform Infra-Red (FTIR) spectroscopy, X-ray Photoelectron Spectroscopy (XPS) and thermogravimetric analysis (TGA). The P(PEGMA)-functionalized nanoparticles were assesed for their ability to reduce phagocytosis by macrophages in vitro. It was found that the uptake of these nanoparticles by macrophages was greatly reduced from 158 pg/cell for the pristine magnetite nanoparticles to <2 pg/cell after grafting with P(PEGMA). Since increasing plasma half-life is a challenge encountered in in vivo applications of nanoparticles, the P(PEGMA)-functionalized nanoparticles offer a distinct advantage in this aspect. The heparinized nanoparticles can also delay phagocytosis by the macrophages, albeit not to the same extent as the P(PEGMA)-functionalized nanaoparticles. However, the heparinized nanoparticles are effective in preventing thrombosis as demonstrated by their ability to prevent blood clotting in vitro, for up to at least 24 hr, as compared to the normal clotting time of about 4 min. Such magnetic nanoparticles with increased plasma circulation time and anti-thrombotic properties may be useful in applications where targeted delivery of heparin is desired, e.g. in the prevention or reduction of restenosis. No cytotoxicity effects were observed with macrophages after 24 hr-incubation with both types of functionalized nanoparticles. These results demonstrate how magnetite nanoparticles can be surface modified by the appropriate functional groups to tailor their applications in biomedicine.

P178 Elastic Analysis for Liquid-Bridging Induced Contact

H. Fan
School of Mechanical and Aerospace Engineering,
Nanyang Technological University, Singapore 639798,
E-mail: mhfan@ntu.edu.sg

The micro-scale contact induced by liquid bridging is studied numerically via FEM with consideration of coupling effect between the liquid bridging and the elastic deformation of the half space. The liquid bridging force and contact area as functions of a dimensionless parameter χ (measurement of relative stiffness of the contact bodies) and the filling angle ψ (measurement of liquid volume) are obtained and discussed. The FEM solution is used to check the accuracy of the approximate analytical solutions based on Hertzian theory. We also studied the configurational stability of the liquid between the two contacting bodies as the volume of the liquid approaches zero. By examining the solutions for describing the shape of the liquid under equilibrium, it was found that these solutions become physically infeasible as the volume of the liquid vanishes. A linear stability analysis was carried out by perturbing the relevant equilibrium configurations and examining the change of the free energy of the system under consideration. The analysis leads to the conclusion that the equilibrium shape of the liquid, that bridges two solids in contact, may become unstable under certain conditions. As its volume diminishes, the liquid may break into smaller droplets.

P179 Biomechanical Modeling of Bone for Needle Insertion

Jackson Shin-Kiat Ong*, Zheng-Yi Lian, Chee-Kong Chui, Zhenlan Wang, Jing Zhang, Jeremy Choon-Meng Teo, Chye-Hwang Yan, Sim-Heng Ong, Chee-Leong Teo and Swee-Hin Teoh
National University of Singapore
*E-mail: mpeoskj@nus.edu.sg

Medical simulators are increasingly being used in surgical training as more medical schools adopt a more human way of treating animals. The study of the bone material property allows medical simulator to have an accurate

computation model of bone for cracking simulation during bone needle insertion. For surgical simulation involving haptics interaction, the force at the needle tip has to compute at an interactive manner. We are developing a predictive model for bone cracking. In this predictive model, we regard the cortical bone as a dense form of cancellous bone that can be considered as a linear elastic material. The porosity of the bone determines the resistance felt as the user inserts the needle into the bone. There is no clear boundary between cortical and cancellous bones. The user will feel less resistance to insert the needle through the cancellous region. Friction at the needle-bone interface is approximated using a static model and hence, is dependent on the distance of needle insertion. An adaptive threshold based image processing method is used to segment the human bone from medical images such as CT and MRI. A volumetric model is then reconstructed from the segmented bone images.

P180 The Preparation of B Site Doping $La_2Ni_{1-x}M_xO_4$ and Its Application for the Methane Selective Oxidation

Jesslin Tan Wei Qi[1], Sun Han[2], Michael Tasrif[3], Chen Luwei*[,3] Lin Jianyi[3], Jiang San Ping[4] and Sam Zhang Shanyong[4]
[1]*Applied Science School, Temasek Polytechnic, 21 Tampines Avenue 1, Singapore 52*
[2]*Department of Physics, National University of Singapore*
[3]*Institute of Chemical and Engineering Science, A*STAR*
[4]*School of Mechanical &Aerospace Engineering, Nanyang technological University*
*E-mail: Chen_luwei@ices.a-star.edu.sg

K_2NiF_4 structure perovskites have attracted more and more attention since the superconductivity was found over La_2CuO_4. This kind of material can accommodate a wide variety of oxygen stoichiometries by introducing excess oxygen into interstitial sites of the structure.

In this study, La_2NiO_4 with B site doping $La_2Ni_{1-x}M_xO_4$ (M=Cu, Co, Fe, x=0, 0.3, 0.5) were prepared and the doping effect on the structure and catalytic activity for selective methane oxidation for H_2 production was studied.

It was found that Cu doping with content up to $x = 0.5$ causes very little change on the K_2NiF_4 structure. When this K_2NiF_4 sample reacted with methane, the maximum evolution of H_2 temperature increased from 650°C to 810°C with increasing Cu doping content from 0 to 0.5, while total oxygen content decreased. When K_2NiF_4 was doped with Fe and Co at the level of < 0.3 and 0.1, respectively, La_2O_3 phase appears obviously while the K_2NiF_4 structure still maintains The characteristic K_2NiF_4 structure disappeared if Fe and Co content reached 0.5 and 0.3, respectively. Methane reaction with Fe- and Co-doped La_2NiO_4 did not find a linear correlation as that observed for Cu-doped samples.

P181 Bone Material Estimation in Statistical Model Aided Elastic Deformation

Jing Zhang*[,1,2], Changwei Yeo[1], Chee Kong Chui[1], Chye Hwang Yan[2], Sim Heng Ong[2,3] and Swee Hin Teoh[1]
[1]*Department of Mechanical Engineering, National University of Singapore*
[2]*Department of Electrical Engineering, National University of Singapore*
[3]*Division of Bioengineering, National University of Singapore*
*E-mail: mpezj@nus.edu.sg

Knowledge in mechanical properties of bone is important for deformable modeling method in computer assisted bone surgeries. In deformable modeling method, finite element (FE) is typically used to elastically map a template model to the target image dataset. Nevertheless, bone material property is complex and is highly heterogeneous. It is difficult to represent these properties in numerical simulation. We assume a linear elastic material model for bone with varying elastic modulus between 10 GPa and 30 GPa. Bone is considered as an almost incompressible material with Poisson's ratio fixed at 0.3. Prior to deformation, a statistical shape model guided method is used to select a template model that is closest to the target image. To deform this template, an elastic modulus within the predefined range was first picked by analyzing the input images. If the model fails to match the image by deformation, the process is repeated to update the bone elastic modulus. The iteration ends successfully with an optimal modulus when the selected model is deformed to a good match with the target images. This method ensures a good match of the bone geometry. We will investigate the correctness of the selected elastic modulus value in future studies.

P182 A Study on Paclitaxel Release from Single and Double Layer Biodegradable Poly (Lactide-Co-Glycolide)/Poly (L-Lactide) Films for Coronary Stent Application

Luciana Lisa Lao and Subbu S. Venkatraman*
School of Materials Science and Engineering
Nanyang Technological University
Singapore
*E-mail: assubbu@ntu.edu.sg

Due to some limitations of permanent metallic stents, a new generation of biodegradable polymeric stents has been actively researched. Besides its temporary residence, such biodegradable stents have high capacity for local drug delivery. In the case of coronary stents, antiproliferative drugs are required to prevent excessive smooth muscle cells proliferation that can lead to restenosis (artery reclosure).

This paper presents the in vitro release of paclitaxel, an effective antiproliferative drug, from a single layer poly (lactide-co-glycolide) 53/47 and bilayer poly (L-lactide)/poly(lactide-co-glycolide) films, which can then be processed into a helicoidal stent. Some of the factors affecting release kinetics were investigated: film layer thickness, drug loading and directionality of release. In addition, a separate degradation study was conducted to correlate to the release profiles obtained.

The release profiles show a consistent triphasic pattern: early diffusional release, followed by degradation controlled release and finally a slower completion phase.

P183 Influence of Process Parameters on the Properties of Scaffolds Developed by Robot-Based Rapid Prototyping (RP) Technique

M. Enamul Hoque[1,2]; Hutmacher Dietmar, W.[2]; Feng, Wei[1]; S. Li[3], M.-H. Huang,[3] M. Vert[3] and Wong, Y.S.[1]
[1] *Department of Mechanical Engineering*
National University of Singapore
10 Kent Ridge Crescent
Singapore 119260
[2] *Division of Bioengineering, Faculty of Engineering,*
National University of Singapore,
10 Kent Ridge Crescent
Singapore 119260
[3] *Research Center for Aritificial Biopolymers, CRBA-UMR CNRS 5473,*
University Montpellier 1, Faculty of Pharmacy,
15 Avenue Charles Flahault, BP 14 491,
34093 Montpellier Cedex 05, France

Often there are patients suffering from tissue loss or organ failure due to maladies such as trauma, tumor resection or birth defect. Tissue engineering which utilizes scaffold as a temporary support for the cells' survival and growth, provides an alternative way to treat such patients. Different tissues require different scaffold properties depending on their structures and functions. This study focuses on how the process parameters influence the structural properties of the scaffolds. The scaffolds were fabricated as layer-by-layer via robot-based rapid prototyping (RP) technology using triblock co-polymer, namely PCL-PEG-PCL. The polymer is melted electrically in a metallic chamber and extruded out of a minute nozzle by compressed air while the robot moves according to the precise computer control. The process parameters like temperature, pressure and dispensing speed were varied to evaluate their effects on the porous characteristics and mechanical properties of the scaffolds. The scaffold morphology was observed by SEM and the porosity was measured by pycnometer method. Compression tests were performed to obtain scaffolds' mechanical properties. This study shows that the scaffolds' structural properties are influenced by the process parameters. Therefore, by varying process parameters scaffolds with various properties can be manufactured which could fulfill the requirements of targeted tissues.

P184 Growth and Characterization of Cobalt Doped Zinc Oxide Films

Tay Maureen*, Wu Yi Hong, Han Gu Chang, Chong Tow Chong and Zheng Yuan Kai
Department of Electrical and Computer Engineering,
National University of Singapore
*E-mail: TAY_Maureen@dsi.a-star.edu.sg

We report a systematic study of structural, optical, electrical and magnetic properties of $Zn_{1-x}Co_xO$ ($x = 0.08 - 0.41$) thin films co-doped with Al. Both co-doped (in which Co is co-sputtered with other elements) and δ-doped (in which Co is doped digitally in the host matrix) samples have been prepared and studied. Prior to the doping of Co, the growth conditions were optimized to produce ZnO:Al films with a resistivity of about 1–2 $m\Omega \cdot cm$. All the films with x in range of $0.08 - 0.41$ showed clear hysteresis curves at room temperature and Curie temperatures for the most heavily doped samples (both co-doped and δ-doped) are over 400 K. Although absorption peaks associated with the d-d transitions of Co^{2+} ions have been observed in all the samples with different Co compositions, only the most heavily doped samples have shown clear anomalous Hall effect. The latter also showed strong, but photon energy–dependent, magnetic circular dichroism and negative magnetoresistance at room temperature. All these results clearly suggest that the samples are inhomogeneous ferromagnets which has also been confirmed by transmission electron microscope observations and differential conductance measurements.

P185 Synthesis and Characterization of Novel DNA Bis-Intercalators for Electrochemical Nucleic Acid Sensors

Natalia C. Tansil and Zhiqiang Gao
Institute of Bioengineering and Nanotechnology,
School of Materials Science and Engineering, Nanyang Technological University
*E-mail: nataliachen@ibn.a-star.edu.sg

Herein we report the synthesis and characterization of a series of novel electroactive DNA bis-intercalators that can be applied for ultrasensitive biosensing. Each molecule consists of two DNA-intercalating units N,N'-bis[1(3-propyl)-imidazole]-1,4,5,8-naphthalene diimide (PIND) linked by a polypyridine complex of osmium or ruthenium. These materials display unique intercalative and electrocatalytic properties, allowing their usage as hybridization indicators and electron-transfer mediators at the same time. This can lead to a simpler, more sensitive, and selective detection platform for nucleic acids. Electrochemical characterization showed that substitution on the polypyridine ligand of the metal complexes varied the redox potential values, providing different pathways for nucleic acid detection. The binding mechanism of the bis-intercalators to DNA was also studied in detail. UV-Vis spectra showed hypochromism and red shift of naphthalene diimide absorption peaks, two signatures of intercalative binding. Preliminary study using circular dichroism spectroscopy confirmed that the binding of these bis-intercalators altered the DNA structure. The apparent binding constant of these new bis-intercalators was found to be at least 2.5 times higher than that of YOYO-3.

P186 Preparation of Al/Al2O3-Matrix Composite as Phase Change Material for Thermal Energy Storage

Shenglin Wang*,[1] and Hua Wang†,[2])
[1] *Faculty of Thermal Energy and Power Engineering,*
[2] *Faculty of Materials and Metallurgical Engineering,*
Kunming University of Science and Technology, Kunming 650093, P. R. China
E-mail: *wsllinda04@sina.com;
†wanghuaheat@hotmail.com

A phase change material (PCM) is able to absorb or release large quantities of latent heat at a fairly constant temperature during its phase transition. For these advantages, The research of phase change materials (PCMs) has attracted

much attention in recent years. This paper presents a kind of Al/Al_2O_3 composite used as thermal energy storage of high temperature.

The preparation process of Al/Al_2O_3composite was mainly discussed, including molding pressure, sintering temperature and component of Al and Al_2O_3. To promote the heat storage ability, additives were added, and the function of the additive was also discussed.

X-ray diffraction (XRD) was engaged for the phase analysis of composite, Scanning electronic microscopy (SEM) was used to examine the microstructures of Al/Al_2O_3 composites, and Differential scanning calorimetry–temperature weight (DSC-TG) analysis was used to determine heat storage density of the composites.

P187 Microstructure Study of the Effect of Wire EDM on Silicon

Sadiq M. Alam*, Mustafizur Rahman and Han Seok Lim
Department of Mechanical Engineering, National University of Singapore
*E-mail: sadiq@nus.edu.sg

The monocrystalline silicon is a very important material from its application point of view, especially in the field of microelectronics. To enhance the practical applications, fabrication in the micron level is of great importance and also the post-process phenomena at the microstructure level are necessary to understand. Micro Wire Electro Discharge Machining (μ WEDM) is now an accepted machining process that has great potential for micro-fabrication. Both in the theoretical and practical arena, there have been only a limited number of studies on the implication of EDM on silicon. Especially there is even little work on the application of wire EDM on silicon material. In this paper the possibility to fabricate micro-components on silicon material with μ WEDM technique has been examined. At the same time how the process impact the material after machining has been carefully observed. The process effect on the microstructure of silicon has been examined with the help of high-resolution microscope and scanning electron microscope. As a practical application, attempts have been taken to fabricate a micro-spring made of monocrystalline silicon. Such spring can find its application in micro-mirrors, sensor and other microelectrocmechanical systems.

P188 Velocity Dependent Fracture Toughness in Creeping Polymeric Materials

S. Tang, T.F. Guo and L. Cheng
Department of Mechanical Engineering, National University of Singapore, 9 Engineering Drive 1, Singapore 117576
*E-mail: mpecl@nus.edu.sg

The deformation of polymers differs considerably from metals. One important aspect of polymers is its rate dependent inelastic behavior even at ambient room temperatures; this rate dependence characteristic can cause fracture toughness to depend on crack speed. In this study, mode I, quasi-static steady-state crack growth is analyzed for rate dependent polymeric materials under plane strain small scale yielding conditions. An embedded process zone (EPZ) encompassing a single row of void-containing cells is placed ahead of the crack. The void growth and coalescence behavior of these cells is governed by a Gurson-like model, while the background material is described by an elastic nonlinearly viscous power-law creep. Results show the competition between decreasing creep zone and rate strengthening of the fracture process zone in the polymeric material under varying crack velocities can cause non-monotonic fracture toughness trends.

P189 The Application of Functionalized SBA-15 for Controlled Adsorption and Release of Model Protein Drug

Shiwei Song, K. Hidajat and S. Kawi*
Department of Chemical and Biomolecular Engineering, National University of Singapore
*E-mail: chekawis@nus.edu.sg

The fragile nature and complex molecule structure pose a great challenge to protein drug delivery, since there are a few problems associated with employment of polymers or liposomes, such as detriment of protein integrity during processing as well as their low drug contents. However, inorganic materials were shown to effectively protect enzymes against denaturation induced by external pH and temperature [1] and to be loaded with a larger amount of proteins [2], which raised their possibility as protein drug carrier.

In this study, inorganic mesoporous SBA-15 material was functionalized with amino groups and has been investigated as a potential matrix for protein drug delivery. Amine-functionalized SBA-15 was prepared by co-condensation of 3-aminopropyltrimethoxy - silane (APTMS) and tetraethylorthosilicate (TEOS), since this method can provide surface functional groups and favorable hydrophilic interface. Bovine serum albumin (BSA) - selected as a model drug — was loaded onto the resulting functionalized SBA-15. By changing molar ratio of APTMS and TEOS during preparation, BSA loading amount on functionalized SBA-15 can reach as high as 30%. FTIR and Raman spectra showed clear peaks at 1600–1700 cm^{-1} due to amide I band of protein, indicating the presence of high loading amount of BSA. After loading and freeze-drying, the resulting materials were soaked into phosphate-buffered saline pH 7.4 to conducting in-vitro release studies. The release profiles showed that release rates can be well-controlled, and subsequent circular dichroism (CD) analysis showed that protein structure after release can be well maintained.

References

1. Jain, T.K. Roy, I., De, T. K. and Maitra, A. Nanometer Silica Particles Encapsulating Active Compounds: A Novel Ceramic Drug Carrier, J. Am. Chem. Soc. 120, pp. 11092–11095. 1998.
2. Katiyar, A.; Ji, L.; Smirniotis, P.; Pinto, N. G. *J. Chromatogr.* A **2005**, 1069, 119–126.

P190 Effect of PVP630000 on Critical Thickness, Morphology and Crystallization of Sol-Gel-Derived PLZT Films

Z.H. Du* and J. Ma
Materials science and engineering, Nanyang Technological University, Singapore, 639798
*E-mail: Duze0001@ntu.edu.sg

Increasing the critical thickness (the maximum film thickness of one coating before crack formation) is a key factor for efficiently preparing thick films(above 1 um) by sol gel processing. In order to increase the critical thickness of lanthanum doped lead zircornate titanate (PLZT, 9/65/35) films, PVP630000 (polyvinylpyrrolidone, with the molecular weight of 630000) was used as stress-relaxing agent to modify the sol gel processing. The effect of PVP630000 concentration on the critical thickness, morphology and crystallization of the PLZT films was studied by surface profiler, FESEM and XRD. It is found that the critical thickness of PLZT films increased remarkably with PVP concentration increasing. When the ratio of PVP630000 monomer/PLZT was 1.5, the critical thickness reached 926.7 nm (compared with 77.5 nm in the case of no-PVP modified PLZT films). It is also found that the increase in the critical thickness of PLZT films can be attributed to the morphology evolution of the films. According to FESEM, the morphology of PLZT films turned to be nano-porous with the PVP concentration increasing, which helped to suppress crack formation so that the critical thickness increased. From XRD results, it is indicated that the formation of perovskite phase was suppressed with the PVP630000 concentration increased.

P191 Apatite Formation on Mesoporous Bioactive Glass CaO-P_2O_5-SiO_2

Yufeng Zhao and Jan Ma
School of Materials Engineering, Nanyang Technological University

Mesoporous bioactive glasses (MBGs) are believed to bring new opportunities in many biomedical aims such as implanting, drug delivery etc., for their superior bioactivities related to their special mesostructure. Formation of apatite onto the bioactive glass has recently attracted great interest. In this work, highly ordered MBGs (CaO-P_2O_5-SiO_2) with apatite composition was sol-gel derived using block copolymer pluronic F127 ($EO_{99}PO_{65}EO_{99}$) as the template. At the same time, another group of samples with apatite layer formed on the pre-synthesized MBGs surface through immersion in the simulated body fluid (SBF) were also investigated. The materials produced were characterized using X-ray diffraction, energy dispersive X-ray (EDX) as well as field emission scanning electron microscopy (FESEM). The pore morphology of both groups of samples was studied through nitrogen absorption/desorption isotherm plot. BJH nitrogen desorption curve presented an accurate pore size distribution. The mesoporous structure was observed under transmission electron microscopy (TEM) field. Small angle X-ray scattering (SAXS) results showed that in the small angle range ($2\theta \sim 1$–$10°$), the peak shape changed depending on the ratio between apatite and the glass composition.

P192 Finite Element Method for Simulating the Normal Impact of Adhesive Microspheres with a Substrate

Xi-Qiao Feng*, Huan Li and Shou-Wen Yu
Department of Engineering Mechanics, Tsinghua University, Beijing 100084, P. R. China
*E-mail: fengxq@tsinghua.edu.cn

The impact of microspheres/microparticles with a surface has been a long-time issue of extensive interest because of its importance in various industrial processes, e.g., powder transportation, gases filtration, surface contamination, particle deposition, and aerosol collection. A question is often required to answer in these processes: when and why do microspheres/microparticles stick to or rebound from a surface? The physical mechanisms associated with particle impact at the micro- and nano-scales and the dependence relationship of the impact behaviors upon such factors as material properties and adhesion have attracted considerable attentions in the past decades but are yet not very clear.

A finite element model is presented in the present paper to study rebound behaviors of an elastic or elasto-plastic microsphere impacting normally against a rigid wall. The interface adhesive forces are introduced by adding distributed elastic springs with constitutive relation characterizing the adhesion property. The effect of adhesion hysteresis is taken into account by assuming that the adhesion work during the incident process is smaller than that during the rebounding process. The dependence relationships of the coefficient of restitution (COR) on the sphere size, adhesion parameters, constitutive relations as well as the impacting velocity of the sphere are analyzed. We also examined the changing tendency of the kinetic energy and adhesion work and their inter-exchange. It is also found that beside interface adhesion and plastic dissipation, the residual stress field caused by the incompatible plastic deformation also has a considerable influence on the impact behavior of spheres and leads to a further decrease in the COR. For smaller impacting velocities, the interface adhesion plays the most significant role in the impact process, while for higher incident velocities, the COR depends mainly on the plastic deformation. In addition, the COR shows a distinct size dependence on the sphere size. Our numerical results show a reasonable agreement with experiment results.

Finally, the above method was extended to the impact of microspheres with a rough surface.

P193 Synthesis and Mechanism Study of Thermal Stable Mesoporous SnO_2/SiO_2 Composite on Neutral Surfactant

Jie Zhu, Bee Yen Tay and Jan Ma
School of Materials Engineering, Nanyang Technological University
E-mail: X030037@ntu.edu.sg

Highly thermal stable mesoporous SnO_2/SiO_2 composed of nanocrystalline SnO_2 and amorphous SiO_2 was fabricated using neutral surfactant as structure directing agent. The synthesis involved the pre-formation of SnO_2 sol solution from $SnCl_4$. Subsequently, SnO_2 nanocrystals were

covered with amorphous SiO_2 in a pH controlled colloidal solution. Upon mixing with surfactant, 1-D hexagonal mesophase composite was obtained. Due to the presence of SiO_2, crystal growth of SnO_2 (<30 Å) was hindered effectively during the removal of surfactant from 400 to 600°. As a result, mesoporous inorganic framework with large surface area (362 m^2/g), pore volume (0.33cc/g) and narrow pore size distribution in the range of 30 to 70 Å were obtained. Primary synthesis parameters such as Si/Sn molar ratio, and calcination temperature were investigated using TGA, X-ray diffraction, BET, HRTEM, and FTIR techniques. Mechanism on the mesostructure formation was also proposed with detailed discussion.

P194 Plasticity and Toughness in Bulk Metallic Glasses

Upadrasta Ramamurty
Department of Metallurgy, Indian Institute of Science, Bangalore-560 012, India

The absence of long range periodicity and hence dislocations in amorphous metals poses difficulty in understanding of the plastic deformation in them. The discovery of bulk metallic glasses (BMGs) revived the interest in studying their mechanical properties, because of the possibility of characterization through conventional mechanical testing. At low temperatures and high stresses, metallic glasses undergo inhomogeneous plastic deformation by the formation of shear bands. The reduction of viscosity due to the stress-induced creation of free volume explains the instability for localized deformation. We have employed a variety of experimental and computational techniques to study deformation and fracture mechanisms in the BMGs. This presentation will highlight on the results primarily in three important areas, (1) impact toughness, (2) indentation (3) fatigue, with focus on the following issues. (i) The effect of structural relaxation on mechanical properties of BMGs. (ii) Ductile to brittle transition due to changes in temperature. (iii) Strain softening due to plastic deformation. (iv) Morphology of shear bands underneath the Vickers indenter. (v) Validation of pressure sensitivity in BMGs using FEM simulations. (vi) Nanocrystallization under fatigue loading.

P195 Constitutive Grain Growth Model for 3Y-TZP Nanocrystalline Powder

Xue Feng* and Ma Jan
Nanyang Technological University, School of Materials Science and Engineering
*E-mail: Pg05264446@ntu.edu.sg

A model to predict the grain growth of a nanocrystalline ceramic compact during free sintering has been developed. In this paper, the dominant mechanism of grain growth at different sintering stages has been investigated. It was found that the dominant grain growth mechanism of intermediate sintering stage is controlled by solid-solution dragging and that of final sintering stage is pore-drag controlled. A constitutive grain growth model is also developed in which the densification is described by interface reaction controlled diffusion mechanism. The model predictions are compared with experimental observations on grain growth of 1200, 1250, 1300 and 1350 Å. It is shown the current model can provide better prediction on intermediate stage than the final stage.

P196 Processing Metal Based Materials Using Microwaves

W.L.E. Wong and M. Gupta*
Department of Mechanical Engineering National University of Singapore, 9 Engineering Drive 1, Singapore 117576
*E-mail: mpegm@nus.edu.sg

Microwave processing of materials is an innovative method to process materials that may not be suitable for conventional means of processing or to improve the properties of existing materials that were processed using conventional methods. Metal based powder compact materials are commonly sintered using conventional resistance heating because it is well known that metals reflect microwaves and cannot be heated. However, recent studies have shown that microwaves can be utilized to sinter metal based powder compacts much more rapidly than conventional sintering, producing materials with better microstructural and mechanical properties. In this study, two directional or hybrid heating is used to sinter monolithic metals and metal based composite materials whereby heating is achieved through the use of microwaves and an external microwave susceptor (SiC) that couples with the microwaves generating radiant heat. Microwaves will heat the billet from within while the radiant heat from the susceptor will heat the billet from the surface inwards. This hybrid heating method results in a more uniform temperature gradient within the billet and circumvents the disadvantage of heating using either conventional heating or microwaves only. Characterization studies were conducted following hot extrusion to evaluate the physical, microstructural and mechanical properties of the synthesized materials.

P197 AlGaN/GaN High-Electron-Mobility Transistors on High-Resistivity Silicon Substrate

S. Arulkumaran*, Z.H. Liu, G.I. Ng, J. Bu, K. Radhakrishnan, H. Wang and C.L. Tan
Temasek Laboratories@NTU, Nanyang Technological University, Singapore
*E-mail: arul001@yahoo.com (or) sarulkumaran@pmail.ntu.edu.sg

Due to the high cost and difficulty in the substrate making technology, GaN substrates are not available in the market. Moreover, the characteristics of HEMTs fabricated in bulk GaN substrate are not very much superior to the SiC and sapphire based HEMT structures. Few reports with greater than 100 W output power of AlGaN/GaN high-electron-mobility transistors (HEMTs) on SiC substrate. For high-power operation, the thermal conductivity of the substrate is expected to be an important design issue and the relatively poor thermal conductivity of sapphire (k_{Sapp} = 0.35 W/cm-K) is expected to limit the device output power. SiC on the other hand, has an excellent thermal conductivity (k_{SiC} = 4.9 W/cm-K) and is an obvious choice for a substrate when thermal considerations are important. AlGaN/GaN high-power HEMTs are usually fabricated on

SI-SiC substrates, which are commercially available but not cost effective. The Si substrate can overcome these limitations of sapphire and SiC that limit manufacturability.

In this work, the 0.3-μm-gate-length AlGaN/GaN HEMTs fabrication and its direct current and microwave characteristics have been performed on high-resistivity (HR) (>20,000 Ω-cm) silicon substrate. The metal organic chemical vapor deposited AlGaN/GaN HEMT on HR Si substrate was obtained from commercial supplier. The HEMT structure exhibited 2-dimensional electron gas mobility and the sheet carrier density of 1300 cm^2/Vs and 0.7×10^{13} cm^{-2} at 300 K, and 5470 cm^2/Vs and 0.69×10^{13} cm^{-2} at 77 K, respectively. After mesa isolation and ohmic contact formation, Ni/Au mushroom shaped 0.8- and 0.3-μm-gate-length devices were fabricated using electron beam lithography system. It should be noted that the devices are un-passivated. On-wafer DC and microwave characteristics were performed to characterize the fabricated devices on Si substrate using 4156B semiconductor parameter analyzer and 8510C Vector Network Analyzer, respectively. A maximum drain current density (I_{Dmax}) and a maximum extrinsic transconductance (g_{mmax}) of 717 mA/mm at Vg = +2 V and 212 mS/mm at V_D = 4V, respectively were observed for a 2.5 μm drain-source gap HEMTs. The 0.8- and 0.3-μm-gate-length HEMTs exhibited a current-gain cut-off frequency (f_T) of 12 and 22 GHz and maximum frequency of oscillation (f_{max}) of 28 and 52 GHz, respectively. The fabricated devices exhibited the ratio of $f_{max}/f_T > 1$ which, means that there is no parallel conduction from HR Si substrate. The observed f_{max} and f_T values are comparable to other reported values. The HR Si has been shown to be a viable substrate for the fabrication of low cost high power and high-frequency operating AlGaN/GaN HEMTs.

P198 Thermo-Optic Switch Using Silicon Prism

T. Zhong, J. Li, X.M. Zhang and A.Q. Liu*
School of Electrical and Electronic Engineering, Nanyang Technological University Nanyang Avenue, Singapore 639798
*E-mail: eaqliu@ntu.edu.sg

This paper reports a new optical switching method utilizing the thermo-optic effect (TOE) and total internal reflection (TIR) of a micromachined silicon prism. It has obtained extinction ratios of >40 dB and 28 dB for two output states, respectively. The key idea is first to adjust the input close to the TIR critical angle of the prism, then to change the refractive index of the prism by localized heating, and finally to switch the output from transmission to TIR. This design exhibits its uniqueness and advantages over the other micromechanical switches [1] and optically pumped switches [2]. This switch requires no mechanical movements, thus it is more efficient and reliable. It does not involve extremely high optical power [2], and localized heating is simple. In addition, the innovative use of the TIR prism can tremendously enhance the sensitivity of switching to small change in refractive index.

Figure 1 illustrates the switching mechanism. Initially the input light is transmitted to Output 1 since the incidence angle is slightly less than the TIR critical angle (i.e. transmission state). As localized heating is applied, the refractive index in a small region near the prism back surface is changed due to TOE, making the TIR condition satisfied. Therefore the light will be totally reflected to Output 2 (i.e. total reflection state).

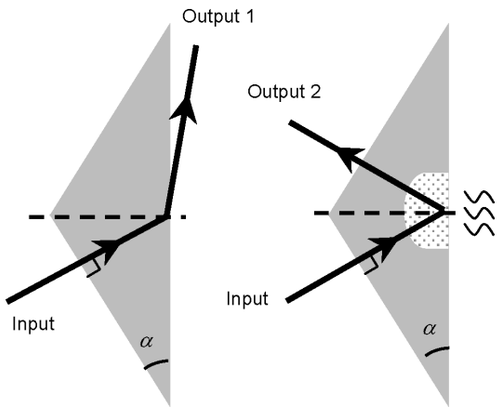

Fig. 1. Schematic diagram of the optical switch using a silicon prism.

Figure 2 shows the simulated plots of the changes of refractive index and refraction angle against the temperature modification relative to the initial 25°C. The refractive index in silicon is increased almost linearly with an

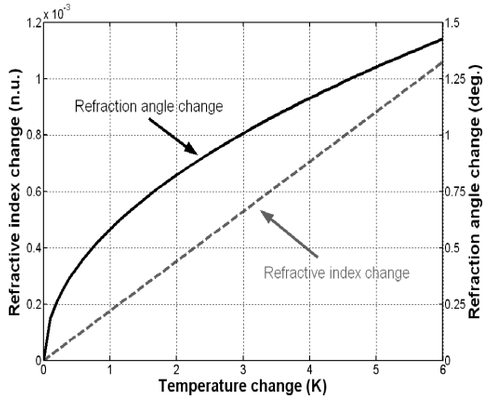

Fig. 2. Theoretical relationships between refractive index variation, refraction angle change and temperature.

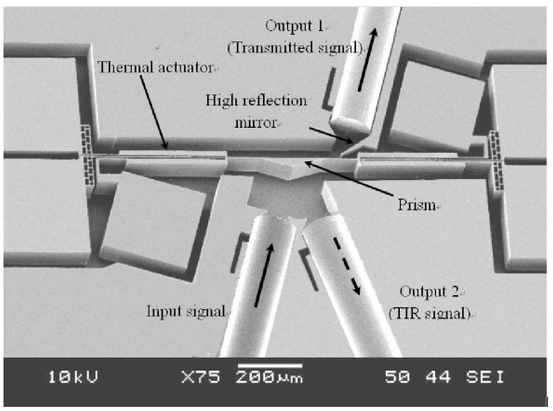

Fig. 3. SEM micrograph of a packaged optical switch.

elevating temperature, as given by [3]

$$\delta n/\delta T = a + b \times T + c \times T^2(K^{-1}) \quad a = 8.61 \times 10^{-s}$$
$$b = 3.63 \times 10^{-7} \quad c = -2.07 \times 10^{-10} \qquad (1)$$

The simulation reveals that a 3K increase of temperature will result in an increase of 5.4×10^{-4} in refractive index, which is sufficient to switch the transmitted output with an 89° initial refraction angle to the TIR output. This indicates an unusual high sensitivity of the switching to the refractive index change.

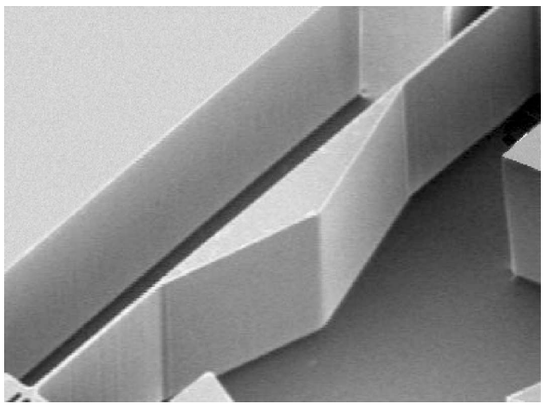

Fig. 4. Close-up of the micromachined silicon prism.

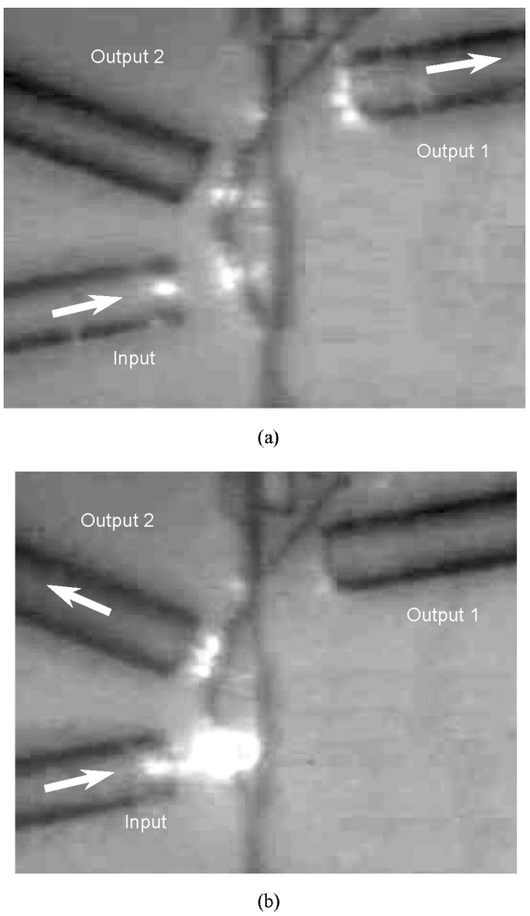

Fig. 5. Infrared snapshots of two switching states. (a) The transmission state; and (b) the total reflection state.

Figure 3 shows the SEM of a packaged optical switch. It consists of a silicon prism, three optic fibers, two thermal actuators and a high reflection mirror (for steering the transmitted light to facilitate the positioning of the Output 1 fiber). The localized heat is generated by a pulsed current through the back surface of the prism.

Figure 4 shows a close-up of the micromachined silicon prism. The prism angle is 16.96° (the critical angle at room temperature) and its initial orientation can be finely tuned by two bi-directional thermal actuators such that the incident angle is slightly less than the critical angle at the silicon-air interface.

Figure 5 presents the infrared snapshots of two switching states. The input is a linearly polarized beam of wavelength 1550 nm. In Fig. 5(a), no heating is applied. The light is transmitted into the Output 1. In Fig. 5(b), 10 mA current is applied, the temperature of the prism back surface is about 78.6°C. The input light is totally reflected into the Output 2. The extinction ratio is >40 dB for Output 1, and 28 dB for Output 2.

In summary, innovative application of total internal reflection and thermo-optic effect of a silicon prism have been demonstrated for optical switching function. This design might bring in a new architecture of optical switches for optical network applications.

References

1. J. Li, *et al*., Advanced fiber optical switches using deep RIE (DRIE) fabrication, *Sens. Actuat. A*, **102(3)**, 286 (2003).
2. V. R. Almeida, *et al*., All-optical control of light on a silicon chip, *Nature*, **431(28)**, 1081 (2004).
3. F.D.G. Corte, *et al*., Temperature dependence analysis of the thermo-optic effect in silicon by single and double oscillator models, *J. Appl. Phys*., **88(12)**, 7115 (2000).

P199 Modeling and Experiment of Time-Varying Electroosmotic Transport in Microchannels

T.N.T. Duong[1], C. Lu[2], P.H. Yap[3] and A.Q. Liu*,[1]
[1] *School of Electrical and Electronic Engineering, Nanyang Technological University, Singapore 639798*
[2] *Institute of High Performance Computing, Singapore Science Park II, Singapore 117528*
[3] *Defence Medical Research Institute, DSO National Laboratories, Singapore 118230*
*E-mail: eaqliu@ntu.edu.sg

This paper investigates and proposes a model to describe the time-varying electroosmotic transport inside a rectangular microchannel that connects two liquid reservoirs. Compared to pressure-driven flow, electroosmosis does not require moving parts, is easy to control but it also has much smaller flow rate and thus a longer time is necessary to achieve a practical volume. The rate of decrease of flow rate depends on the operating conditions and channel geometry mainly due to the build-up of adverse pressure inside the microchannel.

Figure 1 shows (not to scale) the pressure variation along the microchannel. This adverse pressure is caused

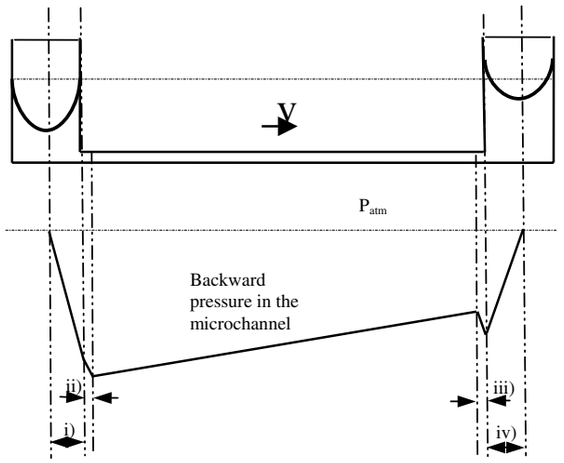

Fig. 1. Schematic diagram (not to scale) to show pressure variation along the microchannel. i) and iii): Laplace pressure and hydrostatic pressure; ii) and iv): pressure head loss at entrance and exit due to sudden fluid contraction and expansion.

by many complex interrelated factors such as the siphoning effect due to difference in liquid levels at the two reservoirs, Laplace pressure at the reservoir menisci, and pressure head losses at the entrances/exits of the channels where the fluid contracts/expands [1,2].

Figure 2 shows the vector field of the flow velocity inside microchannel. The image was shortly after a voltage was applied to effect electroosmotic flow. It can be seen that the flow is laminar and has a plug-like flow profile.

A mathematic model is proposed to describe the flow rate with time as followed:

$$\ln\left[\frac{Q(t)}{Q_0}\right] + 2\alpha\gamma[Q(t) - Q_0] = -\alpha\beta t$$

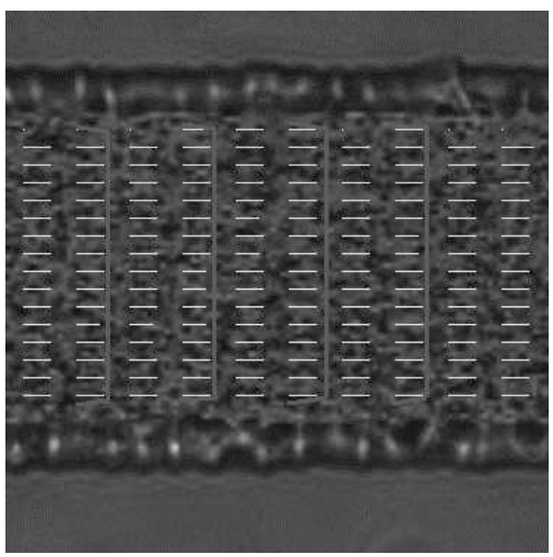

Fig. 2. Experiment results of vector field along microchannel.

where $Q(t)$ is the flow rate at time t seconds, Q_0 is the initial flow rate and α, β, γ are three geometry-determined parameters.

Experiments were conducted in two straight channels with dimensions of 70 μm × 50 μm (C1), 100 μm × 26 μm (C2), the first values being the widths and the second values being the depths.

Figure 3 shows C1 and C2 had similar initial flow rate. This is expected because the two channels have similar cross sectional areas. However, the flow rate of C1 decreases very rapidly whereas the flow rate of C2 only decreases slowly with time. After 140 s, the flow rate of C1 decreases by more than 80% whereas the flow rate of C2 only decreases by 10%.

Figure 4 shows that within the same time interval C2 transports more than two times as much as C1.

In conclusion, it has been shown that the volume flow rate decreases significantly with time and a mechanism to describe how the flow rate varies with time is discussed in order to accurately predict the total volume throughput and the time required to transport a certain volume of sample.

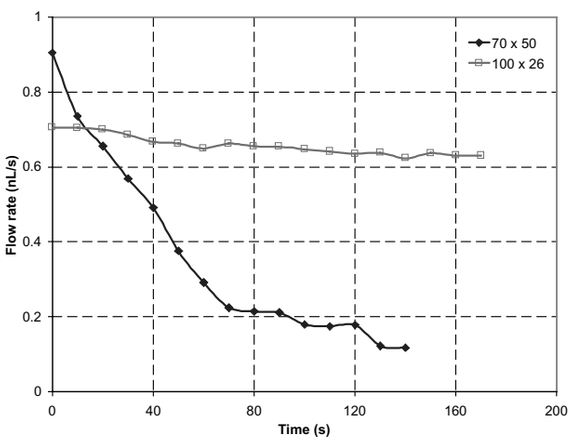

Fig. 3. Experiment results of instantaneous flow rates for two microchannels of different dimensions.

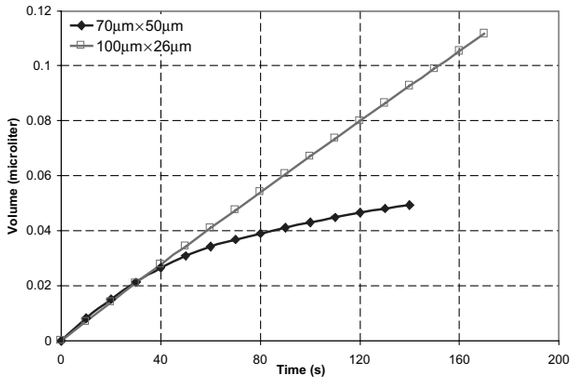

Fig. 4. Experiment results for total transported volumes for two different microchannel of different dimensions.

References

[1] T.N.T. Duong, H.N. Cheang, D.N. Ghista and A.Q. Liu, proceedings of IEEE Conference on Emerging Technologies- Nanotechnology, Singapore, 11–13 Jan 2006.

[2] H.J. Crabtree, E.C.S. Cheong, D.A. Tilroe and C.J. Backhouse, *Anal. Chem.* **73**, 4079 (2001).

P200 Dual Function Photonic Crystal Bandpass Filter Coupler

E.H. Khoo, J.H. Wu, W.M. Tan and A.Q. Liu*
School of Electrical and Electronic Engineering, Nanyang Technological University Nanyang Avenue, Singapore 639798
*E-mail: eaqliu@ntu.edu.sg

This paper presents the combination of a filter and a taper coupler to produce a dual function device called photonic crystal bandpass filter coupler. The advantage of this device is cost reduction, high compactness and coupling efficiency. The two-dimensional crystal structure consists of an array of high refractive index circular rods surrounded by air medium in square lattice arrangement. The rods have a refractive index, $n = 3.45$, which corresponds to silicon at optical communication wavelength. The radius to lattice constant, r/a ratio is 0.2 and there is a bandgap in the TM polarization (E field parallel to the rods axis) at normalize frequency of 0.285–0.413. Figure 1 shows the linear smooth photonic crystal taper waveguide [1] obtain by distorting the crystal lattice.

In the empty area of the taper, a point defect is inserted to act as a multipole source to couple the light. A point defect in the crystal act as a resonator to inrease coupling efficiency. By placing a defect in the empty space, the group velocity of the propagating waves will be reduced and this increase the interaction time of between the defect mode and waveguide mode. Figure 2 shows the dispersion diagram of the point defect mode. The group velocity is related to the dispersion diagram by the following expression [2]

$$v_\varepsilon = \frac{\partial \omega}{\partial k}$$

which implied that the slope of the dispersion diagram gives the group velocity. From Figure 2, we can see that the group velocity is very small in the band gap area. The very low steepness of the slope of the defect mode indicates that the group velocity is very small and this indicates strong interaction between the cavity mode and the resonator mode.

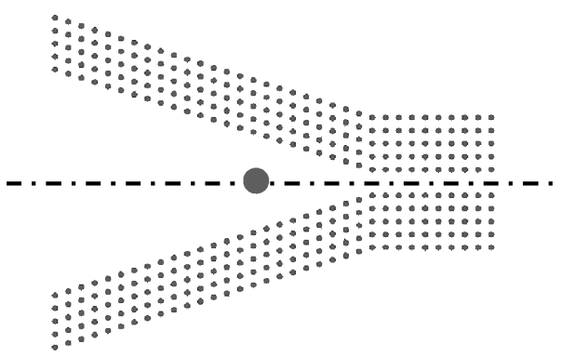

Fig. 1. Band dispersion diagram of a single mode photonic crystal waveguide.

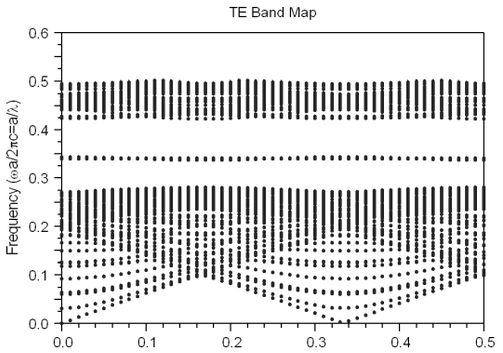

Fig. 2. Band Dispersion Diagram of a point defect.

Figure 3 shows the far field radiation of the point defect resonator. From the figure, we can see the field radiation pattern resemble that of a dipole field pattern. By varying the radius of the defect, we are varying the effective index of the whole system. This means that we are pulling a state from the air or dielectric band and localizing it in the bandgap.

Figure 4 shows the band spectrum after optimising the number of defects, position of defects and the size of defects to be place inside the taper. The defects are

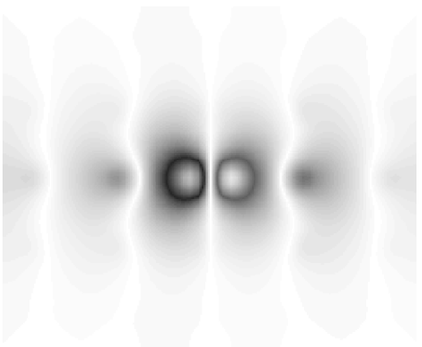

Fig. 3. Far field radiation pattern of a point defect, showing the dipole pattern.

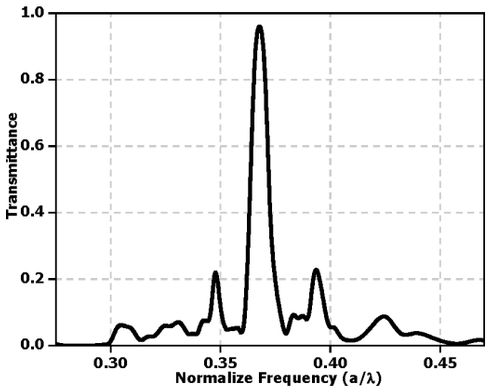

Fig. 4. Bandpass spectrum of the defect taper waveguide.

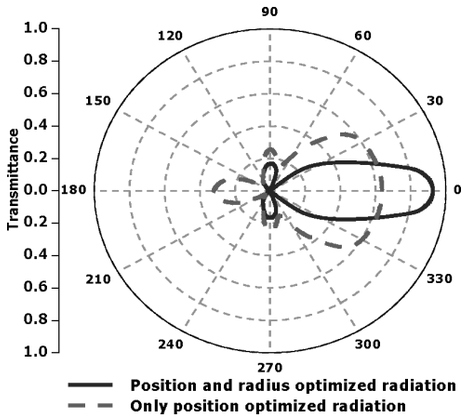

Fig. 5. Power Coupling behaviour for the tapers at each relative position.

placed inside the taper and optimised for maximum transmission and coupling efficiency at 1550 nm. The defects act as a resonator to increase the coupling efficiency from 0.2351 to 0.96 as shown in Figure 4. Apart from coupling efficiency, the defect resonator also reduces the band spectrum of the coupled waves. The spectrum has a bandwidth of 30 nm in the C band.

Figure 5 shows the different in the radiation pattern of the optimised and the un-optimised defects in the photonic crystal taper waveguide. We can see that the radiation pattern of the taper with defects optimise is more directional and has a smaller emitting angle compared to the un-optimised defects.

References

[1] E. H. Khoo *et al*., *Optics Express*, **13**, 7748 (2005).
[2] K. Sakoda, Optical Properties of Photonic Crystals (2001).

Author Index

Typeset and Printed by Stallion Press
e-mail: enquiries@stallionpress.com